



**HAL**  
open science

# Experimental simulation and modeling of sock-to-skin friction during running

Eglantine Baussan

► **To cite this version:**

Eglantine Baussan. Experimental simulation and modeling of sock-to-skin friction during running. Other. Université de Haute Alsace - Mulhouse, 2010. English. NNT : 2010MULH3179 . tel-00871091

**HAL Id: tel-00871091**

**<https://theses.hal.science/tel-00871091v1>**

Submitted on 8 Oct 2013

**HAL** is a multi-disciplinary open access archive for the deposit and dissemination of scientific research documents, whether they are published or not. The documents may come from teaching and research institutions in France or abroad, or from public or private research centers.

L'archive ouverte pluridisciplinaire **HAL**, est destinée au dépôt et à la diffusion de documents scientifiques de niveau recherche, publiés ou non, émanant des établissements d'enseignement et de recherche français ou étrangers, des laboratoires publics ou privés.

UNIVERSITÉ DE HAUTE ALSACE  
ÉCOLE NATIONALE SUPÉRIEURE D'INGÉNIEURS SUD ALSACE  
LABORATOIRE DE PHYSIQUE ET DE MÉCANIQUE TEXTILES  
EMPA LABORATORY FOR PROTECTION AND PHYSIOLOGY

# THÈSE

Pour l'obtention du titre de

**DOCTEUR DE L'UNIVERSITÉ DE HAUTE ALSACE**

DISCIPLINE : MÉCANIQUE

Par

**Églantine BAUSSAN**

**Étude tribologique et modélisation du contact peau - chaussette.  
Application à la course à pied.**

Soutenue publiquement le 6 décembre 2010 devant le jury suivant :

Professeur Guy MONTEIL	ENSMM Besançon	Rapporteur
D. R. CNRS Yves BERTHIER	INSA de Lyon	Rapporteur
Professeur Betty LEMAIRE-SEMAIL	Polytech'Lille	Examinatrice
Docteur René ROSSI	EMPA St Gallen	Co-encadrant
Docteur Siegfried DERLER	EMPA St Gallen	Co-encadrant
Professeur Marie-Ange BUENO	Université de Haute Alsace	Directrice

# REMERCIEMENTS

J'aimerais en premier lieu exprimer ma reconnaissance à Marie-Ange pour avoir initié ce projet de recherche en codirection avec l'EMPA St Gallen et me l'avoir proposé. En plus de m'avoir convaincue d'entreprendre ce travail, elle m'a accompagnée au quotidien par ses conseils et son soutien et je l'en remercie.

Mes pensées vont également à Siegfried et René qui ont supervisé mon travail et m'ont chaleureusement accueillie dans leur groupe de recherche lors de mes travaux à St Gallen.

Je suis aussi très reconnaissante aux professeurs Guy Monteil, Yves Berthier et Betty Lemaire-Semail d'avoir accepté de rapporter et d'examiner mon travail. J'ai apprécié leurs conseils et leurs remarques constructives lors de ma soutenance.

Merci à Dominique Malfait, PDG de Labonal, pour sa disponibilité, pour nous avoir fourni notre base de travail et nous avoir suivi tout au long de ce projet.

Je tiens de même à remercier Alexandre Watzky de l'Université Paris XII pour ses conseils quant au modèle que nous avons développé.

Ce travail n'aurait pas été réalisé sans le financement de la région Alsace, de l'Université de Haute Alsace et de l'EMPA Swiss Federal Laboratories for Materials Science and Technology St Gallen, qu'ils soient assurés de ma reconnaissance.

Je tiens tout particulièrement à remercier Brigitte qui en plus de m'avoir formée et accompagnée tout au long de mon monitorat et de mes années d'ATER, a toujours été disponible pour moi et m'a aidé pour l'exploitation informatique de mes résultats et sur la partie modélisation qu'elle continue d'ailleurs d'améliorer. Son soutien m'a été très précieux lors des passages difficiles de ma thèse, je regretterai notre collaboration et nos sorties sportives.

Un grand merci aussi à Michel pour son amitié et son aide dans la mise en place du tribomètre qui a servi à mes recherches, à Romain pour avoir repris le flambeau et complété mes travaux par son approche mécanique et à Philippe pour m'avoir assistée lors de la partie expérimentale de mon travail.

Merci à Christian Lutz Gerhardt qui m'a familiarisée avec les équipements de l'EMPA et que j'aurais aimé mieux connaître.

Je tiens bien sûr à ne pas oublier mes collègues de bureau ; Céline, Coralie, Mohamed, Romain, Cyril, Jean-Maurice et Mohamed Ali, grâce à qui l'ambiance de travail a toujours été sympathique et qui ont participé à l'aboutissement de mon travail par leur présence, leurs conseils et leur bonne humeur.

Je pense encore aux acteurs du service technique ; Francis, Thien, Sébastien, Philippe, Christian, Jean-Christophe, qui font en sorte que notre quotidien soit le plus aisé possible.

J'ai bien évidemment une pensée pour toutes les personnes qui font et ont fait de cette école un endroit où il fait bon venir, travailler, vivre, qu'ils soient thésards, chercheurs, enseignants, IATOSS, élèves ou extérieurs. Je remercie tous ceux qui se sont intéressés de près ou de loin à qui je suis et ce que je fais.

Enfin, j'aimerais terminer par une pensée pour mon mari, ma famille, celle de mon côté et celle du côté d'Olivier, et mes amis qui m'ont soutenue, écoutée, secouée, encouragée, conseillée, de manière indéfectible tout au long de ma thèse. Leur aide m'a été extrêmement précieuse.

A handwritten signature in black ink, appearing to read 'E. Hank', located in the lower right quadrant of the page.

# CONTENTS

Remerciements _____	2
Textile glossary _____	5
Introduction _____	13
Chapter I: state of the art _____	16
Chapter II: materials and methods _____	71
Chapter III: experimental results _____	100
Chapter IV: modelling of sock-to-skin friction _____	161
Conclusion _____	187

# Textile glossary

### Acetate

Acetate is a manufactured fibre of cellulose ethanoate (acetate) wherein less than 92%, but at least 74% of the hydroxyl groups of the original cellulose are acetylated.

### Acrylic

Acrylic is a manufactured fibre composed of synthetic linear macromolecules having in the chain at least 85% (by mass) of recurring acrylonitrile groups.

### Back

The back is the reverse of a fabric as opposed to the face. Face and back are identified in function of the way the fabric is used or in function of the position of the fabric on the loom.

### Bast fibre (fibre libérienne)

A bast fibre is a fibre obtained from the stems of various plants.

### Burlap

Burlap is a plain cloth made from single yarns of approximately the same linear density in warp and weft, usually made from bast fibres, particularly jute.

### Cast-off position

It is the position in the knitting cycle where the needle is retracted to its lowest point, allowing the new loop to be drawn through the old loop and then casting the latter over the head of the needle hook.

### Compressibility

Compressibility is a term relating to the hand of fabrics and referring to the resistance to squeezing. It ranges from soft (high compressibility) to hard (low compressibility). Measurements of thickness at various pressures provide an objective mean of testing compressibility. This notion is closed to the inverse of hardness for a standard material.

### Compressional resilience

Compressional resilience is the recovery of thickness or energy through a compression and recovery cycle.

### Course

A course is a row of loops across the width of a knitted fabric, i.e. perpendicular to the machine direction.

### Crimp

The crimp of a yarn is the waviness or distortion of the yarn that is due to interlacing in the fabric. In woven fabrics, the crimp is measured by the relation between the length of the fabric sample and the corresponding length of yarn when it is removed there from and straightened under suitable tension. Crimp may be expressed numerically as (a) percentage crimp, which is 100 divided by the fabric length and multiplied by the difference between the yarn length and the fabric length, and (b) crimp ratio, which is the ratio of yarn length to fabric length.

### Elastane

Elastane is a manufactured fibre that is composed of synthetic linear macromolecules having in the chain at least 85% (by mass) of segmented polyurethane groups and that rapidly reverts substantially to its unstretched length after extension to three times that length. The most famous trademark of elastane is Lycra®.

### Face of fabric

The face of a fabric is the side which is intended to be the use surface or which is to be visible in an end product.

### Fibre

(1) *General*. Fibre is the fundamental element used in the fabrication of textile yarns and fabrics.

(2) *Specific*. Fibre is a unit of matter characterized by having a length at least 100 times its diameter or width, and with the exception of noncrystalline glass fibre, having a definitely preferred orientation of its crystal unit cells with respect to a specific axis.

(3) *Textile*. Fibres can be spun into a yarn and made into a fabric by interlacing in a variety of methods, including weaving, knitting and twisting. The essential requisites for fibres to be spun into yarn include a length of at least 5mm, pliability, cohesiveness, and sufficient strength.



### Filament

A filament is a fibre of indefinite length.

### Fleece

A fleece is a fabric with a deep, napped, or pile face.

### Float

*In warp knitting:* a float is a length of yarn not received by a needle and connecting two loops of non-consecutive courses.

*In weft knitting:* a float is a length or lengths of yarn not received by a needle and connecting two loops of the same course that are not in adjacent wales.

### Gauge

The gauge is the number of needles per unit length along a needle bed of a knitting machine. In current practice, the common unit length of one inch (25.4 mm) is used for all types of warp and weft knitting machines.

### Hosiery

Hosiery stands for the knitted coverings for the feet and legs.

### Jute

Jute is the fibre obtained from the bast layer of the plants *Corchorus capsularis* and *Corchorus olitorius*.

### Knitting

Knitting is the process of forming a fabric by the intermeshing of loops of yarn. Warp knitting is a method of making a fabric by normal knitting means in which the loops made from each warp thread are formed substantially along the length of the fabric. It is characterized by the fact that each warp thread is fed more or less in line with the direction in which the fabric is produced. In weft knitting, the loops made by each weft thread are formed substantially across the width of the fabric. It is characterized by the fact that each weft thread is fed more or less at right angles to the direction in which the fabric is produced.

### Knock-over

Knock-over is the action of casting off the old loop over the head of the needle.

### Latch needle

A latch needle is a needle having a small terminal hook closed by a pivoting latch. The action is automatic as the fabric loop overturns the latch and allows the loop to be knocked over. The newly formed loop is drawn by the hook, and loop-forming and knock-over proceed simultaneously.

### Moisture regain

Moisture regain is the ratio of the mass of moisture in a material to the oven-dry mass. It is usually expressed as a percentage for a standard atmosphere of 60% relative humidity and 22°C.

### Nap

A nap is a fibrous surface produced on a fabric or felt by raising in which part of the fibre is lifted from the basic structure.

### Needle bed

A needle bed is a flat slotted plate in which knitting needles operate under the influence of jacks or cams.

### Nylon

Originally Nylon was the trademark of Dupont for polyamide 6.6. It is now a common noun.

### Pile

Pile is a surface effect on a fabric formed by tufts or loops of yarn that stand up from the body of the fabric.

### Plain weft-knitted fabric

A plain weft-knitted fabric is a fabric in which all of the component knitted loops are of the same sort and meshed in the same manner.

### Polyamide

Polyamide is a manufactured fibre composed of synthetic linear macromolecules having in the chain recurring amide groups, at least 85% of which are attached to aliphatic or cyclo-aliphatic groups.

### Polyester

Polyester fibre is a manufactured fibre composed of synthetic linear macromolecules having in the chain at least 85% (by mass) of an ester of a diol and benzene-1,4-dicarboxylic acid (terephthalic acid).

### Polypropylene

Polypropylene is a manufactured fibre composed of synthetic linear macromolecules having an aliphatic saturated hydrocarbon chain in which alternate carbon atoms carry a methyl group, generally in an isotactic disposition and without further substitution.

### Polytetrafluoroethylene

Polytetrafluoroethylene is a fibre made from a synthetic linear polymer in which the chief repeating unit is  $-\text{CF}_2-\text{CF}_2-$ .

### Polyurethane

Polyurethane is a manufactured fibre composed of synthetic linear macromolecules having in the chain recurring aliphatic groups joined via urethane groups which together comprise at least 85% (by mass) of the chain.

### Raising

It consists in producing a layer of protruding fibres on the surface of fabrics by brushing, teasing or rubbing. The fabric, in open width, is passed over rotating rollers covered with teazles, fine wires, etc., whereby the surface fibres are pulled out or broken to give the required effect.

### Relative humidity

Relative humidity is the ratio of the actual pressure of the water vapour in the atmosphere to the saturation pressure of water vapour at the same temperature and same total pressure. The ratio is usually expressed as a percentage.

### Sinker

A sinker is a blade that works in conjunction with knitting needles and assists with loop formation and fabric holding.

### Spandex

Spandex is an elastane fibre.

### Spinning

Spinning is the process or the processes used in the production of yarns or filaments.

### Stitch

A stitch is an intermeshed loop.

### Viscose

Viscose is a manufactured fibre of cellulose obtained by dissolving sodium cellulose xanthate in a dilute solution of sodium hydroxide.

### Wale

A wale is a column of loops along the length of a fabric, i.e. in the production direction of the knitting machine.

### Worsted

Descriptive of yarns spun wholly from combed wool in which the fibres are reasonably parallel, and fabrics or garments made from such yarns. In most countries, fabrics with a small proportion of non-wool decorative threads can be described as worsted.

### Yarn

A yarn is a product of substantial length and relatively small cross-section consisting of fibres and/or filament(s) with or without twist.

*Note:* Assemblies of fibres or filaments are usually given other names during the stages that lead to the production of yarn, e.g., tow, slubbing, sliver, or roving. Except in the case of continuous-filaments or tape yarns, any tensile strength possessed by assemblies at these stages is generally the minimum that can hold them together during processing.

### Yarn count

The count is the mass per unit length. It can be expressed in various units.

*Tex*: it is a recognized international unit which corresponds to the mass in grams of one kilometre of product.

*Metric count* ( $N_m$ ): it is defined as the number of kilometres of yarn to obtain one kilogram.

*Cotton count* ( $N_e(c)$ ): it is the number of hanks of 840 yards per pound.

$$N_m = N_e(c) \times 1.693 = \frac{1000}{Tex}$$

The definitions given here are drawn from the following books [1-3]:

1. Milton Harris, *Handbook of textile fibers*. first edition. 1954, Washington: Harris research laboratories, inc. 356.
2. Textile Institute Textiles Terms and Definitions Committee, *Textile Terms and Definitions*. Ninth Edition. 1991, Manchester: M C TUBBS BSc Tech AMCT CText FTI FRSA P N DANIELS BA MIIInfSc. 367.
3. George E. Linton, *The modern textile and apparel dictionary*. Fourth revised enlarged edition 1973, Plainfield, New Jersey 07060, USA: textile book service, a division of Bonn Industries, Incorporated 716.

# Introduction

Various skin troubles can be caused by sports activities such as allergic reactions, and chafing when swimming, frictional alopecia or occlusive acne when bicycling, blisters, corns, calluses and talon noir when running. We investigated the contact of the sock and the skin of the foot during running. Friction blister is the most common cutaneous disorder for joggers. Blisters are caused by clothes rubbing on the skin. They appear where skin is glabrous and epidermis is thick and result from frictional forces that mechanically separate epidermis cells. The formation of blisters depends on the magnitude of the frictional forces and the number of times that an object cycles across the skin. During jogging, the foot is deformed in each stride. A running shoe has to provide support and shock absorption. Due to its higher stiffness, the shoe will not perfectly follow the skin deformations i.e. relative movements take place and rubbing occurs. Various scientific publications about the structure of running shoes and the fibre composition and properties of running socks are available. However, very few studies investigated the influence of socks structures regarding friction induced on the skin. The influence of the sock structure on friction must be a subject of interest for sock manufacturers but such research seems to be kept confidential.

In this study, we investigated the friction which different running socks structures exert on the skin during running by means of friction experiments using a mechanical skin model. We also modelled the friction of textile surfaces covered with terries on the foot skin. The objectives were to examine and simulate the effect of sock structure on friction for the recreational runner. We aimed to determine whether one specific textile construction provides better performances in terms of friction exerted on the skin and intended to develop a simple and quick model that can predict the friction a given sock structure will induce on the skin of a runner.

The thesis is divided into four chapters.

Chapter 1 gives an overview of the current state of the knowledge in skin injuries, friction and compression properties of textile fabrics and skin and socks technology regarding friction and compression in contact with the skin in the shoe.

Chapter 2 describes the testing conditions, the socks which were investigated and the friction and compression analysers used.

Chapter 3 reports the experimental results of this research; the friction results are first presented and then confronted to compression results in order to conclude on the performances of the different textile structures.

Chapter 4 describes and analyses previous friction and compression models before introducing in details the analytical model of sock-to-skin friction that is proposed.

The conclusion finally highlights the most important findings of this thesis and suggests outlooks for future works.



# Chapter I: state of the art

# Résumé

Ce premier chapitre présente dans un premier temps les affections cutanées qui peuvent être générées lors de pratiques sportives. Le cas de la course à pied et plus spécifiquement les phlyctènes sont abordés en détail. Dans un deuxième temps, les principales lois de la tribologie sont exposées ainsi que les propriétés de frottement et de compression des surfaces textiles et de la peau. Pour terminer, l'influence de certaines caractéristiques comme par exemple la composition ou bien l'épaisseur d'une chaussette de course sur le frottement généré au niveau de la peau est discutée.

La peau est une barrière de protection pour les organes et les tissus qui forment le corps humain. Lors de pratiques sportives, elle peut être exposée de manière prolongée ou répétitive au frottement, à la pression, à l'humidité, au soleil, au froid ou à la chaleur. Différentes affections cutanées peuvent s'ensuivre, nous n'en citerons ici que quelques unes. Les cors et callosités sont des zones où la peau s'est épaissie de manière à mieux résister aux frottements répétitifs. Selon le sport pratiqué et l'équipement utilisé, les callosités peuvent apparaître à divers endroits. Les cors sont le plus souvent localisés au niveau des proéminences osseuses des pieds. Les cors durs apparaissent là où les doigts de pieds sont en contact avec la chaussette alors que les cors mous apparaissent entre les doigts de pieds. Une malformation ou bien le fait de porter des chaussures et des chaussettes mal adaptées augmente le risque d'apparition de cors. Parmi les problèmes cutanés fréquemment rencontrés chez les marathoniens, les phlyctènes sont les plus fréquentes. Nous avons donc concentré nos recherches sur cette affection particulière.

Il y a principalement quatre contraintes qui s'exercent sur le pied lorsque l'on court : le choc dû au contact initial entre la chaussure et le sol lors de la foulée, la pression de l'ensemble chaussure + chaussette, le frottement et le cisaillement dus au mouvement du pied dans la chaussure. La probabilité d'apparition d'une ampoule dépend de l'intensité des forces qui s'exercent sur la peau et du nombre de foulées. Plus les forces sont importantes plus l'apparition de phlyctènes est rapide. Les étapes de formation d'une ampoule sont les suivantes :

- Les couches superficielles de l'épiderme subissent tout d'abord une exfoliation et une zone rougie et douloureuse apparaît.

- Ensuite, il y a séparation de deux couches de l'épiderme et l'espace laissé vide entre les deux couches se remplit de liquide sous l'effet de la pression hydrostatique.

Les phlyctènes apparaissent communément aux endroits où la peau est glabre et l'épiderme épais tandis que les zones pileuses de la peau où l'épiderme est fin sont sujettes à l'exfoliation mécanique et aux irritations. En ce qui concerne la course, les ampoules sont plus nombreuses à l'avant du pied. La peau est pourtant plus fine à l'avant qu'à l'arrière du pied mais l'avant du pied est soumis à plus de pression et de cisaillement que la région du talon. Plusieurs facteurs jouent sur l'apparition de phlyctènes : selon le terrain choisi, les forces de cisaillement qui s'exercent sur le pied sont plus ou moins importantes, la transpiration, la chaleur ou des exercices inhabituels contribuent à accélérer l'apparition d'ampoules, tandis que le fait de bien lacer ses chaussures permet de réduire leur nombre.

Nous étudions le contact tribologique entre la chaussette de sport et la peau de manière à mesurer, simuler et diminuer le frottement s'exerçant sur la peau. Le contact tribologique est déterminé par les deux corps en contact (rugosité, composition, propriétés mécaniques), l'interface ou troisième corps, l'environnement (température, humidité relative) et le système mécanique (force normale appliquée, vitesse, géométrie du contact). Les forces de frottement dépendent, à l'échelle macroscopique, du système tribologique, à l'échelle mésoscopique, des mécanismes de déformation des deux corps en contact au niveau de leurs aspérités de surface et, à l'échelle moléculaire, des mécanismes d'adhésion entre les deux corps. Deux matériaux en contact subissent des déformations i.e. des modifications dimensionnelles. On distingue trois types de déformation. Les déformations élastiques apparaissent dès l'application de la contrainte et disparaissent immédiatement et complètement lorsque celle-ci cesse. Les déformations plastiques sont elles irréversibles tandis que les déformations viscoélastiques disparaissent totalement mais pas immédiatement. Une partie de la déformation disparaît immédiatement (effet élastique) et l'autre partie disparaît au fil du temps (effet visqueux).

Les principales lois du frottement sont celles d'Amontons, de Coulomb et de Bowden et Tabor. Les lois d'Amontons indiquent que la force de frottement est indépendante de l'aire de contact, que cette force est proportionnelle à la force normale appliquée i.e.  $F = \mu \times W$  avec F force de frottement tangentielle en Newton, W force normale en Newton et  $\mu$  coefficient de frottement qui dépend des matériaux en contact, et que la force de frottement est indépendante de la vitesse de déplacement. Coulomb a introduit la notion de frottement statique et dynamique. La force de frottement statique est la force requise pour initier le

mouvement entre les deux corps alors que la force de frottement dynamique est la force requise pour entretenir ce mouvement, généralement moins importante que la première. Selon Bowden et Tabor, les lois du frottement dépendent des mécanismes d'adhésion et de déformation qui sont tous deux liés à la notion d'aire de contact réel. L'aire de contact réel est généralement bien inférieure à l'aire de contact apparente et dépend des rugosités des surfaces en contact, des propriétés des matériaux, de la force normale appliquée et de l'échelle considérée.

Certaines de ces lois ne s'appliquent pas dans le cas des matériaux textiles, notamment la deuxième loi d'Amontons (la force de frottement est proportionnelle à la force normale appliquée). Pour les fibres textiles, la relation  $F = KW^n$  où  $K$  et  $n$  sont des constantes déterminées empiriquement,  $0 \leq n \leq 1$ , est admise. C'est en fait l'aire de contact réelle qui dépend de  $W$ . Si l'on considère une surface recouverte d'aspérités sphériques, dans le cas d'une déformation purement plastique, l'aire de contact est directement proportionnelle à  $W$  alors que dans le cas d'une déformation purement élastique, elle est proportionnelle à  $W^{\frac{2}{3}}$ . Pour une surface réelle, dans le cas d'une déformation purement élastique, l'aire de contact réelle sera donc proportionnelle à  $W^n$  où  $\frac{2}{3} \leq n \leq 1$ . Pour des forces normales très élevées, la déformation plastique du matériau sera importante et la force de frottement pourra alors être modélisée par la relation  $F = \alpha W + KW^n$  où  $\alpha$  est une constante empirique.

En ce qui concerne la peau, la force de frottement sur cette dernière est proportionnelle à  $W^{\frac{2}{3}}$ . Les propriétés tribologiques de la peau dépendent de sa souplesse et de son hydratation. Le coefficient de frottement de la peau en contact avec une surface textile augmente avec l'humidité. L'hydratation de la peau entraîne en effet une adhésion plus forte entre la peau et la surface textile.

Les chaussettes de sport sont principalement tricotées soit en jersey simple, soit en jersey bouclette qui a la même structure que le jersey simple mais est tricoté avec deux fils ; un fil de fond pour former la structure et un fil de bouclette qui forme des boucles sur la face envers du tricot lui donnant ainsi de l'épaisseur. La composition d'une chaussette influence de manière importante ses propriétés, comme par exemple sa compressibilité, son coefficient de frottement et son taux de reprise. Pour une vitesse de frottement de  $0,6 \text{ m.s}^{-1}$ , les coefficients de frottement de différentes matières textiles peuvent être classés du plus grand au plus petit dans cet ordre : coton, lin, coton peigné, laine, et soie. Cet ordre est indépendant des

conditions atmosphériques. Le taux de reprise d'un textile permet de quantifier son caractère hydrophile. La laine est la fibre la plus hygroscopique ; l'eau représente 12 à 15% de son poids dans des conditions normales d'humidité et peut atteindre jusqu'à 30 à 50% de celui-ci dans un environnement humide. La laine absorbe l'humidité de manière lente et sèche aussi lentement. La soie est presque aussi hydrophile que la laine mais sèche beaucoup plus rapidement. Les chaussettes en coton sont également très hydrophiles, elles retiennent l'humidité au contact de la peau ce qui provoque une sensation désagréable et de nombreuses affections cutanées. En revanche, les fibres de polyester comme les fibres de Coolmax® sont très hydrophobes et évacuent l'humidité. Pour donner un ordre de grandeur, les fibres de coton retiennent trois fois plus d'humidité que les fibres d'acrylique et quatorze fois plus que celles de Coolmax®. Plus la surface spécifique de la fibre est importante plus la fibre évacue l'eau facilement. Les fibres artificielles et synthétiques présentent des sections droites de formes très variées. À titre d'exemple, entre une section ronde et une section scalloped oval comme celle du Coolmax®, la surface spécifique augmente de 20%. Si l'on compare les fibres synthétiques aux fibres naturelles, les fibres synthétiques provoquent moins d'affections cutanées car leurs coefficients de frottement et leurs taux de reprise sont plus bas.

Une bonne chaussette de sport doit absorber l'humidité mais aussi la drainer vers l'extérieur et permettre également l'évacuation de la chaleur générée par le frottement. Les chaussettes en coton ne sont pas recommandées car leur conductivité thermique est faible ; 0,07 W/m/K, et qu'elles sont hydrophiles. Le polyester avec un taux de reprise de 0,4% et une conductivité thermique de 0,14 W/m/K est un assez bon compromis, le polyamide également bien qu'avec un taux de reprise de 3% car sa conductivité thermique atteint 0,25 W/m/K. De plus, il est conseillé de choisir un produit qui permette d'avoir un coefficient de frottement faible avec la peau de manière à ce que le pied soit libre de bouger et ne subisse pas de contraintes de cisaillement importantes et en même temps un coefficient de frottement important avec la chaussure de manière à limiter l'amplitude du mouvement dans la chaussure.

Malgré de très nombreuses recherches sur les phlyctènes, il est difficile de prévoir l'apparition et la sévérité d'une ampoule et aucune solution simple et efficace n'existe pour prévenir sa formation. Le meilleur moyen consiste à réduire au maximum la pression et le frottement exercés sur la peau en choisissant des chaussures et des chaussettes adaptées. Le choix des chaussures dépend des caractéristiques des pieds de la personne et de l'activité pratiquée. Les chaussettes doivent être adaptées aux chaussures et à la manière de les porter. Afin de réduire la pression exercée sur la peau, l'aire de contact entre la chaussette et la

chaussure doit être maximale ; la distance entre la chaussure et la peau doit donc être si possible égale à l'épaisseur de la chaussette non comprimée. Si cette distance est plus petite, cela augmente la pression de contact et si elle est plus grande, cela augmente la distance de frottement du pied dans la chaussure.

# CONTENTS

<b>Chapter I: state of the art</b>	<b>16</b>
<b>I. SKIN INJURIES AND FOOTWEAR</b>	<b>24</b>
1. Human skin structure	24
2. Sport-induced skin injuries due to mechanical influences	25
A. Damages from friction and pressure	26
B. Skin erythema due, among others, to running practise	27
a. Jogger's toe	27
b. Chafing and abrasion	27
c. Friction blister	27
3. Blister formation	27
4. Factors influencing the formation of skin blisters	29
A. Footwear influence	29
B. Influence of the lacing technique	30
5. Prevention of blisters	31
<b>II. FRICTION AND COMPRESSION OF FABRICS AND SKIN</b>	<b>33</b>
1. Tribology overview	33
A. Tribological contact	33
B. Laws of friction	35
a. Laws of Amontons	35
b. Laws of Coulomb	35
c. Bowden and Tabor approach	36
2. Friction behaviour of textiles	38
A. Effect of load on the friction of fibres	38
B. Variation of the area of contact with load	39
C. Case of high normal stresses	40
D. Effect of fibre cross-section shape	40
E. Effect of yarn sett and hairiness	41
F. Other factors affecting friction	41
3. Frictional properties of human skin	41
A. Influence of the applied load on skin friction	41
B. Influence of skin humidity	42
C. Influence of anatomical site and age	43
4. Fabric to skin friction measurements	44
A. Fabric friction measurement methods	44

B.	Fabric to skin friction devices	45	
C.	Investigations on friction blisters	46	
D.	Skin models	46	
5.	Plantar pressure measurements	47	
A.	Measurement devices	47	
B.	Plantar pressure in normal foot	48	
6.	Fabric compression measurements	49	
III.	SOCKS TECHNOLOGY		52
1.	Textile overview	52	
A.	Fibres	52	
B.	Yarns	52	
C.	Knitted Fabrics	53	
2.	Common knitted structures for sport socks	54	
A.	Simple jersey	55	
B.	Terry jersey	59	
3.	Influence of fibre composition	61	
A.	On coefficient of friction	61	
B.	Moisture regain	62	
4.	Influence of sock thickness	64	
5.	Are there ideal socks?	65	
	Literature cited		67



In this chapter, skin injuries that may occur during sports activities will be described. Running induced skin disorders, especially friction blisters will be detailed. The influence of external factors on blisters incidence will also be dealt with. We will see that blister formation is mainly due to friction and pressure forces. General principles of tribology, friction and compression properties of textiles and skin will then be exposed. Finally, the effect of different properties of a sock, such as its fibre composition and its thickness, on skin friction and compression will be tackled.

## **I. SKIN INJURIES AND FOOTWEAR**

### **1. Human skin structure**

Human skin has a surface of about 2 m<sup>2</sup>, a weight of 5 kg and a thickness from 1 to 4 mm for an adult. It has two functions: it protects our organs and tissues against mechanical, biological, thermal and solar stresses and it enables perspiration to be evacuated while it prevents water from penetrating in our body. It is composed of several layers, from the most superficial to the deepest: the corneal layer, the epidermis, the dermis and the hypodermis [1]. The multilayered structure of skin is illustrated in figure 1.

The corneal layer is a superficial layer which covers the epidermis and acts as a barrier against the environment aggressions. The epidermis is composed up to 90% by keratinocytes; cells which insure cutaneous regeneration and healing. Its thickness can vary from 0.07 mm for the eyelid to 1.4 mm for the sole of the foot [2, 3]. It depends in part on the thickness of the stratum corneum which is largest at the hands and feet [4]. The stratum corneum is the upper layer of the epidermis. It is around 0.015 mm thick and is renewed continuously i.e. new cells are continuously integrated in the stratum corneum, but on the other hand, superficial cells are permanently abraded and lost. The epidermis is separated from the dermis by the basal membrane. This junctional zone has a complex structure. Under the epidermal layer, the lamina lucida is located, followed by the lamina densa which is interlinked through anchoring filaments and fibrils with the basal cells and the dermal fibrous tissues. This structure is subjected to bullous skin diseases. The dermis is composed of collagen fibres<sup>§</sup> and elastin matrix. It is responsible for the skin tear resistance and elasticity. Its thickness ranges

---

<sup>§</sup> This symbol indicates that the word definition is given in the textile glossary.

from 1 mm for the face to 4 mm for the back. The deformation of the dermis presents an elastic and a viscous part. The hypodermis or subcutaneous tissue has a loose structure whereby the dermis can slide on the bone or the muscle and it absorbs a great part of the shearing energy.

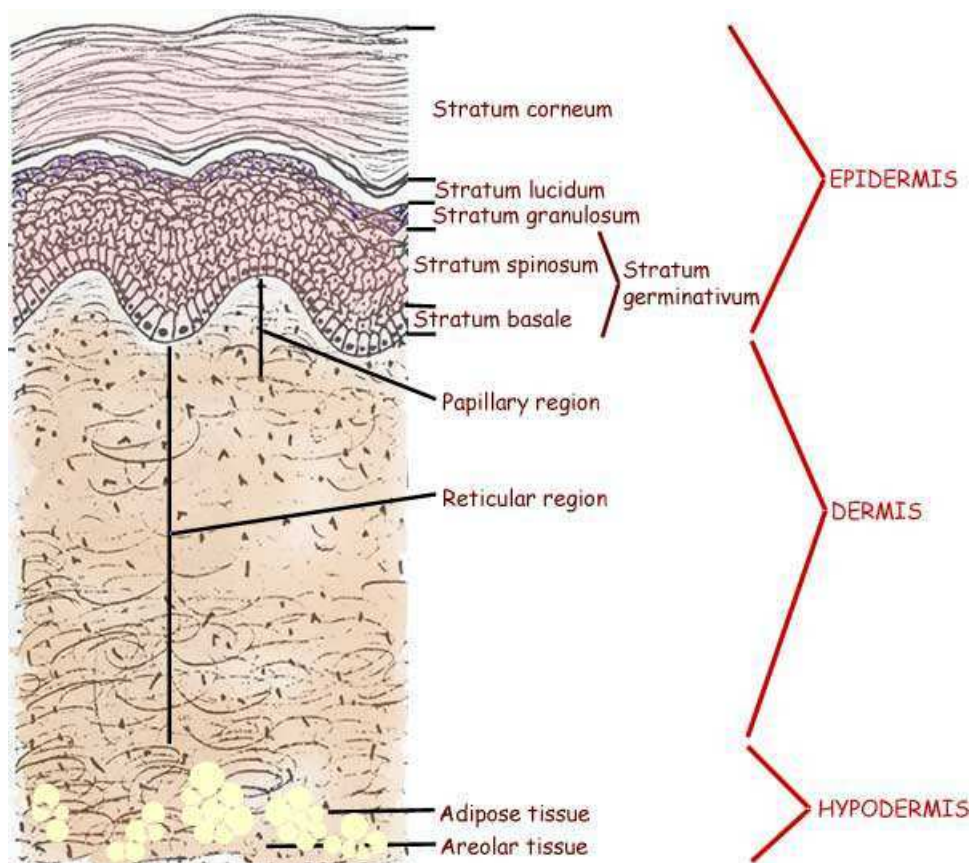


Figure 1: Human skin layers [5].

## 2. Sport-induced skin injuries due to mechanical influences

The skin is the primary human protective barrier. During sports activities, the skin is exposed to multiple prolonged stresses such as friction, pressure from clothing and equipment, high level of skin humidity from perspiration, sunlight, cold or heat. Various skin injuries can result, for example infections and dermatoses. Skin injuries may be caused either by sun, cold, chemicals or contact and friction [6]. Many publications investigated the affections of skin relative to sports activity [7-13].

## **A. Damages from friction and pressure**

During use and because of mechanical loads during sport activity, sport clothes and equipment can generate friction, pressure, heat and occlusion on the athlete skin thus provoking superficial folliculitis called acne mechanica. Many pieces of athletic equipment have been reported to cause this acneiform eruption such as sweatbands, face guards, helmets, football paddings or backpacks [7, 9, 12, 13].

Human skin also develops protective response to chronic and repetitive friction. Calluses and corns are thus thickened, hyperkeratotic plaques which occur at points of continuous friction like palms and soles. Depending on the sport and the equipment, calluses may develop in various locations. Corns have a deep central core and can be hard or soft [13]. They occur as often as not over foot bony prominences, especially over the metatarsal heads, along the inner aspect of the large toe, or over structurally or functionally defective areas of the foot. Poor fitting footwear and skeletal deformities increase the risk of developing corns. Hard corns occur on the external surface of the toes where drying occurs while soft corns are interdigital and result from sweating.

Black heel (also called talon noir) is an asymptomatic lesion which often occurs on the post lateral aspect of the heel of teenagers and young adults. It is characterized by discrete brown or blue-black macules caused by the rupture of small peripheral blood vessels [9, 10]. It is frequently observed in sports which require frequent sudden stops i.e. basketball or handball. Repeated stop-and-start motions, changes in direction and constant pounding on hard surfaces lead to injury of the heel against the back of the shoe. The macules of talon noir occur on the posterior, medial, and lateral sides of the heel, just above the thick plantar skin where blood vessels are less protected by fatty tissue.

Most of the cutaneous reactions related to sports activities can be developed during running practice, especially foot lesions.

## **B. Skin erythema due, among others, to running practise**

### ***a. Jogger's toe***

Approximately 0.1 to 14% of runners reported injuries to the toenails on marathon day [10]. It is a subungual hematoma which commonly appears on the hallux, on the second toenail, or on the lateral aspects of the third, fourth and fifth toes. It presents a black discoloration, oedema and erythema and is due to repetitive shocks of the longest toe against the toe box\* of the shoe. It often occurs with downhill running.

### ***b. Chafing and abrasion***

The friction of moist skin can result in chafing which is a superficial inflammatory dermatitis. The keratin is separated from the granular sub layer of the epidermis by friction in a warm and humid environment. In the marathon literature, chafing was reported by 0.4 to 16% of runners [8, 10].

Long distance runners commonly suffer from jogger's nipples which is a painful and crusted abrasion of the areolae and nipples. Jogger's nipples are caused by repetitive friction against coarse shirts and occur in 2 to 16.3% of runners on marathon day.

### ***c. Friction blister***

Friction blister is the most common injury in marathon participants. Up to 39% of marathon runners who participated to the surveys had post marathon blisters [8]. For infantry soldiers carrying heavy equipment over long distances, blisters can account for 48% of the total injuries [14]. We therefore focused our research on this particular skin phenomenon which occurs at the interface between foot and sock. As blister is the subject of our research, it will be fully detailed in the next paragraphs.

## **3. Blister formation**

Knapik et al. reported that most activity-related blisters may be due to frictional shearing forces [15]. However, frictional shearing forces do not seem to be sufficient for a blister to occur. For Reynolds et al., it is the combination of pressure, shear and moderate level of moisture which generates friction blisters [16]. Comaish suggested that mechanical fatigue might be the most important mechanism in blister formation [17]. Four main stresses

---

\* The toe box is the part of the shoe where the toes are.

actually act on the foot: step shock, pressure, friction and shear. Step shock is the impact force which arises from the initial contact of the foot with the ground. For a running athlete, this force can be up to three times the body weight [18]. Friction results from the rubbing of the footwear (shoe and sock) on the skin of the foot. It is often localized and provokes heat and skin exfoliation. While friction corresponds to the external aspect of skin rubbing, shear can affect both foot contact surface and deeper tissues. The initial contact between the foot and the ground is made with the heel. When the heel touches the ground, friction between the foot and the footwear is generated whereby a horizontal shear force acting backwards against the foot is produced. The shearing forces are thought to be more damaging to the skin than vertical forces [18]. Step shock, pressure, friction and shear are usually occurring at the same time which results in injuries of the foot structures and the skin [19]. The magnitude of forces and the number of times an object cycles across the skin determine the probability of blister development: the higher the forces, the fewer the cycles necessary to produce a blister. According to Knapik [20], there is a minimal force below which no blister will form, regardless of the number of shear cycles.

The forces detailed above lead to an exfoliation of the stratum corneum and the formation of a reddened region in and around the area of rubbing which is referred as a “hot-spot” [20]. Then a cleavage of the epidermal layers occurs, usually between the stratum granulosum and the stratum spinosum layers [3, 8, 10, 11, 13, 14, 20-23]. The three most superficial skin layers, i.e. the stratum corneum, the stratum lucidum and the stratum granulosum are then left intact and form the blister roof [21]. The separation of skin cell layers may also take place subepidermally [11]. Once the layers are separated, hydrostatic pressure causes the resulting free space to fill with blood or tissue transudation [8, 14, 20].

Friction blisters commonly occur on glabrous skin where epidermis is thick whereas friction on hairy skin with thin epidermis usually leads to mechanical skin exfoliation and irritation as illustrated figure 2.

Herring and Richie reported that friction blisters are peculiar to the skin of the hand palms and foot soles where the thickened stratum corneum, stratum lucidum and stratum granulosum develop an interfacial movement with the stratum spinosum [22]. According to Mailler, Adams and Bergeron, blistering events usually occur on the tips of the toes, the balls of the feet and the posterior heel [8, 11]. Forefoot region is more affected than heel region.

60.2 % of the blisters observed by Herring and Richie [22] on the feet occurred in the forefoot region, 33.3 % in the midfoot region and 6.5% in the rearfoot area. The skin is actually thinner on the forefoot than on the heel area. Moreover, Dai et al. measured larger magnitudes of the plantar pressure and shear on the forefoot region than on the heel region thus explaining this difference [24]. The size of blisters is very dependent on the region of the skin, the contact and the environment, Herring and Richie [22] observed blisters from 8.7 to 81.2 mm<sup>2</sup>. For Bergeron [11], blisters of less than 5 mm in diameter are small blisters.

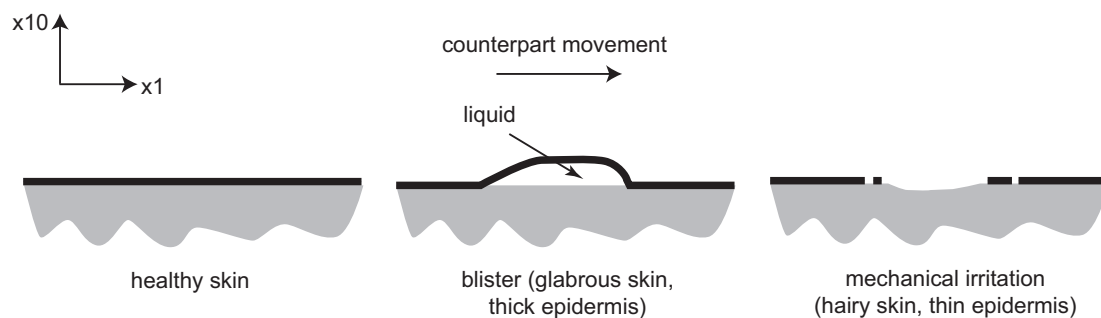


*Figure 2: Friction blister and mechanical skin irritation phenomena.*

#### 4. Factors influencing the formation of skin blisters

The type of ground surface may increase the shearing forces on the foot thus promoting blisters [18]. Skin moisture, heat or unusual exercises are others factors which contribute to blisters formation [8, 16]. The number and severity of previous foot skin blisters are also crucial. Patterson et al. studied the blistering events among 100 cadets in a summer camp [6]. They found that women and cadets with a history of blisters in the 2 years before camp had higher relative risk of blister formation. They recommended as well the preconditioning of the foot to its footwear in order to reduce severe blisters. They thus suggested a significant influence of the footwear on the formation of skin blisters.

##### A. Footwear influence

Running shoes can be classified according to their level of stability. A runner should buy running shoes corresponding to his weight and way of running. Running shoes that bring

a high level of stability are indicated for severe overpronators, flat-footed and bigger runners while neutral shoes correspond to lighter and underpronating runners. Finally, running shoes that give a moderate level of stability are designed to fit the majority of runners [25]. Richie includes the footwear, notably the type of insole and the socks, in the environmental parameters that can increase foot blisters formation [18]. He reported studies have been carried out which investigated the role of footwear on foot lesions. These studies showed that appropriate footwear reduce the occurrence of foot affections by redistributing and decreasing plantar pressure and shear. The importance of footwear in blistering events will be further discussed later in this manuscript. Footwear includes the shoe and the sock; consequently one must be careful in the choice of both (size and technical properties) but also in the way of wearing them. Shoe lacing system is thus of great importance.

## **B. Influence of the lacing technique**

In 2001, Sandrey et al. [26] compared the ability of different soccer shoes to control rear foot motion and showed that a shoe with a special “pronated lacing technique” presented a better effectiveness than others. In 2002, Polster [27] recommended X-lacing as the best lacing technique. These studies inspired Hagen and Hennig [28] who investigated the effects of different shoe lacing systems on rear foot motion, plantar pressure distribution and shock attenuation during running.

The latter study investigated nine different lacing conditions varying the number of laced eyelets. An additional test was carried out fixing the shoe lacing conditions and changing the shoe lacing tightness from weak to normal and strong. Various parameters were recorded during the running sequences: foot pronation during contact, tibial acceleration of the right leg and plantar pressure under seven locations, i.e. medial and lateral heel, lateral midfoot, first, third and fifth metatarsal heads and hallux.

Strong tightness and maximum number of eyelets laced conditions gave identical results. The shoe lacing technique highly impacted foot-shoe coupling. Stronger lacing induced a tighter coupling of foot to shoe leading to reduced peak vertical loading rates, peak heel pressures and pronation velocity. On the other hand, the important sliding of foot within the shoe in the weak tightness and low laced shoe conditions reduced peak vertical impact forces and peak pressures under the forefoot. Hagen and Hennig could conclude that the important thing was to well lace running shoes which is, to my point of view, the most important thing because the better lacing conditions may surely differ according to which

shoe and which sock are worn and also among individuals. The footwear is a closed environment, every part of it, i.e. the foot, the sock and the shoe interferes with the others so the whole system should always be considered. Appropriate shoes and lacing system are therefore not sufficient; one should also wear appropriate socks. This will be the matter of this chapter third part. Besides adapted footwear, there are a couple of methods which may prevent blisters to occur.

## 5. Prevention of blisters

Healthy and well hydrated skin can bear more stress before breaking down and is then less likely to develop friction blisters [29]. There are several products which can help reduce friction and shear on the skin and thus prevent blister formation such as lubricants or skin surface drying agents [6, 8]. Rubbing moist skin produces higher frictional forces than rubbing very dry or very wet skin which suggests that reducing sweating, e.g. using antiperspirants, may reduce friction and consequently reduce blisters [15].

Reynolds et al. [16] investigated the influence of an antiperspirant with emollient\* additives on frequency and severity of frictional blisters, hot spots, and irritant dermatitis. The antiperspirant may cause irritant dermatitis; the emollient was thus added to reduce the incidence of this specific skin disorder. They investigated 23 healthy subjects free of lower extremity skin lesions and with no history of hypersensitivity to topical skin products. Their feet were treated with either the antiperspirant (20% aluminium zirconium tetrachlorohydrate glycine concentration plus water) with emollient additives, emollient additives alone (placebo control), or nothing for 4 consecutive days. They were asked to walk on a treadmill for 200 minutes. During the walk, the amount of foot sweat, the number of injuries and the size of blisters were assessed. The subjects were also asked to rate the severity of the blisters and hot spots on a pain scale of 0 to 10. No differences were seen among treatment conditions for sweat accumulation, blister incidence, hot spot formation, or blister severity. However, mean blister size and perceived severity increased with exercise duration. As antiperspirants are proved to decrease sweat rate, the authors thought that the emollients may have affected the antiperspirant's chemical properties and may have also acted as moisturizing agents, increasing friction and macerating the outer epidermis.

Knapik and his colleagues [15] later examined whether an antiperspirant can reduce foot blisters during hiking. They carried out a double-blind study separating into two groups

---

\* emollient: an emollient is a substance which relaxes and softens the skin (*émollient* in French).



cadets attending the United States Military Academy. One group used an antiperspirant (20% aluminium chloride hexahydrate in anhydrous ethyl alcohol), the second group used a placebo preparation (anhydrous ethyl alcohol). Their feet were examined for blisters before and after a 21 km hike. It was observed that the antiperspirant may be efficient to reduce foot blisters during prolonged cross-country hiking if applied at least three times on 3 separate days before a hike. Compared to the placebo group, cadets using the antiperspirant at least 3 nights before the hike had indeed a 56% lower incidence of blisters. The lower incidence of blisters is correlated to the number of participants who reported that their feet did not sweat during the experiment. The results are detailed in tables 1 and 2.

PREPARATION USED	APPLICATION FOR 0 TO 2 DAYS	APPLICATION FOR 3 TO 5 DAYS
Antiperspirant	39%	21%
Placebo	41%	48%

*Table 1: Overall incidence of blisters [15].*

PREPARATION USED	APPLICATION FOR 0 TO 2 DAYS	APPLICATION FOR 3 TO 5 DAYS
Antiperspirant	15%	45%
Placebo	9%	17%

*Table 2: Percentage of participants whose feet did not sweat [15].*

Cadets who used the antiperspirant nevertheless reported significantly more irritation than those using the placebo. The overall incidence of self-reported irritation was 57% in the antiperspirant group and 6% in the placebo group. Knapik et al. suggested that using antiperspirants less concentrated in aluminium chlorohydrate, applying antiperspirants every other or every third night or combining the active ingredients of antiperspirants with a cortisone-based preparation may be methods of reducing skin irritation while preserving the favourable antiperspirant property.

## II. FRICTION AND COMPRESSION OF FABRICS AND SKIN

### 1. Tribology overview

The tribology is the academic discipline which studies the interactions between contacting surfaces [30]. It essentially deals with solid-solid contacts, solid-fluid contacts, friction, wear and lubrication. All domains of activities are concerned by the tribology as contacts contribute to the mechanisms of solid to solid bonds in live systems or in devices.

The first practical aspects of friction have their roots in prehistory [31]. More than 400,000 years ago, our hominid ancestors were making use of friction when they chipped stone tools. By 200,000 B.C., Neanderthals had achieved a clear mastery of friction, generating fire by the rubbing of wood on wood and by the striking of flint stones. The second application showing understanding of friction phenomena, namely the use of lubricants to minimize the work required to transport heavy objects, dates back more than 4000 years. However, the tribology has been recognized for less than fifty years.

Friction forces are opposed to the movement of a solid in contact, in our case, with another solid. The rolling friction is usually lower than the sliding friction; it is the wheel principle. The sliding friction slows down or stops the relative movement of rotation or translation of two bodies in contact.

#### A. Tribological contact

The different actors of a tribological contact are:

- The two contacting bodies which are characterised by their surface roughness, their composition, their mechanical properties etc...
- The interface or third body is constituted of contaminants, lubricants, etc...It can be solid, fluid, introduced on purpose in the contact (lubricant for example) or generated by the contact mechanism (such as abraded particles).
- The environment (temperature, relative humidity, etc...).

- The mechanical system which includes the applied normal load, the velocity, the contact geometry, etc...

The contact geometry is the general shape of the bodies' surfaces around the contact area. There are three main contact geometries:

- Point-shaped contacts (typically ball on a flat surface).
- Linear contact (cylinder on a flat surface).
- Surfaced contact (parallelepiped on a flat surface).

The friction forces depend on:

- The tribological system on a macroscopic scale.
- The deformation mechanisms of the two contacting bodies at the surfaces asperities (mesoscopic scale).
- The adhesion mechanisms between the two bodies at the atomic or molecular scale.

Lubrication aims to reduce friction i.e. to increase sliding or reduce wear and heat generation or both at the same time. It consists in generating a free-motion thin (from 0.1 and 100  $\mu\text{m}$  thick) film between the two contacting surfaces. This thin film can be a gas, a liquid or a solid film and should have the lowest possible shear resistance; it will separate the two surfaces and make the movement easier. The choice of the lubricant depends on its role in the system. Wear is characterised by material dislocation. It can be adhesive, abrasive, corrosive or with fatigue and does not necessarily follow the friction evolution. Adhesion is characterised by the creation of interfacial bonds between the contacting surfaces. Abrasion is due to the action of hard particles which tear off material from the contacting surfaces. When two materials are in contact, deformations i.e. modifications of shape and/or dimensions may occur.

There are three different types of deformations:

- Purely elastic deformations which occur immediately under stress and disappear immediately and completely when the stress stops. These are reversible deformations.
- Plastic deformations which are irreversible.

- Viscoelastic deformations which disappear in part or totally when the stress stops acting. Two stages are distinguished: a part of the deformation clears immediately (elastic effect) and the other part wears off with time (viscous effect).

## B. Laws of friction

### a. Laws of Amontons

The first recorded systematic study in the field of tribology is due to Leonardo da Vinci (1452-1519) who, in the XV<sup>th</sup> century, measured the force of friction between objects on both horizontal and inclined surfaces. Cords attached to the object to be moved were allowed to pass over fixed rollers or pulleys to weights which gave a measure of the resisting force. Leonardo da Vinci also studied the influence of the apparent contact area upon friction resistance. He wrote: “the friction made by the same weight will be of equal resistance at the beginning of its movement although the contact may be of different breadth and length” [32] and “friction produces double the amount of effort if the weight is doubled” but the first laws of friction were attributed to Amontons (cf. figure 3):

- First law: the friction force is independent of the contact area.
- Second law: the friction force is proportional to the applied normal load (weight). The friction can therefore be expressed as  $F = \mu \times W$  where  $F$  is the tangential friction force in Newton,  $W$  the normal load in Newton and  $\mu$  the friction coefficient (without dimension).  $\mu$  depends on the materials in contact.
- Third law: the friction force is independent of the sliding velocity.

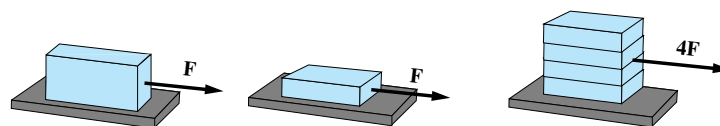
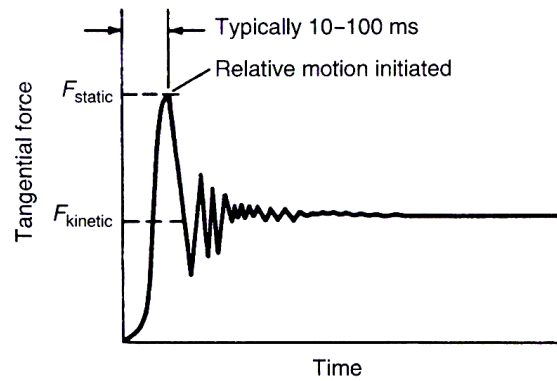


Figure 3: Amontons' laws of friction (1699).

### b. Laws of Coulomb

In 1782, Coulomb rounded out Amontons second law introducing the concept of static and dynamic friction (cf. figure 4). The static friction force is the force required to initiate motion while the dynamic or kinetic friction force is the force required to sustain motion. Static friction is usually higher than dynamic friction.



*Figure 4: Static and dynamic friction forces.*

Coulomb observed that the kinetic friction is almost independent of the sliding velocity and this is sometimes referred to as the third law of friction. He also considered the possibility that friction arises from adhesion between the surfaces in contact but abandoned this theory when he observed that the friction was independent of the area of the bodies. He then suggested that friction arises from the asperities present on the surfaces, the frictional energy expended in sliding representing the work necessary to lift one surface over the asperities of the other [33].

In many cases, the laws of Amontons and Coulomb are not verified. Nevertheless, the coefficients of friction of several materials can be compared provided that they were measured in the same conditions.

### *c. Bowden and Tabor approach*

The current theory of basic friction mechanisms was proposed in 1950 by Bowden and Tabor. According to this theory, two mechanisms permit to physically explain friction laws; adhesion and deformation. These two phenomena are related to the notion of real contact area.

When two surfaces are in contact, high local stresses and possible increase in surface

temperatures lead to bonds generation. Macroscopic bodies always have rough surfaces, at least on a microscopic level. When two solid materials are placed in contact, some regions on their surfaces will be so close together that the surface atoms of one material “touch” the surface atoms of the other material, while in other regions, the surface atoms are separated by large distances (around 1 μm). The regions of contact are referred to as junctions (cf. figure 5). The real contact area is the sum of the junctions’ areas. The real contact area is commonly a lot lower than the apparent contact area. Real contact area depends on:

- Surfaces roughness: the rougher the surfaces, the lower the real contact area.
- Material properties: the higher the hardness, the lower the real contact area.
- Normal load: when the normal load increases, the contact areas are deformed and new junctions are created.
- The scale which is considered.

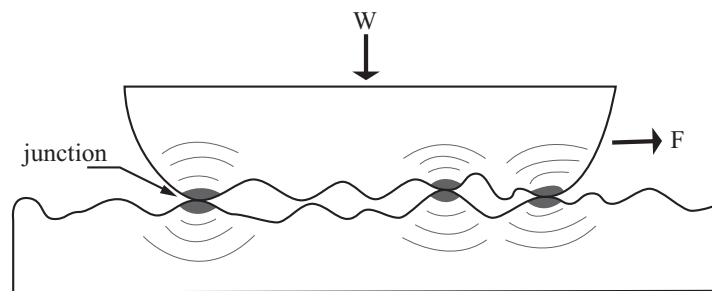


*Figure 5: Contact between two solids; junctions.*

The junctions are formed by adhesive contact. The adhesion between the contacting bodies results from atomic, chemical or physical attractions at the junctions. The adhesion force is the normal force  $F_a$  which is necessary to separate the two bodies by shearing under a given normal load  $W$ . The adhesion coefficient is thus  $\mu_a = \frac{F_a}{W}$ . The adhesion force depends on the two materials in contact and on the real contact area. It may be increased with a prolonged contact as the number and the surface area of the junctions may get higher with the time of contact thus increasing the real contact area (by creep). Moreover, the adhesion force is all the more important that the two contacting bodies are close together and usually gets higher linearly with normal force.

During friction, a displacement of material to the side and to the front of the contact or even a removal of material can occur. The deformation force depends on the volume of material that has been displaced. If the contacting bodies have different hardness, the hardest body creates an imprint on the softest. Two actions are then combined; junctions are sheared and materials are removed from the softest body.

To resume, if the interaction between adhesion and deformation is supposed negligible, the friction force between two bodies in contact can be written as:  $F = F_a + F_d$  with  $F_a$ : adhesion force and  $F_d$ : deformation force. This approach is adapted to viscous materials, but in this case, the deformation force will also depend on the speed of deformation.

## 2. Friction behaviour of textiles

Studies conducted during the latter half of the twentieth century, on natural and synthetic fibres, have shown that the coefficient of friction is not a material property, but is a function of the normal force and the geometric area of contact [34]. An increase in normal force causes a decrease in the coefficient of friction. The size of the fibre, the smoothness of the surface and the mode of contact (point, line or area) also affect the value of the coefficient of friction. In the classical materials like metals, frictional force  $F$  is directly proportional to the normal force  $W$ . However, a non-linear relation occurs with most polymeric materials.

Aliouche [35] investigated the friction of woven textiles and observed that the coefficient of friction  $\mu$  began to decrease sharply when the normal load increased from 0 to a positive value then the coefficient of friction still got lower but slowly and became roughly constant for high normal loads. He explained the stabilization of the value of the coefficient of friction by the integration of the hairiness in the volume of the woven fabric. At high normal loads, the distribution of loads on the contact surface is thought to be more homogeneous and the number of points of contact to be maximal.

### A. Effect of load on the friction of fibres

It seems satisfactory to use a simple relationship like:  $F = KW^n$  where  $K$  and  $n$  are empirical constants whose values are found by fitting the data on the model and conducting a least square analysis [34, 36],  $n$  is less than unity. All workers in the field of fibre friction who adopt this relationship have assumed firstly that friction arises from adhesion at the points of

real contact and secondly that the junctions at the interface have a constant shear strength  $s$ . Therefore, they have all explained the variation of  $F$  with  $W$  in terms of the variation of the true area of contact  $A$  with  $W$  [33]. If  $s$  is a constant, it follows from the previous equation that  $A = k_1 W^n$  where  $n$  has the same value as in the previous equation. Lincoln (1952) examined the friction between a sphere and a flat nylon surface at low loads and found that  $F$  varied as  $W^{\frac{2}{3}}$ . He then measured the geometrical area of contact between a nylon sphere and a glass flat by optical interference methods and found that the area of the circle of contact varied as  $W^{\frac{2}{3}}$ . Howell and Mazur (1953) investigated the friction between crossed fibres at right angles and found a relationship of the form  $F = kW^n$  where  $n$  was 0.8 for drawn nylon, 0.9 for undrawn nylon and 0.96 for cellulose acetate. In 1951, Finch studied the imprint formed by curved cylinders of nylon on a glass flat and found the area of the imprint to be proportional to  $W^{0.89}$ . This appears to be in excellent agreement with the frictional dependence on  $W$ . However, Howell and Mazur used an optical interference method similar to that used by Lincoln and obtained a different result. They wound the fibre round a cylindrical rod and pressed the curved fibre against an optical flat. The optical area was observed and often had very irregular boundaries, varied from fibre to fibre, and was time-dependent. Under standard loading conditions of 15 seconds, they found that for practically all the fibres examined the optical area varied as  $W^{0.73}$ . In addition, they observed that a fibre bent over a rod of larger diameter gave a larger optical area for a given load. This is in agreement with the type of behaviour to be expected for elastic deformation. Howell pointed out that these optical measurements of the area of contact have marked limitations. First, the exact location of the boundary of the ellipse or circle of contact is uncertain. Secondly, the optical area of contact is the same as the true area of contact only if the surfaces are smooth. With surfaces covered with asperities the real or true area of contact will always be smaller than the optical area. The recognition of this difficulty has led to the development of a number of models showing how the true area of contact may be expected to vary with load.

## **B. Variation of the area of contact with load**

Archard (1951) considered a surface covered with asperities of spherical shape [33]. The two extreme types of deformation are purely plastic and purely elastic. For purely plastic



deformation the area of contact is directly proportional to the load. For purely elastic deformation the area of contact of each asperity is proportional to  $W^{\frac{2}{3}}$ . Two possible ways in which elastic deformation can take place were foreseen:

- Contact occurs over a fixed number of asperities and the effect of increasing the load is simply to increase the elastic deformation of each asperity. In this case the area of real contact is proportional to  $W^{\frac{2}{3}}$  (smooth contact).
- Contact occurs over a large number of asperities, the average area of each deformed asperity being constant. Increasing the load in this case increases the number of regions of contact and the area of real contact is directly proportional to  $W$  (rough contact).

With real surfaces an intermediate behaviour may be expected. Consequently, for pure elastic deformation, the true area of contact will be proportional to  $W^n$  where  $n$  lies between  $2/3$  and  $1$ . If this is the only parameter affecting the friction, the friction will also follow a similar relationship.

### **C. Case of high normal stresses**

At high normal stresses, a textile will have significant plastic deformation. A plausible model for characterizing the behaviour in this region may be  $F = \alpha W + KW^n$  where  $\alpha$  is an additional empirical constant [33]. Using the classical definition of the coefficient of friction,  $\mu = \alpha + KW^{n-1}$ . This model, initially proposed by Gralen for applying to fibre friction in general, was used by Briscoe for characterizing friction in ballistic textiles. Under the ballistic levels of stresses, the material is expected to lose its elastic recovery properties and be mostly deformed plastically. The second term of the model will then be small and friction will largely be given by the first term.

### **D. Effect of fibre cross-section shape**

El-Mogahzy and Gupta [34] investigated the effects of structural and morphological factors on the friction of fibrous materials. They measured the friction of monofilaments of polypropylene of three different cross-sectional shapes namely circular, triangular and

trilobal. In both the line and the point contact tests, the circular fibre gave a significantly higher value of  $\mu$  than did the triangular or the trilobal materials, the average difference being about 31%. The values of  $K$  and  $n$  for the circular fibres were also higher by 28% and 3.6% respectively than the corresponding average values for the non-circular materials. It was visualized that the trilobal and triangular fibres were transversely stiffer and thus less deformable than the circular.

### **E. Effect of yarn sett and hairiness**

Ajayi [37] investigated the influence of yarn sett and surface hairiness on the friction of woven fabrics. He found that the frictional resistance to motion of these fabrics increases with the yarn sett and for the case of pile-type fabrics with the height of fibre tufts.

### **F. Other factors affecting friction**

Some other factors that affect friction are the mode of contact (line, point or area) during tests, the morphology of the surfaces (degree of roughness or smoothness), the testing environment (temperature, and relative humidity), and the time of contact (time before sliding and speed of sliding) [34]. The mode of contact used will affect the number of points of contact ( $m$ ) and through it the values of  $K$ ,  $A$ ,  $F$  and  $\mu$ . One would generally expect that the larger the area the larger would be the value of  $\mu$ . Differences in surface morphology can affect friction as a rougher surface, with fewer contacts per unit area, would mean a smaller value of  $m$  and therefore should result in lower friction. Finally, since fibres are viscoelastic materials, their properties can change with the time of loading. It is expected that the contact area will increase as the sliding speed is decreased thus leading to an increase in the coefficient of friction [36].

## **3. Frictional properties of human skin**

### **A. Influence of the applied load on skin friction**

Amontons' law stipulating the non-variance of the coefficient of friction with load does not apply to the skin [38, 39]. Sivamani et al. [38] found that  $\mu$  is proportional to  $W^{-0.32}$  where  $W$  is the applied normal load. Koudine et al. [39] found that the coefficient of friction  $\mu$

was proportional to  $W^{-0.28}$ . These results are very similar to the theoretical relationship deduced by Wolfram [40] from the Hertz theory:

$$\mu \propto S \left( \frac{K}{E} \right)^{2/3} W^{-1/3}$$
 where E is the Young's modulus of skin, K is a term including

average dimension of adhesive contacts, their number, and frequency per unit area, and S is the shear strength of the adhesive contacts.

These three studies showed that the friction force on the skin is proportional to  $W^{\frac{2}{3}}$ .

## B. Influence of skin humidity

Friction properties of human skin depend on the skin texture, suppleness and hydration. The stratum corneum can absorb up to 8 times its weight in water [2]. The stratum corneum hydration degree is a very important parameter. When the stratum corneum is dry, it is brittle and less resistant but when it is highly hydrated, it becomes delicate. The brittle-to-ductile transition for skin has been reported to occur at 70% RH [41]. The stiffness and coefficient of friction of the stratum corneum increase with humidity whereas an extreme dryness and wetness will tend to decrease skin friction [6, 21]. Numerous studies investigated the evolution of the coefficient of friction of skin in contact with textiles in function of skin humidity [32, 38, 41-46]. They all reported an increase of the coefficient of friction with higher skin humidity.

In a recent study, Gerhardt et al. [42] systematically varied the hydration state of skin of the volar forearm in 22 subjects and found a highly positive linear correlation between skin moisture and friction coefficients against textiles. They found that the evolution of skin friction with moisture is gender influenced; the friction of female skin showed significantly higher moisture sensitivity. Coefficients of friction increased typically by 43% in women and by 26% in men when skin hydration varied from very dry to normally moist skin.

A study on the effects of wearing diapers on skin was carried out by Zimmerer et al. [43]. They observed that skin wetness was proportional to diaper wetness and that with increased skin wetness, there were increased coefficients of friction and increased abrasion damage.

Gwosdow et al. [44] pulled fabrics across skin in different humid conditions from neutral to hot-dry and hot-humid. For them, greater humidity involves greater degree of hydration of the stratum corneum which may lead to a better adhesion between skin and fabrics. Greater adhesion could result in a higher fabric to skin contact area thus explaining the increase of friction coefficient and friction force. Herring [29] proposed the same explanation stating that skin moisture increases friction, torque and shearing forces by increasing the adhesion of the skin to the sock.

Kenins [41] showed that fibre type and moisture influenced fabric-to-skin friction. Moreover, it could be concluded that moisture on the skin was more important than fibre type or fabric construction in determining the intensity and nature of fabric-to-skin friction and also that glabrous skin friction is less affected by moisture than hairy skin.

Nacht et al. [45] investigated the changes in skin friction coefficient induced by skin hydration and emollient application. They observed that when a drop of water is put on the skin, the coefficient of friction immediately increases sharply and then decreases rapidly to its initial value. They explained this phenomenon by the absorption of water in the stratum corneum thus increasing the contact area between the probe and the skin and leading to an increase in friction coefficient. As water is lost through evaporation, the stratum corneum returns to its original state and the friction coefficient decreases to its baseline value.

### **C. Influence of anatomical site and age**

In 1990, Elsner, Wilhelm and Maibach [47] studied the frictional properties of human skin in two localised areas: the forearm and the vulva. 44 healthy female volunteers participated to this study whereby the dynamic friction coefficient between skin and a teflon probe was measured. Elsner et al were looking for correlations between the dynamic friction coefficient and particular parameters which could influence skin properties: age, body weight, height, transepidermal water loss, and skin capacitance. They found a higher coefficient of friction for vulvar skin ( $0.66 \pm 0.03$ ) than for forearm skin ( $0.48 \pm 0.01$ ) which can be explained by the important hydration of vulvar skin compared to forearm skin. Age seems to influence transepidermal water loss and friction coefficient in forearm but not in vulvar skin.

Cua, Wilhelm and Maibach [48] also measured the dynamic friction coefficient of skin and the skin lipid content in 11 different anatomical regions: the forehead, the upper arm, the volar and dorsal forearm, the post auricular, the palm, the abdomen, the upper and lower back, the thigh and the ankle of 29 volunteers of different age and gender. They found no particular difference in dynamic friction coefficient when varying age and sex group, but dynamic friction coefficient does vary significantly depending on the anatomical site.

Zhang and Mak [49] measured the coefficient of friction of skin in contact with several materials over six anatomical regions, namely the dorsum of the hand, the palm of the hand, the anterior side of the forearm, the posterior side of the forearm, the anterior leg and the posterior leg. The highest coefficient of friction was measured at the palms of the hand.

Gerhardt et al. [50] studied skin-textile friction and skin elasticity in young and aged people. They confirmed that skin elasticity is lower in elderly persons. For seniors, more pronounced skin tissue displacements also occurred and greater shear forces took place during frictional contact. These observations showed that deformation plays an important role in the friction of aged skin.

#### **4. Fabric to skin friction measurements**

##### **A. Fabric friction measurement methods**

The measurement methods of friction behaviour of fabrics are based on a signal treatment in temporal domain by a statistical analysis of the friction force, on the difference between static and dynamic friction or either on the analysis of the coefficient of friction variation in function of the applied normal load [36, 51]. The classical measures can be unidirectional or multidirectional. The unidirectional method the most commonly used consists in fixing the fabric on a horizontal support. A probe connected to a force sensor is then rubbed on the fabric. A statistical treatment of the temporal signal is realised whereby a mean friction coefficient can be calculated. This is the principle of the friction and roughness module of the Kawabata's Evaluation System (KES; a range of measurements devices

developed by Kawabata and the Hand Evaluation and Standardization Committee and commercialised by Kato Tech Co., Ltd) [52].

A multidirectional tribometer was developed by Bueno [51] because the KES friction and roughness module was found not sufficiently sensible to characterise the effects of finishing treatments. This device combines two characteristics; a study of the fabric in all the directions of its surface and the use of the periodical character of a fabric surface which is harnessed using a signal treatment in the frequency domain. Its use is thus limited [53]:

- The textile fabric tested should have a periodical surface with a small period.
- This tribometer is based on the “frequential signature” of a textile fabric; it consists in computing the Fourier transform of the temporal signal of the fabric during rubbing. The autospectrum obtained shows one or several frequency peak(s). The peak(s) height characterizes the fabric state with great sensitivity. This tribometer thus quantifies a modification of the surface but can hardly compare different fabrics.

Another multidirectional device was therefore developed, using a new probe. This apparatus consists in a very thin steel plate (50 to 75 mm long, 10 to 30 mm wide and 30 to 50  $\mu\text{m}$  thick) which is excited in vibration by the rotating textile fabric. The steel plate is prestressed before a measure i.e. bent on the textile surface. The vibration of the plate is measured with strain measurement gauges. The steel plate has natural frequencies which are independent of the rubbed textile surface. The energy of each mode of vibration is analysed in order to characterize the textile surface whatever structure it has [54, 55].

## **B. Fabric to skin friction devices**

Fabric to skin friction was usually assessed by using panels of volunteers. It generally consisted in slowly pulling fabric samples across the surface of a subject’s skin. The pressure between fabric and skin was often applied by suspending a weight to the free end of the fabric and the frictional force required to pull each fabric across the skin was recorded by a force transducer [6, 44].

Friction between hand and object or between skin and textiles can also be analysed by rubbing the skin against objects and surface samples attached to a multi-axial force plate or a force transducer. Normal and friction forces are thus recorded whereby friction coefficients can be calculated [56].

An alternative approach consists in using a tribometer whereby probes made of different materials can be slid over the skin of subjects [46].

### **C. Investigations on friction blisters**

Studies on friction blister formation and prevention are usually performed by recording the prevalence and size of blisters among a group of subjects which either have routinely heavy load of activities, such as athletes or military personals or are asked to perform specific trials [8, 15, 16].

A device was designed in the late 1960s and early 1970s in order to produce friction blisters on human skin [6]. The rubbing head of this apparatus could be moved over the surface of any chosen skin site at a selected stroking rate under a chosen load. Various materials, including textiles, could be attached to the rubbing head. Frictional coefficient and temperature could be recorded. It was observed that the rubbing head geometry, weight and attached material all affect the friction coefficient measurements. The effect of skin moisture was also studied and it was shown that a dry skin reduced the friction, while a moist skin increased the friction [6, 14, 32].

### **D. Skin models**

Fabric-to-skin friction was often assessed by measurements on voluntary subjects' skin but the appearance of skin models is providing new possibilities to scientists who study human skin. To model fabric-to-skin friction and compare this model to experiments, the best is to use a skin model rubbing on the fabric as it will present a very low variability in frictional properties. Skin models have indeed the advantage to be reproducible compared to human skin and enable scientists to use classical friction measurement devices to assess fabric to skin friction.

Derler et al. [57] investigated the friction of untreated human finger skin against a reference textile with 12 subjects using a force plate. Fabric samples were attached to a dynamometer and rubbed by the participants with the index finger. The sliding movements of the finger ranged from 5 to 10 cm and were parallel to the longitudinal axis of the force plate. The stroke frequencies were  $1 \pm 0.3$  Hz and the contact areas between finger and fabric were between 1.5 and 3 cm<sup>2</sup>. For roughness assessments, the subjects used normal loads of

$1.5 \pm 0.7$  N which resulted in typical contact pressures between 3 and 10 kPa. The results for the human skin were compared with friction measurements of different silicone and polyurethane materials as mechanical skin equivalents. A polyurethane coated polyamide fleece with a surface structure similar to that of skin; Lorica®, showed the best correspondence with human skin under dry conditions. The artificial leather Lorica® Soft is also used for testing the slip resistance of floor coverings in barefoot areas.

## 5. Plantar pressure measurements

Plantar pressure is the distribution of force over the foot sole. Early investigations of foot pressure patterns were obtained from the imprint in soft materials [58, 59]. These methods gave qualitative results as they only recorded the shape of the foot and the deepest impressions in the surface. The first quantitative measurements of foot pressure were carried out using an air filled chamber by Carlet and Marey respectively in 1872 and 1873. Arrays of deformable materials which left an ink print or were recorded by optical methods were later developed.

Nowadays, a wide variety of plantar pressure measurement systems are available which rely on electromechanical sensors. Pressure sensors are force transducers whereby the force exerted on a known surface can be measured. Pressure is then calculated dividing force by area. Electromechanical transducers usually convert a mechanical stress into an electrical signal which can be recorded and stored for later analysis.

The characteristics of the pressure measurement apparatus should be adapted to the research subject. For example, a higher spatial resolution is needed to measure children's feet pressure than adults' feet pressure because a child's foot is smaller than an adult's foot. To measure pressure on small anatomical structures, one should not use a too large sensor as it will underestimate the real pressure due to the lower pressures around the structure. There are different sensor principles such as resistive or capacitive methods and different measurement devices i.e. insoles or single transducer systems. All the sensors detailed below [58] measure the normal component of the ground reaction but neglect shear forces.

### A. Measurement devices

In-shoe systems are used to record the pressure at the foot-shoe interface. Multiple steps can be recorded and easily averaged and analysed provided that the orientation of the



foot remains the same with respect to the sensor. Some systems include a portable data logger which allows field measurements.

Matrix devices are a succession of rows or columns of sensors whereby the whole plantar surface of the foot can be covered by an active sensor area.

Sole systems are composed of sensitive elements placed at selected anatomical sites on the sole. They offer faster sampling rates as less data has to be processed.

## **B. Plantar pressure in normal foot**

Many parameters may affect foot pressure. These include shoe construction, foot shape, age, gender, body mass and gait velocity. Body mass does not seem to influence plantar pressure as much as one would expect. A low correlation was found between these two parameters and only under the lateral midfoot and the third metatarsal head [58]. This correlation was more pronounced in female subjects than in men. The whole plantar pressure increases linearly with higher gait velocity but the same behaviour is not observed in all the anatomical areas. The pressure at the heel and under the medial forefoot follows the whole plantar pressure evolution while under the midfoot and the lateral forefoot the pressure decreases with increasing speed [58].

Many studies investigated plantar pressure distributions, but either these investigations were carried out on abnormal feet such as diabetic feet or the subjects were walking or jogging barefoot [23, 60-65]. One can assume that abnormal feet may feel higher pressure than normal feet and that in-shoe pressure may be lower than barefoot pressure but it depends on the area of the foot and the footwear. It is thus difficult to estimate the pressure exerted on normal feet during jogging with adapted footwear. However, the analysis of the running gait and the structure of the foot indicate which foot areas suffer from higher pressures. Gait analysis of running is indeed well-known: first the heel contacts the ground, then the others structures of the foot are used from the heel to the toes and finally propulsion is given with the forefoot. The heel and the forefoot are thus subjected to higher pressure than other elements of the foot. Moreover, the structure of the foot shows bone prominences which also experience high pressures e.g. the metatarsal and hallux [59, 66].

## 6. Fabric compression measurements

A fabric is not an elastic solid; it presents a hysteresis during a compression - decompression test. To test the dynamic compression of a fabric, one can either use the compression module of KES-F or an extensometer.

Peirce [67] studied compression test curves which provide the thickness of a fabric in function of the applied pressure. He interpreted them as exponentials of which shape depends on the fabric. Three different phases can be distinguished on these curves (cf. figure 6). The first phase corresponds to the fabric surface hairiness squashing. The hairier the fabric, the slower the reduction of thickness with increasing pressure. The second stage refers to the compression of the fabric structure; the way yarns are organized may be slightly changed. Once the air trapped in the fabric has been released, the fibres are finally deformed. The curve asymptote corresponds to the material maximum deformation.

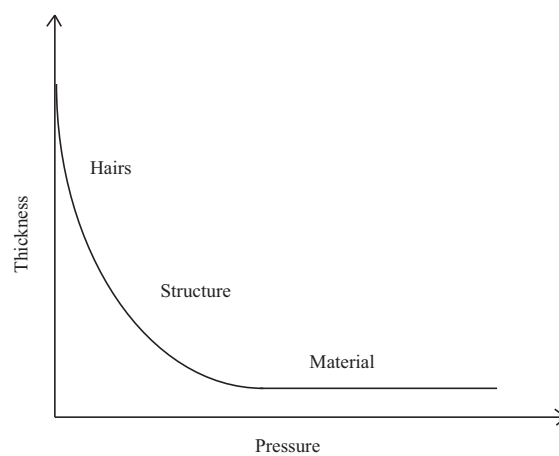


*Figure 6: Pierce curve.*

Kawabata compression module KES-FB3 (cf. figure 7) is composed of a circular presser foot of 2 cm<sup>2</sup>. When the driving motor switch is turned on, the plunger starts to descend and compress the sample. When the compressional force reaches the preset upper-limit force, the motor automatically turns to a recovery process. The compression - decompression cycle is completed at a constant rate of compressional

deformation ( $0.02 \text{ mm.s}^{-1}$  in standard mode,  $0.007 \text{ mm.s}^{-1}$ , and  $0.2 \text{ mm.s}^{-1}$  if changing gear system). The displacement of the plunger is detected by a potentiometer. The compressional force transducer is a steel ring with a linear differential transformer. There are two relevant pressures regarding the analysis of the compression results;  $P_0$  which equals 50 Pa and the maximum pressure  $P_m$  which equals 5 kPa in standard mode.

The following parameters are obtained (cf. figure 8):

- $T_0$ : thickness under  $P_0$ , in mm
- $T_m$ : thickness under  $P_m$ , in mm
- EMC: compressibility  $EMC(\%) = 100 \times \frac{T_0 - T_m}{T_0}$
- WC: compression work  $WC = \int_{x=T_0}^{x=T_m} P \times dx$  where P is the increasing pressure in cN.cm/cm<sup>2</sup>
- LC: compression linearity  $LC = \frac{WC}{\frac{1}{2} \times (T_0 - T_m) \times P_m}$  without unit

It is the compression work of the fabric related to the compression work of an elastic solid with same initial and final thicknesses i.e. divided by the area of the triangle formed by the dotted lines on figure 8.

- RC: resilience or restored energy rate  $RC(\%) = 100 \times \frac{WC'}{WC}$  where WC' is the recovery work  $WC' = \int_{x=T_0}^{x=T_m} P' \times dx$  where P' is the decreasing pressure

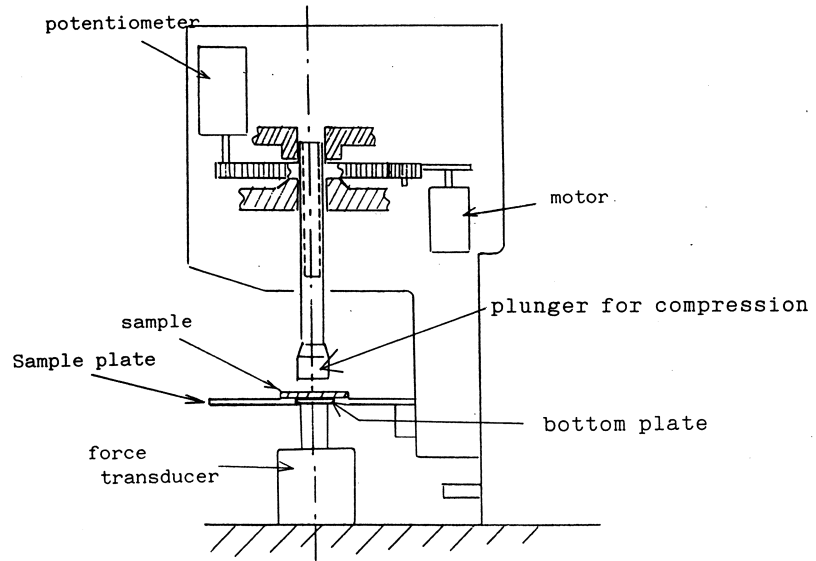


Figure 7: Schematic illustration of Kawabata's compression tester.

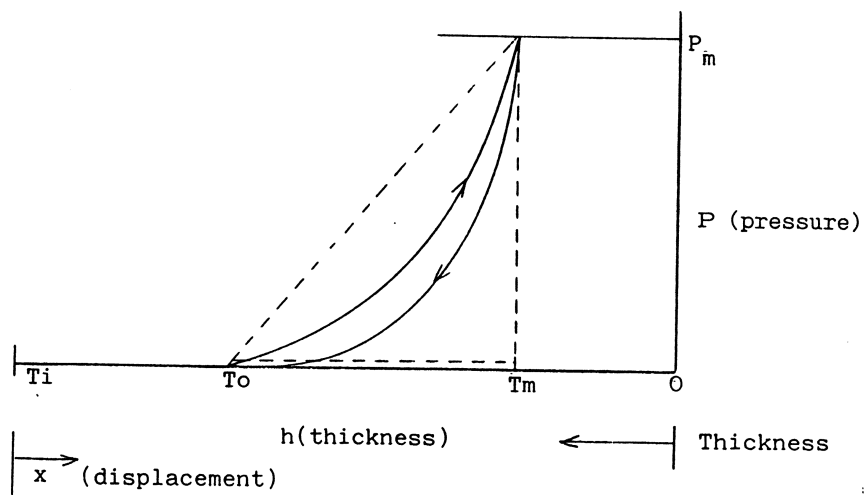


Figure 8: An example of pressure thickness curve.

### III. SOCKS TECHNOLOGY

#### 1. Textile overview\*

##### A. Fibres

Fibres and filaments<sup>§</sup> are the basic elements of textile. Their length is a lot higher than their transversal dimensions, they are therefore very flexible. Fibres lengths can be up to a few centimetres while filaments have lengths of hundreds of meters, even several kilometres. Filaments are obtained spinning<sup>§</sup> either artificial materials such as viscose<sup>§</sup> or acetate<sup>§</sup>, or synthetic materials i.e. polyamide<sup>§</sup>, polyester<sup>§</sup>, acrylic<sup>§</sup>, polyurethane<sup>§</sup>. Silk is a natural filament which length is comprised between 400 m and 1 km. Textile fibres can have a natural origin such as wool, silk, cotton, linen or come from cut or cracked filaments.

The length and the fineness of fibres are two major parameters. The fineness of a fibre can be characterised by its diameter if it has a round cross section or by its count<sup>§</sup> i.e. its mass per unit length. The count is usually given in Tex ( $1 \text{ Tex} = 10^{-3} \text{g.m}^{-1}$ ). Fibres and filaments correspond to the microscopic scale of textiles (from 1  $\mu\text{m}$  to 0.1 mm).

##### B. Yarns

Spinning is the process whereby yarns<sup>§</sup> can be obtained from fibres or filaments. Fibres must be cleaned, individualised and parallelised before being spun. The combing process is a stage whereby the shortest fibres can be eliminated thus giving a better regularity and resistance to the yarn. Yarn cohesion is usually obtained by twisting it but some yarns are obtained by friction spinning.

Yarn twist is characterised by its direction (S if fibres are oriented like follows: \, and Z if they are oriented in the opposite direction: /, cf. figure 9) and its value in turns per meter. Yarn fineness is given in Tex. Yarns correspond to the mesoscopic scale of textiles (from 0.1 to 1 mm).

---

\* The information given in this section is drawn from my courses on textile metrology (taught by Jean-François Le Magnen), spinning (given by Marc Renner and Artan Sinoiméri), and knitting (taught by Marie-Ange Bueno) during my textile engineering education at the École Nationale Supérieure des Industries Textiles de Mulhouse.

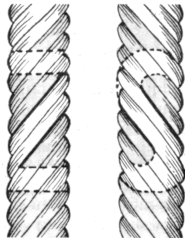


*Figure 9: Z and S yarn twist direction.*

### **C. Knitted Fabrics**

A fabric is a textile surface obtained from yarns, fibres or filaments. The most common textile fabrics are knitted fabrics, woven fabrics and nonwovens.

Knitting<sup>s</sup> is the process whereby knitted fabrics are obtained. It consists in interlacing one or several yarns to form stitches<sup>s</sup>. The kind of knit is the loops interlacing basic pattern. In addition to the kind of knit, a knitted fabric is characterised by the yarns used to knit it, and its stitch length. There are two different knitting methods: weft and warp knitting (cf. figures 10 and 11).

In a weft knitted fabric, a single yarn forms successive courses of stitches; it is the principle of hand knitting. In a warp knitted fabric, several yarns are knitted at the same time and the stitches formed with the same yarn are in different courses. The thickness of a knitted fabric depends, among others, on the yarn twist. The higher the twist, the thicker the knitted fabric [53].

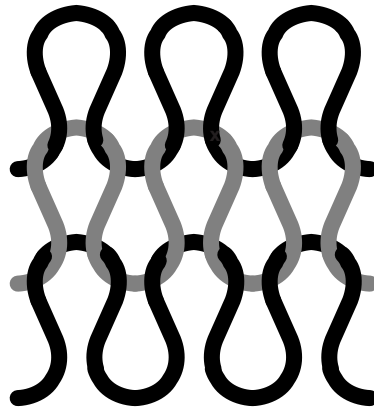


*Figure 10: Example of weft knitted fabric; simple jersey. A course<sup>s</sup> of stitches is coloured in grey. This knitted structure is realised with a single yarn.*



*Figure 11: example of warp knitted fabric; 1 and 1 lapping structure.*

Fabrics correspond to the macroscopic scale of textiles (from 1 mm to 1 m). They are flexible, deformable and viscoelastic materials. Fabrics behaviour depends on the three scales that have been described. Fibres, yarns and fabric structure contribute to fabric mechanical properties.

## 2. Common knitted structures for sport socks

Knitted fabrics are composed of curved yarns to form interlaced loops [68]. With regard to the method of using the yarn, there are two knitting principles, warp knitting and

weft knitting. Socks are weft knitted fabrics. In weft knitted fabrics, a single yarn is used to knit the fabric. This yarn travels horizontally to make a succession of loops. To form a loop in a weft knitted fabric, each needle is inserted through each one of the original loops and thus draws a yarn through the original loop to form a loop on the next course. The newly formed loop takes the place of the original loop on the needle and remains there until the needle pulls the next yarn through it [69].

There are two widely used weft knitted structures for socks products; simple and terry jersey. These two kinds of knit are detailed and illustrated below.

### **A. Simple jersey**

In simple jersey, all the stitches are identical; they are straight loops. The two faces are very different. The face<sup>§</sup> shows tightened wales<sup>§</sup> of V which fit together. On the back<sup>§</sup>, one can see successive and parallel waves (cf. figure 12). It is the weft knitted fabric the most widely used in clothing (tee-shirt, pull-over, socks, stockings, etc...) and also in technical textiles applications (coating support, composites reinforcements ...).

This kind of knit is produced with a single needle bed<sup>§</sup> knitting machine. Figure 13 shows the parts of the knitting machine which are involved in the loop formation. The needle (1) is mobile in the vertical groove of the cylinder (2) via the action of the cams (3). It is kept in place by the spring which is all around the cylinder (4). The sinkers<sup>§</sup> (5) move horizontally and slide in the grooves of the sinker ring (6) and in the grooves of the upper part of the cylinder (9). They slide in a cam track (7) whereby they can be moved forward and back. The different parts of a sinker and of a latch needle<sup>§</sup> are respectively detailed in figures 14 and 15. The yarn guides (8) are fixed on the cam track. The needles and the sinker ring rotate whereas the cams and the yarn guides are immobile. The jersey loop formation is illustrated in figure 16.



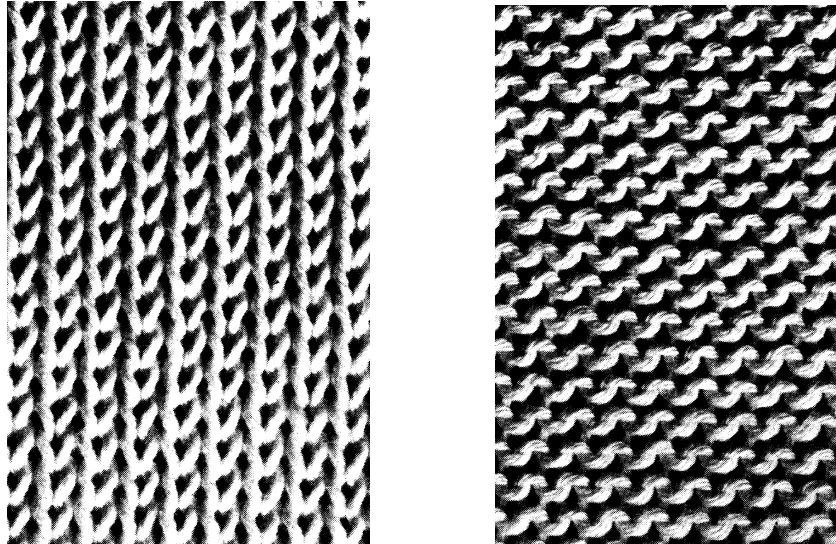


*Figure 12: Face (left) and back (right) of a simple jersey fabric.*

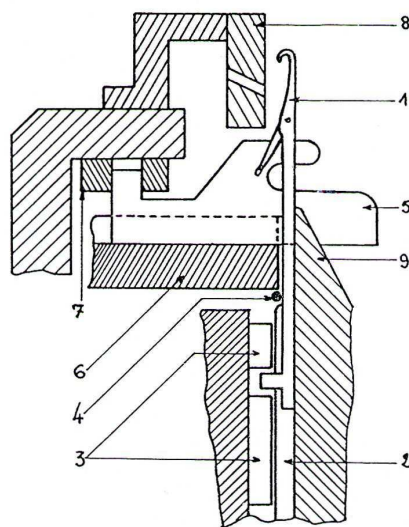


*Figure 13: Parts of the knitting machine involved in the jersey loop formation. The knitted fabric is inside the machine (on the right hand side). The needle hooks are turned towards the outside of the knitting machine.*

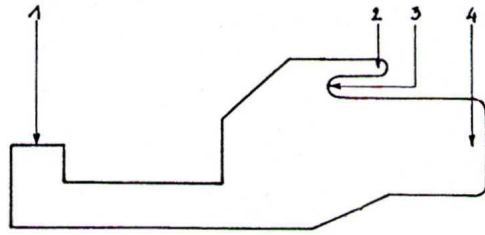


Figure 14: The different parts of a sinker; 1) the butt, 2) the nose, 3) the throat, 4) the body. The body behaves as a casting-off device and the nose prevents the knitted fabric from moving up.

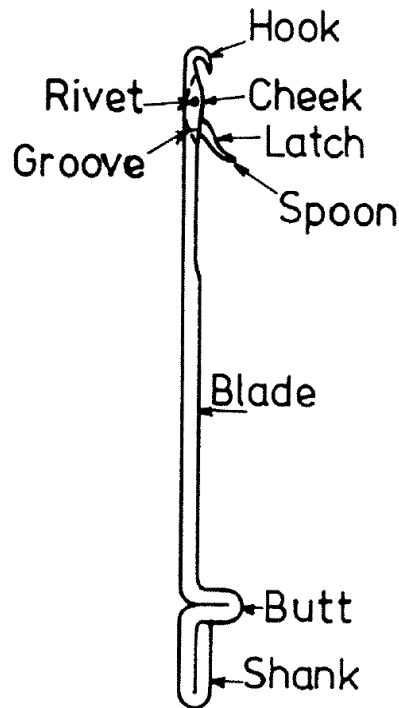


Figure 15: The different parts of a latch needle [70].

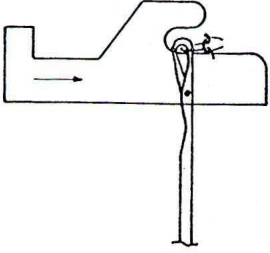
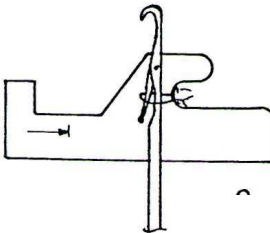
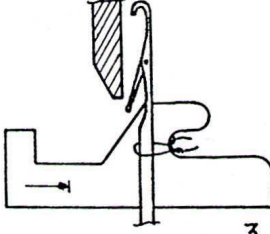
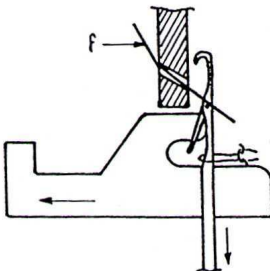
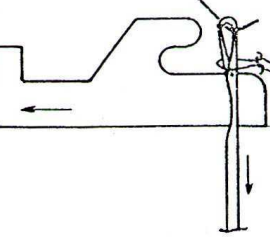
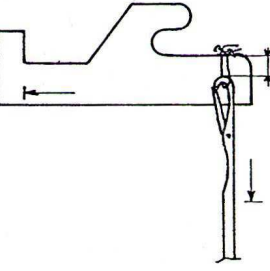
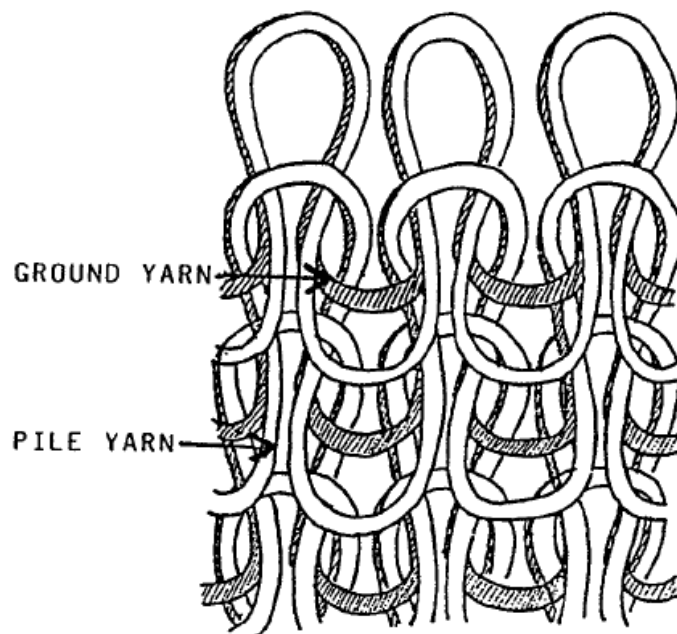
	<p>The needle has just moved up from its casting-off position<sup>s</sup>. Sinkers are moving towards the knitting machine centre. The throat and the nose of the sinkers will therefore keep the fabric in place while the needles will move up.</p>
	<p>The needles are moving up, the needle latch is opened by the previous loop. The fabric is maintained by the sinkers in their final forward position via the connecting floats.</p>
	<p>The needle is in its highest position, the previous loop falls on the needle blade. The yarn guide prevents the latch from closing.</p>
	<p>The needle is moving down and takes the yarn in its hook. The sinkers are moving back.</p>
	<p>The needle keeps moving down pulling the yarn. The needle latch is closed by the previous loop. The sinkers keep moving back.</p>
	<p>The needle reaches its lowest position pulling the yarn through the previous loop. The sinkers reached their final back position.</p>

Figure 16: Main phases of the jersey loop formation.

## B. Terry jersey

Terry jersey is usually covered with loops on one side. Two yarns are knitted together, the ground yarn and the pile<sup>s</sup> yarn (cf. figure 17). The ground yarn is held while the pile yarn is released to form loops [71]. The pile yarn must therefore be much more crimped<sup>s</sup> than the ground yarn in order to form terries on the back side of the fabric. The face has the same aspect as simple jersey face while terries are visible on the back [68]. The formation of the terry jersey loop is illustrated in figure 18.



*Figure 17: Terry jersey knitted structure.*

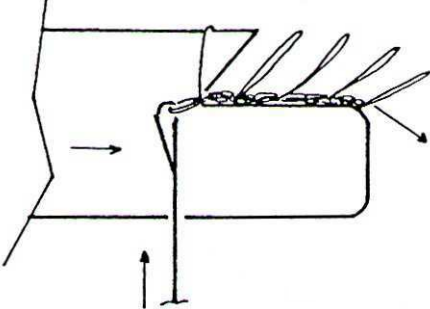
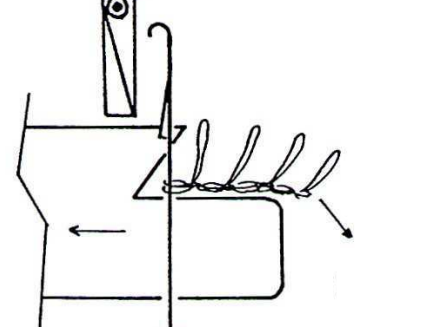
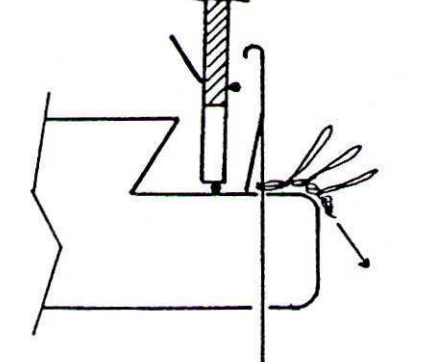
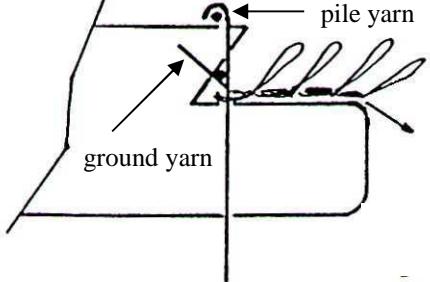
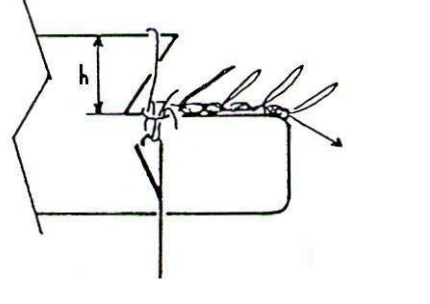
	<p>The stitch of the previous course has just been knocked over<sup>s</sup> and the needle is moving up. The sinker is in its final forward position; the stitches are maintained by the throat of the sinker and the terry by the nose of the sinker.</p>
	<p>The needle reaches its highest position. The yarn guide prevents the latch of the needle from closing. The sinker is moving back and the terry is released.</p>
	<p>The sinker is in its final back position and the yarn guide is near to the needle.</p>
	<p>The sinker moved forward for the terry to be formed when the pile yarn is taken by the needle. The ground yarn is at the back of the sinker throat.</p>
	<p>The needle is in its casting-off position. The ground and the pile yarns are drawn through the previous stitch. The height of the terry depends on the height <math>h</math> of the sinker nose. The higher the sinker nose, the higher the terry. 2.5, 3.1 and 3.5 mm are classical heights for a sinker nose.</p>

Figure 18: Main phases of the terry jersey loop formation.

### 3. Influence of fibre composition

Sock fibre composition may influence many sock properties such as tensile strength, compressibility<sup>§</sup>, heat transfer, friction coefficient and moisture regain<sup>§</sup>. Only the last two will be treated below as coefficient of friction and moisture regain are essential parameters with regard to fabric to skin friction and can thus have an effect on the size and the frequency of blisters.

For example, Herring and Richie [22] carried out a double-blind study about the effect of sock fibre composition on the frequency and the size of blistering events in long-distance runners. The socks tested were identical in every aspect except fibre composition; one was 100% acrylic-made and the other was composed of 100% natural cotton fibres. They observed less blisters and their size was smaller with the acrylic-made socks.

Mailler and Adams [8] suggested to wear moisture wicking synthetic socks in order to prevent the formation of blisters.

Knapik and his colleagues also investigated the effect of sock composition on the incidence and severity of foot blisters. Three boot-sock systems were tested namely the standard military boot sock composed of a wool-cotton-nylon<sup>§</sup>-spandex<sup>§</sup> combination, this standard military boot sock with an additional thin inner polyester sock and a very thick outer wool-polypropylene<sup>§</sup> sock with the same liner as before. In terms of reduction of the incidence of blisters and severe blisters, the socks can be ranged in this order: thick outer sock with thin liner, then the standard military sock with the liner and finally the standard military sock alone [6]. In this study, not only the fibre composition but also the thickness of the socks was varied, the results may then be a combination of both effects. The influence of sock thickness on sock to skin interaction will be discussed in the next paragraph.

#### A. On coefficient of friction

Gwosdow et al. [44] tested six different unwashed fabrics on eight healthy male volunteers in an environmental chamber. Worsted<sup>§</sup> wool, combed cotton, cotton, silk, linen and burlap<sup>§</sup> were pulled across the inner surface of the volunteers' forearm at  $0.6 \text{ m}\cdot\text{s}^{-1}$ . The fabrics can be ranged from the highest friction force to the lowest: cotton, burlap, linen, combed cotton, wool and silk. This order was independent of the ambient conditions.

Zhang and Mak [49] investigated in vivo frictional properties of human skin in contact with the following materials: aluminium, nylon, silicone, and cotton sock. Nylon showed an

average coefficient of friction of 0.37 with skin, while the mean coefficients of friction between skin and cotton sock and between skin and silicone were 0.51 and 0.61 respectively.

## **B. Moisture regain**

Fabrics absorb water in stages. Water vapour first penetrates the fibre mass. The amount of absorption depends on the chemical composition of the fibres; it is low for most synthetics and high for most natural fibres. With increasing humidity, many layers of water molecules may be bound and water may condense on the fibre surface. Then the fibres may swell as plasticization of the monocrystalline structures occurs and liquid water will penetrate the fibre mass. The amount of water taken up during these processes is called regain [41].

Moisture regain is a parameter whereby the hydrophilicity of a textile material can be quantified. Wool is the most hygroscopic textile fibre. It carries moisture up to 12 or 15% of its weight under ordinary conditions and can take up 30 to 50% of its weight in a moist environment. It absorbs moisture and dries slowly. Silk is nearly as hygroscopic as wool but it loses moisture much more rapidly [72]. Cotton socks are also highly hydrophilic, they hold moisture against the foot which leads to less cushioning and more moisture related cutaneous problems like blisters and athlete's foot. On the opposite, polyester fibres such as Coolmax<sup>®</sup> are hydrophobic; they draw moisture away from the foot [73]. Cotton fibre retains three times the moisture of acrylic and fourteen times the moisture of Coolmax<sup>®</sup>.

Moisture regain depends on relative humidity and temperature. It increases with relative humidity but the order of fibres from the highest to the lowest regain does not change with humidity [71]. Swelling properties are linked to moisture regain, the more hydrophilic a fibre, the more it swells in water. Swelling is usually expressed as a percentage, for example cotton fibre surface increases by 44 to 49% when plunged in water (cf. table 3). When a fibre swells, it reduces the free space in the shoe and thus decreases the sweat transport from the inside to the outside of the sock.

Moisture regain is not the only characteristic that determines the degree of hydrophobicity of a fibre; overall wicking performance should also be considered. Fibres should also have a great specific surface in order to facilitate water transport from the inside to the outside of the sock. Spinning is a process whereby artificial and synthetic fibres can be obtained. Textile material goes through the holes of a die and is then stretched. Artificial and synthetic fibres cross-sections can thus be varied changing the shape of the die holes (cf. figure 19). For example, Coolmax<sup>®</sup> section is scalloped oval increasing its specific

surface by 20% compared to a round cross-sectional geometry of fibre. Vapour transport is thus easier for a Coolmax<sup>®</sup> than for a cotton sock.

	COTTON	WOOL	SILK	POLYESTER	ACRYLIC	NYLON (PA 6-6)
Moisture regain at 21°C and 65% relative humidity in percentage	8.5	17	11	0.4	1.6	3
Swelling in water in percentage	44-49	32-38	30-41	None	0-5	0-2

Table 3: Moisture regain and swelling of textile fibres [71]. The abbreviation PA 6-6 stands for polyamide 6-6.

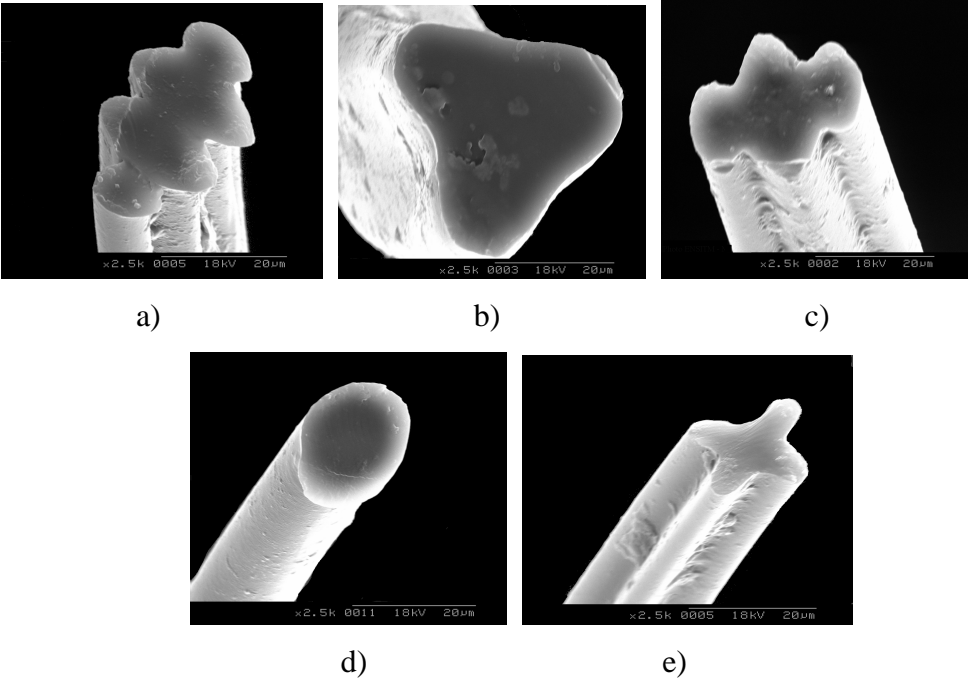


Figure 19: Different cross-sections of Polyester fibres photographed with a scanning electron microscope: a) hexachannel, b) trilobal, c) scalloped oval, d) round and e) cruciform [74].

When comparing synthetic fibre compositions to natural fibre contents, synthetic fibres are more efficient to prevent friction induced skin injuries because of lower friction coefficients and moisture regain.



#### 4. Influence of sock thickness

Socks manufacturers propose various friction-reducing socks. In most of the case, thick paddings are placed at selected areas such as the toes, the forefoot and the heel. Double layer socks are also widely used. With these sock systems, designers try to make the friction occur between the two layers of socks instead of on the skin [29, 75]. Using thick paddings or double layer socks, the aim is to increase the thickness of the sock in order to decrease the pressure exerted on the foot skin.

Mailler and Adams [8] suggested wearing two pairs of socks from different materials. Richie [18] also advocates the use of double layer sock material of which he detailed the composition: a synthetic inner layer coupled with a natural fibre outer layer. As high plantar pressure is an acknowledged risk factor in the development of plantar ulcers in the diabetic neuropathic foot and of skin irritations and blisters in healthy foot, Garrow et al. [19] studied the ability of a multilayered sock (preventive foot care PFC) to reduce plantar foot pressure in a sample of high-risk patients with diabetes. PFC socks have a double-layer construction consisting of a padded outer layer to cushion the feet combined to a low-friction inner layer to reduce friction at the sock/foot interface. They compared PFC socks to ordinary supermarket socks recording in-shoe plantar pressure measurements with F-Scan, an in-shoe system marketed by Tekscan, Boston, MA. They measured the differences in maximum foot contact area and plantar pressure for the whole foot, forefoot and peak plantar pressure areas. They found an increase of 8% in maximum foot contact area when subjects wore the PFC socks. Total foot pressure was also decreased by 9%. Similar results were observed at the forefoot with a 14.2% increase in contact area and a 10.2% reduction in peak forefoot pressure.

Wearing thicker socks seems therefore to increase the contact area between foot and sock thus decreasing foot pressure. However, it is important to remember that hosiery<sup>§</sup> offering thicker construction will reduce the volume within the shoe. Compared to the supermarket socks which were around 0.7 mm thick, the maximum thickness of the PFC hosiery was 2.7 mm around the toes, metatarsal phalangeal area and the heel. Although 2 mm may not represent a huge increase in bulk inside the shoe, additional care in the fitting of shoes is nonetheless required because such hosiery may induce localised increase in foot pressure.

## 5. Are there ideal socks?

Perspiration can exceed 0.5 litre per foot during sport activity [18], moisture absorption is thus needed. However, in addition to the perspiration of the foot, moisture produced elsewhere on the body may accumulate in the sock due to gravity and this amount far exceeds the absorption capacity of any sock product. Moisture absorption capacity is not sufficient; a good athletic sock must also draw water away from the foot. Ideally, one should wear hydrophobic socks and shoes with a hydrophilic inner liner. The socks should not be too hydrophobic because they may not allow water transfer. It is also important that the sock allows the evacuation of the heat produced by friction. Cotton fibres are not recommended since they have a low thermal conductivity of 0.07 W/m/K and are hydrophilic. Polyester is hydrophobic (moisture regain of 0.4%) and has an average thermal conductivity of 0.14 W/m/K, it can thus be a good compromise. Polyamide is also a good solution even if its moisture regain equals 3% because its thermal conductivity reaches 0.25 W/m/K [76].

Dai et al. [24] investigated the effect of wearing socks with different frictional properties on plantar shear. They simulated the foot-sock-insole contact using a 3-D finite element model. With this model, they studied the dynamic plantar pressure and shear stress during the stance phases of gait. They simulated three cases: a barefoot with a high frictional coefficient against the insole (0.54), a sock with a high frictional coefficient against the skin (0.54) and a low frictional coefficient against the insole (0.04) and another sock with opposite frictional properties. They found that wearing socks of low friction against the insole allow more relative sliding between the foot and footwear and thus reduce the shear force compared to the barefoot. If the foot cannot move in the shoe, high pressure and shear can result in blisters or other lesions on the forefoot. To avoid cutaneous lesions, the foot must be free to slide in the shoe. Therefore, low friction is required between foot and the insole and there must be a certain space in the shoe for the foot to slide. However, rubbing in the shoe includes friction between the foot and the inner surface of sock and friction between the outer surface of sock and the shoe, and if the friction is too low on both interfaces, it may lead to an excessive movement of the foot in the shoe and to discomfort and insecurity. Ideally, a sock should have low friction with the skin to allow movement of the foot and high friction with the insole.

Sport-specific socks appeared in the 1980s [18]. Soon, a small range of specific socks were available for key sports such as tennis and running. Nowadays, there are special socks for every conceivable sport activity; it has become a marketing issue. Actually, there is very little difference in hosiery products design within any particular company but it is extremely profitable. Socks should rather be designed specific to the shoe and the foot as it seems to be the case for professional athletes.

Despite extensive research on friction blisters, scientists can hardly predict the apparition and severity of a blister and there is still no simple and sure solution to prevent its formation. It may be due to the dramatic variation of skin conditions (surface roughness, hydration, adhesion between skin layers, etc.) among individuals as well as among different anatomical sites of the same person. The best way to avoid blisters is to reduce the mechanical factors that provoke their formation i.e. pressure and friction. This can be achieved choosing well adapted footwear. The choice of the shoes depends on the characteristics of the feet and the sport practise. The socks should be fitted to the shoes and the way the runner tightens his shoes. In order to reduce the pressure on the skin, the contact surface between the sock and the shoe should be as large as possible; the distance between the shoe and the skin should ideally be equal to the thickness of the sock when it is not compressed. A lower distance will lead to an increase of the contact pressure while a higher distance will increase the sliding distance. The design of a sock may reduce the friction and pressure forces acting on the foot skin. The aspects of sock fibre composition and thickness have been discussed. For Richie [18], the ability of a sock to dissipate damaging forces on the foot surface depends more on its structure than on its fibre composition. Our research is precisely focused on studying the effect of the sock structure on the friction between the fabric and the skin. The friction force between terry jersey socks and the skin is also modelled.

## Literature cited

1. Régnier, M. and M.-J. Staquet, *La peau reconstruite*. Pour La Science, 1999(266): p. 154-159.
2. Breugnot, C., *Contribution à la caractérisation mécanique du toucher des surfaces textiles à partir de critères neurosensoriels*, in *Sciences Pour l'Ingénieur*. 2005, Université de Haute Alsace: Mulhouse. p. 209.
3. Sanders, J.E., B.S. Goldstein, and D.F. Leotta, *Skin response to mechanical stress: Adaptation rather than break down-A review of the literature*. Journal of Rehabilitation Research and Development, 1995. **32**(3): p. 214-226.
4. Elsner, P., *What textile engineers should know about the human skin*. Curr Probl Dermatol, 2003. **31**: p. 24-34.
5. [cited 2010 2010/10/12]; Available from: <http://www.lionden.com/ap1out-skin.htm>.
6. Zhong, W., et al., *Textiles and Human Skin, Microclimate, Cutaneous Reactions: An Overview*. Cutaneous and Ocular Toxicology, 2006. **25**(1): p. 23 - 39.
7. Reichel, M. and D.A. Laub, *From Acne to Black Heel: Common Skin Injuries in Sports*. the physician and sportsmedicine, 1992. **20**(2): p. 111-118.
8. Mailler, E.A. and B.B. Adams, *The wear and tear of 26.2: dermatological injuries reported on marathon day*. British Journal of Sports Medicine, 2004. **38**: p. 498-501.
9. Kirkland, R. and B.B. Adams, *Dermatological problems in the football player*. International Journal of Dermatology, 2006. **45**: p. 927-932.
10. Mailler-Savage, E.A. and B.B. Adams, *Skin manifestations of running*. Journal of the American Academy of Dermatology, 2006. **55**(2): p. 290-301.
11. Bergeron, B.P., *A Guide to Blister Management*. The physician and sportsmedicine, 1995. **23**(2): p. 37-46.
12. Basler, R.S.W., C.M. Hunzeker, and M.A. Garcia, *Athletic Skin Injuries. Combating Pressure and Friction*. The physician and sports medicine, 2004. **32**(5): p. 33-40.
13. Pharis, D.B., C. Teller, and J.J.E. Wolf, *Cutaneous manifestations of sports participation*. Journal of the American Academy of Dermatology, 1997. **36**(3): p. 448-459.
14. Xing, M., et al., *Skin friction blistering: computer model*. Skin Research and Technology, 2007. **13**(3): p. 310-316.
15. Knapik, J.J., K. Reynolds, and J. Barson, *Influence of an antiperspirant on foot blister incidence during cross-country hiking*. Journal of the American Academy of Dermatology, 1998. **39**(2): p. 202-206.
16. Reynolds, K., et al., *Effects of an antiperspirant with emollients on foot-sweat accumulation and blister formation while walking in the heat*. Journal of the American Academy of Dermatology, 1995. **33**(4): p. 626-630.
17. Comaish, J.S., *Epidermal fatigue as a cause of friction blisters* The Lancet, 1973. **301**(7794): p. 81-83.
18. Richie, D.H. *Socks: Hosiery - Essential equipment for the Athlete*. [cited 2009/03/11]; Available from: <http://www.aapsm.org/socknov97.html>.
19. Adam P., G., V.S. Carine H.M., and B. Andrew J.M., *Efficacy of Multilayered Hosiery in Reducing In-Shoe Plantar Foot Pressure in High-Risk Patients With Diabetes*. Diabetes Care, 2005. **28**(8): p. 2001-2006.

20. Knapik, J.J., et al., *Friction Blisters - Pathophysiology, Prevention and Treatment*. Sports Medicine, 1995. **20**(3): p. 136-147.
21. Polliack, A.A. and S. Scheinberg, *A New Technology for Reducing Shear and Friction Forces on the Skin: Implications for Blister Care in the Wilderness Setting*. Wilderness & Environmental Medicine, 2006. **17**(2): p. 109-119.
22. Herring, K.M. and D.H. Richie, *Friction blisters and sock fiber composition A double-blind study*. Journal of the American Podiatric Medical Association, 1990. **80**(2): p. 63-71.
23. Yavuz, M. and B.L. Davis, *Plantar shear stress distribution in athletic individuals with frictional foot blisters*. Journal of American Podiatric Medical Association, 2010. **100**(2): p. 116-120.
24. Dai, X.-Q., et al., *Effect of sock on biomechanical responses of foot during walking*. Clinical Biomechanics, 2006. **21**(3): p. 314-321.
25. <http://www.aaspm.org/runshoe.html>, *Running Shoes by Level of Stability*. 2010/04/14.
26. Sandrey, M.A., C.J. Zebas, and J.D. Bast, *Rear-foot motion in soccer players with excessive pronation under 4 experimental conditions*. Journal of Sport Rehabilitation, 2001. **10**(2): p. 143-154.
27. Polster, B., *Mathematics: What is the best way to lace your shoes?* Nature, 2002. **420**(6915): p. 476-476.
28. Hagen, M. and E.M. Hennig, *The influence of different shoe lacing conditions on plantar pressure distribution, shock attenuation and rearfoot motion in running*. Clinical Biomechanics, 2008. **23**(5): p. 673-674.
29. Herring, K.M., *How Socks Make The Feet*. <http://www.aapsm.org/socks-make-the-feet.html>, 2009/04/08.
30. Gras, R., *Tribologie Principes et solutions industrielles*. Mécanique et matériaux, ed. I.u. nouvelle. 2008, Paris: DUNOD. 322.
31. Persson, B.N.J., *Sliding Friction Physical Principles and Applications*, ed. P.D.D.h.c.K.v. Klitzing and P.D.R. Wiesendanger. 1998: Springer-Verlag Berlin Heidelberg. 462.
32. Naylor, P.F.D., *The Skin Surface and Friction*. British Journal of Dermatology, 1955. **67**(7): p. 239-248.
33. Howell, H.G., K.W. Mieszkis, and D. Tabor, *Friction in textiles*. 1959, London: Butterworths Scientific Publications. 263.
34. Gupta, B.S., *Friction in textile materials*. 2008, Cambridge, England: Woodhead Publishing Limited. 462.
35. Aliouche, D., *Contribution à l'étude des mécanismes de frottement des étoffes*, in *Sciences de l'Ingénieur*. 1991, Université de Haute Alsace: Mulhouse. p. 152.
36. Virto, L. and A. Naik, *Frictional Behavior of Textile Fabrics. Part I: Sliding Phenomena of Fabrics on Metallic and Polymeric Solid Surfaces*. Textile Research Journal, 1997. **67**(11): p. 793-802.
37. Ajayi, J.O., *EFFECTS OF FABRIC STRUCTURE ON FRICTIONAL PROPERTIES*. Textile Research Journal, 1992. **62**(2): p. 87.
38. Sivamani, R.K., et al., *Friction coefficient of skin in real-time*. Skin Research and Technology, 2003. **9**(3): p. 235-239.
39. Koudine, A.A., et al., *Frictional properties of skin: proposal of a new approach*. International Journal of Cosmetic Science, 2000. **22**: p. 11-20.
40. Wolfram, L.J., *Friction of skin*. Journal of the Society of Cosmetic Chemists, 1983. **34**(8): p. 465-476.
41. Kenins, P., *Influence of Fiber Type and Moisture on Measured Fabric-to-Skin Friction*. Textile Research Journal, 1994. **64**(12): p. 722-728.

42. Gerhardt, L.-C., et al., *Influence of epidermal hydration on the friction of human skin against textiles*. Journal of the Royal Society Interface, 2008. **5**: p. 1317–1328.
43. Zimmerer, R.E., K.D. Lawson, and C.J. Calvert, *The Effects of Wearing Diapers on Skin*. Pediatric Dermatology, 1986. **3**(2): p. 95-101.
44. Gwosdow, A.R., et al., *Skin Friction and Fabric Sensations in Neutral and Warm Environments*. Textile Research Journal, 1986. **56**: p. 574-580
45. Nacht, S., et al., *skin friction coefficient: changes induced by skin hydration and emollient application and correlation with perceived skin feel*. J. Soc. Cosmet. Chem., 1981(32): p. 55-65.
46. Sivamani, R.K., et al., *Coefficient of friction: tribological studies in man - an overview*. Skin Research and Technology, 2003. **9**: p. 227-234.
47. Elsner, P., D. Wilhelm, and H. Maibach, *Frictional properties of human forearm and vulvar skin: influence of age and correlation with transepidermal water loss and capacitance*. Dermatologica, 1990. **181**(2): p. 88-91.
48. Cua, A.B., K.P. Wilhelm, and H.I. Maibach, *Skin Surface Lipid and Skin Friction: Relation to Age, Sex and Anatomical Region*. Skin Pharmacology and Physiology, 1995. **8**(5): p. 246-251.
49. Zhang, M. and A.F.T. Mak, *In vivo friction properties of human skin*. Prosthetics and Orthotics International, 1999(23): p. 135-141.
50. Gerhardt, L.-C., et al., *Skin-textile friction and skin elasticity in young and aged persons*. Skin Research and Technology, 2009(15): p. 288-298.
51. Bueno, M.-A., et al., *Tribological investigation of textile fabrics*. Wear, 1996. **195**(1-2): p. 192-200.
52. Kawabata, S., *The Standardisation and Analysis of Hand Evaluation*. 1980, Osaka: The Textile Machinery Society of Japan.
53. Bueno, M.-A., *Caractérisation de l'état de surface des textiles en vue d'une meilleure compréhension de leur toucher*, in *Sciences Pour l'Ingénieur*. 2002, Université de Mulhouse: Mulhouse. p. 107.
54. Fontaine, S., *Contribution à la compréhension des mécanismes tribologiques lors d'une usure abrasive ou chimique de structures fibreuses. Application industrielle aux tissus en PET-laine.*, in *Sciences Pour l'Ingénieur*. 2001, Université de Haute Alsace: Mulhouse. p. 228.
55. Bueno, M.-A., S. Fontaine, and M. Renner, *Dispositif pour mesurer l'état de surface d'un matériau et procédé de mise en oeuvre*, LPMT, Editor. 2000: France.
56. Derler, S., et al., *Friction of human skin against smooth and rough glass as a function of the contact pressure*. Tribology International, 2009. **42**(11-12): p. 1565-1574.
57. Derler, S., U. Schrade, and L.C. Gerhardt, *Tribology of human skin and mechanical skin equivalents in contact with textiles*. Wear, 2007. **263**(7-12): p. 1112-1116.
58. Rosenbaum, D. and H.-P. becker, *Review article. Plantar pressure distribution measurements. Technical background and clinical applications.*. Foot and Ankle Surgery, 1997. **3**: p. 1-14.
59. Lord, M., D.P. Reynolds, and J.R. Hughes, *Foot pressure measurement: A review of clinical findings*. Journal of Biomedical Engineering, 1986. **8**(4): p. 283-294.
60. Hayafune, N., Y. Hayafune, and H.A.C. Jacob, *Pressure and force distribution characteristics under the normal foot during the push-off phase in gait*. The Foot, 1999. **9**(2): p. 88-92.
61. Cock, A.D., et al., *A functional foot type classification with cluster analysis based on plantar pressure distribution during jogging*. Gait & Posture, 2006. **23**: p. 339-347.
62. Burnfield, J.M., et al., *The influence of walking speed and footwear on plantar pressures in older adults*. Clinical Biomechanics, 2004. **19**(1): p. 78-84.

63. Donaghue, V.M., et al., *Longitudinal in-shoe foot pressure relief achieved by specially designed footwear in high risk diabetic patients*. Diabetes Research and Clinical Practice, 1996. **31**(1-3): p. 109-114.
64. Nagel, A., et al., *Long distance running increases plantar pressures beneath the metatarsal heads: A barefoot walking investigation of 200 marathon runners*. Gait & Posture, 2008. **27**(1): p. 152-155.
65. Kernozek, T.W. and E.E. LaMott, *Comparisons of plantar pressures between the elderly and young adults*. Gait & Posture, 1995. **3**(3): p. 143-148.
66. Mills, N.J., *Running shoe case study*, in *Polymer Foams Handbook*. 2007, Butterworth-Heinemann: Oxford. p. 307-327.
67. Peirce, F.T., *The "Handle" of Cloth as a Measurable Quantity*. Journal of the Textile Institute, 1930: p. T377-T416.
68. Troyes, C.d.P.d.l.B.d. and C.d.R.d.l. Bonneterie, *Mémento de technologie bonneterie*. 1968, Troyes: grande imprimerie de Troyes. 25
69. Abrams, A. and L. Mishcon, *Pattern Wheel Designing for Circular Jersey Knitting Machines*. first edition ed. 1949, New York: Supreme knitting machine co., inc. 165.
70. Committee, T.I.T.T.a.d., *Textile Terms and Definitions*. Ninth Edition ed. 1991, Manchester: M C TUBBS BSc Tech AMCT CText FTI FRSA P N DANIELS BA MIIInfSc. 367.
71. Harris, M., *Handbook of textile fibers*. first edition ed. 1954, Washington: Harris research laboratories, inc. 356.
72. Woolman, M.S. and E.B. McGowan, *Textiles: a handbook for the student and the consumer*. third ed. 1946, New York: The macmillan company. 388.
73. Pribut, S. and D. Richie, *Separating the Buzz from the Biomechanics: A guide to Athletic Shoe trends & Innovations*. Podiatry Management, 2004: p. 85-97.
74. Pac, M.-J., *Les surfaces textiles aux échelles micro-méso et macroscopiques : propriétés thermiques et tribologiques*, in *Sciences Pour l'Ingénieur*. 2001, Université de Haute-Alsace: Mulhouse.
75. Bernhardt, F., *Double layer sock with low friction layer to layer interface*. 2000: United States.
76. Bertaux, E., et al., *Textile, Physiological, and Sensorial Parameters in Sock Comfort*. Textile Research Journal, 2010.

# Chapter II:

## materials and methods



# Résumé

L'objectif de ce travail de recherche était d'étudier l'influence de la structure textile sur le frottement entre la peau du pied et la chaussette lors de la course à pied. Le premier chapitre a recensé les différentes affections cutanées qui peuvent survenir lorsque l'on pratique le jogging. Ces affections peuvent apparaître à différents endroits et la pression exercée sur la peau par l'ensemble chaussure + chaussette dépend de la zone considérée. Pour pouvoir mesurer le frottement entre la peau et la chaussette dans les mêmes conditions que lors de la course à pied, il faut déterminer l'aire de contact entre le pied et la chaussette, l'amplitude de frottement, la fréquence de frottement et la force normale appliquée sur la peau. Le chapitre II détaille successivement les zones du pied étudiées, les chaussettes et les dispositifs de mesures de frottement et de compression utilisés.

Les informations disponibles dans la bibliographie sur les zones d'apparition des phlyctènes ne sont pas suffisamment détaillées pour bien les identifier. J'ai par conséquent réalisé un sondage afin de localiser les zones du pied où les ampoules apparaissent en fonction de l'activité sportive pratiquée. Cinq sites ont ainsi été identifiés : le coussinet sous le gros orteil sur la plante des pieds (cité dans 56% des cas), la voule plantaire (citée dans 50% des cas), le talon (cité dans 56% des cas), les côtés externes du gros et du petit orteil (cités dans 25% des cas).

En ce qui concerne les chaussettes de course à pied, les modèles basiques sont en coton renforcé de polyamide ou de polyester. Ils contiennent aussi parfois de l'élasthanne en faible quantité (2 à 3% en masse) aux zones élastiques, ou bien de l'acrylique pour diminuer l'humidité à la surface de la peau ou encore du PolyTetraFluoroEthylène afin de diminuer le coefficient de frottement peau-chaussette. Les chaussettes d'hiver sont à base de laine tandis que certaines marques proposent aussi des chaussettes à base de polyamide ou de polyester qui permettent de garder les pieds au sec. Dans notre étude, nous utilisons des chaussettes en coton car c'est le principal composant des chaussettes basiques. Quant à la structure tricotée, les chaussettes de course à pied sont généralement soit en jersey simple soit en jersey bouclette. Nous avons choisi 4 liages : le jersey simple qui a une structure fine tricotée avec un seul fil, le jersey double qui présente la même structure mais tricotée avec deux fils, le jersey ponts de fils qui, en plus de la structure de base en jersey simple, présente des flottés

formés avec un deuxième fil, et le jersey bouclette dont l'épaisseur importante est obtenue par les boucles que forme le deuxième fil avec le fil de fond. De plus, six autres chaussettes ont été étudiées afin d'évaluer l'influence du titre des fils, du liage et de la longueur de fil absorbée. Les comptes i.e. le nombre de colonnes et de rangées de mailles par cm, ou bien le nombre de ponts de fils ou de bouclettes par cm, ont été mesurés pour chaque type de chaussette ainsi que le diamètre moyen des fils. Pour les jerseys bouclette, l'angle décrit par les bouclettes avec la verticale au tricot et la hauteur des boucles ont également été déterminés. Tous les tests effectués ont été réalisés à sec en atmosphère conditionnée standard i.e. à  $20^{\circ}\text{C} \pm 2^{\circ}\text{C}$  et  $65\% \pm 4\%$  d'humidité relative. Les matériaux textiles ont été conditionnés au préalable durant 48 heures.

Un tribomètre alternatif linéaire à poids mort a été mis en place au Laboratoire de Physique et de Mécanique Textiles afin de reproduire le plus fidèlement possible le frottement de l'ensemble chaussure + chaussette sur la peau lors de la course à pied. La chaussette est collée sur une table oscillante dont le moteur est commandé par un programme informatique. La table oscillante décrit un mouvement sinusoïdal. Le palpeur, fixé sur un bras, va venir frotter la face envers de la chaussette i.e. celle qui est en contact avec la peau au porter. Le dispositif de fixation de la charge normale est placé au dessus du palpeur. Un capteur à jauge de déformation est placé sur le bras afin de mesurer la force de frottement. Le déplacement vertical du palpeur est enregistré grâce à un capteur laser. Le palpeur a une longueur de 1,7 cm et une largeur de 0,9 cm pour une aire de contact de  $1,53 \text{ cm}^2$  ce qui correspond à la surface de l'index, mesurée grâce à un sondage sur 58 personnes. Le palpeur est recouvert d'une peau artificielle en polyamide enduit de polyuréthane, le Lorica®, qui présente une surface similaire à la peau et reproduit de façon satisfaisante les propriétés tribologiques de la peau sèche. Deux autres palpeurs, de forme cylindrique en acier inoxydable de surface égale au premier et qui ne diffèrent que par leur rugosité, ont également été utilisés afin de mieux comprendre les phénomènes qui se produisent lors du frottement. La distance de frottement a été fixée à 5mm. La force normale exercée sur la peau par l'ensemble chaussure + chaussette ainsi que la fréquence des foulées ont été mesurées in situ grâce à un capteur piezorésistif flexible, le Flexiforce®, pour une vitesse de course de 8 à 13 km/h. Nous avons concentré notre étude expérimentale sur la zone de la voute plantaire. Pour cette zone, la fréquence des foulées a été fixée à 1,5 Hz et la force normale appliquée à une plage de 0,44 à 2,14 N.

Un deuxième tribomètre a aussi été utilisé, le Textile Friction Analyser (TFA), qui a été développé par l'EMPA Swiss Federal Laboratories for Materials Science and Technology St Gallen. Un bras d'élévation permet d'ajuster la force normale appliquée. Le mouvement alternatif du support métallique est programmé informatiquement et géré par un moteur. Ce tribomètre est assez différent du précédent ; le palpeur est rond de diamètre 2,8 cm, il a donc une surface de 6,16 cm<sup>2</sup> alors que celui du LPMT est rectangulaire et a une surface de 1,53 cm<sup>2</sup>. Les expériences de frottement ont donc été réalisées pour une pression donnée. De plus, sur le dispositif du LPMT, le palpeur est libre de bouger verticalement selon l'influence de la structure tricotée ce qui n'est pas le cas sur le TFA. Par conséquent, pour le tribomètre du LPMT, la force normale appliquée est constante alors que, dans le cas du TFA, la force normale varie autour d'une valeur d'équilibre plus élevée. Ni le tribomètre du LPMT ni le TFA ne reproduit fidèlement le frottement de la chaussette sur le pied dans la chaussure lors de la course à pied. Ce qui se produit dans la chaussure est probablement un cas intermédiaire, c'est pourquoi il était intéressant de réaliser des mesures de frottement sur les deux tribomètres et de les comparer.

La pression exercée sur la peau du pied par l'ensemble chaussure + chaussette dépend de nombreux facteurs dont le comportement de la chaussette en compression. C'est pourquoi des mesures de compression ont été effectuées sur un appareil KES FB3, dispositif de la chaîne de mesures Kawabata dédié à l'évaluation de la compression des matériaux textiles. Un capteur Flexiforce® a été fixé sur le pied presseur, les chaussettes ont été placées avec la face endroit vers le haut (face en contact avec la chaussure) et l'envers vers le bas (face en contact avec le pied). Ainsi, la pression exercée par le pied presseur sur l'endroit est mesurée par le Flexiforce® et correspond à la pression exercée par la chaussure sur la chaussette tandis que la pression exercée sur l'envers de la chaussette est mesurée par le capteur de force du KES FB3 et correspond à la pression exercée sur la peau. La vitesse de déplacement du pied presseur a été fixée à 0,02 mm/s et la pression maximale à 15 kPa.

# CONTENTS

<i>Chapter II: Materials and methods</i>	<i>71</i>
I. TESTED FOOT AREAS	76
II. RUNNING SOCKS	77
1. Fibre composition	77
2. Textile structure	79
3. Setting, yarn diameter, terry height and orientation	83
4. Textile testing conditions	85
III. LINEAR RECIPROCATING DEAD WEIGHT TRIBOMETER	85
1. Design of the pin	87
A. Surface area	87
B. Artificial skin model	88
C. Additional pins	89
2. Characteristics of the reciprocating movement	89
A. Sliding movement amplitude	89
B. Sliding movement frequency and applied normal force	90
IV. TEXTILE FRICTION ANALYSER (TFA)	92
V. COMPRESSION EXPERIMENTS	95
Literature cited	99

The aim of this research work was to study the influence of the textile structure on the friction between the foot skin and the sock during running. The skin injuries that may be induced by jogging were detailed in chapter I. They may occur on different anatomical sites and the pressure on the skin is highly dependent on the anatomy. In order to measure the friction between the foot and the sock in similar conditions than in a shoe during running, the contact area between the foot and the sock, the sliding movement amplitude and frequency, and the normal force applied on the skin need to be fixed. This chapter successively details the foot areas we studied, the socks we used and the friction and compression measurement devices and settings.

## I. TESTED FOOT AREAS

According to Mailler, Adams and Bergeron, blisters usually occur on the tips of the toes, the balls of the feet and the posterior heel [1, 2]. Herring and Richie [3] found that the forefoot region is more affected than the heel region. 60.2 % of the blisters they observed occurred in the forefoot region, 33.3 % in the midfoot region and 6.5% in the rearfoot area. This information is not sufficiently detailed to identify the preferential areas for blister formation on the foot. I thus carried out a survey asking people to localise on foot anatomy's pictures the zones where they usually have blisters and to specify how often these zones were injured and during which sport activity. 16 participants answered the survey, 7 women and 9 men, from 25 to 55 years old. 5 preferential sites were identified, namely the plantar area under the first metatarsal head, the plantar fascia area, the heel, the external side of the hallux and the external side of the little toe. These five zones are illustrated in figures 1 to 3.



*Figure 20: Zone 1; under the first metatarsal head.*

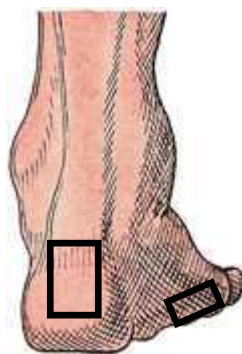


*Figure 21: Zones 2 and 3; respectively the plantar fascia and the heel (left foot).*



*Figure 22: Zones 4 and 5; respectively the external sides of the big and the little toe.*

Zones 1 and 3 were cited by 56% of the participants, half of the people who answered the survey had blisters localised at zone 2 and zones 4 and 5 were mentioned by 25% of the participants.

## **II. RUNNING SOCKS**

### **1. Fibre composition**

Basic running socks are mostly made of cotton, usually combined with polyamide or polyester. Polyester is less expensive but also less resistant than polyamide. When combined with cotton, polyamide or polyester is used as plating\* to increase the sock's lifetime. Socks

---

\* plating: the plating (*vanisage* in French) is a reinforcement technique. For example, the toe and the heel of a sock can be reinforced using an additional yarn.

may also contain elastane<sup>§</sup> in very small quantity (2 to 3% in mass) in specific elastic areas, or acrylic in order to reduce moisture at the sock - foot skin interface or either polytetrafluoroethylene<sup>§</sup> (PTFE) whereby the coefficient of friction between the skin and the sock may be reduced. Winter running socks commonly contain a high percentage of wool fibres for the runner to be warm. The compositions of different worldwide commercialised running socks are given in Tables 1 to 3.

BRAND NAME	% OF COTTON	% OF PA	% OF ACRYLIC	% OF PTFE	% OF PP	% OF ELASTANE
RUN 100	48	32	20			
RUN 500	57	16	25			2
RUN 50	65	35				
RUN 400	60	12	37			1
RUN 300	50	27	20			3
RUN 800		66		32		2
RUN 900 light		69			19	12
RUN 1000	57	16	25			2

*Table 4: Fibre compositions of socks sold by Décathlon. The abbreviations PA, PTFE and PP respectively stand for polyamide, polytetrafluoroethylene and polypropylene.*

BRAND NAME	% OF COTTON	% OF PA	% OF PP	% OF ELASTANE	% OF PET
TACTEL X1		98		2	
RUN X3	80			2	18
RUN X2 CMX	40			2	58
Oasics KAYANO		78		8	14
Oasics RUN QUARTER	60	38		2	
Nike Elite RUN		72		1	27

*Table 5: Fibre compositions of socks sold by Go Sport. The abbreviation PET stands for polyethylene terephthalate.*

BRAND NAME	% OF WOOL	% OF COTTON	% OF PA	% OF ACRYLIC	% OF PP	% OF ELASTANE	% OF PET
New Balance			100				
Rywan			17			3	80
Nike ergonomique			26			3	71
Nike dry-fit			28				68
Oasics			32				68
Rohner winter running	45		16	27	11	1	
Running hurricane		17	72			8	
X Socks Speed One		38	38		18	6	

*Table 6: Fibre compositions of specific sport trademark running socks.*

Sport's brands such as New Balance, Oasics or Nike propose specific running socks which are mostly made of polyamide or polyester for the foot to remain dry. These socks are not commercial successes, maybe because they are expensive for recreational runners. For our study, we selected cotton made socks as cotton is the principal component of basic socks.

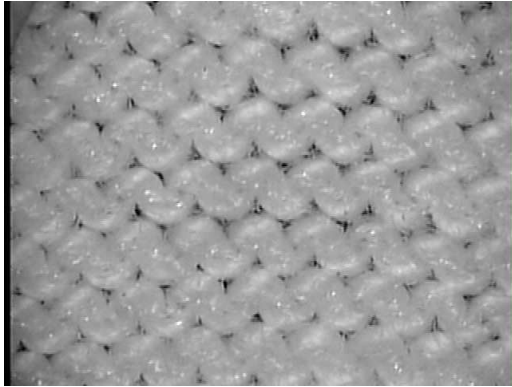
## 2. Textile structure

There are two knitted structures widely used in running socks, namely terry and simple jersey (cf. table 4). These two structures were described in the previous chapter (paragraph III. 1).

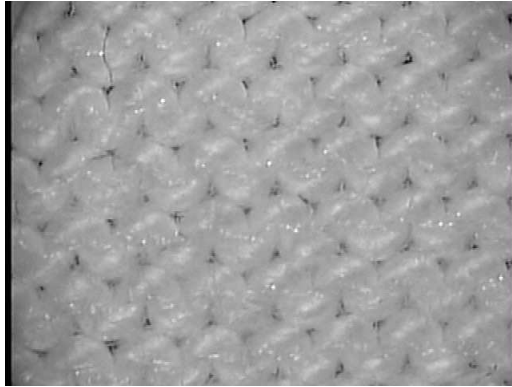


KNITTED STRUCTURE	RUN 100	RUN 500	RUN 50	RUN 400	RUN 300	RUN 800	RUN 900 LIGHT	RUN 1000
Simple jersey	X		X		X			
Terry jersey		X		X		X	X	X

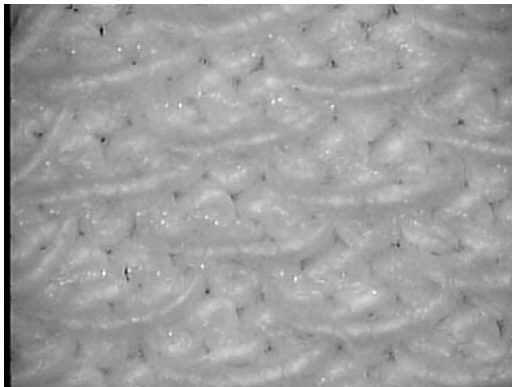
Table 7: Knitted structure of Décathlon's running socks.



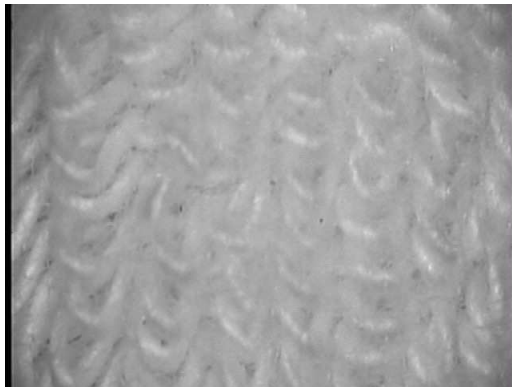
a)



b)



c)



d)

Figure 23: Labonal socks: a) simple jersey, b) double jersey, c) yarn bridges and d) terry jersey.

Four different kinds of knit were selected:

- Labonal simple jersey

This thin structure is knitted with a single cotton yarn.

- Labonal double jersey

The thickness of the structure is slightly increased knitting two cotton yarns together.

- Labonal yarn bridges

This structure is also derived from simple jersey. Here, floats<sup>§</sup> are formed by a second yarn.

- Labonal terry jersey

The important thickness of this kind of knit is due to the loops formed by the pile yarn with the back yarn.

Figure 4 shows these four kinds of knit photographed with a zoom  $\times 40$ . These four structures were knitted with a gauge<sup>§</sup> 14.

Six others cotton-made socks were tested in order to study the influence of the yarn count, the knitted structure and the stitch length:

- Terry jersey 10 – 12, terry jersey 10 – 16 and terry jersey 10 – 20

These socks only differ by their yarn count (cf. table 5).

SOCK	TERRY JERSEY 10 - 12	TERRY JERSEY 10 - 16	TERRY JERSEY 10 - 20
Yarn count in Ne(c)	12	16	20
Yarn count in Tex	141	106	85

*Table 8: Yarn count for terry jersey 10 - 12, terry jersey 10 - 16 and terry jersey 10 - 20.*

- Terry jersey 10 – 16 and simple jersey 10 – 16

They only differ by their knitted structure; one is a terry jersey sock while the other one is a simple jersey sock. The terries of the terry jersey sock are less compact, less homogeneous and more crushed than Labonal terries.

- Terry jersey 9 – 16, terry jersey 10 – 16 and terry jersey 11 – 16

They only differ by their size, respectively 9 ¼, 10 ¼ and 11 ¼ inches which is linked to the stitch length (cf. table 6). The stitch length is the length of yarn contained in one stitch and is expressed in cm of yarn per stitch.

SOCK	TERRY JERSEY 9 - 16	TERRY JERSEY 10 - 16	TERRY JERSEY 11 - 16
Stitch length in cm per stitch	1.19 ± 0.02	1.22 ± 0.01	1.28 ± 0.01

Table 9: Stitch length for terry jersey 9 – 16, terry jersey 10 – 16 and terry jersey 11 – 16. The stitch lengths were measured using a Sodemat device (Troyes, France) in accordance with standards NFG07101 and NFG07311.

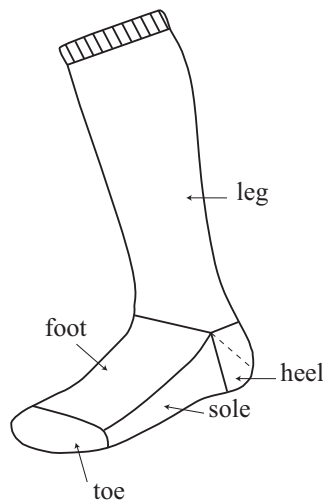


Figure 24: Different sections of a sock.

A sock can be decomposed into five sections (cf. figure 5): the leg, the foot, the toe, the sole and the heel. Three sections, namely the toe, the sole and the heel are in contact with

skin areas where blisters may occur. Only these parts were studied. The way a sock is assembled was not considered. It seems obvious that the more discontinuity and thickness the sock sewing up presents, the higher friction it will induce on the foot skin.

### 3. Setting, yarn diameter, terry height and orientation

The setting i.e. the number of yarns or terries per cm in both directions of the investigated socks in loom-finished state are given in table 7.

The diameters of the yarns were measured using a Projectina® 4002 device (Projectina, Heerbrugg, Switzerland, serial number 8070). Objective 35004 ( $\times 40$ ) and lens 170/10/0.25 were employed whereby a 1 mm read equals to 8  $\mu\text{m}$  in reality. 10 and 6 measures were respectively carried out for Labonal and other socks. The results are shown in table 7.

The height and the angle of terries with the vertical to the textile fabric were measured from photographs. The mean values are reported in table 8 (at least 10 measurements) and figure 6 shows an example of a photograph used to assess these parameters.

SOCK	LENGTHWISE SETTING	WIDTHWISE SETTING	MEAN YARN DIAMETER IN MM
Labonal simple jersey	16 courses	9 wales	$0.36 \pm 0.03$
Labonal double jersey	14 courses	8 wales	$0.43 \pm 0.03$
Labonal yarn bridges	7.5 bridges and 16 courses	4.5 bridges and 10 wales	$0.38 \pm 0.08$
Labonal terry jersey	17	9.5	$0.39 \pm 0.05$
Terry jersey 10 - 12	9	6	$0.51 \pm 0.05$
Terry jersey 10 - 16	8.5	6	$0.36 \pm 0.03$
Terry jersey 10 - 20	9	6	$0.34 \pm 0.03$
Simple jersey 10 - 16	9 courses	6.5 wales	$0.40 \pm 0.06$
Terry jersey 9 - 16	11	7	$0.41 \pm 0.07$
Terry jersey 11 - 16	7.5	6.5	$0.38 \pm 0.04$

*Table 10: Lengthwise, widthwise settings of the socks and mean diameters of the yarns without tension. For double jersey, it is the diameter of one single yarn which is given. For yarn bridges, the values stand for the bridge yarn. For terry socks, the results are given for the terry yarn.*

KNITTED FABRIC	TETAINIT (°)	HEIGHT (MM)
Labonal terry jersey	$5 \pm 5$	$1.38 \pm 0.18$
Terry jersey 10 - 12	$-41 \pm 6$	$1.06 \pm 0.11$
Terry jersey 10 - 16	$-45 \pm 7$	$1.04 \pm 0.09$
Terry jersey 10 - 20	$-51 \pm 8$	$1.07 \pm 0.13$
Terry jersey 9 - 16	$-36 \pm 11$	$1.09 \pm 0.05$
Terry jersey 11 - 16	$-52 \pm 8$	$1.11 \pm 0.16$

*Table 11: Height and orientation of terries. Tetainit is the angle formed by the terries with the vertical to the textile surface, it is positive when the terries are oriented towards the heel of the sock and negative when the terries are oriented towards the toe of the sock.*

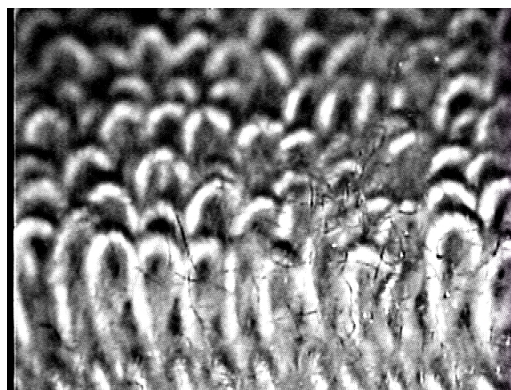


*Figure 25: Example of a photograph used to assess the height and the orientation of terries.*

#### 4. Textile testing conditions

As it has been detailed in the first chapter, textile materials can be highly hydrophilic. In a moist environment, textile fibres absorb water from the air and swell. The properties of textile materials are therefore highly influenced by ambient humidity and temperature. In order to compare different textile materials, international standard conditions have been fixed for textile testing experiments i.e.  $20^{\circ}\text{C} \pm 2^{\circ}\text{C}$  and  $65\% \pm 4\%$  Relative Humidity (european standard NF EN ISO 139). Socks were preconditioned in this climate for at least 48 hours before the experiments.

Comparative friction results of different textile surfaces obtained in dry conditions remain valid in wet conditions [4]. Therefore, all the experiments described in chapters 2 and 3 were carried out in dry conditions.

### III. LINEAR RECIPROCATING DEAD WEIGHT TRIBOMETER

A specific device was designed to simulate the friction of the sock on the foot in the shoe during running. It is composed of an oscillating motor-controlled table (Controls Linear Table x.act LT 100-2 ST controlled by 3 Chanel Stepper-Motor-Controller M50.PCI, LINOS Photonics GmbH & Co. KG, Göttingen, Germany) on which the sock is stuck using a removable and high resistant glue. A computer program has been written in Visual Basic language whereby the oscillating table can have a sinusoidal movement. The back side of the sock i.e. the one which touches the skin in the shoe is in contact with a probe which is mounted on an arm. Weights can be applied overhead of the probe. A strain-gauge sensor (HBM PW4C3 sensor, maximum load 3 N, HBM France SAS, Mennecy, France) is clamped on the arm whereby friction forces can be recorded. A laser sensor has been installed on the tribometer in order to measure the vertical displacement of the pin during a friction experiment.

Figure 7 is a photograph of the tribometer while figure 8 shows the curve shape of the oscillating table displacement in function of time for the settings which will be detailed later.

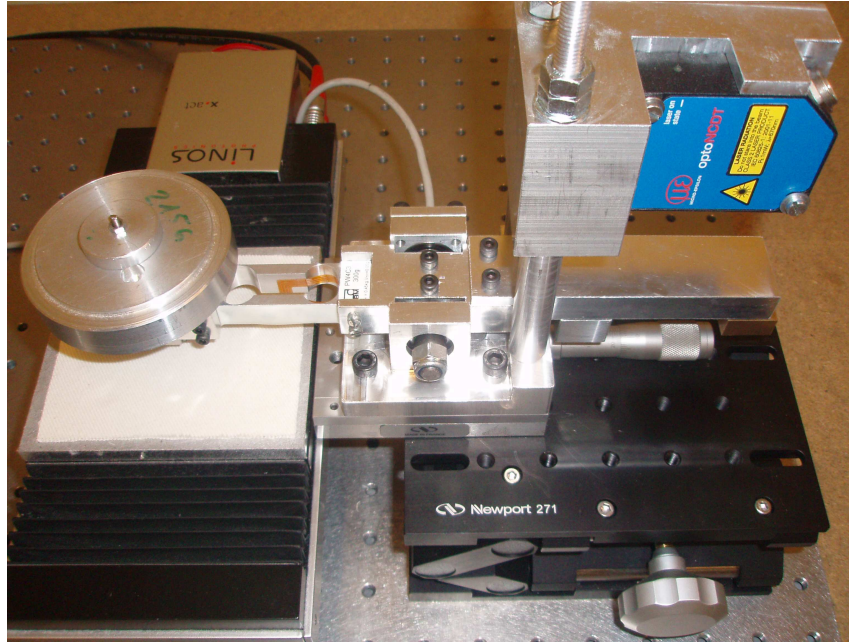


Figure 26: Linear alternating friction device.

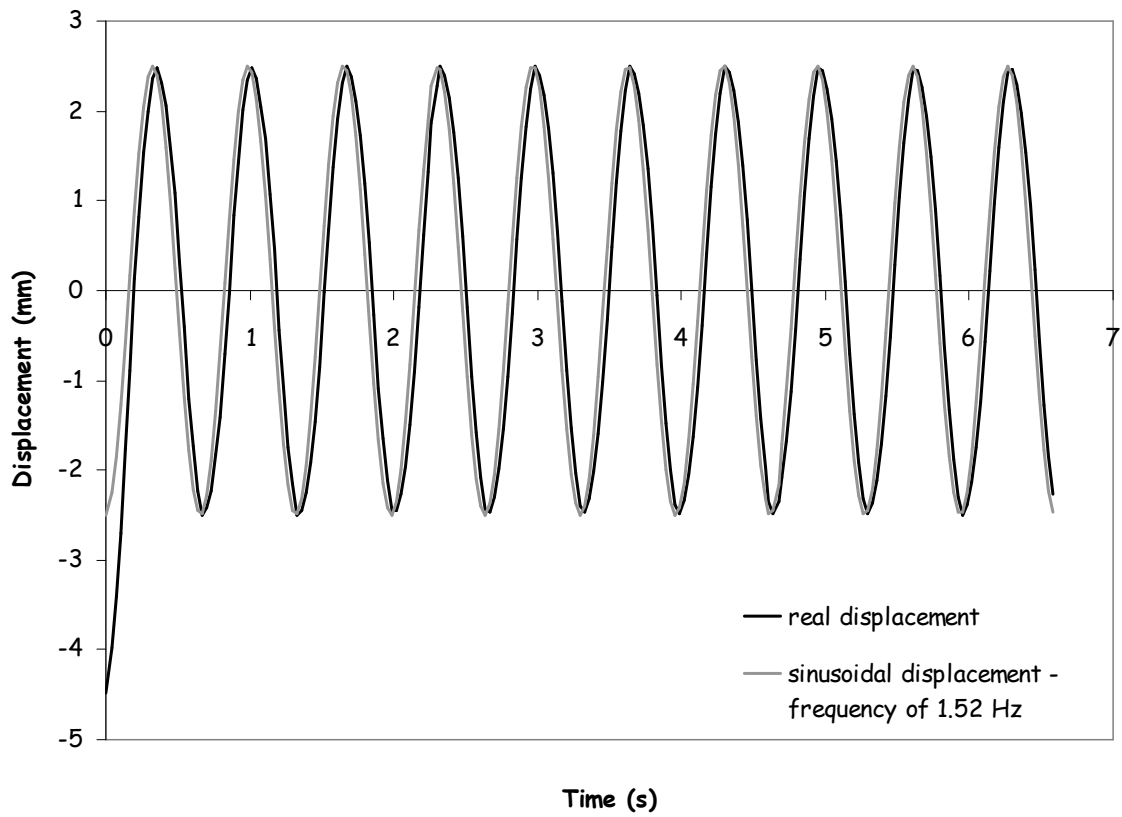


Figure 27: Displacement of the oscillating table versus time.

## 1. Design of the pin

### A. Surface area

When developing our tribometer, we tried to design a highly versatile apparatus which can be used to evaluate at the same time the friction between the sock and the foot in the shoe and the friction between the finger and a fabric. The index is the finger the most commonly used to assess the tactile properties of a fabric. The skin of the index and the skin of the foot are both glabrous and when considering the areas of the foot where blisters commonly occur, the contact area involved in blister formation seems to be similar to the surface area of the index. Moreover, the contact pressure used to evaluate tactile properties ranges from 0.15 to 4.5 N [5] and, as it will be detailed later in section III.2.B, the contact pressure of the foot with the sock during running varies from 0.44 to 20 N. The other parameters namely the sliding distance and the sliding velocity are adjustable. I therefore measured the surface area of the index in order to manufacture a pin with the same surface.

To measure the surface area of the index, 58 volunteers, 40 men and 18 women, aged from 20 to 65 years were asked to tincture their index with red ink using a stamp pad and to press it against a paper sheet placed on a precision balance. They placed their index on the paper sheet as if they were touching a textile fabric and pressed it until they reached a force of 0.78 N (i.e. 80g read on the precision balance). I then scanned the fingerprints, converted each image into jpeg format and analysed them using ImageJ program. The calibration was realised with a square of 2 cm side length. The fingerprints were considered ellipsoidal. The mean contact area of the index with the paper sheet was  $1.56 \pm 0.38 \text{ cm}^2$ . It was slightly higher for men ( $1.60 \pm 0.37 \text{ cm}^2$ ) than for women ( $1.46 \pm 0.37 \text{ cm}^2$ ). The pin used in friction experiments was thus 1.7 cm long and 0.9 cm wide i.e. it has a surface area of  $1.53 \text{ cm}^2$ . This result is similar to the values given by Breugnot [5] and Derler [6] who respectively used a surface area of  $1.6 \text{ cm}^2$  for the mean contact area between the finger and fabrics and measured contact areas from 1.5 to  $3 \text{ cm}^2$  in touch experiments. The pin has fully rounded edges in order to reduce boundary effects.



## B. Artificial skin model

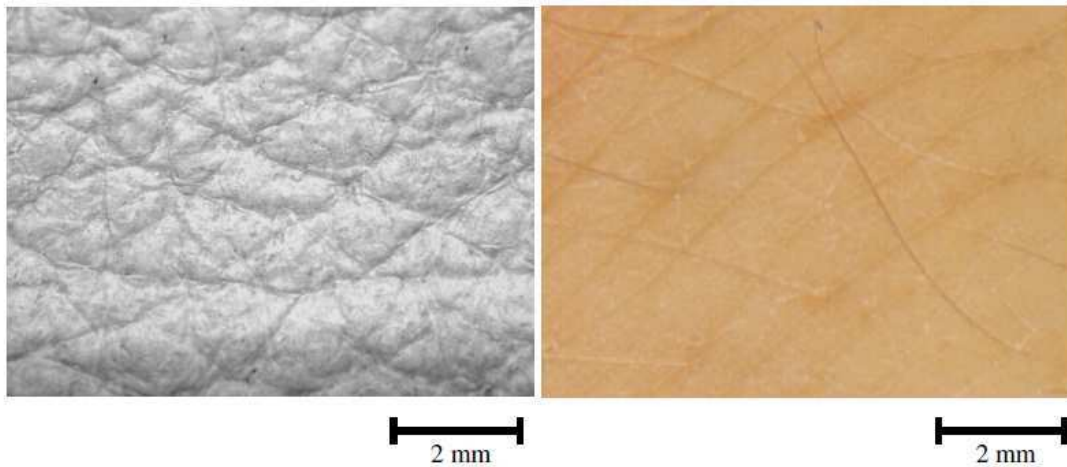


*Figure 28: Light-optical micrograph showing, on the left, the typical surface topography of the skin model Lorica® and, on the right, that of in vivo human skin (back of the hand) [7].*

The pin is covered with a polyurethane coated polyamide microfibre fleece; Lorica® (polyurethane-coated polyamide, Lorica® Soft, Lorica Sud, Milano, Italy). Lorica® presents a surface structure similar to that of skin (cf. figure 9) and was found to simulate the friction behaviour of human skin in dry conditions [6]. The pin is covered with Lorica® using double-face scotch-tape as shown on figure 10.

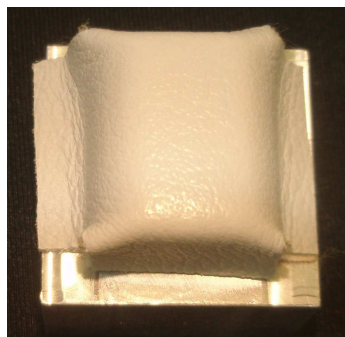


*Figure 29: Tribometer pin recovered with Lorica®.*

### C. Additional pins

In order to better understand the phenomena which take place during the friction of the socks, we wanted to compare the friction results obtained with two pins which only differ by their roughness. A product having the same material properties than Lorica® Soft combined with a smooth surface is not available. Comparative friction tests were therefore carried out with two cylinder-shaped pins made of stainless steel: a smooth one and one with 1mm diameter balls made of stainless steel stuck on its surface which will be called the “rough” one (figure 11).



*Figure 30: the smooth and “rough” pins made of stainless steel. These pins have the same surface area (in contact with the sock) than the Lorica® pin.*

To investigate the influence of the counterpart material on the friction performances, the socks were rubbed against smooth polyurethane because Lorica® is a polyurethane coated polyamide. The mean arithmetic roughness of Lorica® and smooth polyurethane was measured using a Taylor – Hobson Surtronic 3 roughness meter under 100 mN with a tip of 5 mm. It respectively equals  $19.44 \pm 1.69 \mu\text{m}$  and  $0.51 \pm 0.16 \mu\text{m}$  for Lorica® and smooth polyurethane.

## 2. Characteristics of the reciprocating movement

### A. Sliding movement amplitude

The distance over which the foot slides in the shoe during running is not easy to measure. However, the size of blisters can give us an idea of this distance. According to Knapik et al. [8], the size of blisters corresponds indeed to the area where the rubbing is applied. Herring and Richie [3] observed blisters from 0.087 to 0.812 cm<sup>2</sup>. Moreover, blisters

of less than 5 mm in diameter were qualified as small blisters by Bergeron [2]. We therefore presumed that the sliding distance of the foot in the shoe should not far exceed 5mm and thus fixed the sliding distance of the pin on the sock to this value.

## B. Sliding movement frequency and applied normal force

We have seen in the previous chapter that the pressure the shoe – sock system applies on the foot skin depends on the area of the foot and on the running speed. The literature indicates the areas of the foot which experience the highest forces but no data is available on the forces exerted on the areas we wanted to study (section I). We therefore measured the force at these specific areas. We thus needed a force measurement system which can be inserted in the shoe of a volunteer without modifying the force exerted by the footwear on its foot skin and without disturbing the runner so that its running gait remained unchanged. Insoles systems have a nonnegligible thickness and therefore reduce the force on the foot. Moreover, we needed to record the force on skin areas outside the foot sole. A flexible piezoresistive force sensor FlexiForce® (Tekscan, South Boston, USA) matched our needs (figure 12).

FlexiForce® is 208  $\mu\text{m}$  thick, 14 mm wide and its length can vary from 51 to 203 mm. Its active zone is round shaped and has a diameter of 9.53 mm i.e. it has a 0.71  $\text{cm}^2$  active surface. The electrical resistance of the sensor is inversely proportional to the applied load. The response time of this sensor is 5  $\mu\text{s}$ ; impact forces can thus be recorded. When running, the force applied on a specific area of the foot may change very quickly as the foot is hardly ever motionless; a low response time was therefore necessary. FlexiForce® can work either in cold or hot environments (from  $-9^\circ\text{C}$  to  $60^\circ\text{C}$ ) and can support forces up to 440N depending on the model.



Figure 31: FlexiForce® sensor.

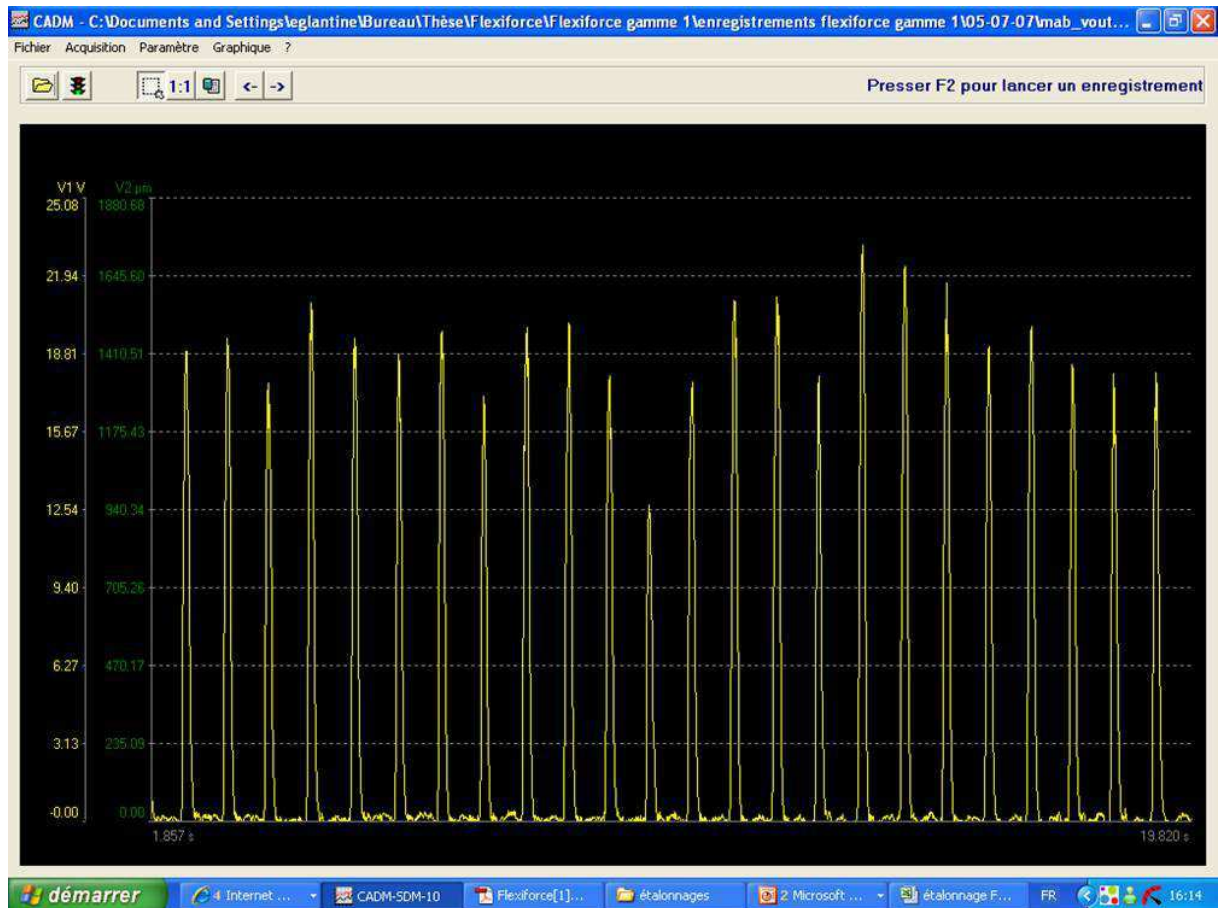


Figure 32: Record of a run at 8 km/h with FlexiForce® placed at the plantar fascia.

Signals are recorded using a data acquisition system SDM 10 and CADM software (Doerler Mesures, Vandoeuvre-lès-NANCY, France). Figure 13 shows a record obtained with a FlexiForce® sensor. On this graph, the voltage, which corresponds to the force (sensor calibration), is plotted in function of time. From the recorded force signal, peak forces, mean force and stride frequency can be calculated.

5 volunteers were asked to run on a treadmill with their own footwear in a climate controlled room (20°C and 65% RH). Three women and two men, aged from 25 to 47 years old, with weights between 52 and 76 kg participated in this study. The sensor was fixed on their foot with adhesive tape. Then, they chose their running speed and first got used to the treadmill. Thereafter, one run was recorded for each foot area (zones 1 to 5). Running speeds varied from 8 to 13 km/h. The sliding frequency of the foot in the shoe was assumed to be equal to the stride frequency i.e. 1.2 to 1.5 Hz for a running velocity of 8 to 13 km/h. The forces and sliding frequencies recorded are given in table 9.

We focused our measurements on the plantar fascia area. The sliding frequency was then fixed to 1.5 Hz and the vertical forces ranged from 0.5 to 2.2 N.

AREA OF THE FOOT	FIRST METATARSAL HEAD	PLANTAR FASCIA	HEEL	BIG TOE	LITTLE TOE
Force range (N)	5 to 20	0.44 to 2.14	0.87 to 4.4	1 to 15	1.89 to 9.33
Sliding frequency range	1.2 to 1.5 Hz				

*Table 12: Force and frequency ranges.*

#### **IV. TEXTILE FRICTION ANALYSER (TFA)**

This device has been developed by the EMPA [9] to monitor normal and friction forces at the same time. It includes an elevation arm (cf. figure 14) whereby friction test functionalities can be implemented by measuring and controlling vertical load over an adjustable force range up to 20 N. The reciprocating motion of the metallic support is created by a stepper motor which is operated by a programmable controller. Friction forces are measured using a highly sensitive quartz load cell (Type 9203, Kistler, Winterthur, Switzerland) with a maximum resolution of 5 mN connected to a charge amplifier (Type 5011B, time constant: 10s). Vertical forces are recorded using a strain-gauge force transducer (Type U9B, HBM, Darmstadt, Germany) with a maximum resolution of 10 mN. The position of the manoeuvrable weight can be changed whereby the normal load can be adjusted. The weight is driven by a DC motor (A-max 26, Maxon, Sachseln, Switzerland).

The TFA is different from the LPMT's tribometer in terms of contact surface, applied normal load and sliding velocity. Firstly, the LPMT's tribometer has a chamfered rectangular

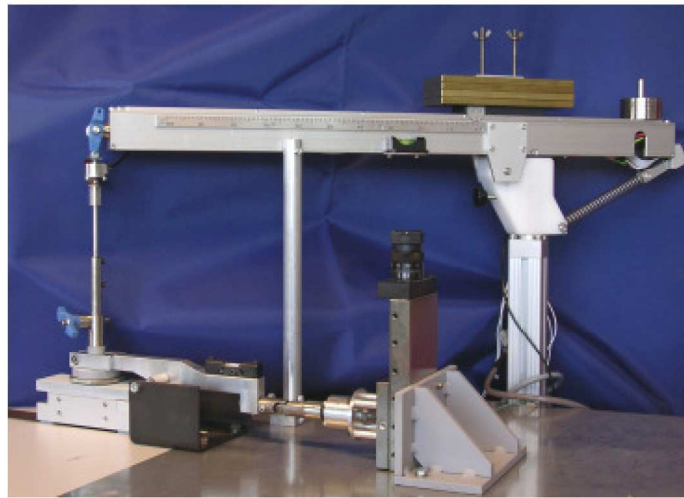
pin of 1.53 cm<sup>2</sup> surface while the TFA pin is round shaped with a diameter of 2.8 cm i.e. a surface of 6.16 cm<sup>2</sup>. Friction experiments were then realised for the same pressures.

Secondly, the LPMT's tribometer is a dead weight tribometer i.e. the pin is free to move up and down under the influence of the textile structure during a friction test. On the TFA, the distance between the pin and the elevation arm is fixed when setting the device (the manoeuvrable weight is moved until the strain-gauge sensor perceives the desired normal load). In fact, the system is also composed of a dead weight but the elevation arm is linked to its support by a pivot and a spring gives rigidity to the system (cf. figure 14). The pin thus cannot raise itself up freely. Therefore, for the LPMT's tribometer, the applied normal load is constant and corresponds to the dead weight whereas for the TFA, the applied normal load varies around a mean value which is higher than the dead weight of the LPMT's tribometer for the same setting value. The vertical load applied by the TFA versus time for a set point of 9.49 N is given figure 15.

Thirdly, the sliding velocity is triangular shaped for the LPMT's tribometer while for the TFA, the sliding velocity signal is 40% ramp shaped (20% ascending ramp to reach the set point velocity then 60% constant velocity and 20% descending ramp).

Finally, friction force signals recorded using the LPMT's tribometer are noisy compared to the signals recorded using the TFA because on the LPMT's tribometer the friction force signal is not filtered while a low-pass filter is applied to the data recorded on the TFA.

Neither the linear alternating dead weight tribometer nor the TFA exactly reproduces the friction of the foot with the sock in the shoe. For the LPMT's tribometer, the weight is free to move vertically while in the case of the TFA, the system is fixed. In-shoe conditions are probably an intermediate between these two cases. Friction experiments were therefore carried out on both tribometers. Both the TFA and the LPMT's tribometer can be improved in order to better reproduce the friction between the sock and the foot of a runner during jogging. The materials in contact, the pressure and the sliding frequency have been adapted but the experimental measures do not entirely simulate the frictional conditions on anatomical body shapes. The use of curved rubbing elements could, in a further study, simulate the contact of textile fabrics against skin overlying bony prominences. The pin may also be designed in order to reproduce the shape of the tested foot area. Moreover, a shoe insole may be placed under the sock.



15 cm

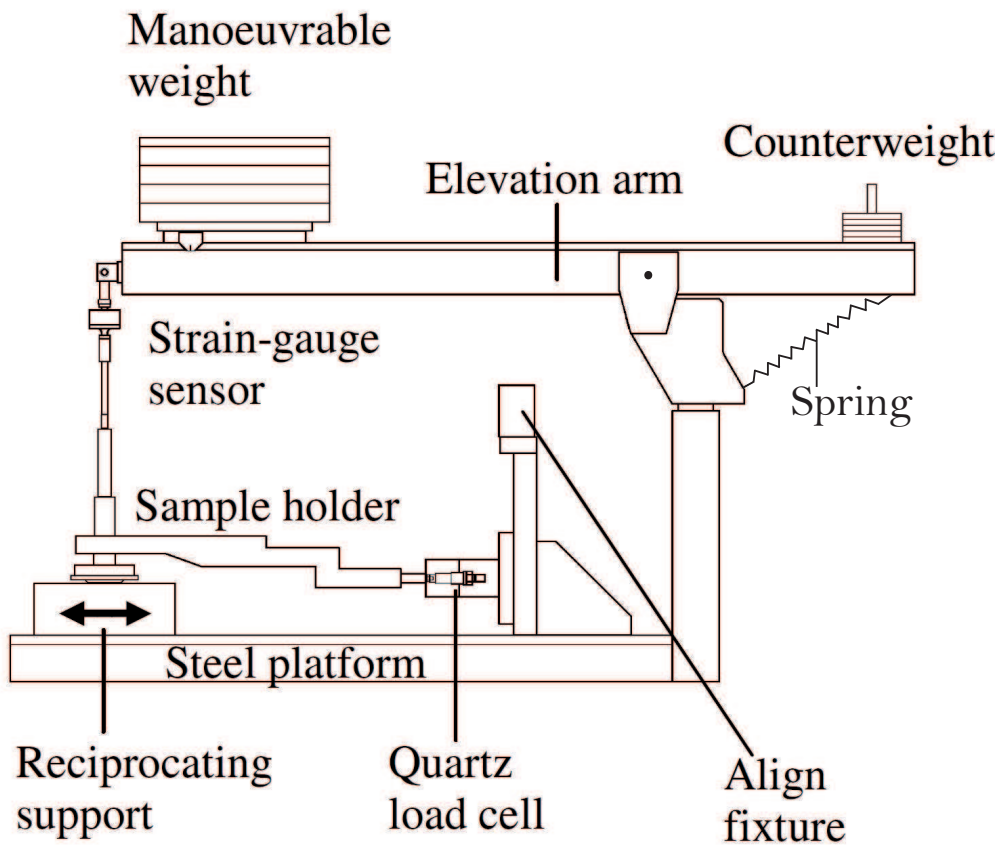


Figure 33: TFA device [7].

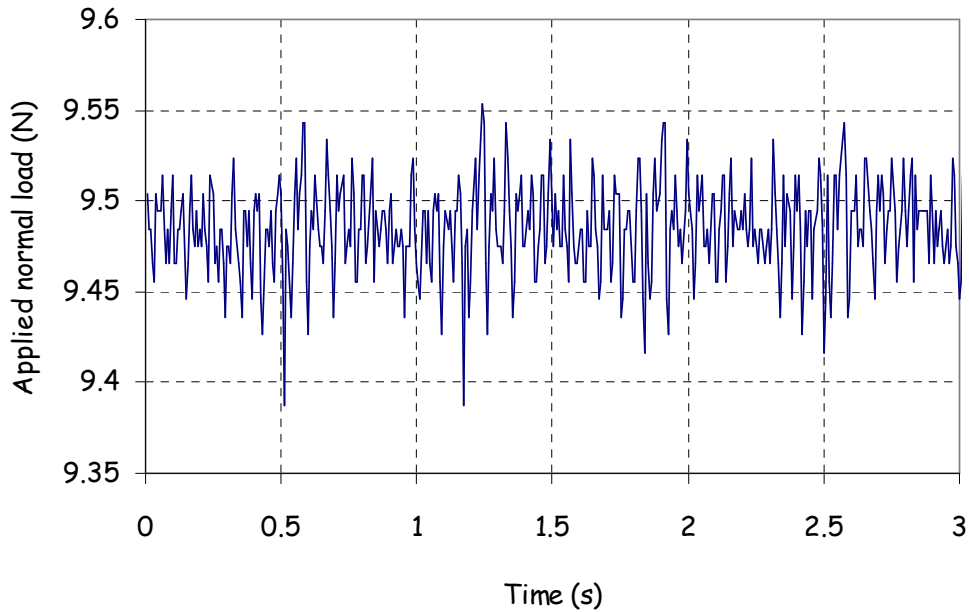


Figure 34: Normal load applied by the TFA in function of time for a set point of 9.49 N.

## V. COMPRESSION EXPERIMENTS

The pressure exerted on the foot by the footwear depends on the shape and the cushioning properties of the shoe, the friction and compression behaviour of the sock and on the skin characteristics. Compression tests for socks were implemented on KES FB3 [10]. A FlexiForce® sensor was placed on the compression plunger surface with double-face scotch-tape and the socks were positioned with the face up and the back side down as shown on figure 16. The pressure the plunger applied on the face of the sock was recorded by the FlexiForce® sensor and corresponds to the pressure exerted by the shoe on the sock. The pressure transmitted to the back of the sock is recorded by the force transducer of the KES FB3 and corresponds to the pressure exerted by the footwear on the foot skin. The FlexiForce® signal was recorded on a computer using the related software and the KES FB3 signal was saved using an oscilloscope.



The following settings were chosen:

FlexiForce® software and oscilloscope:

- 100 points/s.
- The measure is manually and automatically started for the FlexiForce® and the oscilloscope respectively.
- The measure lasts for 200 s for terry jersey socks and for 100 s for the other knitted structures.

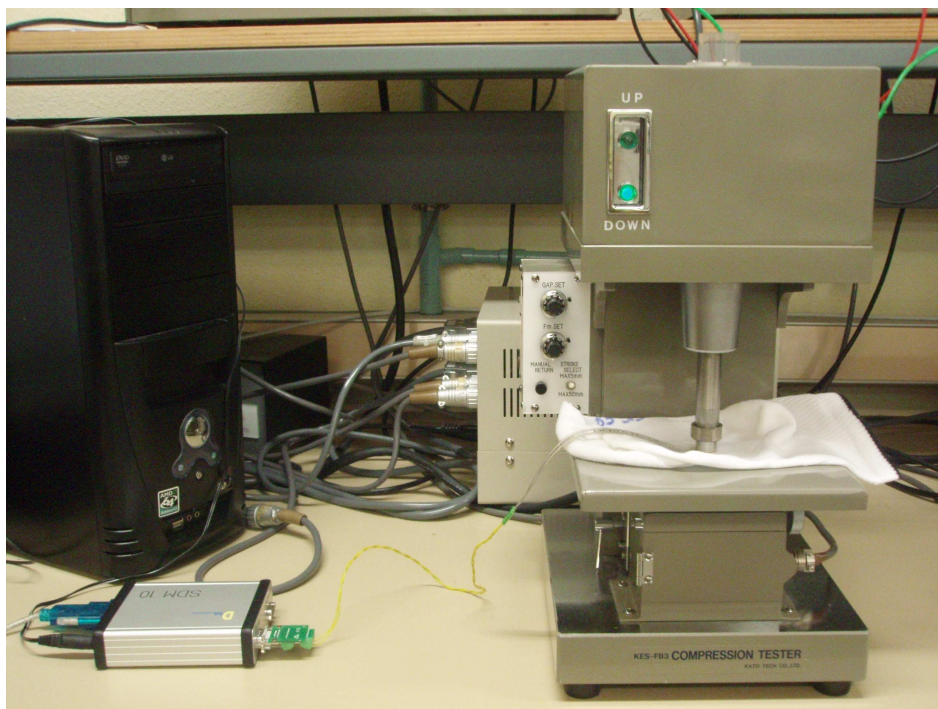


*Figure 35: KES FB3 equipped with FlexiForce®.*

KES FB3:

- Plunger velocity:  $0.02 \text{ mm.s}^{-1}$ .

This velocity is of course very low compared to the velocity with which the foot touches the ground when running; it was limited by the sampling frequency of the Flexiforce®. However, compression experimentations realised on velvet fabrics by Camillieri [11] at velocities from  $0.02$  to  $0.2 \text{ mm.s}^{-1}$  show a negligible influence of the velocity on the compression results.

- Maximum pressure of 15 kPa.

Calibration test without sample

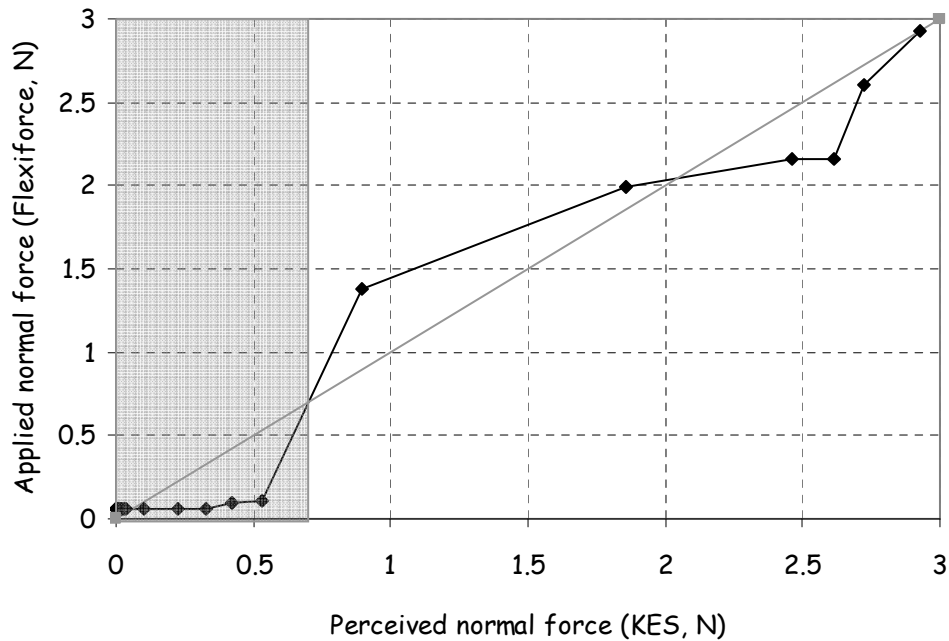


Figure 36: One calibration test; applied normal force (measured with Flexiforce®) versus perceived normal force (measured with KES transducer). The black curve is the calibration curve while the grey line is the expected result.

A calibration test was first carried out. During the calibration test, the KES plunger applied a force on the surface of the Flexiforce® i.e. on 0.71 cm<sup>2</sup> while the force measured by the KES force transducer was measured on 2 cm<sup>2</sup>. As there is no sample on the compression tester, the transmitted force should be equal to the applied force. On the other hand, for tests with textile fabrics, as the plunger of the KES sinks in the textile sample, the applied force is distributed over the entire surface of the plunger i.e. 2 cm<sup>2</sup>, the same surface on which the transmitted force is measured. Calibration test results are thus displayed in force while the results of the compression tests with textile samples are given in pressure.

Calibration test results are reported in figure 17 which displays the applied normal force i.e. the force measured by the Flexiforce® in function of the perceived normal force i.e. the force measured by the KES force transducer. It can be noticed that the behaviour of the Flexiforce® is not linear, the grey area corresponds to a perceived normal force higher than the applied normal force which is not possible physically. The compression results will be analysed without considering this zone. The latter zone will be identified by a grey area on the compression curves.

## Literature cited

1. Mailler, E.A. and B.B. Adams, *The wear and tear of 26.2: dermatological injuries reported on marathon day*. British Journal of Sports Medicine, 2004. **38**: p. 498-501.
2. Bergeron, B.P., *A Guide to Blister Management*. The physician and sportsmedicine, 1995. **23**(2): p. 37-46.
3. Herring, K.M. and D.H. Richie, *Friction blisters and sock fiber composition A double-blind study*. Journal of the American Podiatric Medical Association, 1990. **80**(2): p. 63-71.
4. Gwosdow, A.R., et al., *Skin Friction and Fabric Sensations in Neutral and Warm Environments*. Textile Research Journal, 1986. **56**: p. 574-580
5. Breugnot, C., *Contribution à la caractérisation mécanique du toucher des surfaces textiles à partir de critères neurosensoriels*, in *Sciences Pour l'Ingénieur*. 2005, Université de Haute Alsace: Mulhouse. p. 209.
6. Derler, S., U. Schrade, and L.C. Gerhardt, *Tribology of human skin and mechanical skin equivalents in contact with textiles*. Wear, 2007. **263**(7-12): p. 1112-1116.
7. Gerhardt, L.-C., *Tribology of human skin in contact with medical textiles for decubitus prevention*, in *Sciences*. 2008, ETH Zurich: Zurich. p. 206.
8. Knapik, J.J., et al., *Friction Blisters - Pathophysiology, Prevention and Treatment*. Sports Medicine, 1995. **20**(3): p. 136-147.
9. Gerhardt, L.-C., et al., *Study of skin-fabric interactions of relevance to decubitus: friction and contact-pressure measurements*. Skin Research and Technology, 2008(14): p. 77-88.
10. Kawabata, S., *The Standardisation and Analysis of Hand Evaluation*. 1980, Osaka: The Textile Machinery Society of Japan.
11. Camillieri, B., J.-M. Praëne, and M.-A. Bueno, *Simulation du frottement des surfaces fibreuses à partir de la compression transversale*, in *22èmes Journées Internationales et Francophones de Tribologie*. 2010: Albi, France.

# Chapter III: experimental results

## Résumé

Des expériences de frottement et de compression ont été réalisées afin d'étudier le contact mécanique entre la chaussette et la peau lors de la course à pied. Une étude phénoménologique identifiant le mouvement relatif du palpeur du tribomètre du LPMT et des différents tricots a pu être effectuée en observant l'évolution simultanée de la force de frottement et de la position verticale du palpeur. Pour le jersey bouclette, le palpeur s'enfonce dans la structure en couchant les bouclettes dans le sens aller du mouvement. Plus le palpeur s'enfonce plus la force de frottement augmente car l'aire de contact entre les deux corps et la déformation augmentent. Une fois les bouclettes complètement couchées, le palpeur ne bouge plus et la force de frottement reste constante. Au moment du changement de sens, les bouclettes se relèvent avant d'être couchées dans le sens opposé. Pour des pressions relativement faibles de 3 et 6 kPa, le palpeur se relève immédiatement lors du changement de direction. Pour des pressions plus élevées de 10 et 15 kPa, il faut un nombre suffisant de bouclettes sous le palpeur pour qu'il se relève, c'est pourquoi le palpeur remonte plus tard quand la pression normale augmente. De plus, au moment du changement de sens, il s'enfonce un peu plus profondément dans la structure de la chaussette car sa vitesse décroît. On observe les mêmes phénomènes pour le jersey ponts de fils, le déplacement vertical du palpeur est moindre car les ponts sont moins orientés que les bouclettes. En ce qui concerne les structures jerseys simple et double, elles semblent symétriques, la force de frottement en sens aller est très similaire à celle en sens retour mais le déplacement vertical du palpeur montre une anisotropie de tribologie de surface. Si l'on mesure la longueur des têtes et des pieds de mailles dans les deux structures, on constate que les pieds de mailles sont plus courts que les têtes de mailles. En sens aller, le palpeur passe au-dessus des têtes de mailles avant de frotter les pieds de mailles c'est pourquoi il est entraîné vers le haut, et inversement en sens contraire.

Une étude sur l'influence de la Longueur de Fil Absorbée et du titre des fils sur les propriétés tribologiques des chaussettes a également été menée. Aucune influence du titre des fils n'a été constatée tandis que pour une pression normale faible de 3 kPa, la force de frottement évolue en sens inverse de la LFA. Cela s'explique par la forme des boucles dans le

tricot, pour un titre de fil donné, plus la LFA augmente, plus les boucles sont plates. La rugosité de la surface tricotée augmente donc lorsque le LFA diminue. Pour une pression normale importante de 15 kPa, les boucles des tricots sont écrasées et la LFA n'a aucune influence sur la force de frottement.

Nous nous sommes intéressés à l'influence de la structure tricotée sur le frottement induit sur la peau d'un coureur amateur lors d'un jogging. Nous avons pu observer que la forme et l'amplitude de la courbe de force de frottement dépend fortement de la structure considérée. Les jerseys simple et double présentent des propriétés tribologiques similaires avec un comportement symétrique tandis que le jersey bouclette a un comportement asymétrique du fait de l'orientation des bouclettes. Pour une distance de frottement inférieure à 2,5 mm, le jersey bouclette induit un frottement moindre que les jerseys simple et double. Pour une distance supérieure à 2,5 mm, le jersey bouclette produit une force de frottement égale ou supérieure à celle induite par les autres structures tricotées. Les bouclettes des chaussettes Labonal sont orientées de la pointe de la chaussette vers le talon lorsqu'elles sont portées en contact avec la peau. Or, lorsque le pied entre en contact avec le sol, il glisse vers l'avant de la chaussure donc en sens opposé de l'orientation des bouclettes ce qui va générer un frottement élevé sur la peau. Il serait plus approprié de tricoter les chaussettes en commençant par la jambe de manière à avoir des bouclettes orientées dans le sens le plus préférable. Deux qualités de chaussettes bouclettes ont été étudiées, les chaussettes Labonal présentent des bouclettes plus homogènes, plus compactes et moins faciles à écraser. Les courbes de frottement du jersey bouclette Labonal sont différentes de celles des jerseys simple et double tandis que le comportement des autres jerseys bouclette se rapproche de celui des jerseys simple. Nous pouvons donc conclure que la forme particulière des courbes de frottement du jersey bouclette Labonal est due à la rotation des bouclettes lors d'un cycle de frottement.

Nous avons aussi étudié l'influence de la rugosité du palpeur sur les signaux de frottement des différentes structures tricotées. Nous avons observé que pour les jerseys simple et bouclette la force de frottement augmente avec la rugosité du palpeur. Le frottement est dû à de la déformation et à de l'adhésion. Ici, les contributions respectives de la déformation et de l'adhésion ne sont pas mesurées indépendamment, on ne peut donc que comparer leur

importance relative dans le frottement. Les phénomènes d'adhésion augmentent avec l'aire de contact i.e. quand la rugosité du contact diminue. Vu qu'ici la force de frottement croît lorsque la rugosité du palpeur augmente, nous en déduisons que la contribution de la déformation dans le frottement est essentielle. En comparant les courbes de frottement obtenues pour les jerseys simple et bouclette en contact avec le palpeur lisse en acier et le palpeur recouvert de Lorica®, on observe une force de frottement plus importante dans le cas du palpeur recouvert de Lorica®, cependant la différence entre les deux résultats est importante dans le cas du jersey simple et faible dans le cas du jersey bouclette. Dans le cas du jersey bouclette, les propriétés du palpeur sont donc moins importantes que dans le cas du jersey simple, la part de l'adhésion dans le frottement est moindre et la contribution de la déformation est donc plus importante.

Nous avons comparé les différentes structures de chaussettes en termes de frottement induit sur la peau. Cependant, la chaussette, de par sa structure et son épaisseur, peut atténuer la pression ressentie sur la peau et ainsi réduire les risques de génération de phlyctènes. Des mesures de compression ont donc été réalisées afin de mesurer, pour une pression appliquée donnée (même sol, même chaussure et même coureur), la pression exercée sur la peau pour les différentes chaussettes étudiées. On observe que la pression exercée sur la peau augmente lorsque le titre des fils augmente. Pour une même LFA, lorsque le titre des fils augmente, les fils sont moins souples et la chaussette moins compressible. Les résultats de compression montrent que le jersey simple présente un meilleur « amortissement statique » que le jersey bouclette. Cependant, la pression maximale ressentie est obtenue pour une profondeur de pénétration plus importante dans le cas du jersey bouclette que dans le cas du jersey simple, ce qui nous a fait penser que le jersey bouclette pourrait présenter un meilleur « amortissement dynamique » que le jersey simple. Nous avons donc testé la capacité de dissipation de l'énergie de ces deux tricots lors d'un choc en lâchant une bille sur ces deux chaussettes d'une hauteur donnée et en mesurant la hauteur du premier rebond de la bille. Il s'avère que le jersey bouclette dissipe effectivement plus d'énergie que le jersey simple.

Les structures jersey double et jersey ponts de fils ont été étudiées en tant qu'intermédiaires entre le jersey simple et le jersey bouclette. Leurs résultats de frottement révèlent effectivement un comportement intermédiaire mais beaucoup plus proche de celui du



jersey simple que de celui du jersey bouclette. Quant à leurs résultats de compression, ils montrent que ces structures sont plus dures que les deux autres et donc moins adaptées pour des chaussettes de sport. C'est pourquoi les conclusions de cette étude ne porteront que sur les structures jerseys simple et bouclette. L'épaisseur d'une chaussette bouclette est un moyen simple, efficace et bon marché d'améliorer le confort de personnes dont les pieds présentent des proéminences osseuses et des ampoules préexistantes. Les expériences de frottement, de compression et d'absorption des chocs ont montré que :

- Pour une force normale donnée, une chaussette en jersey bouclette induit un frottement sur la peau moins important qu'une chaussette en jersey simple à conditions que les bouclettes soient compactes, homogènes et orientées dans la direction de la force de frottement.

- Lors d'une compression progressive, pour la même énergie de compression reçue, le jersey simple transmet sur la peau une énergie de compression moins importante que le jersey bouclette. Le jersey simple apporte donc un meilleur « amortissement statique » ou quasi-statique.

- Quand on lâche une bille d'une hauteur donnée sur des chaussettes en jersey simple et bouclette, le premier rebond de la bille est moins haut dans le cas du jersey bouclette. Le jersey bouclette présente par conséquent un meilleur « amortissement dynamique ».

La confrontation des résultats de frottement, de compression et d'absorption des chocs permet de conclure que :

- Lors de la marche, quand le pied est soumis à la fois à du frottement et à de la compression progressive, la structure tricotée la plus indiquée est le jersey simple.

- Lors de la course à pied, la peau est d'abord soumise à un choc puis à de la compression progressive et du frottement. Il reste à déterminer l'influence de ces trois sollicitations sur la génération de phlyctènes. Le jersey simple présente de meilleurs résultats en termes de frottement et d'« amortissement quasi-statique » tandis que le jersey bouclette est plus performant en termes d'« amortissement dynamique ». Dans le cas du jersey bouclette, il est à noter que sa structure peut être améliorée significativement par des bouclettes compactes et homogènes orientées vers la pointe du pied de manière à réduire le frottement exercé sur la peau lorsque le pied glisse dans la chaussure.

- Si le coureur amateur n'a que des chaussettes en jersey bouclette, il lui faut déterminer l'orientation des bouclettes. Si les boucles sont orientées du talon vers la pointe de la chaussette lorsque la face bouclette est en contact avec la peau, il est alors recommandé de

les porter en contact avec la peau. Si les boucles sont orientées en sens inverse, ce qui est le cas de la plupart des chaussettes vendues dans le commerce, il est préférable de porter les bouclettes en contact avec la chaussure et l'autre face en contact avec la peau ce qui permettra de réduire le frottement sur la peau.

# CONTENTS

<i>Chapter III: experimental results</i>	<u>100</u>
I. FRICTION EXPERIMENTS	<u>107</u>
1. Phenomenological study	107
2. Pressure influence	116
A. On the friction force	116
B. On the coefficient of friction	123
3. Stitch length and yarn count influence	128
4. Sock structure influence	131
5. Influence of the pin material and roughness	139
A. Experiments using the Lorica® and the smooth polyurethane pins	139
B. Experiments using the smooth and the “rough” pins made of stainless steel	146
II. COMPRESSION EXPERIMENTS	<u>149</u>
1. Sock structure impact	149
2. Yarn count influence	152
3. Energetic approach	154
III. CONCLUSION	<u>155</u>

Friction and compression experiments were carried out in order to investigate the mechanical contact between the sock and the foot skin during running.

These experiments will be successively detailed, friction tests in a first part and compression experimentations in a second part. The influence of the applied pressure, the yarn count, the stitch length and structure, the pin material and roughness will be investigated within the following pages.

## **I. FRICTION EXPERIMENTS**

### **1. Phenomenological study**

When considering the evolution of both friction force and vertical position of the pin versus time, the phenomena which occur during a friction test between the Lorica® pin and the different socks can be identified. The vertical position of the pin is a relative position i.e. 0 corresponds to the lowest position of the pin. The laser sensor has a sensibility of 5  $\mu\text{m}$  in dynamic experiments and 1  $\mu\text{m}$  in static experiments.

It can be seen in figures 1a and 1b that, for Labonal terry jersey socks under 3 and 6 kPa, the pin first sinks in the terry structure as it flattens the loops. The more it sinks the higher the friction force due to the increase in contact area and deformation. Once the terries are laid down, the pin stays at the same position and the friction force keeps constant. When the direction of the movement changes, the pin flattens the terries in the opposite direction, it thus moves upwards until all the terries are laid down. For pressures of 10 and 15 kPa, Figures 1c and 1d show the same phenomena except that when the direction of the movement changes, the pin does not go up immediately but sinks little more in the textile structure before going up flattening the terries. In the reverse direction, the number of terries under the pin has to be sufficient for the pin to go up and lay down the terries. The pin therefore moves upwards later when normal pressure increases and it before sinks deeper in the structure because its velocity decreases at the direction change. These explanations are corroborated by videos.

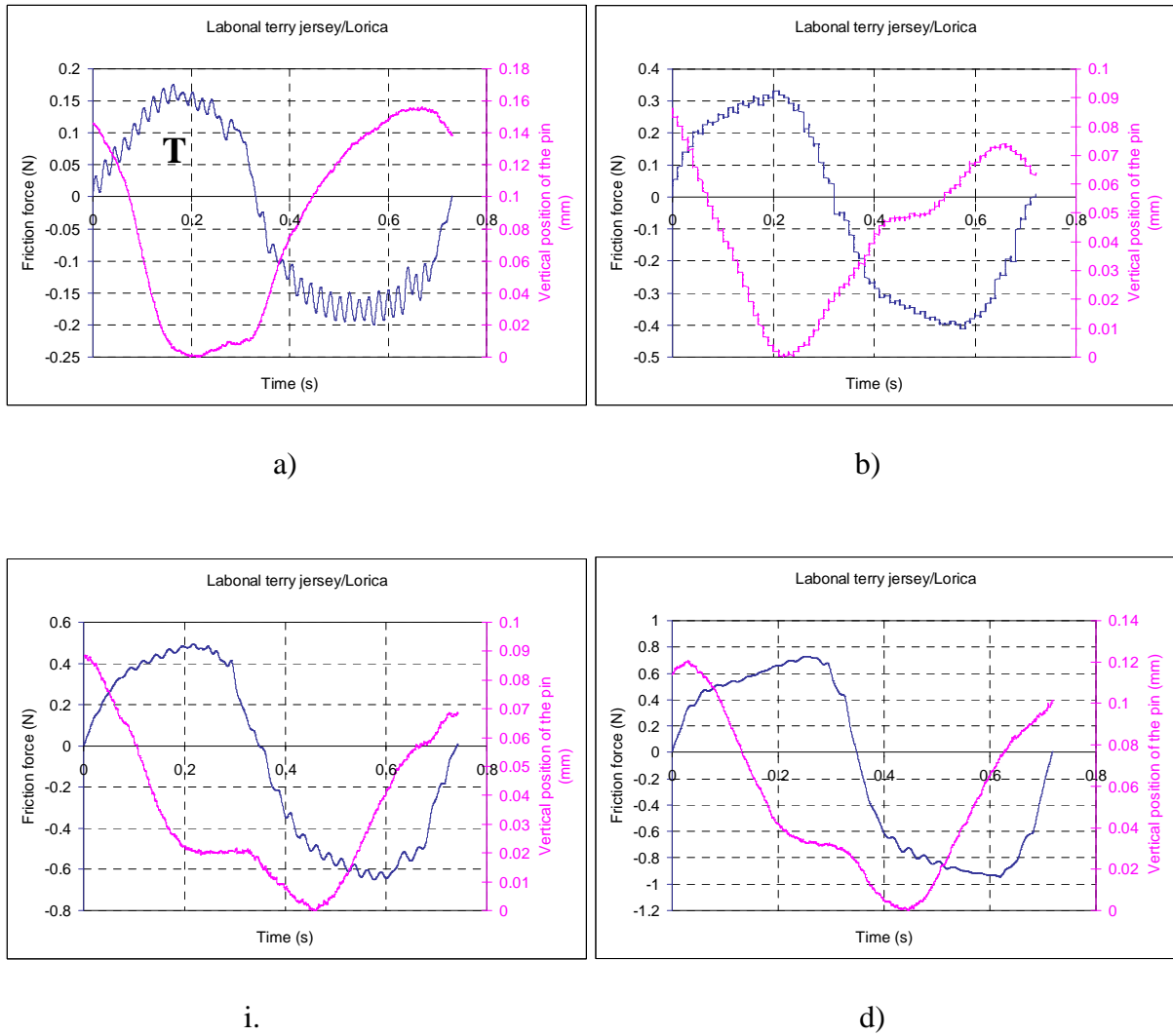


Figure 37: Friction force and vertical position of the pin for Labonal terry jersey socks in contact with the Lorica® pin for a friction cycle. The mean curves were calculated from 10 experiments for a friction distance of 5 mm, a friction frequency of 1.5 Hz and a pressure of respectively a) 3 kPa, b) 6 kPa, c) 10 kPa and d) 15 kPa. The letter T identifies the half period where the movement of the pin follows terries orientation.

The same phenomena were observed for Labonal yarn bridges (cf. figure 2). The bridges are indeed oriented in the same direction than the terries with a smaller angle. As bridges are less oriented than terries, the phenomena are less pronounced, i.e. the vertical pin displacement is smaller in the case of the Labonal yarn bridges.

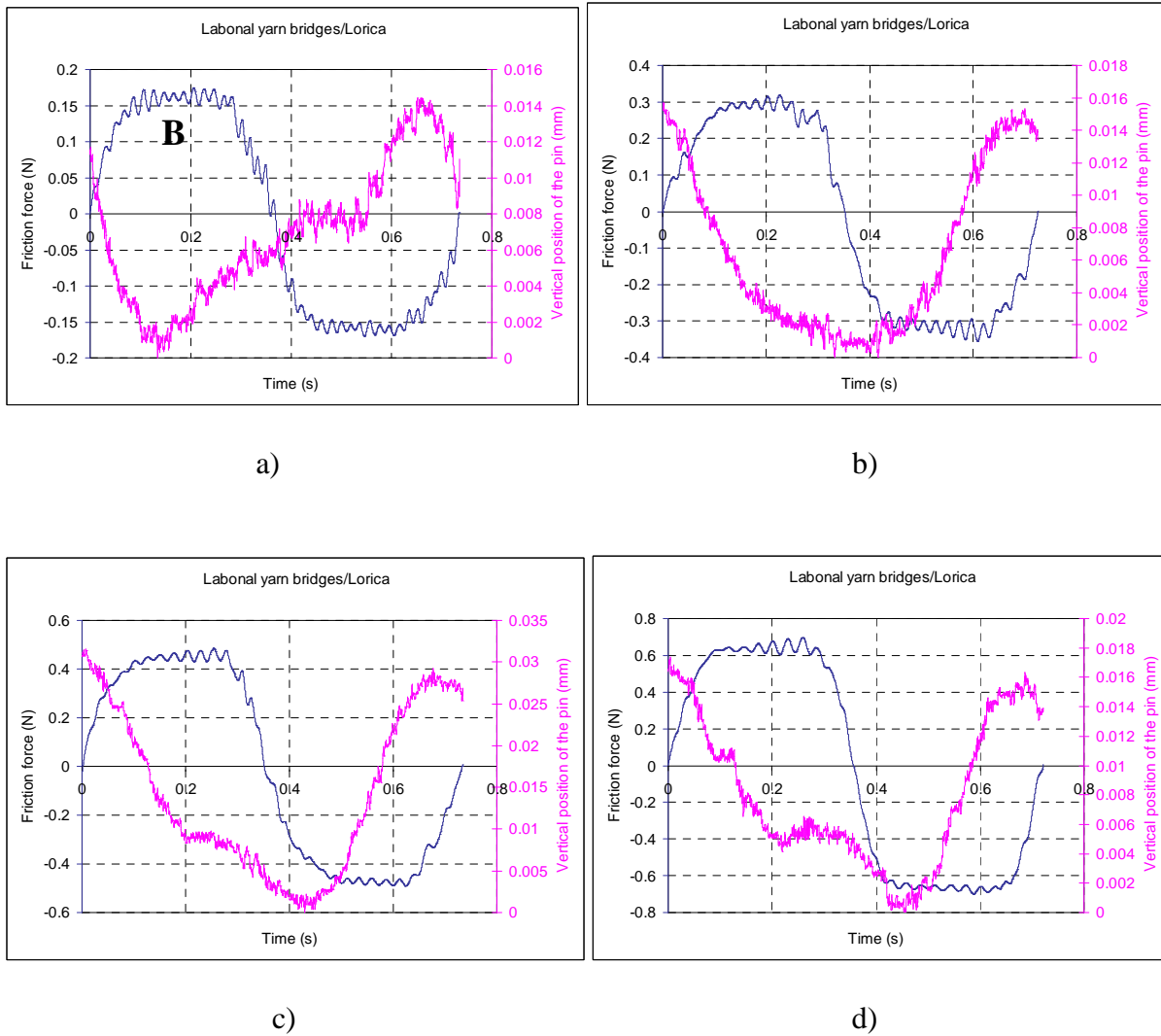


Figure 38: Friction force and vertical position of the pin for Labonal yarn bridges socks in contact with the Lorica® pin for a friction cycle. The mean curves were calculated from 10 experiments for a friction distance of 5 mm, a friction frequency of 1.5 Hz and a pressure of respectively a) 3 kPa, b) 6 kPa, c) 10 kPa and d) 15 kPa. The letter B identifies the half period where the movement of the pin follows bridges orientation.

As for Labonal double and simple jersey socks (cf. figures 3 and 4), it seems that these two structures also present an anisotropy of surface tribology even if these structures seem to be symmetrical relative to an axis in the course direction. The friction force for the forward and the reverse direction show very small difference but the laser sensor that gives the vertical position of the pin is sensible to this anisotropy. In order to understand this anisotropy, it is necessary to consider the different parts of a stitch (cf. figure 5). When looking at figures 6a

and 6b, it is not obvious that the top arcs and the bottom arcs of Labonal double and simple jersey do not have the same length but the bottom arcs are indeed smaller than the top arcs (cf. table 1).

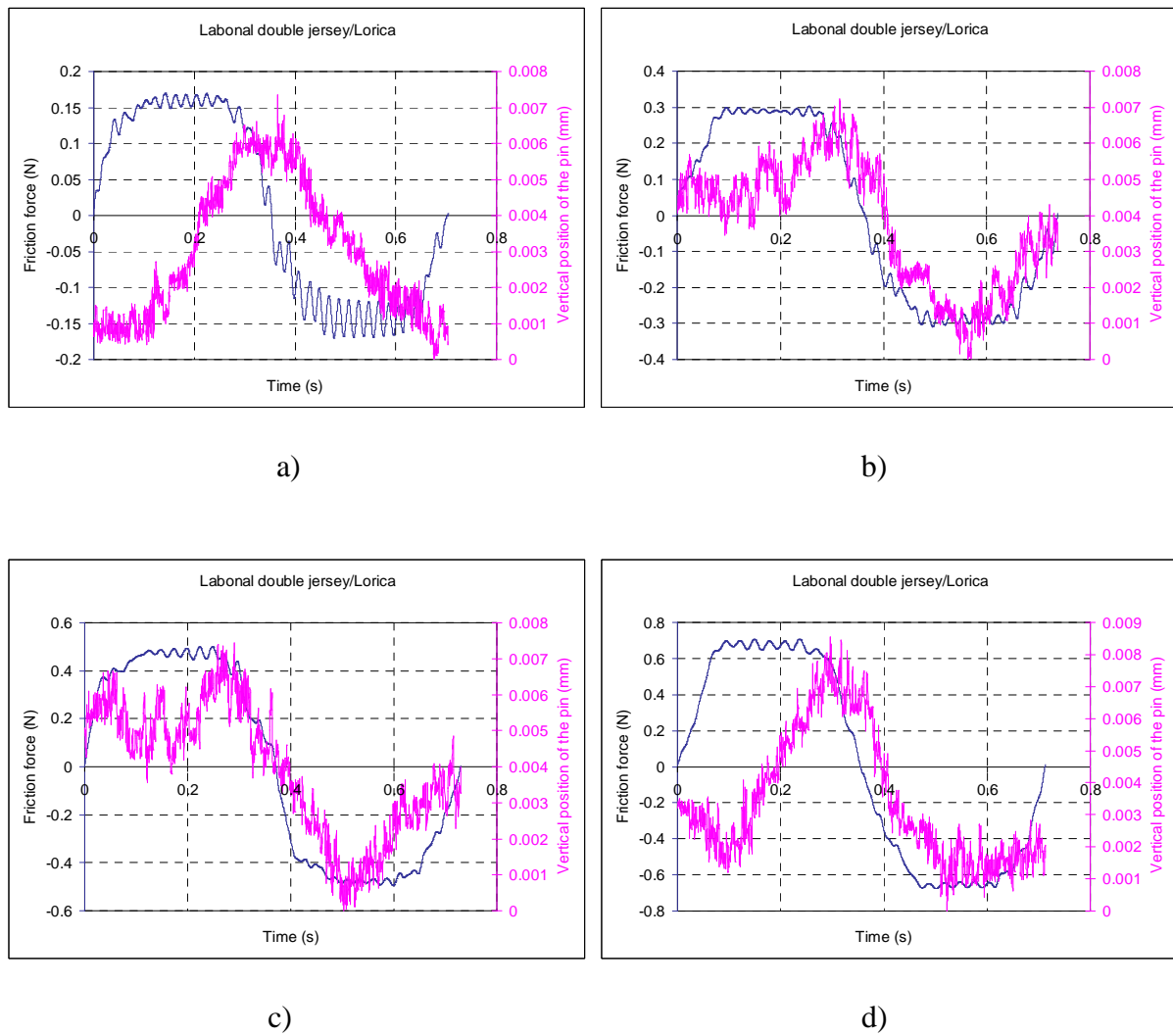


Figure 39: Friction force and vertical position of the pin for Labonal double jersey socks in contact with the Lorica® pin for a friction cycle. The mean curves were calculated from 10 experiments for a friction distance of 5 mm, a friction frequency of 1.5 Hz and a pressure of respectively a) 3 kPa, b) 6 kPa, c) 10 kPa and d) 15 kPa.

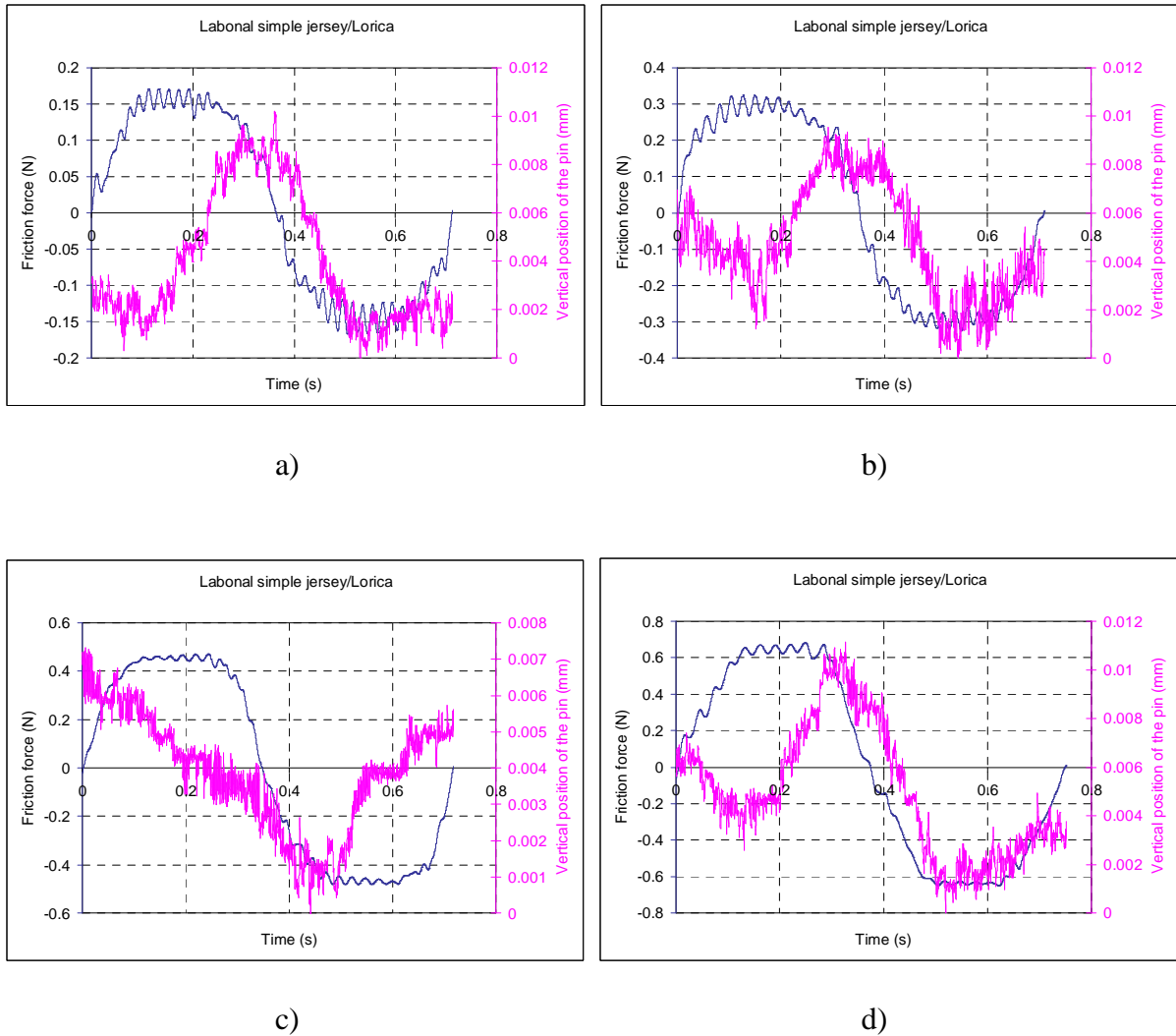


Figure 40: Friction force and vertical position of the pin for Labonal simple jersey socks in contact with the Lorica® pin for a friction cycle. The mean curves were calculated from 10 experiments for a friction distance of 5 mm, a friction frequency of 1.5 Hz and a pressure of respectively a) 3 kPa, b) 6 kPa, c) 10 kPa and d) 15 kPa.

In the forward direction, the pin goes up the top arcs of the stitches and sinks in the bottom arcs of the stitches and inversely for the reverse direction. Considering the sensibility of the laser sensor (5  $\mu\text{m}$  in dynamic), figures 3 and 4 show that the pin goes up before the direction change and goes down once the direction has changed which can be explained by the larger length of top arcs compared to the bottom arcs of the stitches.



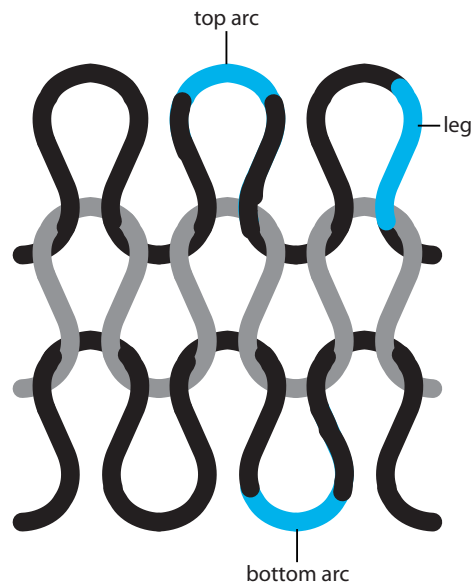


Figure 41: Different parts of a stitch.

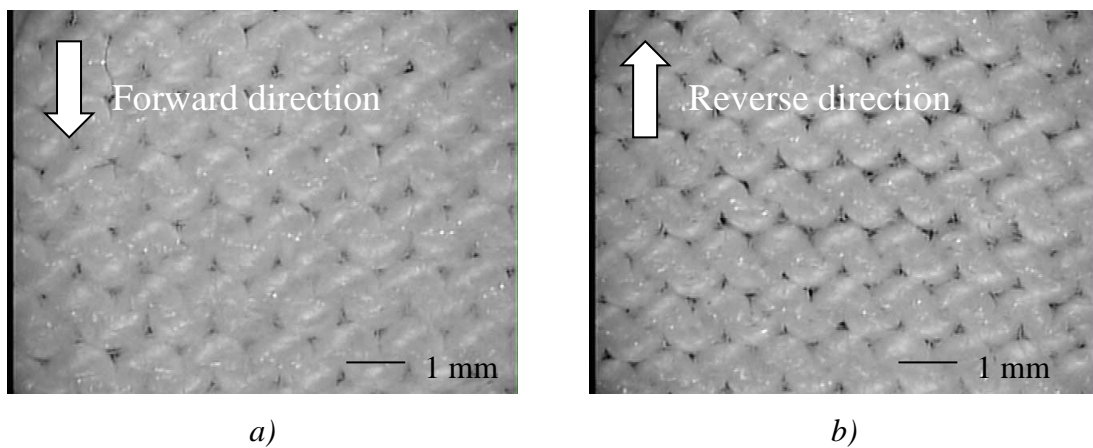


Figure 42: Back of a) Labonal double jersey and b) Labonal simple jersey.

SOCK	MEAN LENGTH OF THE BOTTOM ARCS (MM)	MEAN LENGTH OF THE TOP ARCS (MM)
Labonal double jersey	1.08	1.22
Labonal simple jersey	0.97	1.10

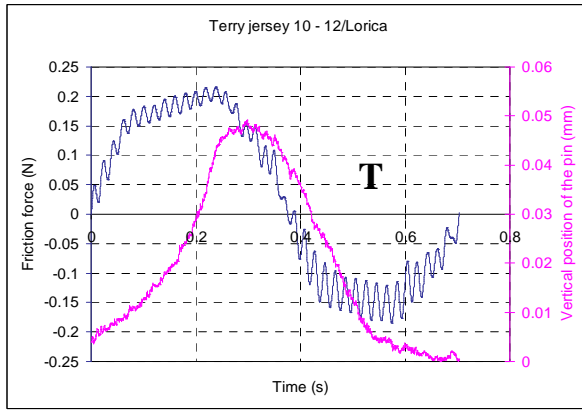
Table 13: Mean length of the bottom and the top arcs of Labonal double and simple jersey socks.

In this chapter, I present experimental results concerning the friction behaviour for Labonal socks and for the six other socks. It has to be noticed that the terries of these socks are oriented towards the toe of the sock i.e. in opposite way compared to Labonal terry jersey and yarn bridges.

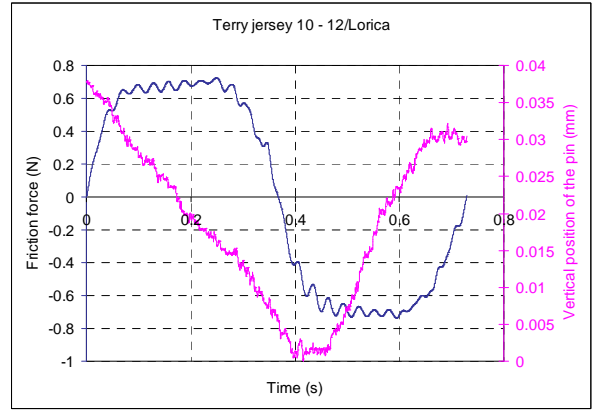
For terry jersey 10 - 12, 10 - 16, 10 - 20, 9 - 16 and 11 - 16, the curves given in figures 7 and 8 show the same behaviour. These terry jersey socks have different behaviours for low and for higher pressures. For a low pressure of 3 kPa, it can be noticed in figures 7a, 7c, 7e, 8c and 8e that they behave in the same manner than Labonal terry jersey and yarn bridges socks. The vertical movement of the pin is just inversed compared to Labonal terry jersey and yarn bridges socks i.e. the pin first goes up because it lifts and pushes the terries to the vertical as the terries of these socks are oriented in opposite way compared to Labonal terry jersey and yarn bridges socks (cf. table 8 chapter II). When the sliding direction switches, the pin sinks in the terry structure flattening the terries.

The terries and yarn bridges of Labonal socks are more elastic and less easy to swat than the other terries. They thus have the same behaviour for low and higher pressure while, in the case of terry jersey 10 - 12, 10 - 16, 10 - 20, 9 - 16 and 11 - 16, for a pressure of 15 kPa, the vertical displacement of the pin is inversed compared to the case of a pressure of 3 kPa, When sliding in the opposite direction of terries orientation, the pin does not lift and push the terries but goes down crushing the terry structure and when the sliding direction changes, the pin goes up sliding along the terries which came back to their initial position (figures 7b, 7d, 7f, 8d and 8f).

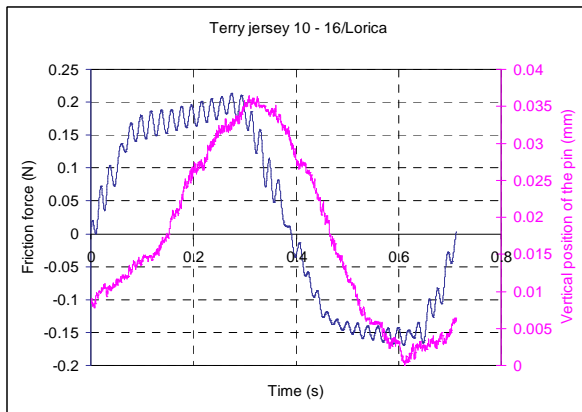
Simple jersey 10 - 16 (figures 8a and 8b) presents the same surface anisotropy as Labonal double and simple jersey. The top arcs of the stitches are 6% longer than the bottom arcs. In the forward direction, the pin goes up the top arcs of the stitches and sinks in the bottom arcs of the stitches and inversely for the reverse direction. The pin therefore goes up before the direction change and goes down once the direction has changed.



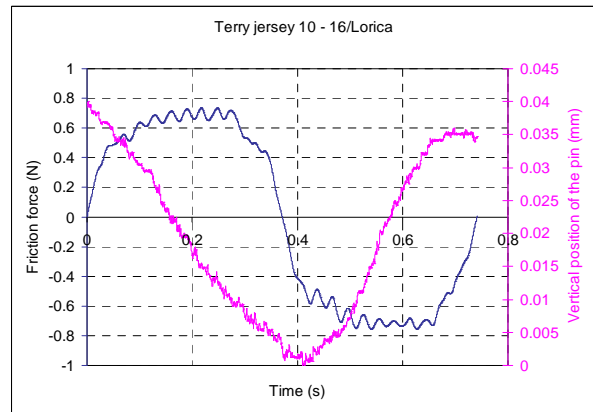
a)



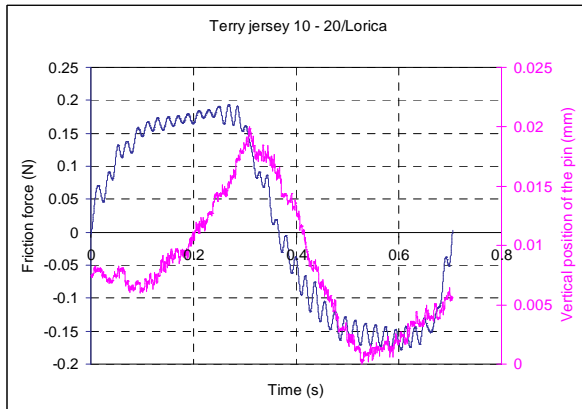
b)



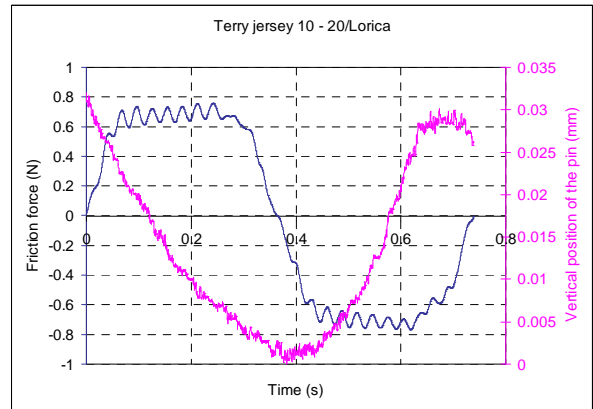
c)



d)



e)



f)

Figure 43: Friction force and vertical position of the pin for terry jersey socks in contact with the Lorica® pin for a friction cycle. The mean curves were calculated from 10 experiments for a friction distance of 5 mm, a friction frequency of 1.5 Hz and a pressure of respectively 3 kPa for cases a, c and e and 15 kPa for cases b, d, and f. The letter T identifies the half period where the movement of the pin follows terries orientation.

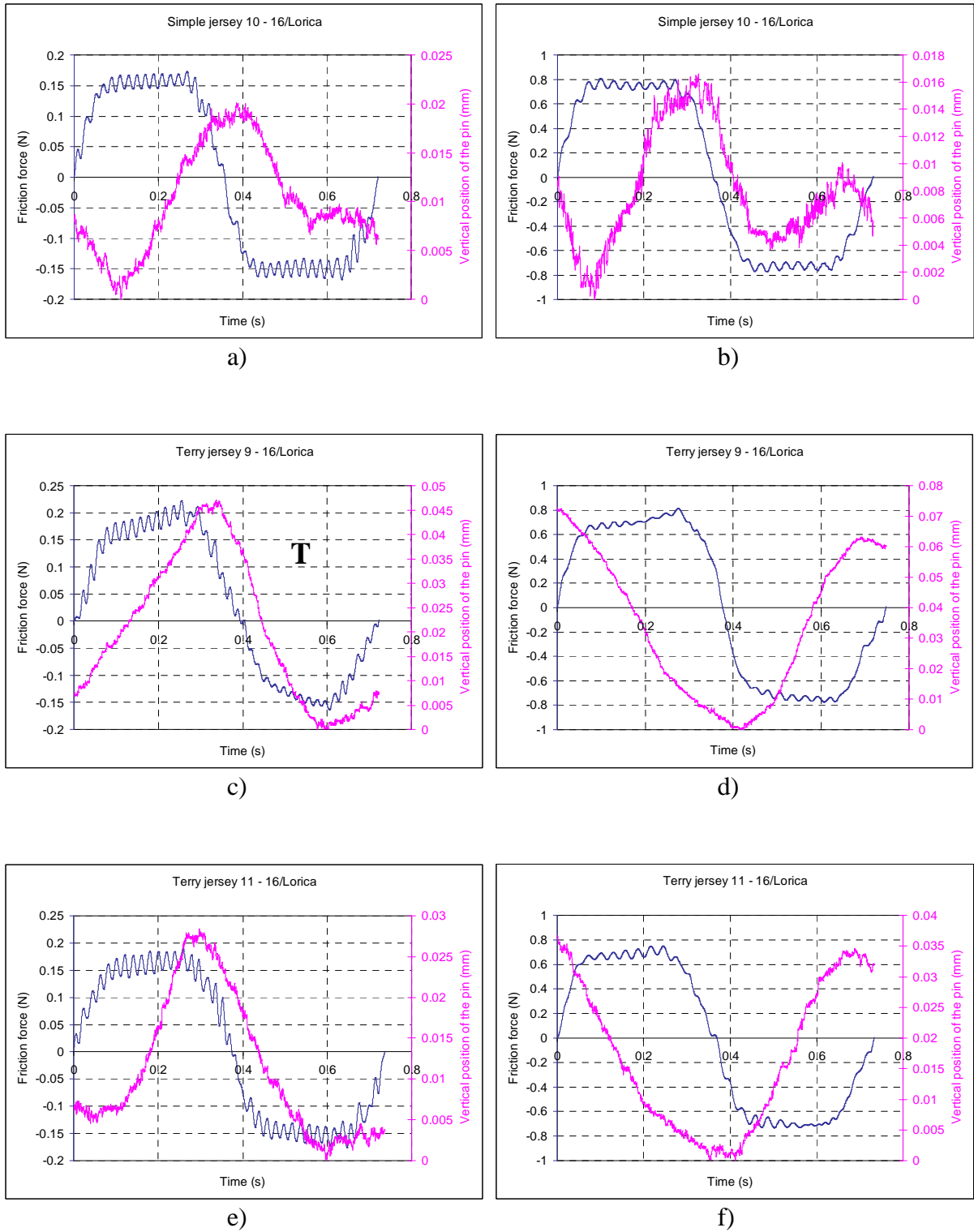


Figure 44 : Friction force and vertical position of the pin for terry and simple jersey socks in contact with the Lorica® pin for a friction cycle. The mean curves were calculated from 10 experiments for a friction distance of 5 mm, a friction frequency of 1.5 Hz and a pressure of respectively 3 kPa for cases a, c and e and 15 kPa for cases b, d, and f. The letter T identifies the half period where the movement of the pin follows terries orientation.

## 2. Pressure influence

### A. On the friction force

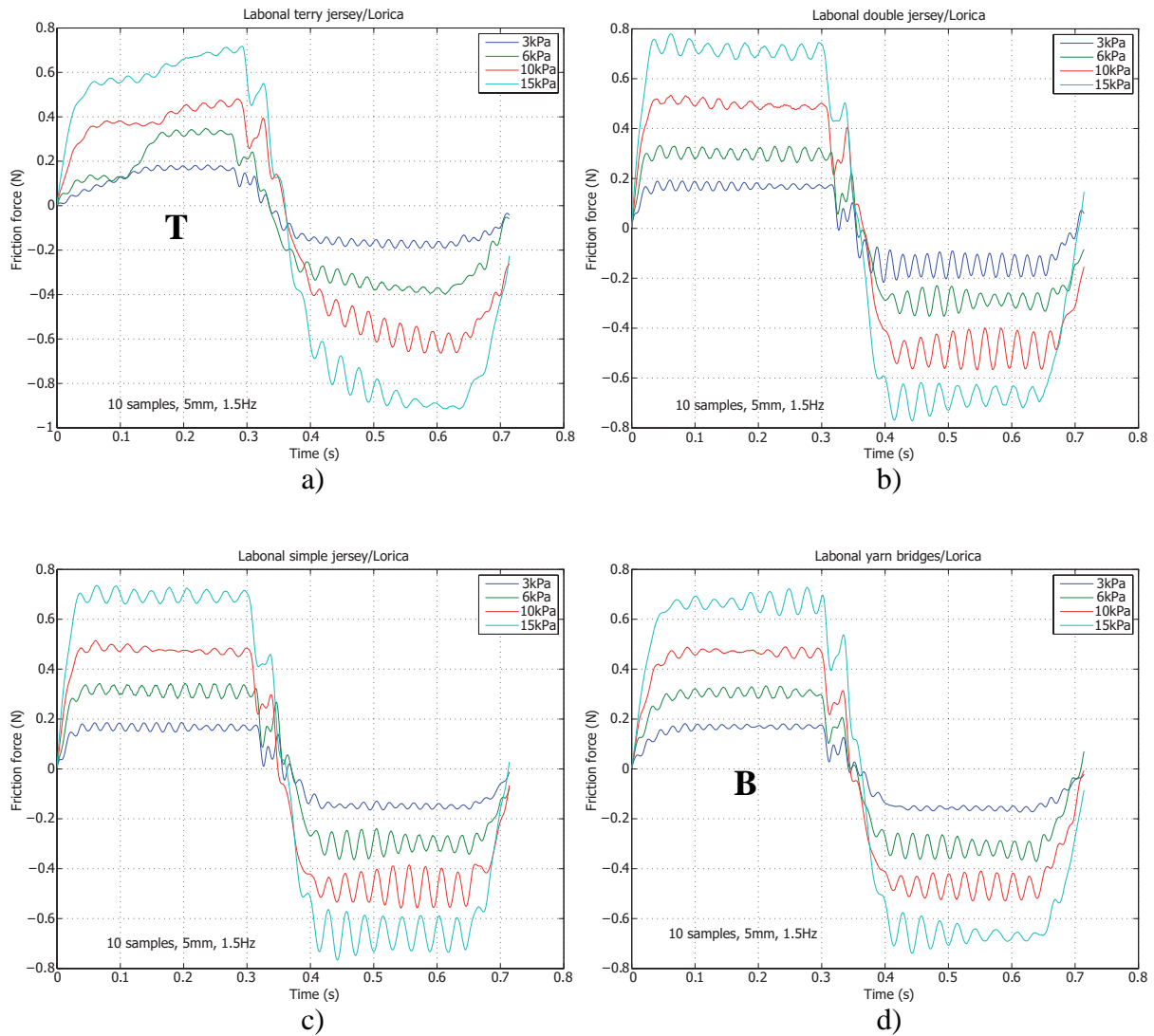
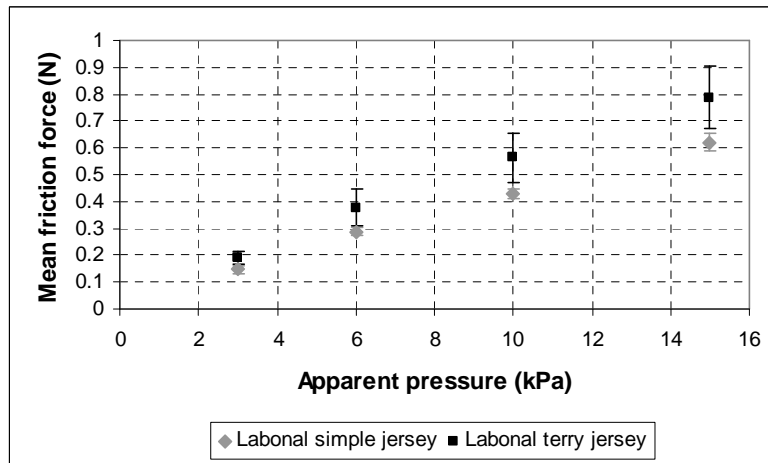
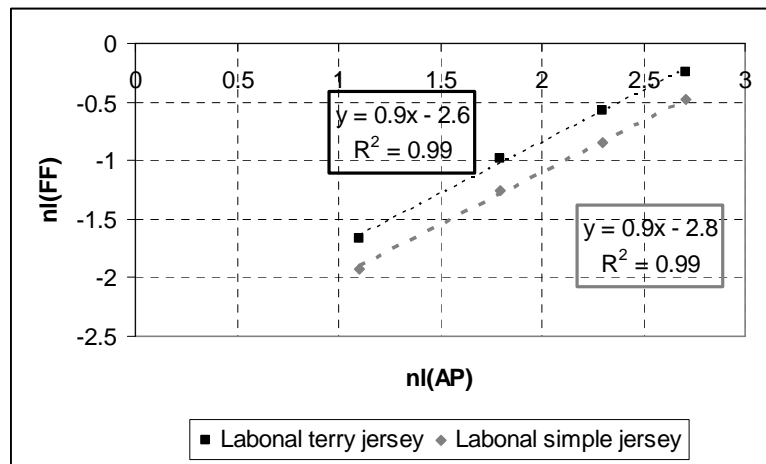


Figure 45: Friction force for a) Labonal terry jersey, b) Labonal double jersey, c) Labonal simple jersey and d) Labonal yarn bridges socks in contact with the Lorica® pin for a friction cycle. The mean curves were calculated from 10 experiments for a friction distance of 5 mm, a friction frequency of 1.5 Hz and pressures from 3 to 15 kPa on LPMT's tribometer. The letters T and B identify the half period where the movement of the pin follows respectively terries orientation and bridges orientation.



a)

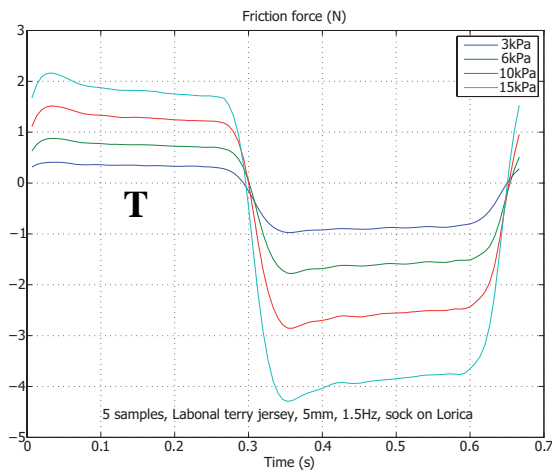


b)

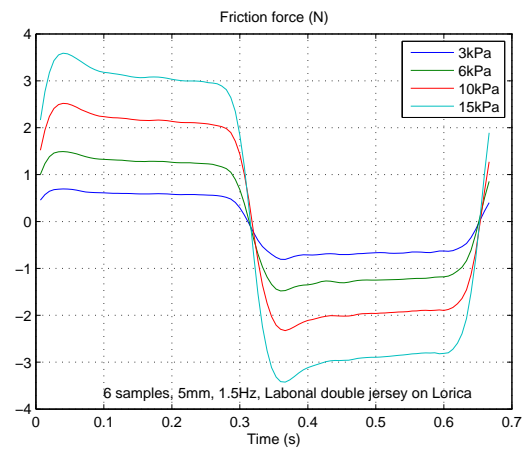
Figure 46: a) Mean friction force versus apparent pressure and b) fitting of the mean friction force in function of the apparent pressure using the empirical equation  $FF = K \times AP^n$  for Labonal terry and simple jersey socks. The abbreviation nl stands for the logarithm, FF is the friction force, AP is the apparent pressure and K and n are empirical constants. The mean friction force was calculated from 3 experimental friction curves of one friction cycle and corresponds to the mean value of the plateaus of the curves.

The well-known fact that the friction force gets higher when the pressure increases can be observed on figures 9 to 13. The mean friction force versus the apparent pressure is shown for Labonal terry jersey and simple jersey socks in figure 10a. The fitting of the mean friction

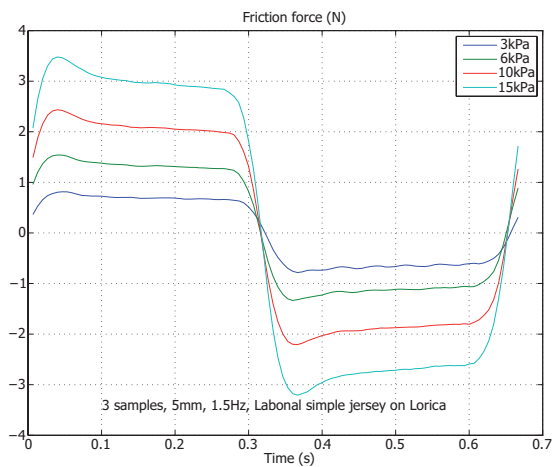
force using the empirical equation  $FF = K \times AP^n$  gives  $n = 0.9$  for both Labonal terry jersey and simple jersey socks which is conform to the theory i.e.  $\frac{2}{3} \leq n \leq 1$ .



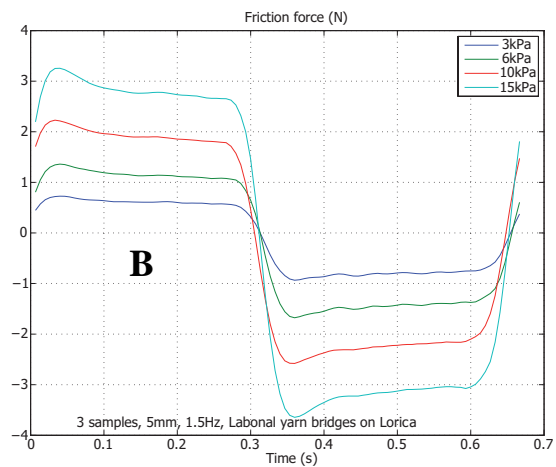
a)



b)



c)



d)

Figure 47: Friction force for a) Labonal terry jersey, b) Labonal double jersey, c) Labonal simple jersey and d) Labonal yarn bridges socks in contact with Lorica® for a friction cycle. The mean curves were calculated from at least 3 experiments for a friction distance of 5 mm, a friction frequency of 1.5 Hz and pressures from 3 to 15 kPa on the TFA. The letters T and B identify the half period where the movement of the pin follows respectively terries orientation and bridges orientation.

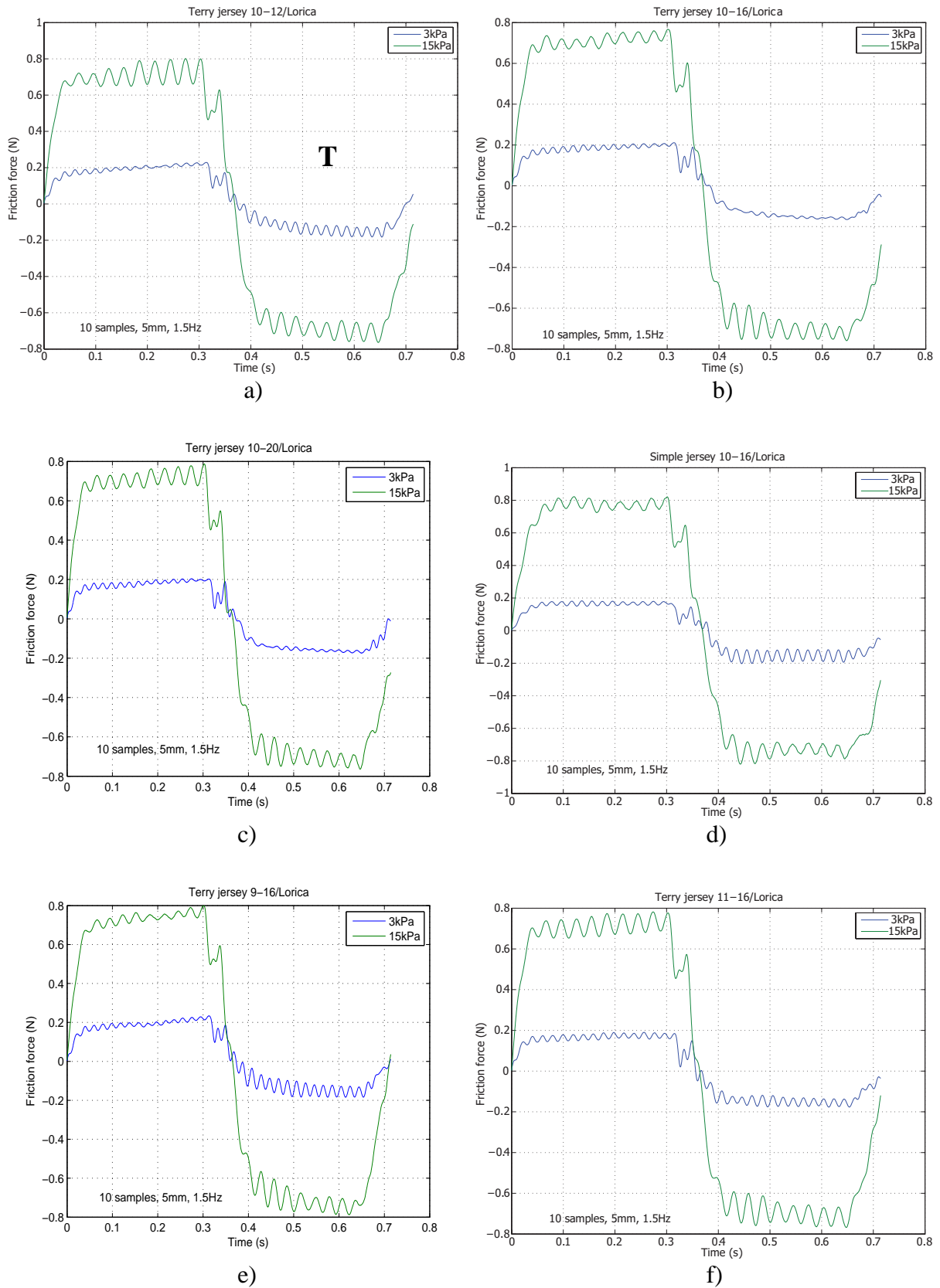


Figure 48: Friction force for a) terry jersey 10 – 12, b) terry jersey 10 – 16, c) terry jersey 10 – 20, d) simple jersey 10 – 16, e) terry jersey 9 – 16 and f) terry jersey 11 – 16 in contact with the Lorica® pin for a friction cycle. The mean curves were calculated from 10



*experiments for a friction distance of 5 mm, a friction frequency of 1.5 Hz and pressures of 3 and 15 kPa on LPMT's tribometer. The letter T identifies the half period where the movement of the pin follows terries orientation.*

For a fixed sock and a given friction device, the shape of the friction curve is the same for all the pressures. The lower the friction force, the flatter the curve. It can be noticed on figure 11 that friction tests carried out using the TFA present two static peaks which correspond to the change of the sliding direction. These static peaks do not occur for friction experiments on the LPMT's tribometer as the pin is free to move up and down while the TFA pin is kept to the same vertical position by the elevation arm. TFA curves show less variations as the friction force signal is filtered while the signal of LPMT's tribometer is not filtered.

The values of the friction force related to the apparent contact surface are of the same order of magnitude for both LPMT's tribometer and TFA for Labonal socks (cf. tables 2 and 3). For terry jersey socks, when the sliding direction corresponds to terries orientation (forward sliding direction), we can suppose that the deformation component of the friction force due to the rotation of terries may induce more friction than the crushing of the structure which explains the higher friction force values in the case of the LPMT's tribometer (cf. table 2). On the other hand, when the sliding direction is opposed to the terries orientation, terries withstand the pin movement, and the phenomena differ upon the tribometer which is considered. For the LPMT's tribometer, the terries under and at the front of the pin are carried along by the pin and rotate. As the pin is free to move vertically, it is lifted by the rotating terries and does not exert extra pressure on the terries. On the other hand, for the TFA, the pin cannot move vertically and is opposed to the natural movement of terries leading to an additional pressure and a higher friction force (cf. table 3). For the others structures, the values of the friction force related to the apparent contact surface are comparable for both tribometers or slightly higher for TFA which may be due to the fact that the pressure can get higher in the case of the TFA measurements. The effect of the hairiness orientation of Labonal terry jersey and yarn bridges is visible in the friction force and the vertical displacement of the pin measured on LPMT's tribometer but is more pronounced in TFA measurement data.

PRESSURE (KPA)	LABONAL TERRY JERSEY		LABONAL DOUBLE JERSEY		LABONAL SIMPLE JERSEY		LABONAL YARN BRIDGES	
	LPMT	TFA	LPMT	TFA	LPMT	TFA	LPMT	TFA
3	0.098	0.049	0.111	0.097	0.111	0.114	0.111	0.097
6	0.144	0.114	0.196	0.211	0.196	0.227	0.196	0.195
10	0.261	0.211	0.327	0.357	0.314	0.357	0.294	0.308
15	0.392	0.292	0.458	0.519	0.458	0.487	0.425	0.455

*Table 14: Comparison of the LPMT's tribometer and the TFA. Labonal socks friction force in N for 1 cm<sup>2</sup> of apparent contact area for pressures from 3 to 15 kPa for the forward sliding direction i.e. the first half of a friction cycle. No standard deviation is given here as these data have been calculated from mean curves.*

PRESSURE (KPA)	LABONAL TERRY JERSEY		LABONAL DOUBLE JERSEY		LABONAL SIMPLE JERSEY		LABONAL YARN BRIDGES	
	LPMT	TFA	LPMT	TFA	LPMT	TFA	LPMT	TFA
3	0.111	0.146	0.111	0.114	0.098	0.114	0.111	0.146
6	0.229	0.260	0.196	0.211	0.196	0.179	0.209	0.260
10	0.392	0.422	0.327	0.325	0.327	0.292	0.307	0.373
15	0.523	0.617	0.458	0.487	0.438	0.438	0.438	0.519

*Table 15: Comparison of the LPMT's tribometer and the TFA. Labonal socks friction force in N for 1 cm<sup>2</sup> of apparent contact area for pressures from 3 to 15 kPa for the back sliding direction i.e. the second half of a friction cycle. No standard deviation is given here as these data have been calculated from mean curves.*

Friction experiments were also carried out changing the counterpart (the material the socks are rubbing). The influence of the counterpart material and roughness will be discussed later. At this stage we just check that the pressure influence is the same whatever the

counterpart material. It can thus be noticed on figure 13 that, for Labonal socks in contact with smooth polyurethane, the friction force increases with pressure.

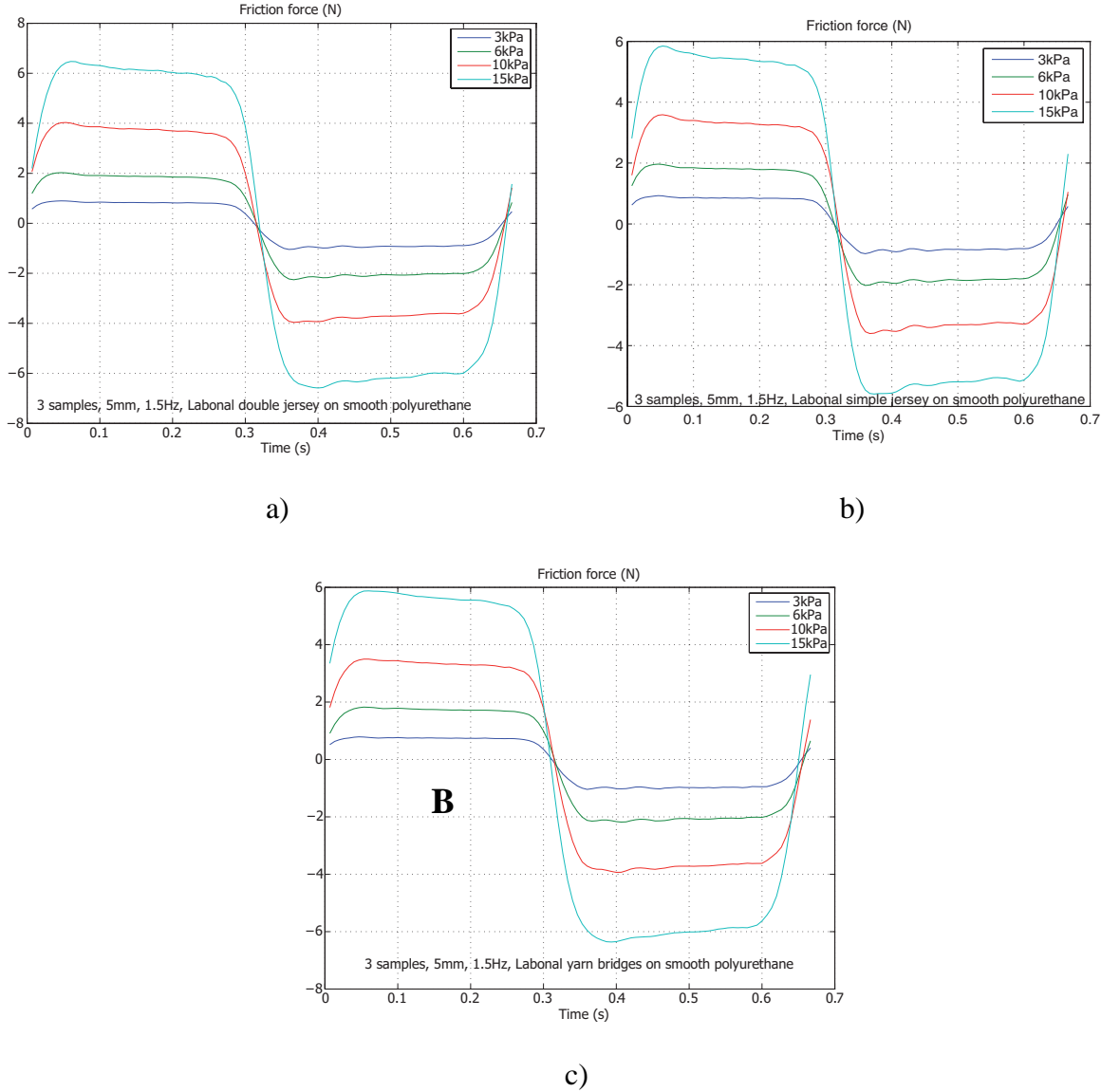


Figure 49: Friction force for a) Labonal double jersey, b) Labonal simple jersey and c) Labonal yarn bridges socks in contact with smooth polyurethane for a friction cycle. The mean curves were calculated from 3 experiments for a friction distance of 5 mm, a friction frequency of 1.5 Hz and pressures from 3 to 15 kPa on the TFA. The letter B identifies the half period where the movement of the pin follows bridges orientation.

## B. On the coefficient of friction

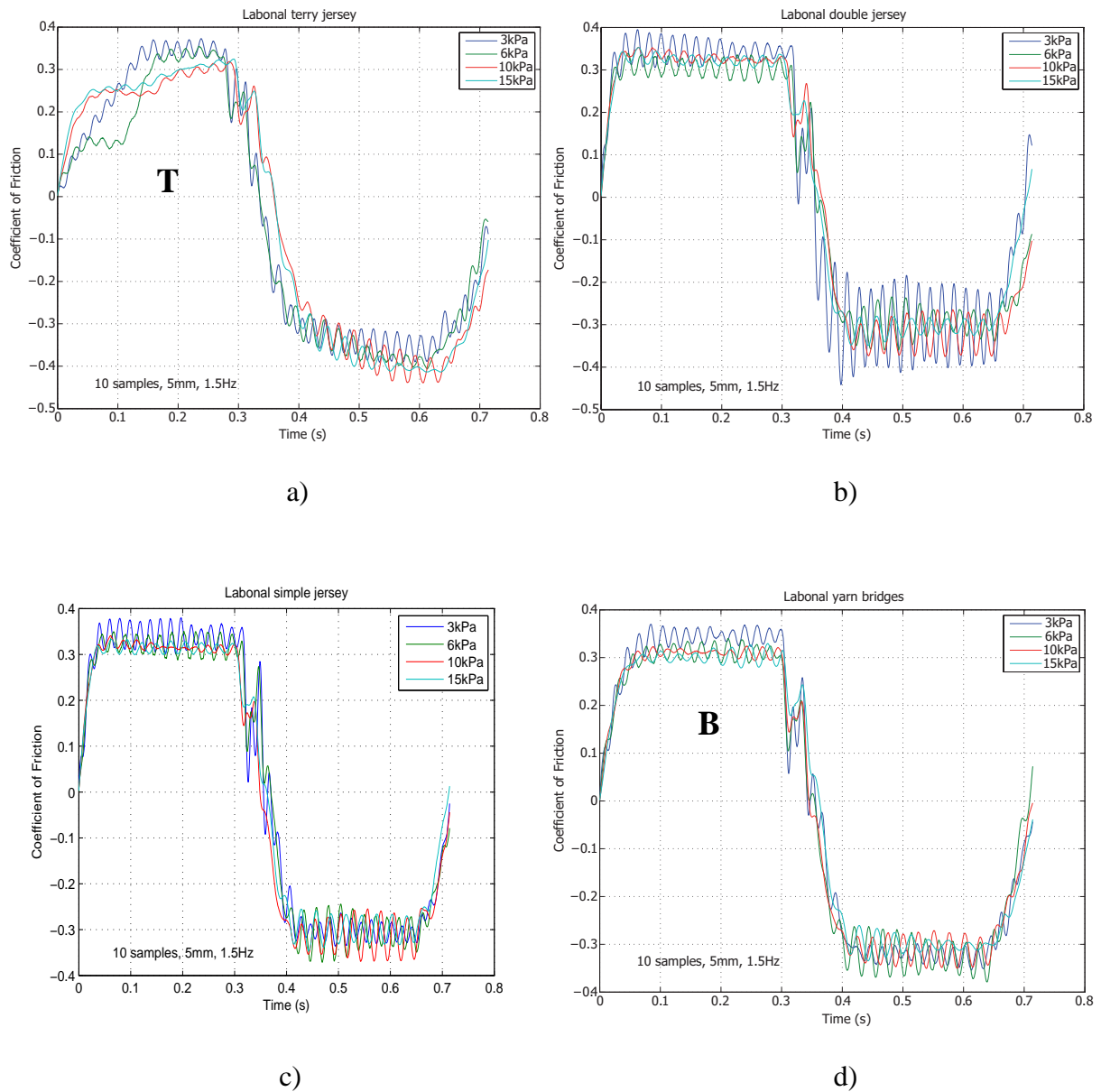
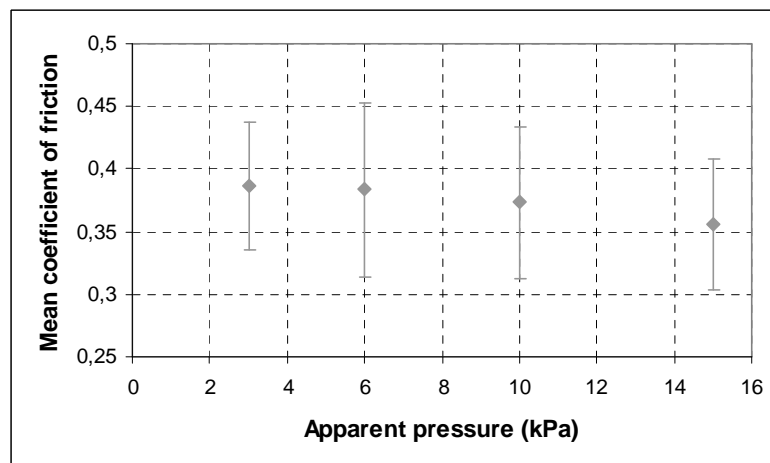
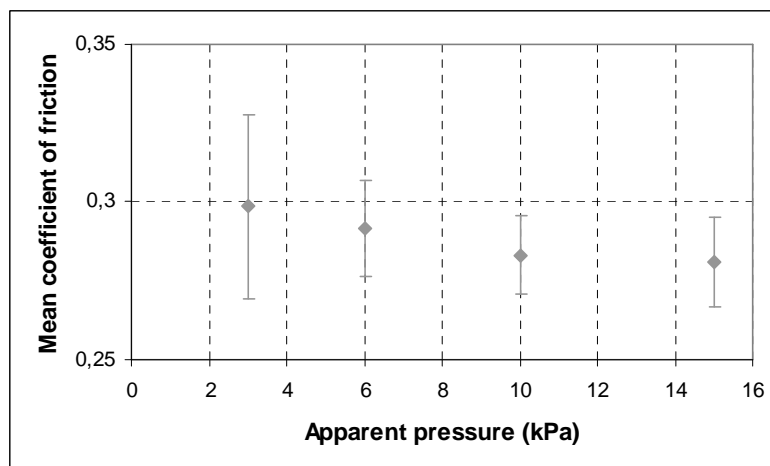


Figure 50: Coefficient of friction for a) Labonal terry jersey, b) Labonal double jersey, c) Labonal simple jersey and d) Labonal yarn bridges socks in contact with the Lorica® pin for a friction cycle. The mean curves were calculated from 10 experiments for a friction distance of 5 mm, a friction frequency of 1.5 Hz and pressures from 3 to 15 kPa on the LPMT's tribometer. The letters *T* and *B* identify the half period where the movement of the pin follows respectively terries orientation and bridges orientation.

The mean coefficient of friction was obtained by dividing the mean friction force by the normal force. It can be seen in figures 14 to 17 that the mean coefficient of friction either remains stable or slightly decreases when pressure increases for the couple cotton / Lorica®. The mean coefficient of friction versus the apparent pressure is detailed for Labonal terry jersey and simple jersey socks respectively in figures 15a and 15b.

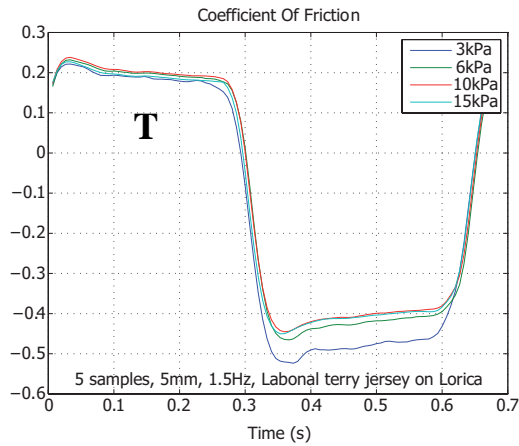


a)

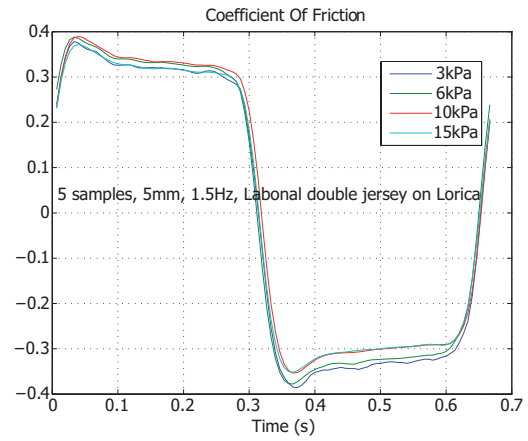


b)

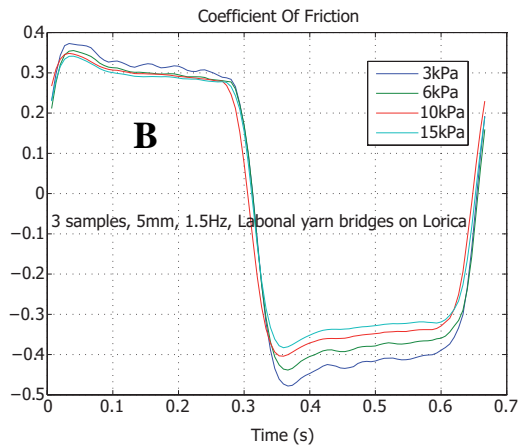
Figure 51: Mean coefficient of friction versus apparent pressure for a) Labonal terry and b) simple jersey socks. The mean coefficient of friction was calculated from 3 experimental curves of 1 friction cycle on the LPMT's tribometer and corresponds to the mean value of the plateaus of the curves.



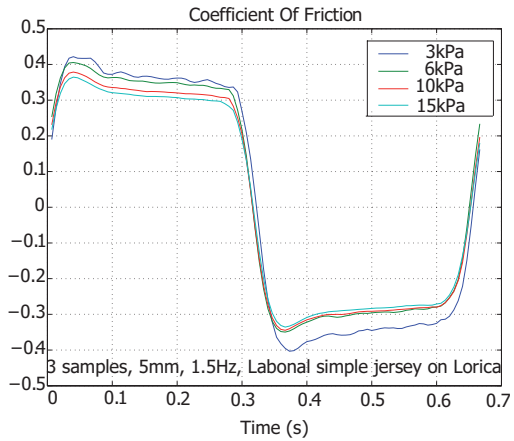
a)



b)

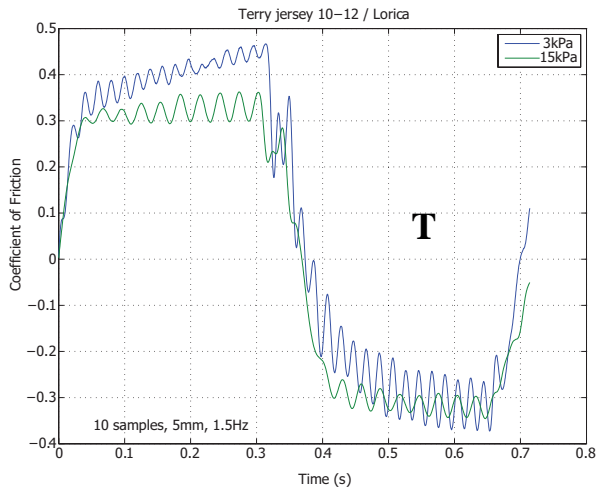


c)

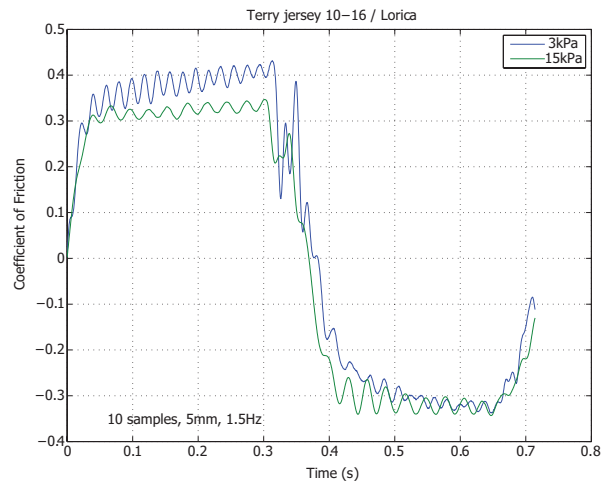


d)

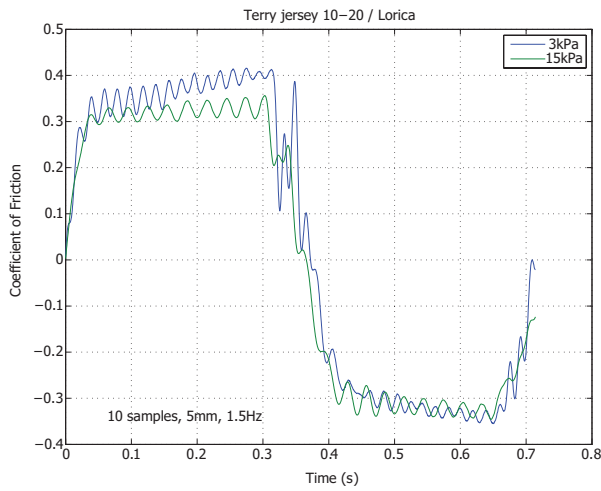
Figure 52: Coefficient of friction for a) Labonal terry jersey, b) Labonal double jersey, c) Labonal yarn bridges and d) Labonal simple jersey socks in contact with the Lorica® pin for a friction cycle. The mean curves were calculated from at least 3 experiments for a friction distance of 5 mm, a friction frequency of 1.5 Hz and pressures from 3 to 15 kPa on the TFA. The letters T and B identify the half period where the movement of the pin follows respectively terries orientation and bridges orientation.



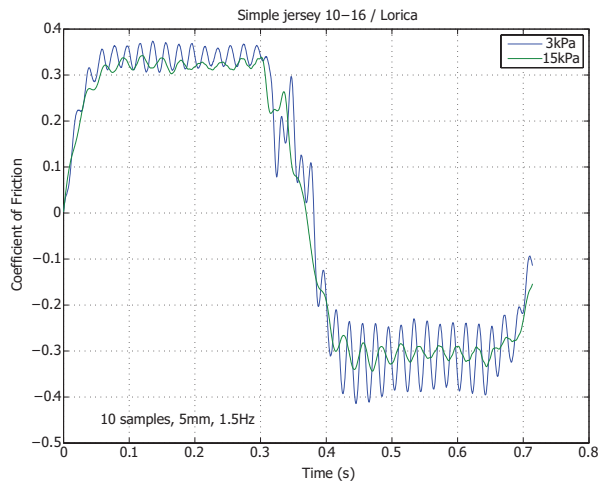
a)



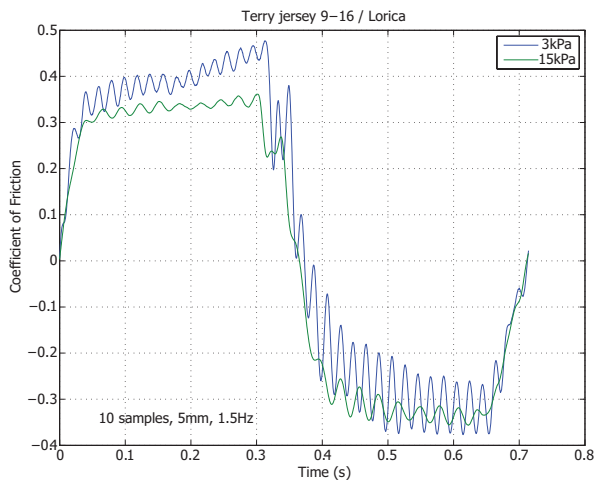
b)



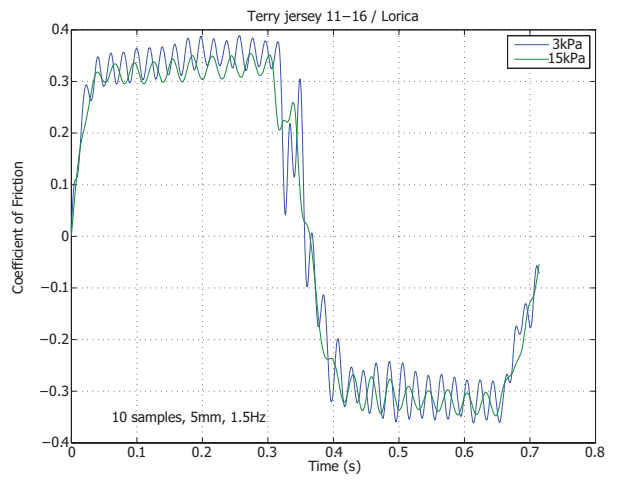
c)



d)



e)



f)

Figure 53: Coefficient of friction for a) terry jersey 10 – 12, b) terry jersey 10 – 16, c) terry jersey 10 – 20, d) simple jersey 10 – 16, e) terry jersey 9 – 16 and f) terry jersey 11 – 16 in contact with the Lorica® pin for a friction cycle. The mean curves were calculated from 10

experiments for a friction distance of 5 mm, a friction frequency of 1.5 Hz and pressures of 3 and 15 kPa on the LPMT's tribometer. The letter T identifies the half period where the movement of the pin follows terries orientation.

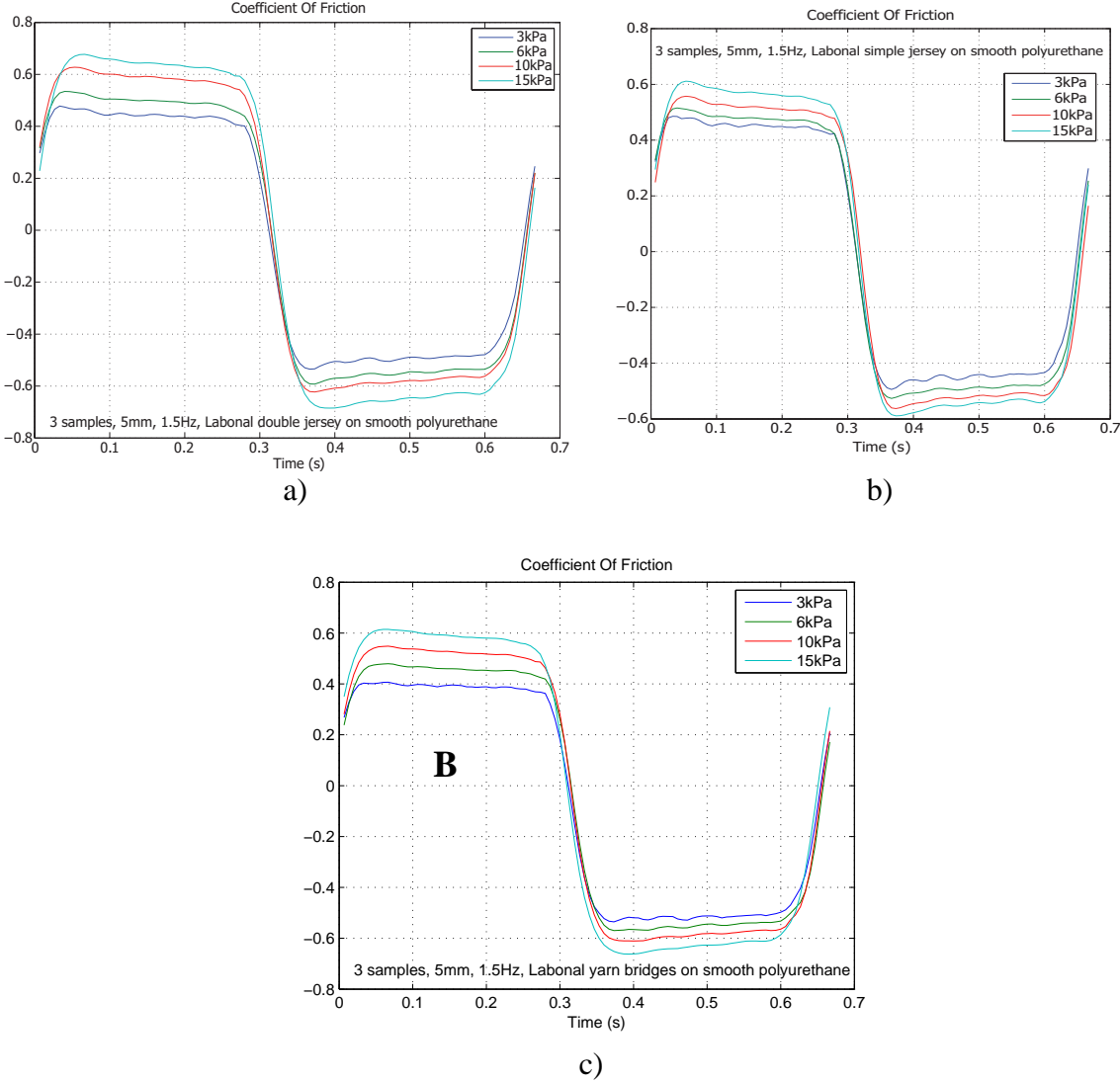


Figure 54: Coefficient of friction for a) Labonal double jersey, b) Labonal simple jersey and c) Labonal yarn bridges socks in contact with smooth polyurethane for a friction cycle. The mean curves were calculated from 3 experiments for a friction distance of 5 mm, a friction frequency of 1.5 Hz and pressures from 3 to 15 kPa on the TFA. The letter B identifies the half period where the movement of the pin follows bridges orientation.



The evolution of the coefficient of friction in function of the pressure depends on the materials in contact. The couple cotton / smooth polyurethane does not react like the couple cotton / Lorica® (cf. figures 16 and 18). The coefficient of friction indeed increases when pressure gets higher as it is shown in figure 18. Friction includes a part of deformation and a part of adhesion. When the normal load is increased, both the deformation part and the adhesion part of friction get higher but the rise in deformation is less important compared to the increase of the real contact area and the decrease of the distance between the two contacting bodies. Figures 16 and 18 thus indicate that the deformation part of friction is more important for the couple cotton / Lorica® than for the couple cotton / smooth polyurethane and that the adhesion contribution to friction is higher for the couple cotton / smooth polyurethane than for the couple cotton / Lorica®.

### **3. Stitch length and yarn count influence**

Three terry jersey socks that only differ by their stitch length namely terry jersey 9 - 16, terry jersey 10 - 16, and terry jersey 11 - 16 and three terry jersey socks that only differ by their yarn count namely terry jersey 10 - 12, terry jersey 10 - 16, and terry jersey 10 - 20 were at our disposal. We could therefore investigate the influence of the stitch length and the yarn count on the friction force and the coefficient of friction (cf. chapter 2 paragraph II.2).

Figures 19 and 20 respectively show the friction force and the coefficient of friction for the socks that have just been cited. By these figures, the yarn count does not impact the friction results. On the other hand, when the fabrics are loaded with a low pressure of 3 kPa, the values of the friction force and the coefficient of friction increase when the stitch length decreases. This is due to the shape of the loop in the knitted fabric. For the same yarn count, the higher the stitch length, the flatter the loop. The fabric surface roughness is thus lower for terry jersey 11 – 16 than for terry jersey 9 – 16 and the values of the friction force and the coefficient of friction get higher with surface roughness. For a pressure of 15 kPa, the loops are compressed and the stitch length has no influence on friction.

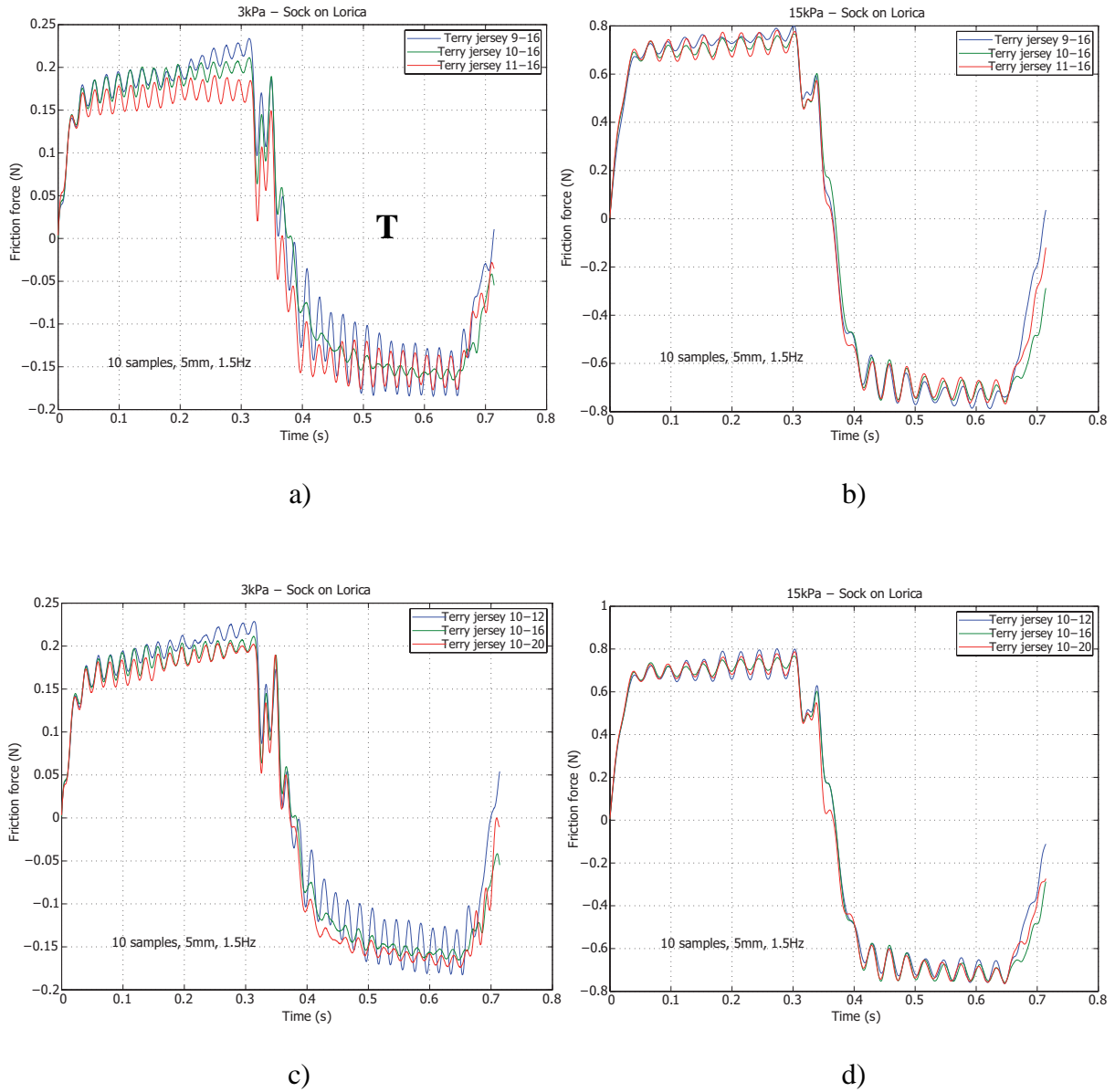


Figure 55: Friction force for a) terry jersey 9 – 16, terry jersey 10 – 16 and terry jersey 11 – 16 under 3 kPa, b) terry jersey 9 – 16, terry jersey 10 – 16 and terry jersey 11 – 16 under 15 kPa, c) terry jersey 10 – 12, terry jersey 10 – 16 and terry jersey 10 – 20 under 3 kPa and d) terry jersey 10 – 12, terry jersey 10 – 16 and terry jersey 10 – 20 under 15 kPa in contact with the Lorica® pin for a friction cycle. The mean curves were calculated from 10 experiments for a friction distance of 5 mm and a friction frequency of 1.5 Hz on the LPMT's tribometer. The letter T identifies the half period where the movement of the pin follows terries orientation.

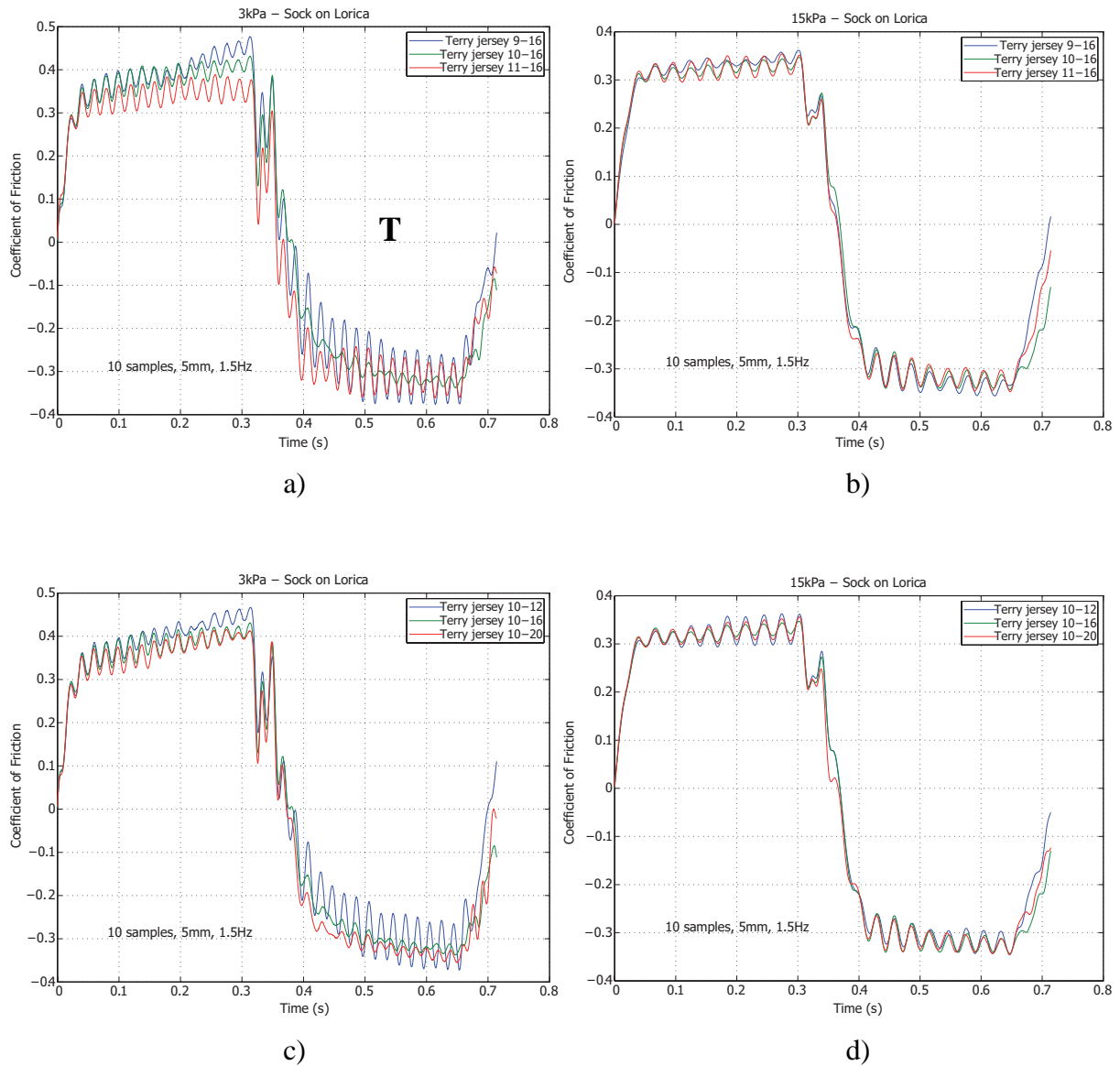


Figure 56: Coefficient of friction for a) terry jersey 9 – 16, terry jersey 10 – 16 and terry jersey 11 – 16 under 3 kPa, b) terry jersey 9 – 16, terry jersey 10 – 16 and terry jersey 11 – 16 under 15 kPa, c) terry jersey 10 – 12, terry jersey 10 – 16 and terry jersey 10 – 20 under 3 kPa and d) terry jersey 10 – 12, terry jersey 10 – 16 and terry jersey 10 – 20 under 15 kPa in contact with the Lorica® pin for a friction cycle. The mean curves were calculated from 10 experiments for a friction distance of 5 mm and a friction frequency of 1.5 Hz on the LPMT's tribometer. The letter T identifies the half period where the movement of the pin follows terries orientation.

#### 4. Sock structure influence

We aimed to determine the influence of the knitted structure of the sock on the friction generated on the skin of the foot during running. We found that the shape and the value of the friction force and the coefficient of friction curves depend on the sock structure (cf. figures 21 to 27).

Figures 21a to 21d and 22a to 22d show that Labonal double and simple jerseys have similar friction forces and coefficients of friction when rubbing against Lorica®. Their friction signals increase sharply before getting stable during the first half of the friction cycle and when the sliding direction of the pin changes, the values of the friction force and the coefficient of friction decrease sharply before stabilizing. Their curves are symmetrical.

On the other hand, for the Labonal terry jersey sock, the values of the friction force and the coefficient of friction progressively increase without getting stable. For sliding distances lower than 2.5 mm, Labonal terry jersey socks induce less friction than the Labonal simple and double jersey structures while beyond 2.5 mm sliding distance, Labonal terry jersey socks present similar or slightly higher friction than other Labonal structures. It can also be noticed that the friction signals of Labonal terry jersey are asymmetrical. The friction force and the coefficient of friction are indeed higher in the second half of the friction cycle i.e. when the pin rubs the sock in the direction opposed to the terries orientation.

It has to be noted that for Labonal terry jersey socks, the terries are oriented towards the heel and when the foot contacts the ground, it slides within the shoe towards the toe i.e. it rubs the sock in the direction opposed to the terries orientation which is the less suitable case regarding skin irritations as it induces higher friction on the skin. It is thus recommended to knit the socks from the leg to the toe in order to reduce the friction when the foot contacts the ground and is loaded with significant normal and tangential forces. As mentioned above, Labonal and others socks are not from the same line of products. Labonal products are higher quality socks. The terries of the socks that were not supplied by Labonal are easy to crush i.e. they do not rotate during a friction cycle. Figures 21e, 21f, 22e and 22f show that one of these terry jersey structure has similar friction force and coefficient of friction than a simple jersey structure. It may thus be concluded that the particular shape of Labonal terry jersey friction force is due to the rotation of terries during a friction cycle.

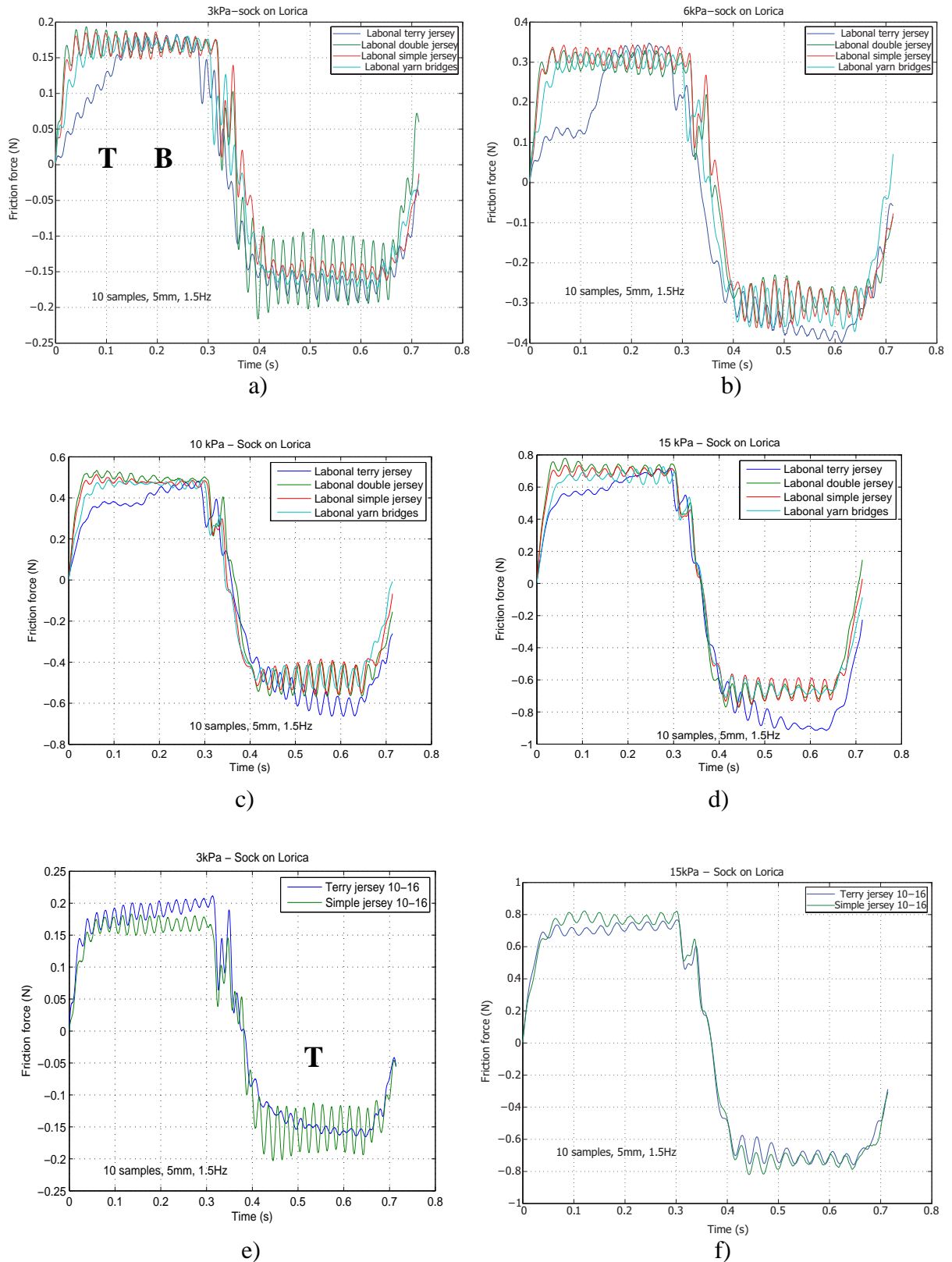


Figure 57: Friction force for Labonal socks under a) 3 kPa, b) 6 kPa, c) 10 kPa, d) 15 kPa and for terry jersey 10 – 16 and simple jersey 10 – 16 under e) 3 kPa and f) 15 kPa in contact with the Lorica® pin for a friction cycle. The mean curves were calculated from

*10 experiments for a friction distance of 5 mm and a friction frequency of 1.5 Hz on the LPMT's tribometer. The letters T and B identify the half period where the movement of the pin follows respectively terries orientation and bridges orientation.*

Yarn bridges structure behaves as an intermediate between terry jersey and simple or double jersey; the bridges are indeed slightly oriented. The asymmetry of Labonal terry jersey and yarn bridges friction curves must be due to the orientation of the terries and bridges; in the terries or bridges direction, the structure rotate quite easily while in the opposite direction, the structure resists to the movement.

Labonal socks friction experiments on the TFA are reported in figures 23 and 24. It can be seen that for friction tests on the TFA, the shape of the friction force and the coefficient of friction curves does not depend on the sock structure; all the curves have the same shape. As the distance between the pin and the sock is constant, the terries and bridges cannot rotate during a friction cycle and only the values of the friction force and the coefficient of friction differ from one sock to another.

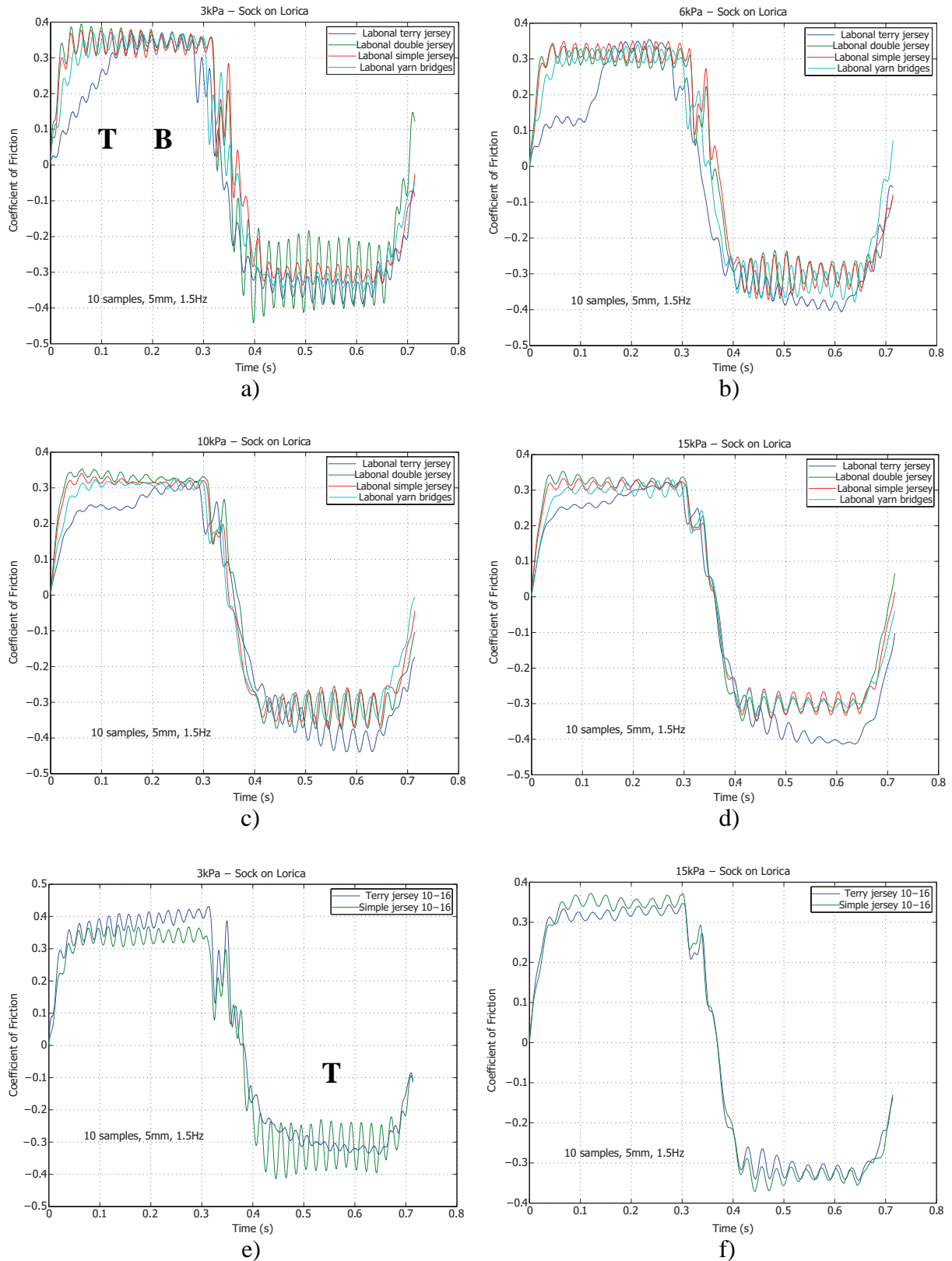


Figure 58: Coefficient of friction for Labonal socks under a) 3 kPa, b) 6 kPa, c) 10 kPa, d) 15 kPa and for terry jersey 10 – 16 and simple jersey 10 – 16 under e) 3 kPa and f) 15 kPa in contact with Lorica® pin for a friction cycle. The mean curves were calculated from 10 experiments for a friction distance of 5 mm and a friction frequency of 1.5 Hz on the LPMT's

tribometer. The letters *T* and *B* identify the half period where the movement of the pin follows respectively terries orientation and bridges orientation.

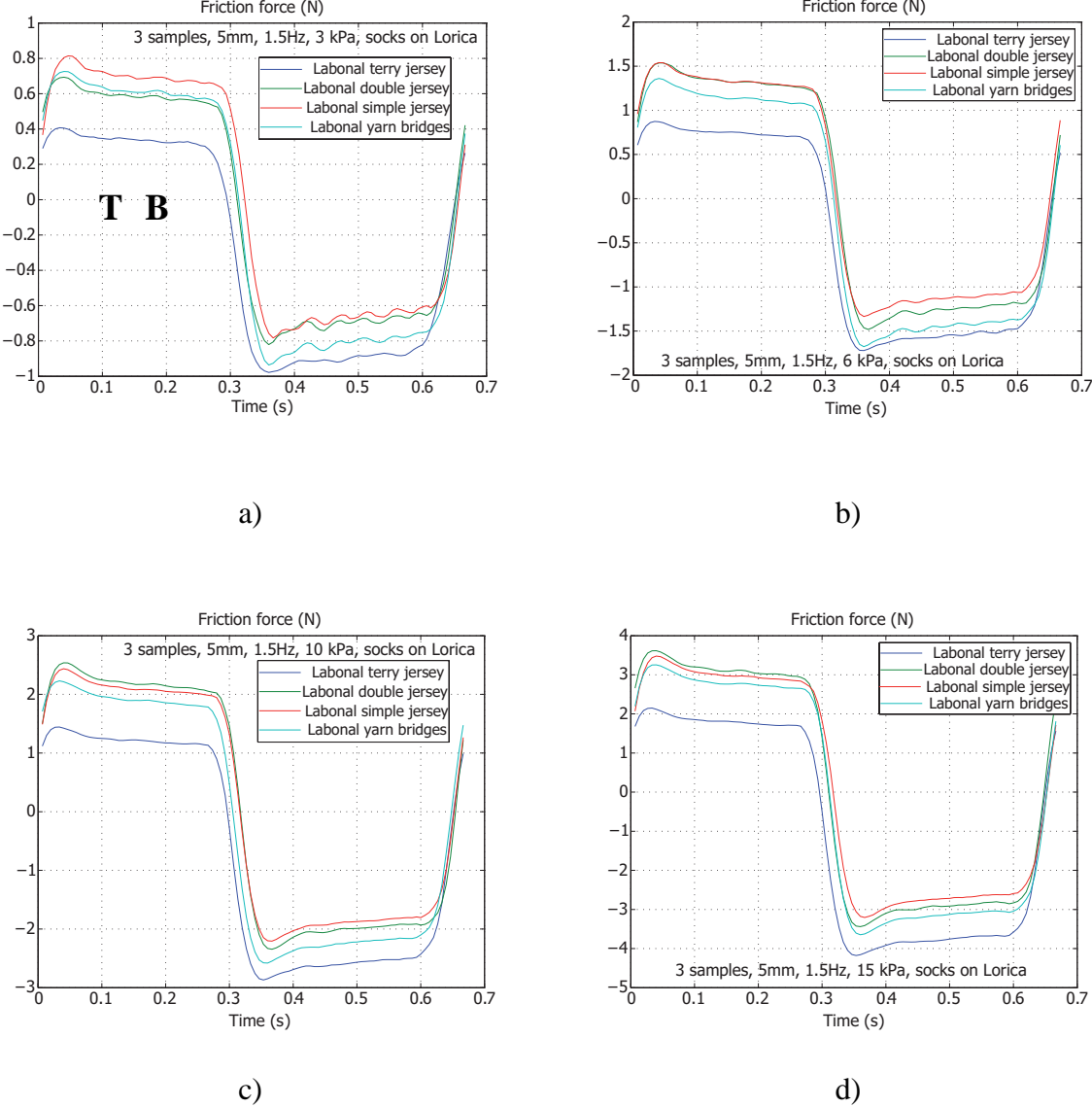


Figure 59: Friction force for Labonal socks under a) 3 kPa, b) 6 kPa, c) 10 kPa and d) 15 kPa in contact with Lorica® for a friction cycle. The mean curves were calculated from 3 experiments for a friction distance of 5 mm and a friction frequency of 1.5 Hz on the TFA. The letters *T* and *B* identify the half period where the movement of the pin follows respectively terries orientation and bridges orientation.



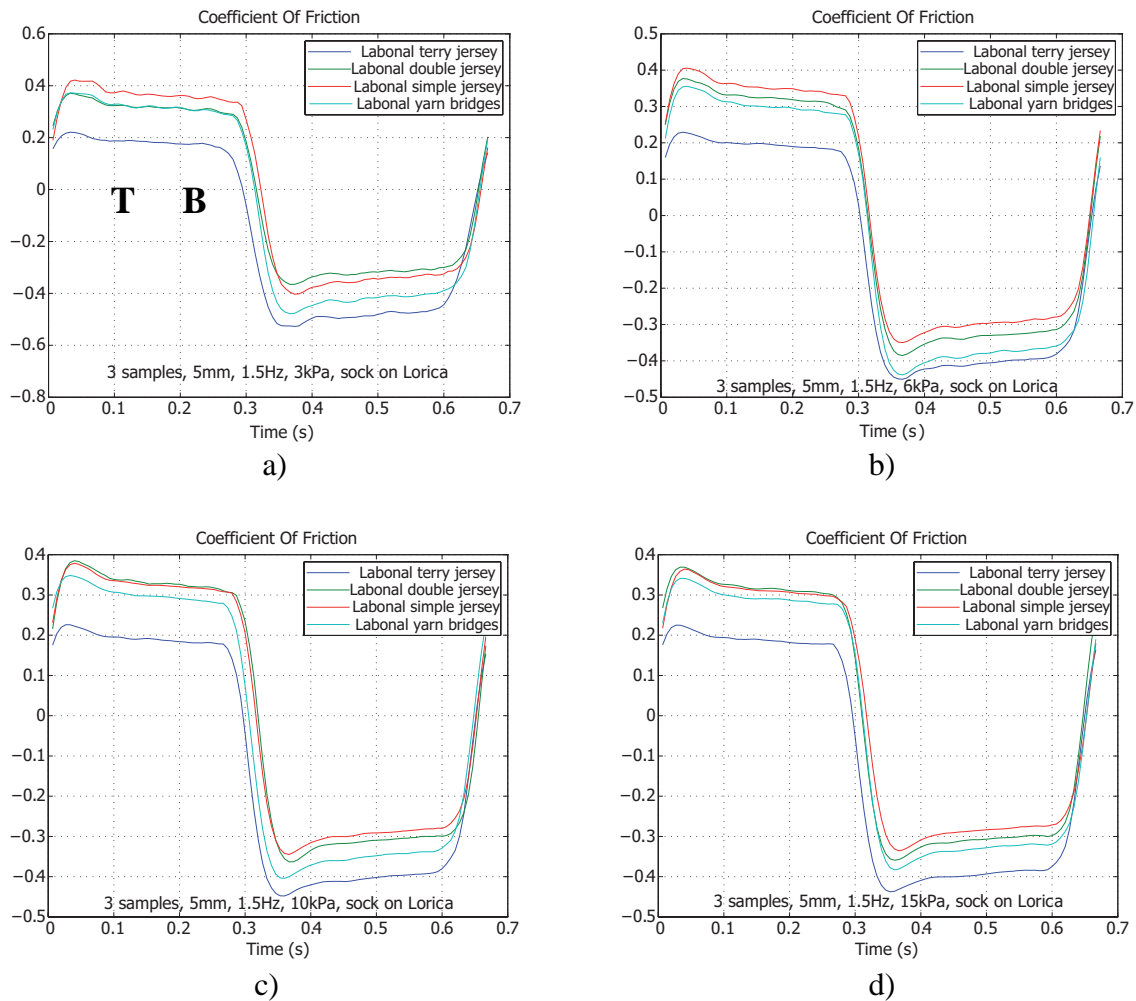


Figure 60: Coefficient of friction for Labonal socks under a) 3 kPa, b) 6 kPa, c) 10 kPa and d) 15 kPa in contact with Lorica® for a friction cycle. The mean curves were calculated from 3 experiments for a friction distance of 5 mm and a friction frequency of 1.5 Hz on the TFA. The letters T and B identify the half period where the movement of the pin follows respectively terries orientation and bridges orientation.

When the sliding direction corresponds to the terries and bridges orientation, Labonal terry jersey is the sock structure which induces less friction, followed by Labonal yarn bridges and simple and double jerseys. For the opposite sliding direction, we find, from the lowest to the highest friction: simple jersey, double jersey, yarn bridges and terry jersey structures. The curves for Labonal simple and double jersey are almost identical.

As it has already been outlined for friction experiments on LPMT's tribometer, the friction curves of simple and double jersey structures are symmetrical while terry jersey and yarn bridges socks curves are asymmetrical because of their oriented structure. The

asymmetry is more important in the case of terry jersey because terries are more numerous and longer, therefore they are more oriented than bridges. Moreover, the asymmetry is also more important when the friction test is carried out on the TFA; for terry jersey, the friction force in the back direction is about 2 times the friction force in the forward direction for experiments on the TFA (cf. figure 23) while the friction force in the back direction is about 1.5 times the friction force in the forward direction for LPMT's tribometer tests (cf. figure 21). This is due to the way the pin is loaded in both devices.

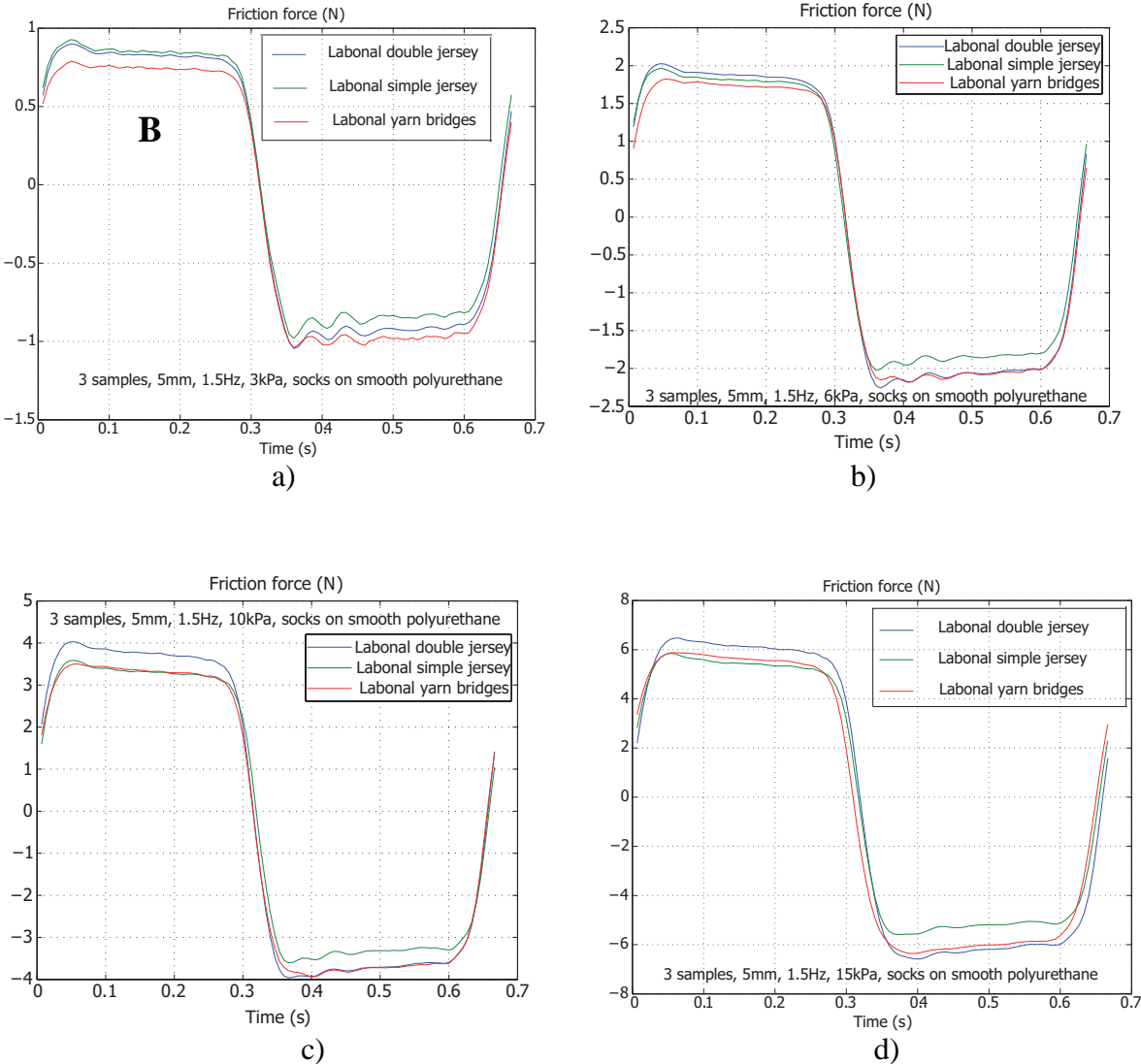


Figure 61: Friction force for Labonal socks under a) 3 kPa, b) 6 kPa, c) 10 kPa and d) 15 kPa in contact with smooth polyurethane for a friction cycle. The mean curves were calculated from 3 experiments for a friction distance of 5 mm and a friction frequency of

1.5 Hz on the TFA. The letter *B* identifies the half period where the movement of the pin follows bridges orientation.

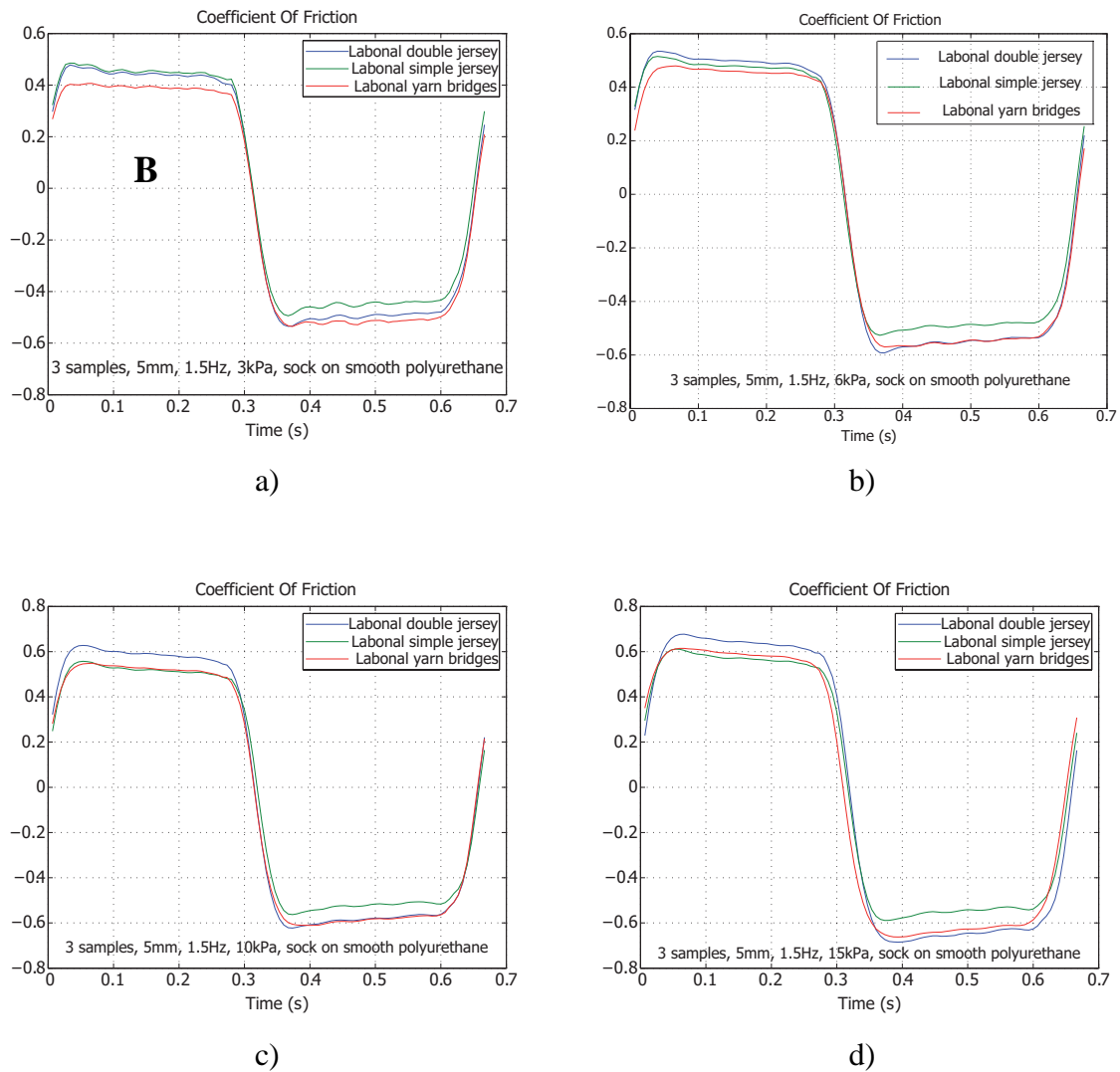


Figure 62: Coefficient of friction for Labonal socks under a) 3 kPa, b) 6 kPa, c) 10 kPa and d) 15 kPa in contact with smooth polyurethane for a friction cycle. The mean curves were calculated from 3 experiments for a friction distance of 5 mm and a friction frequency of 1.5 Hz on the TFA. The letter *B* identifies the half period where the movement of the pin follows bridges orientation.

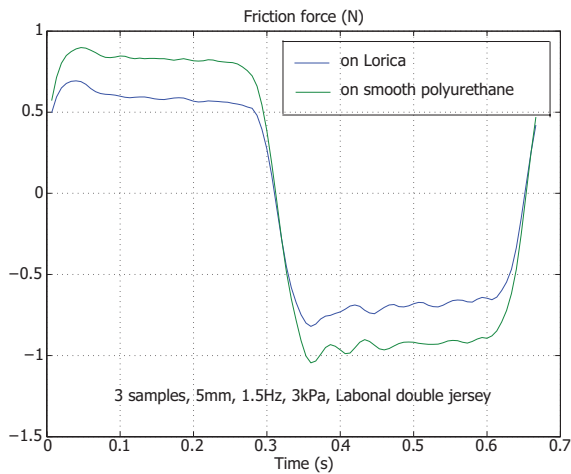
As one can observe in figures 25 and 26, friction experiments with smooth polyurethane counterpart gave similar results than friction experiments with Lorica® counterpart. The friction force and coefficient of friction values are however 1.3 to 2 times

higher in the case of smooth polyurethane which is probably due to a greater real contact area and adhesion force.

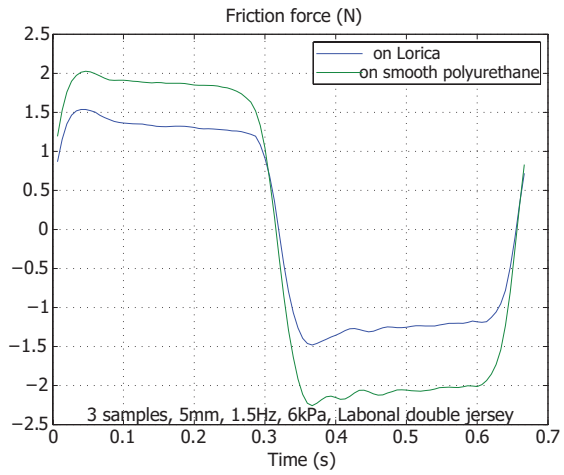
## 5. Influence of the pin material and roughness

### **A. Experiments using the Lorica® and the smooth polyurethane pins**

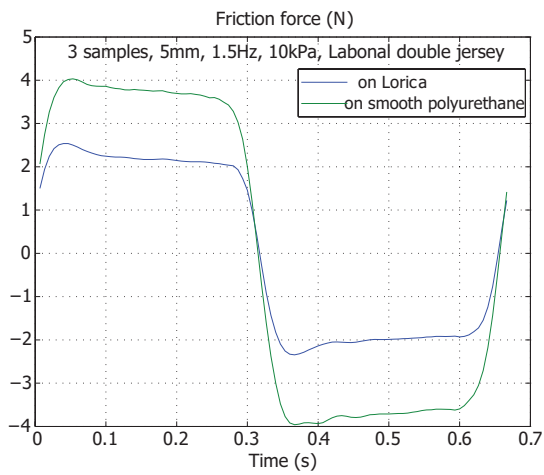
Figures 27 to 32 give the friction force and the coefficient of friction of Labonal socks for a friction cycle for two different counterparts; Lorica® and smooth polyurethane. These curves confirm that friction is higher when the socks are rubbed against smooth polyurethane; friction force and coefficient of friction are multiplied by about 1.2, 1.4, 1.7 and 1.9 for pressures respectively equal to 3, 6, 10 and 15 kPa. The adhesion part of friction is more important for the smooth polyurethane counterpart than for the Lorica® counterpart. For a same increase in pressure, the real contact area therefore increases more in the case of cotton rubbing against smooth polyurethane than in the case of cotton rubbing against Lorica® which explains that the difference between the curves gets higher with pressure.



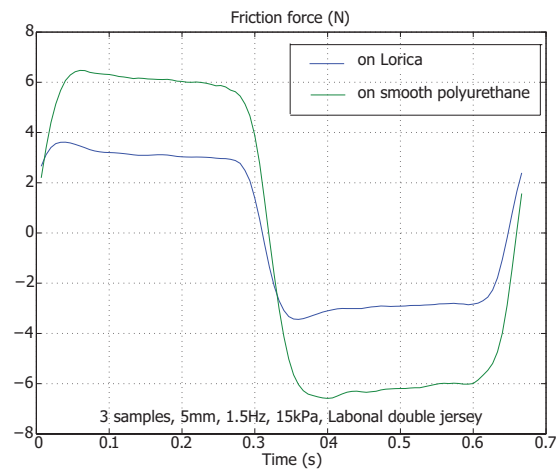
a)



b)

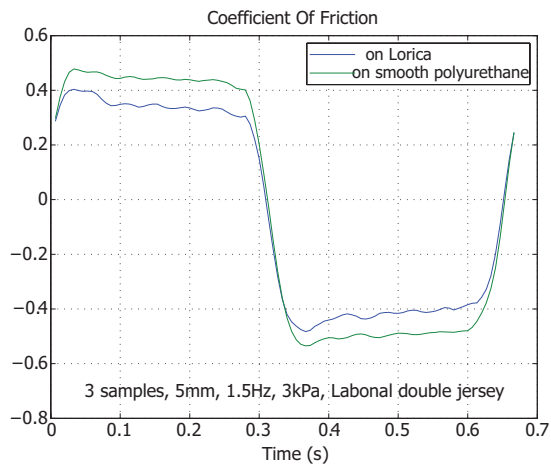


c)

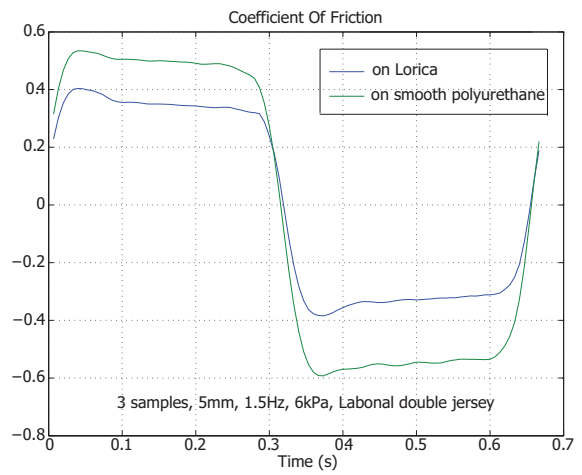


d)

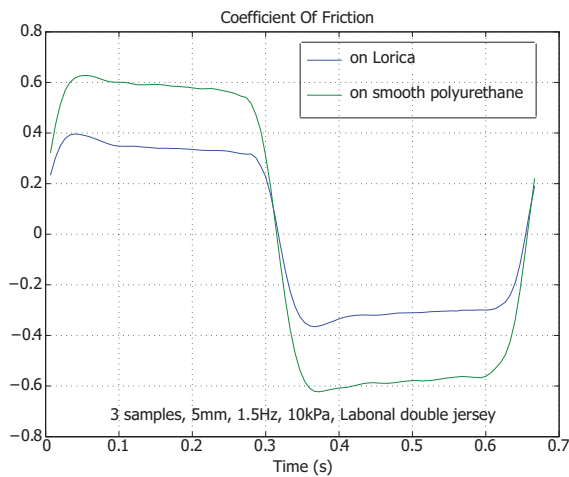
Figure 63: Friction force of Labonal double jersey in contact with Lorica® and smooth polyurethane under a) 3 kPa, b) 6 kPa, c) 10 kPa and d) 15 kPa. The mean curves were calculated from 3 experiments for a friction distance of 5 mm and a friction frequency of 1.5 Hz on the TFA.



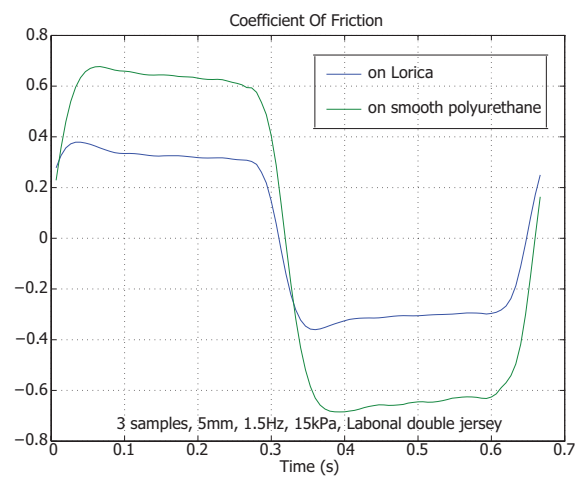
a)



b)

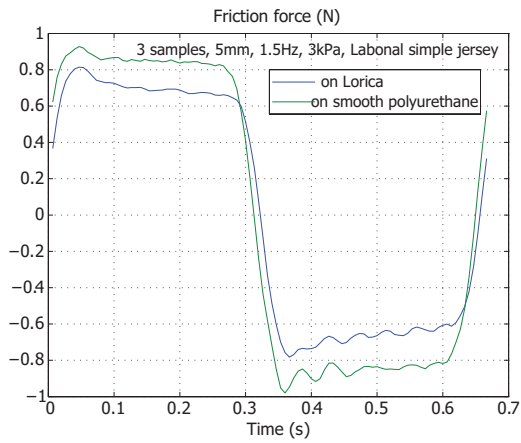


c)

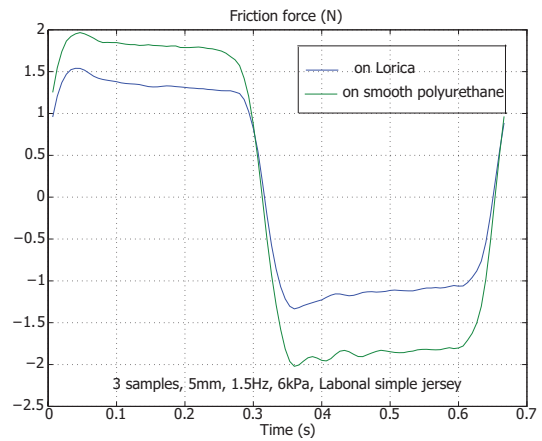


d)

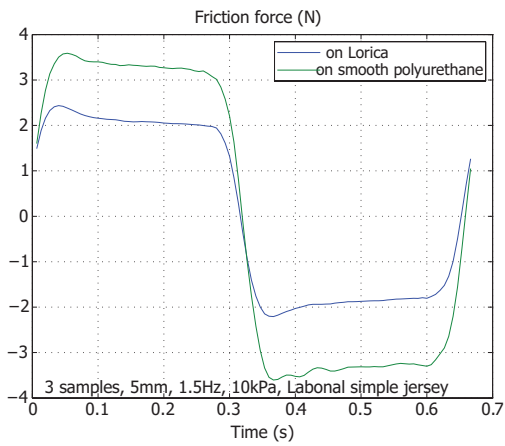
Figure 64: Coefficient of friction of Labonal double jersey in contact with Lorica® and smooth polyurethane under a) 3 kPa, b) 6 kPa, c) 10 kPa and d) 15 kPa. The mean curves were calculated from 3 experiments for a friction distance of 5 mm and a friction frequency of 1.5 Hz on the TFA.



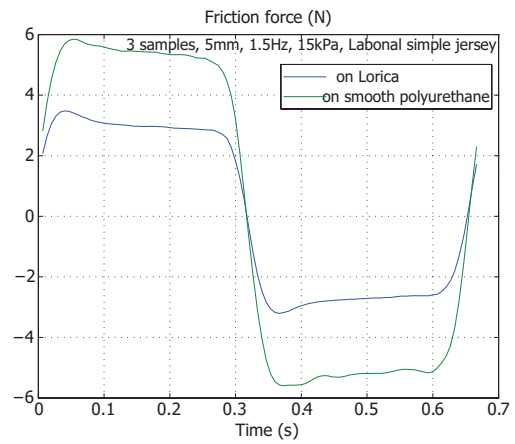
a)



b)

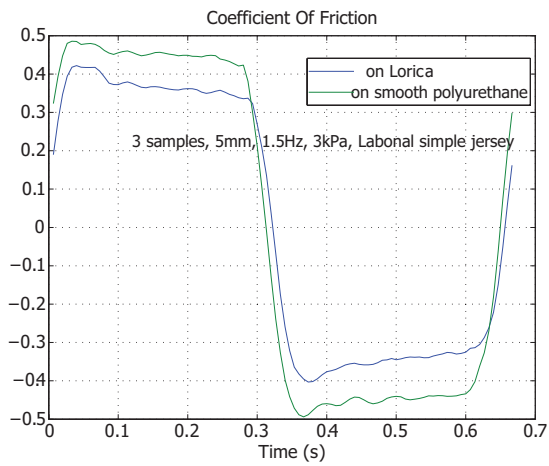


c)

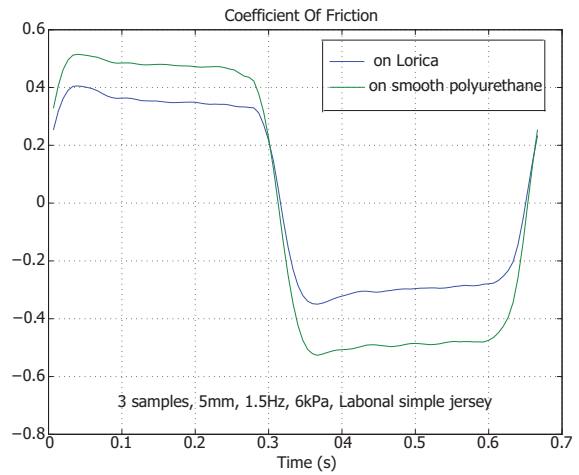


d)

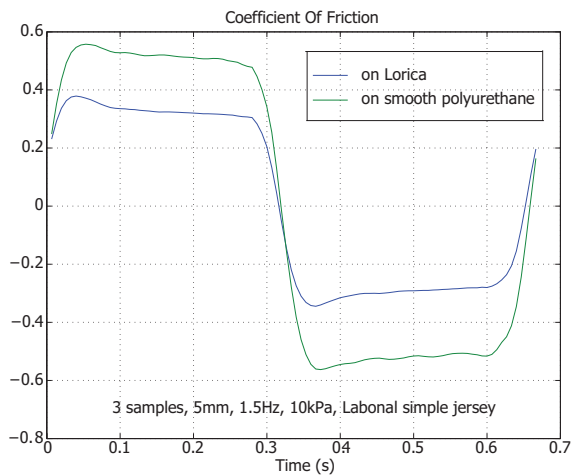
Figure 65: Friction force of Labonal simple jersey in contact with Lorica® and smooth polyurethane under a) 3 kPa, b) 6 kPa, c) 10 kPa and d) 15 kPa. The mean curves were calculated from 3 experiments for a friction distance of 5 mm and a friction frequency of 1.5 Hz on the TFA.



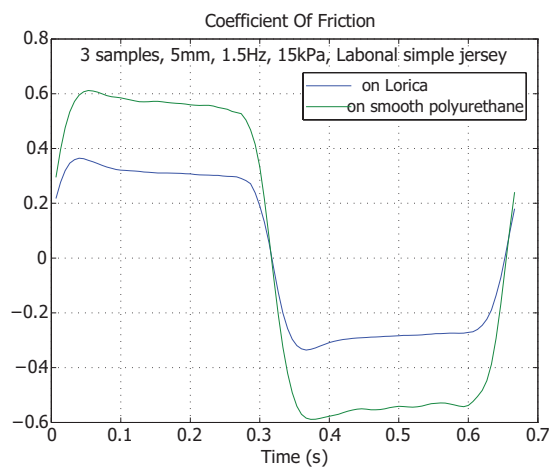
a)



b)



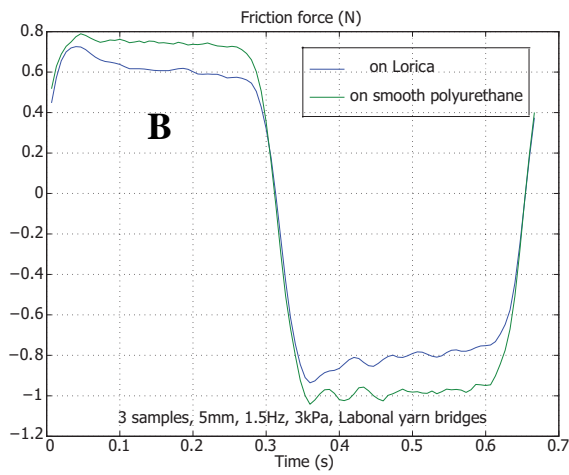
c)



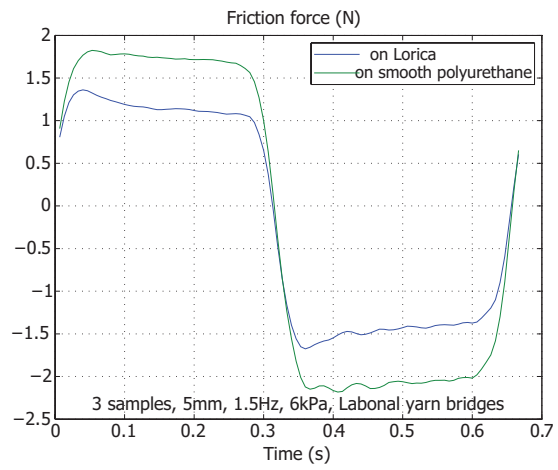
d)

Figure 66: Coefficient of friction of Labonal simple jersey in contact with Lorica® and smooth polyurethane under a) 3 kPa, b) 6 kPa, c) 10 kPa and d) 15 kPa. The mean curves were calculated from 3 experiments for a friction distance of 5 mm and a friction frequency of 1.5 Hz on the TFA.

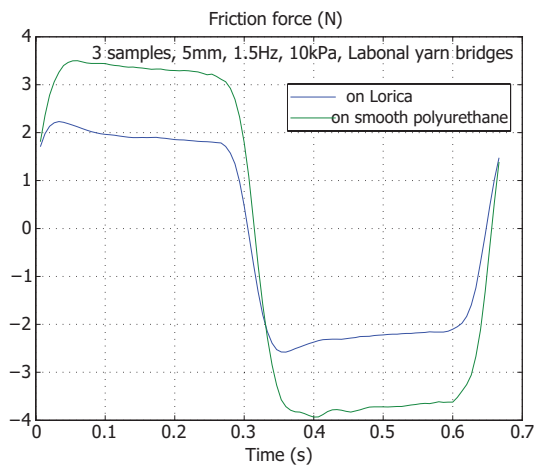




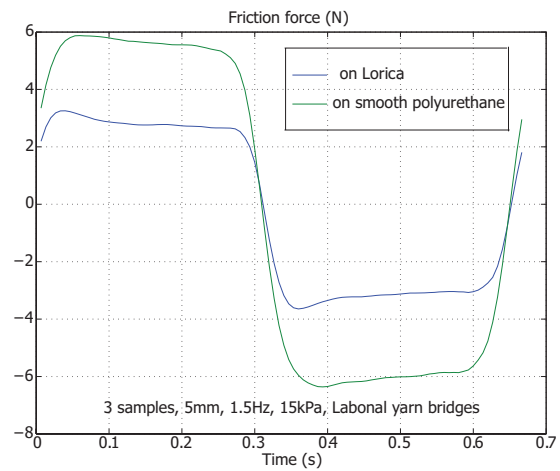
a)



b)

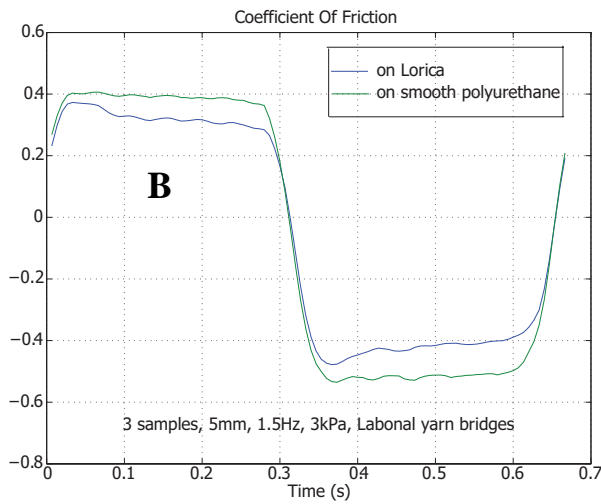


c)

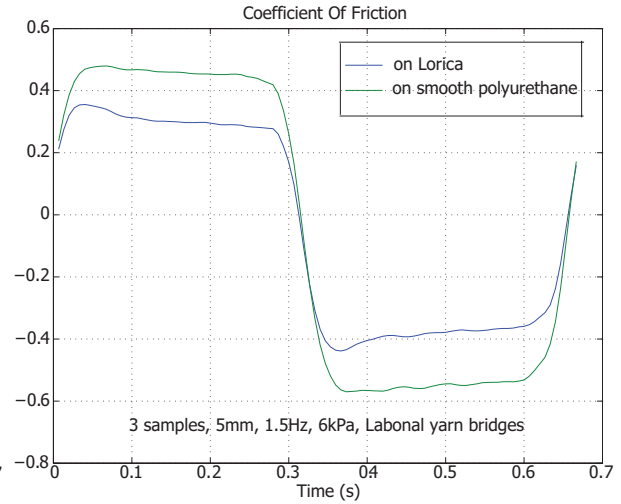


d)

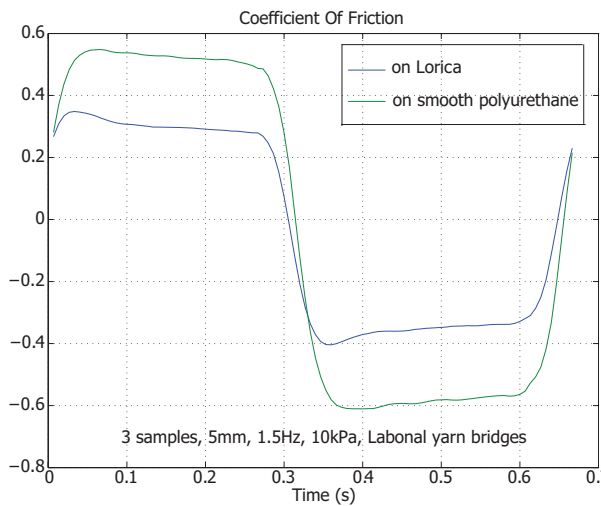
Figure 67: Friction force of Labonal yarn bridges in contact with Lorica® and smooth polyurethane under a) 3 kPa, b) 6 kPa, c) 10 kPa and d) 15 kPa. The mean curves were calculated from 3 experiments for a friction distance of 5 mm and a friction frequency of 1.5 Hz on the TFA. The letter B identifies the half period where the movement of the pin follows bridges orientation.



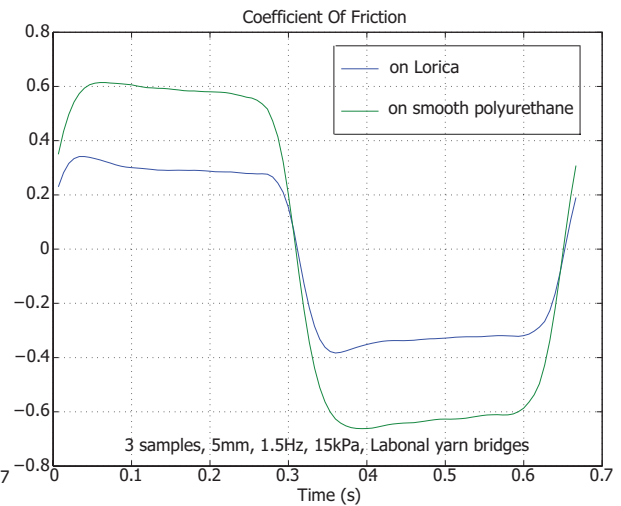
a)



b)



c)



d)

Figure 68: Coefficient of friction of Labonal yarn bridges in contact with Lorica® and smooth polyurethane under a) 3 kPa, b) 6 kPa, c) 10 kPa and d) 15 kPa. The mean curves were calculated from 3 experiments for a friction distance of 5 mm and a friction frequency of 1.5 Hz on the TFA. The letter B identifies the half period where the movement of the pin follows bridges orientation.

## B. Experiments using the smooth and the “rough” pins made of stainless steel

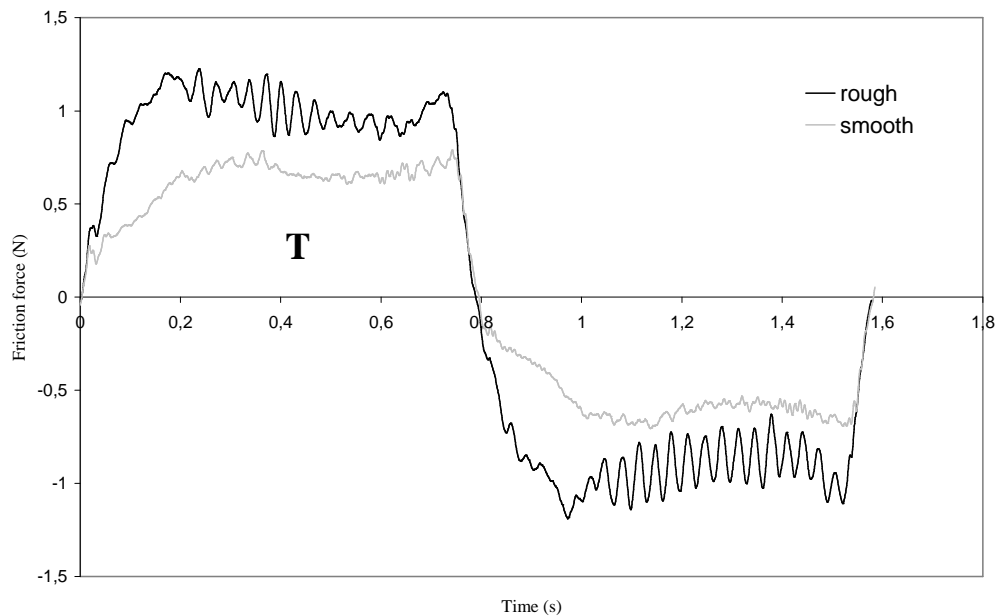
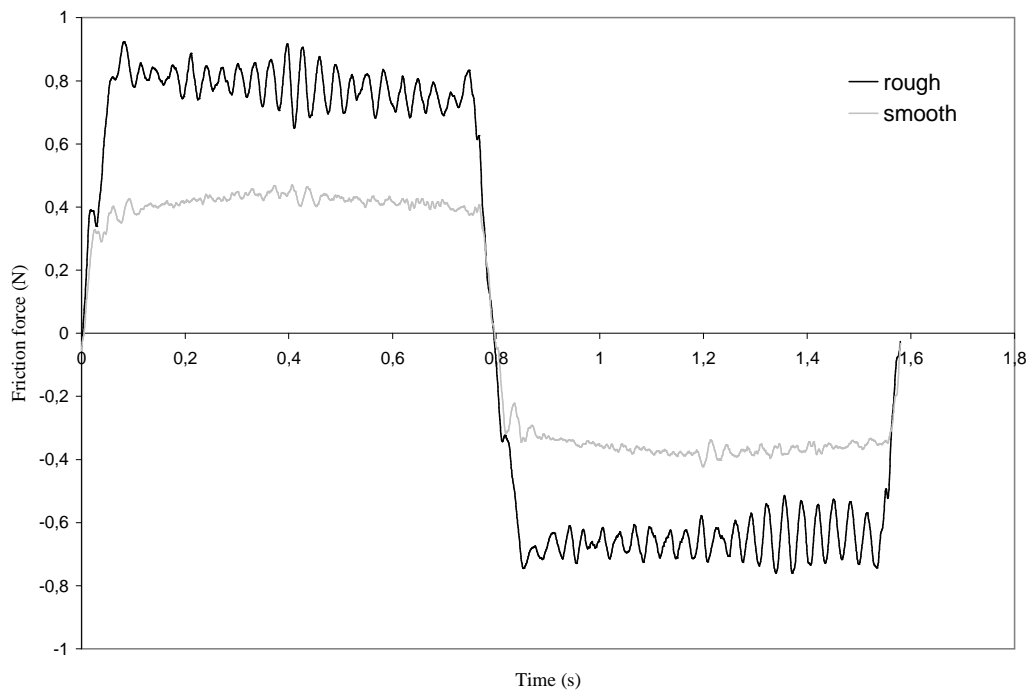


Figure 69: Friction force of Labonal terry jersey in contact with both rough and smooth stainless steel pins. The experiment was carried out on the LPMT's tribometer for a sliding distance of 30 mm, a sliding frequency of 0.63 Hz and a pressure of 15 kPa. The letter T identifies the half period where the movement of the pin follows terries orientation.

As can be observed in figures 33 and 34, the friction force gets higher when the pin roughness increases. Friction is due to deformation and adhesion. As the contributions of adhesion and deformation can not be measured independently, it is not possible to compare absolute values and one can only conclude on the relative importance of the two friction components. Deformation mechanisms are important for the structured steel and Lorica® surfaces. Adhesion usually gets higher when the contact surface increases, i.e., when the surface roughness decreases. Here, the friction force rises with the surface roughness, therefore it can be deduced that the contribution of the deformation component of friction is essential. It is nevertheless interesting to see that basic and terry jersey structures are not

reacting in the same way when the pin roughness is changed. The difference between both signals is less important in the case of terry jersey (40% rise) than for basic jersey (100% growth); the contact area between the sock and the pin is indeed assumed to be smaller for the terry jersey than for the simple jersey.

Moreover, experiments with the smooth stainless steel pin and the pin covered with Lorica® give the same trend (figures 35 and 36). It can be observed that the friction force is higher when the sock is in contact with Lorica® for both terry and simple jersey structures. The difference is quite small for terry jersey socks while it is greater in the case of simple jersey socks. Figure 35 indicates that the deformation of the textile structure is important (the properties of the pin seem relatively unimportant) whereas figure 36 indicates that the properties of the pin are important. It can therefore be assumed that the contribution of deformation in friction is more important for the terry jersey structure than for the simple jersey.



*Figure 70: Friction force of Labonal simple jersey in contact with both rough and smooth stainless steel pins. The experiment was carried out on the LPMT's tribometer for a sliding distance of 30 mm, a sliding frequency of 0.63 Hz and a pressure of 15 kPa.*

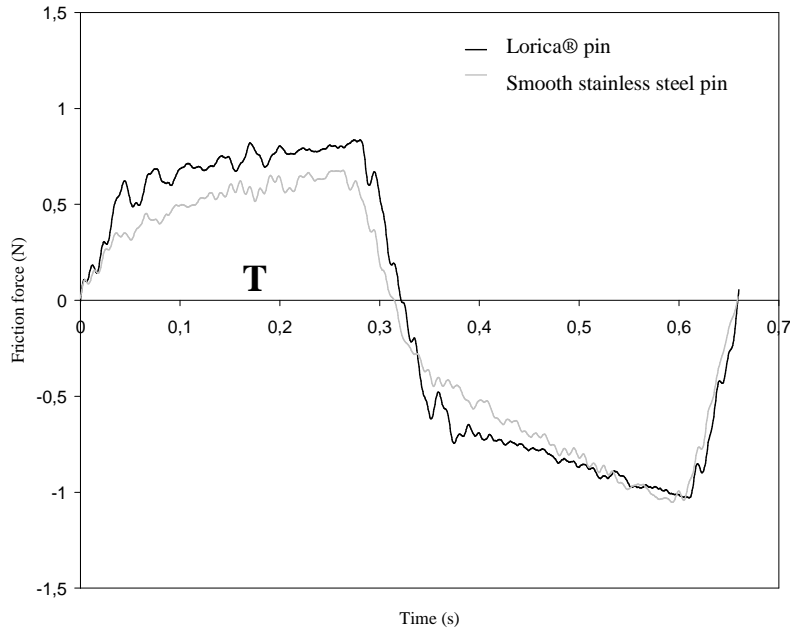


Figure 71: Friction force of Labonal terry jersey in contact with Lorica® and smooth stainless steel pins. The experiment was carried out on the LPMT's tribometer for a sliding distance of 5 mm, a sliding frequency of 1.5 Hz and a pressure of 15 kPa. The letter T identifies the half period where the movement of the pin follows terries orientation.

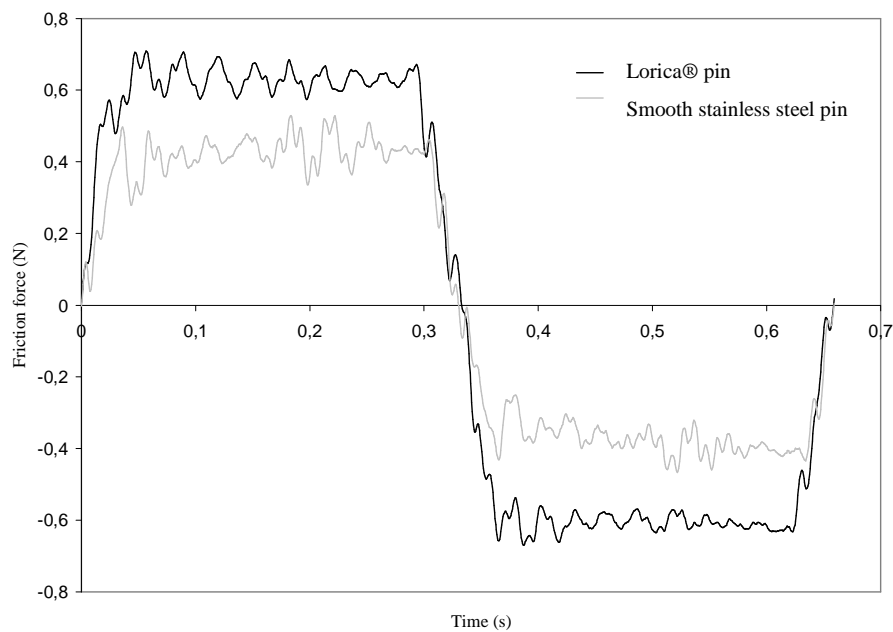


Figure 72: Friction force of Labonal simple jersey in contact with Lorica® and smooth stainless steel pins. The experiment was carried out on the LPMT's tribometer for a sliding distance of 5 mm, a sliding frequency of 1.5 Hz and a pressure of 15 kPa.

## II. COMPRESSION EXPERIMENTS

The TFA and the LPMT's tribometer allowed us to compare different sock knitted structures in terms of friction. We have seen that the terry jersey and the yarn bridges structures give higher friction than the simple and the double jersey when rubbed against Lorica®. However, the friction exerted on the foot skin is not the only parameter to take in account when choosing a running sock. The sock, by its structure and thickness, can reduce the pressure on the skin which may lead to less severe skin irritations. Compression experiments were therefore realised.

The terry jersey structure intuitively seemed better than the simple jersey structure for running application because it is thicker and therefore is expected to present a higher static “damping effect” i.e. a higher distribution of the mechanical stresses through the sock structure. For a given applied pressure on the sock structure, the pressure perceived by the skin is expected to be lower for the terry jersey than for the simple jersey. Compression experiments were carried out in order to investigate this argument. The objective of these experimentations was to measure, for a given applied pressure (same soil, same shoe and same runner), the pressure perceived by the foot skin for the different sock structures. As shown figure 17 chapter II, there is a zone that will not be considered for the compression results. This zone is identified by a grey area.

### 1. Sock structure impact

The plunger stops sinking in the sock structure when the perceived pressure reaches 15 kPa. The maximal perceived pressure is thus the same for all the socks while the maximal applied pressure necessary to get 15 kPa through the sock depends on the knitted structure. It has to be specified that no saturation of the Flexiforce® was observed during the compression experiments. Figures 37 and 38 respectively show the compression results of Labonal socks and of terry jersey 10 – 16 and simple jersey 10 – 16. Figure 37a gives the maximal applied pressure for Labonal socks, the socks can be ranged from the lowest to the highest maximal pressure: yarn bridges, terry jersey, double jersey and simple jersey. Figure 38a confirms that the maximal applied pressure is higher for simple jersey than for terry jersey structure.

Moreover, for a given applied pressure, figures 37c and 37d indicate that simple jersey gives the lowest pressure on the skin, terry jersey and yarn bridges show similar perceived pressure and the highest pressure is obtained with double jersey structure. Double jersey is

thicker than simple jersey but may not be soft like terry jersey so that less cushioning is expected. This is supported by table 4 which gives the thickness of the socks under 49 Pa ( $T_o$ ) and 15 kPa ( $T_m$ ) and the difference  $T_o - T_m$  which corresponds to the compressible thickness of the socks. Figures 38c and 38d corroborate the fact that, for the same applied pressure, simple jersey produces less pressure on the skin than terry jersey.

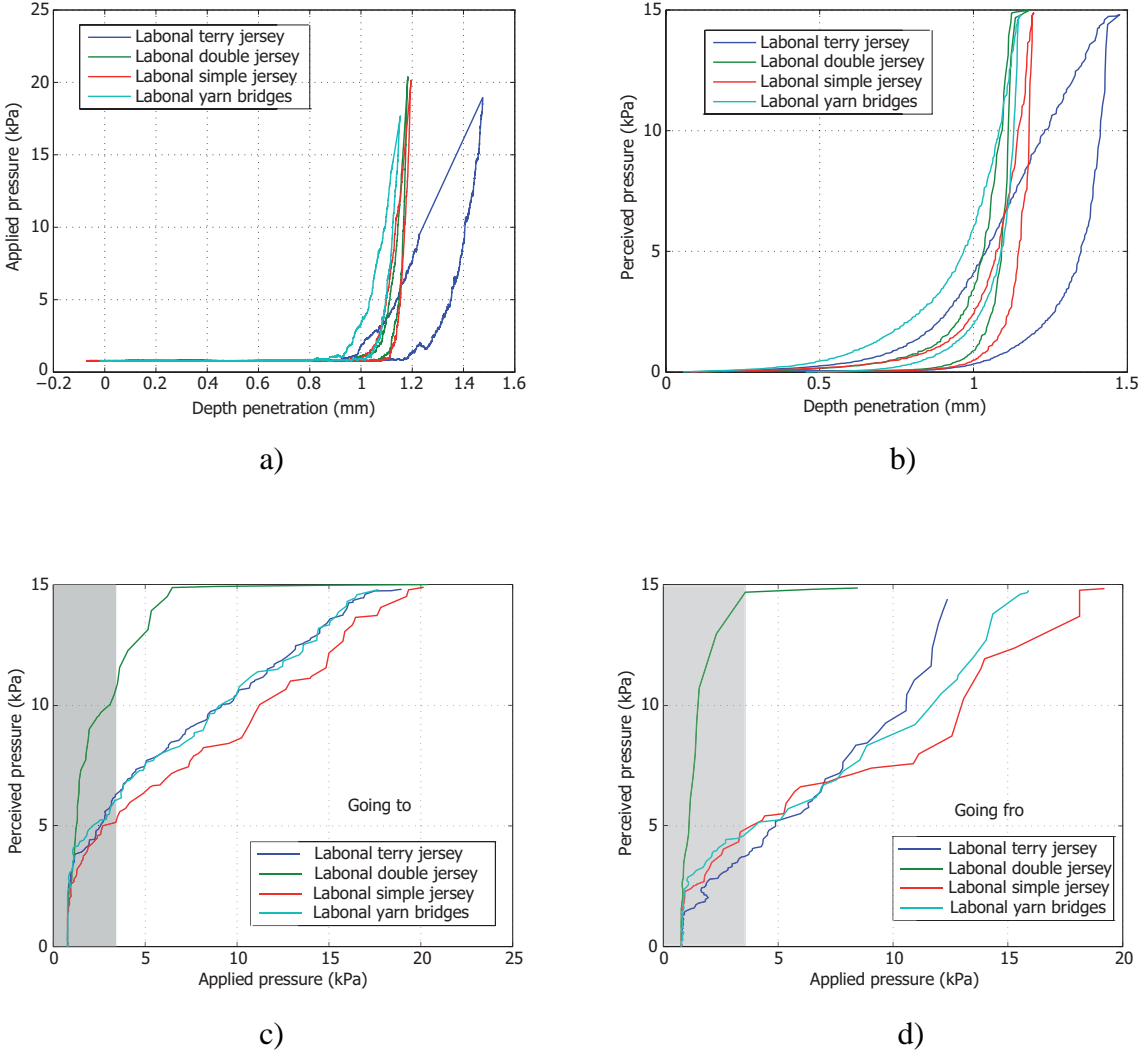
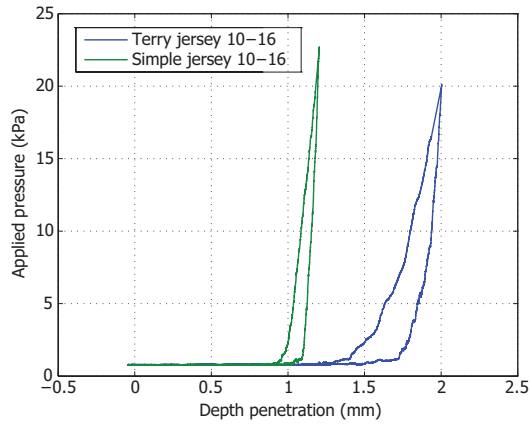
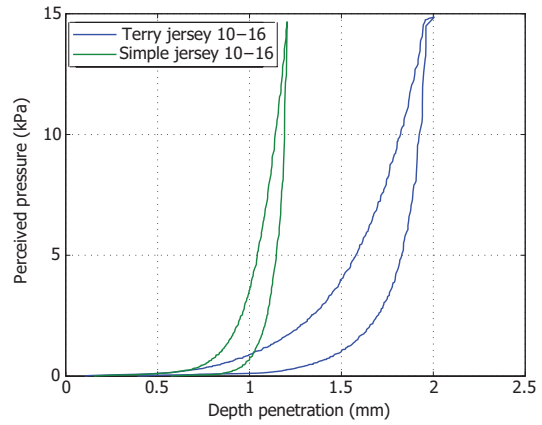


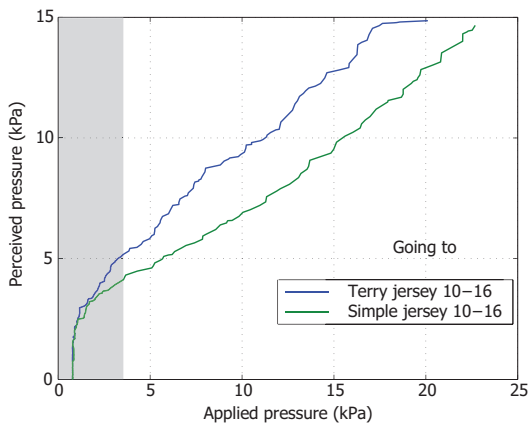
Figure 73: Compression results of Labonal socks; a) applied pressure versus depth penetration, b) perceived pressure versus depth penetration, c) perceived pressure versus applied pressure for the forward direction (compression) and d) perceived pressure versus applied pressure for the back direction (decompression). These mean results are calculated from 10 experiments.



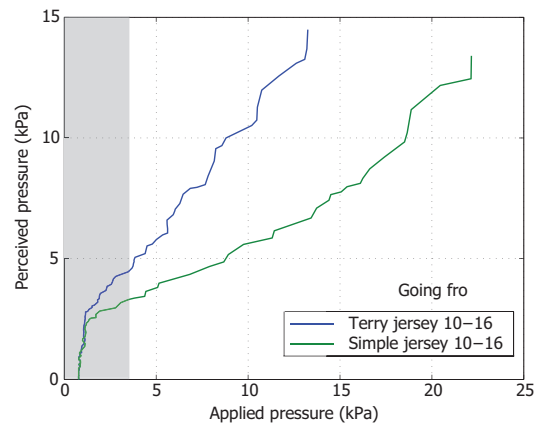
a)



b)



c)



d)

Figure 74: Compression results of terry and simple jersey socks; a) applied pressure versus depth penetration, b) perceived pressure versus depth penetration, c) perceived pressure versus applied pressure for the forward direction (compression) and d) perceived pressure versus applied pressure for the back direction (decompression). These mean results are calculated from 10 experiments.



KNITTED STRUCTURE	MEAN $T_O$ (MM)	MEAN $T_M$ (MM)	$T_O - T_M$ (MM)
Terry jersey	$3.64 \pm 0.06$	$2.43 \pm 0.07$	$1.21 \pm 0.13$
Double jersey	$1.95 \pm 0.09$	$1.16 \pm 0.01$	$0.79 \pm 0.10$
Simple jersey	$1.89 \pm 0.05$	$0.98 \pm 0.02$	$0.91 \pm 0.07$
Yarn bridges	$2.25 \pm 0.05$	$1.27 \pm 0.02$	$0.98 \pm 0.07$

Table 16: Labonal socks thickness under 49 Pa ( $T_o$ ) and 15 kPa ( $T_m$ ), mean results from 10 experiments.

## 2. Yarn count influence

Figure 39 gives the compression results of terry jersey socks which only differ in their yarn count (same stitch length).

It can be observed in figure 39a that the maximal applied pressure is similar for these three socks. However, figure 39b points out that, for a given depth penetration, terry jersey 10 – 16 and 10 - 20 give similar perceived pressure while terry jersey 10- 12 induces higher pressure. Moreover, it can be noticed in figures 39c and 39d that, for a given applied pressure, the socks can be ranged from the lowest to the highest perceived pressure as follows: terry jersey 10 – 20, terry jersey 10 – 16 and terry jersey 10 – 12.

The perceived pressure thus increases with the yarn count which can be related to the sock softness. When the yarn count increases i.e. when the diameter of the yarn gets bigger, the yarn gets less easy to bend and the sock structure gets less soft. Therefore, for a given applied pressure and the same stitch length, the pressure the sock exerts on the skin increases with the yarn count.

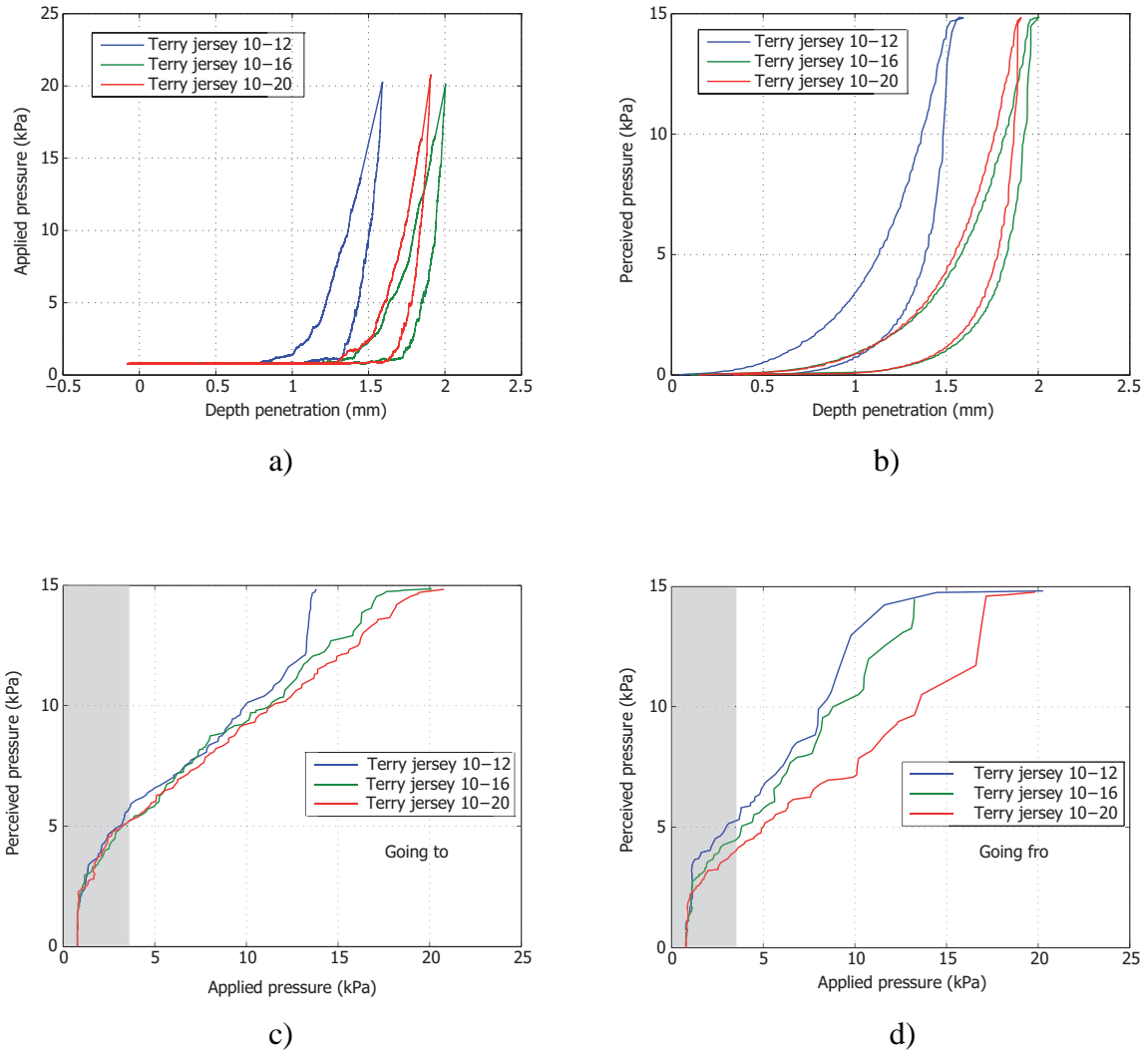


Figure 75: Compression results of terry jersey 10 – 12, 10 – 16 and 10 – 20; a) applied pressure versus depth penetration, b) perceived pressure versus depth penetration, c) perceived pressure versus applied pressure for the forward direction (compression) and d) perceived pressure versus applied pressure for the back direction (decompression). Let's remind that these three structures only differ by their yarn count which respectively equal to 12, 16 and 20 Ne(c) i.e. 141, 106 and 85 Tex. These mean results are calculated from 10 experiments.

### 3. Energetic approach

The ratio of the perceived energy divided by the applied energy was calculated for the socks that have previously been studied in compression. As it has been outlined in chapter 2, the Flexiforce® does not have a linear behaviour for low pressures, consequently the data given here are qualitative ratios; the sock which transmitted the highest amount of energy has a ratio equal to 1. These ratios are indicated in table 5.

SOCK	RATIO PERCEIVED ENERGY / APPLIED ENERGY
Labonal simple jersey	0.69
Labonal double jersey	0.92
Labonal yarn bridges	1.00
Labonal terry jersey	0.73
Terry jersey 10 - 12	0.81
Terry jersey 10 - 16	0.84
Terry jersey 10 - 20	0.80
Simple jersey 10 - 16	0.58

*Table 17: Socks energetic ratios. These ratios were calculated from the mean curves of the applied pressure and the perceived pressure in function of the depth penetration.*

This table indicates that Labonal double jersey and Labonal yarn bridges absorb less energy than Labonal simple and terry jersey which have similar ratios. On the other hand, the energetic ratio of terry jersey 10 – 16 is 50% higher than simple jersey 10 – 16 ratio. Terry jersey 10 - 16 is thicker than simple jersey 10 – 16 but may not present enough softness to absorb the energy transmitted to the sock (unlike Labonal terry jersey). The yarn count does not seem to impact the energetic ratio.

### III. CONCLUSION

The pressure on the foot depends on the shoe (shape, size), the foot shape and the way people tighten their shoes. If the space between the shoe and the foot is not sufficient, the sock will exert a non negligible pressure on the foot even when it does not touch the ground inducing a great friction force between the sock and the skin. On the other hand, shoes which are not tightened enough will lead to excessive friction on the skin due to a higher sliding distance. The footwear should thus be adapted to the runner foot. The sock structure should notably be considered when choosing the size of the shoe. The size of the shoe has to be higher for a thick sock structure like terry jersey than for a thin sock structure like simple jersey.

Compression experiments indicated (figure 37 and table 5) that double jersey and yarn bridges structures do not present a good static “damping effect”. These two structures will then not be recommended.

The friction results obtained on the LPMT’s tribometer showed that, when friction began, terry jersey coefficient of friction was lower than simple jersey coefficient of friction and progressively got higher. Figure 40 shows the distance along which the coefficient of friction of Labonal terry jersey is lower than the one of Labonal simple jersey versus the applied pressure. It can be seen that this distance increases with the applied pressure. Labonal terry jersey may therefore be a good compromise especially when high pressures are exerted on the skin i.e. for stoutly built people. To be recommended, terry jersey socks need to present compact, homogeneous and rather elastic terries which are oriented towards the toe of the sock.

Moreover, in-shoe conditions are probably an intermediate between the conditions of the LPMT’s tribometer and TFA’s conditions. Figure 41 gives the coefficient of friction (calculated from figures 14 and 16 as the value of the coefficient of friction for the first half of the curve) in function of the applied pressure for Labonal terry and simple jersey for both tribometers. An intermediate between both tribometers would give a higher coefficient of friction for Labonal simple jersey than for Labonal terry jersey.

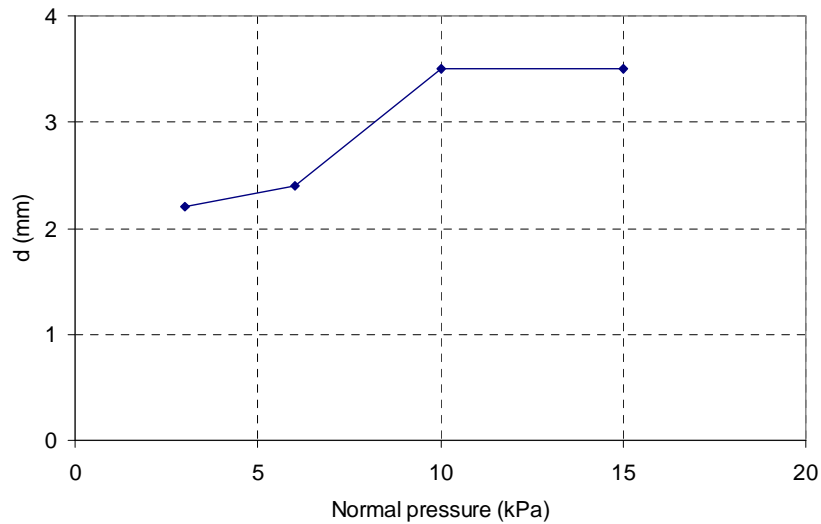


Figure 76: Distance along which the coefficient of friction of Labonal terry jersey is lower than the one of Labonal simple jersey ( $d$ ) versus the applied pressure. The data are taken from friction experiments with the Lorica® pin on the LPMT's tribometer for a friction distance of 5 mm and a friction frequency of 1.5 Hz (cf. figure 22).

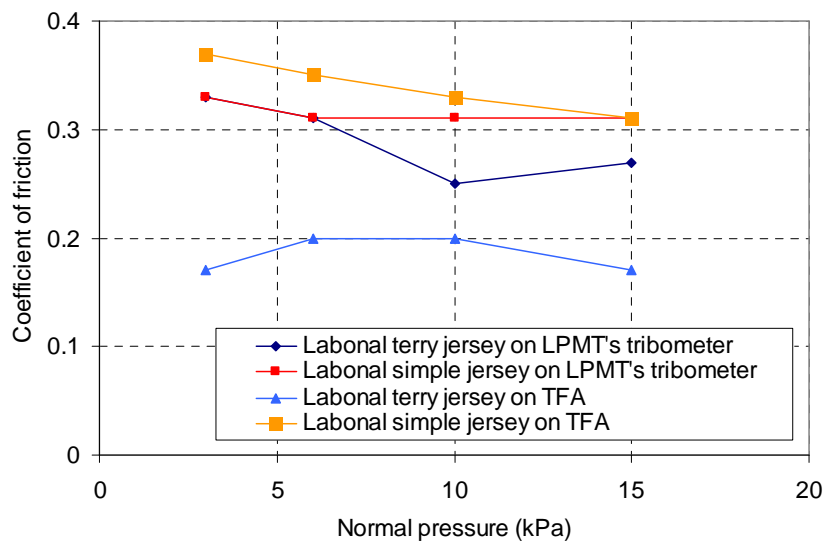


Figure 77: Coefficient of friction of Labonal terry and simple jersey in contact with Lorica® versus the applied pressure. The results are given for both the LPMT's tribometer and the TFA for a friction distance of 5 mm and a friction frequency of 1.5 Hz for the forward sliding direction.

The thickness of terry jersey socks may be appreciated by people with bony prominences at specific areas of the foot or with pre-existing blisters. In this case, the terry jersey structure will reduce the pain. In addition, terry jersey structure is easy and inexpensive to realise whereas the technique of knitting socks with different thicknesses (higher thickness at selected areas) is expensive. Terry jersey structure better corresponds to recreational runners.

However, figures 37, 38 and table 5 indicate that the static “damping effect” of simple jersey sock is greater than the static “damping effect” of terry jersey. It can be seen in figure 37d that for an applied pressure of 12.8 kPa, the perceived pressure equals to 10 kPa for Labonal simple jersey and to 15 kPa for Labonal terry jersey. When comparing the friction force of these two socks in contact with Lorica® (cf. figure 42), terry jersey under 15 kPa induces 20 to 60 % more friction than simple jersey under 10 kPa. If we only consider the static “damping effect” of the sock structure, it would therefore be recommended to wear simple jersey rather than terry jersey socks.

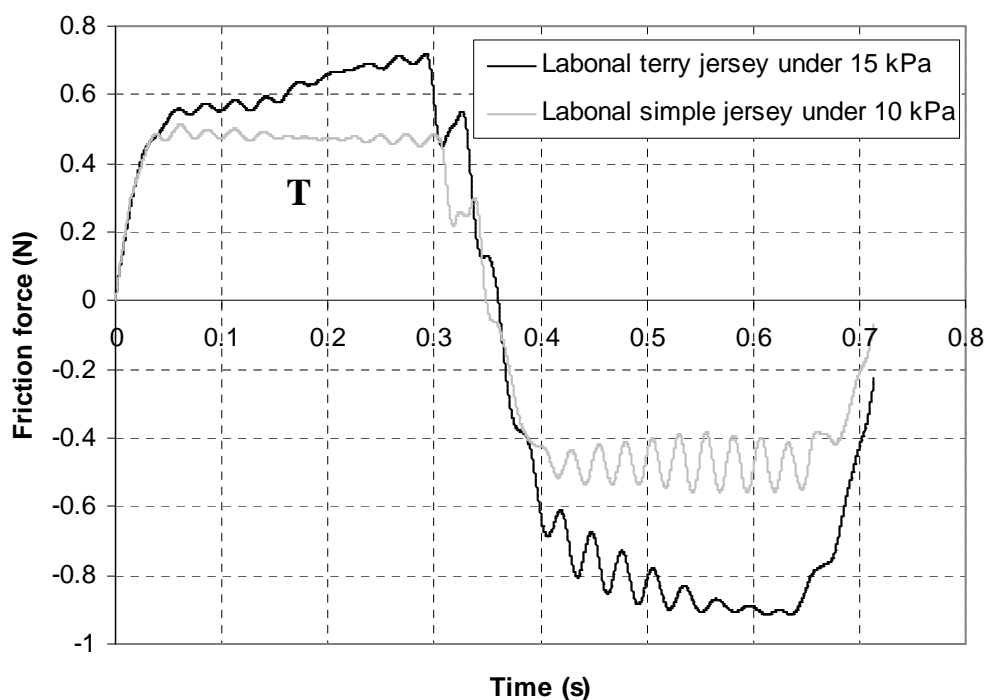


Figure 78: Friction force of Labonal terry jersey under 15 kPa and Labonal simple jersey under 10 kPa in contact with the Lorica® pin. The experiment was carried out on the LPMT's

tribometer with a sliding distance of 5 mm and a sliding frequency of 1.5 Hz. The letter T identifies the half period where the movement of the pin follows terries orientation.

Table 4 shows that the maximal perceived pressure is obtained for a greater depth penetration in the case of the terry jersey compared to the simple jersey i.e. the maximal perceived pressure is reached later in the case of the terry jersey. Terry jersey socks may then provide a better dynamic damping than simple jersey socks. A vibratory analysis of terry and simple jersey socks would determine which structure best resists to a shock and is proposed as an outlook. We nevertheless investigated the ability of the different sock structures to dissipate the energy of a shock dropping a ball of 9g from an initial height of 31.5 cm and observing the height of the first rebound of the ball to calculate the coefficient of restitution  $e$  which is given by the following expression:  $h_n = e^{2n} \times h_0$  where  $h_n$  is the height of the  $n^{\text{th}}$  rebound of the ball and  $h_0$  is the initial height. The terry jersey structure dissipated more energy i.e. has a lower coefficient of restitution than the simple jersey structure as it is reported in table 6.

SOCK	COEFFICIENT OF RESTITUTION
Labonal terry jersey	0.39 ± 0.03
Labonal simple jersey	0.55 ± 0.02
Labonal double jersey	0.45 ± 0.01
Labonal yarn bridges	0.46 ± 0.02
Terry jersey 10 - 16	0.46 ± 0.02
Simple jersey 10 - 16	0.54 ± 0.02
Support	0.75 ± 0.01

Table 18: Coefficients of restitution. The coefficient of restitution of the support is given because the socks are thin and smooth compared to the support and it therefore has an influence on the quantitative results of shock absorption.

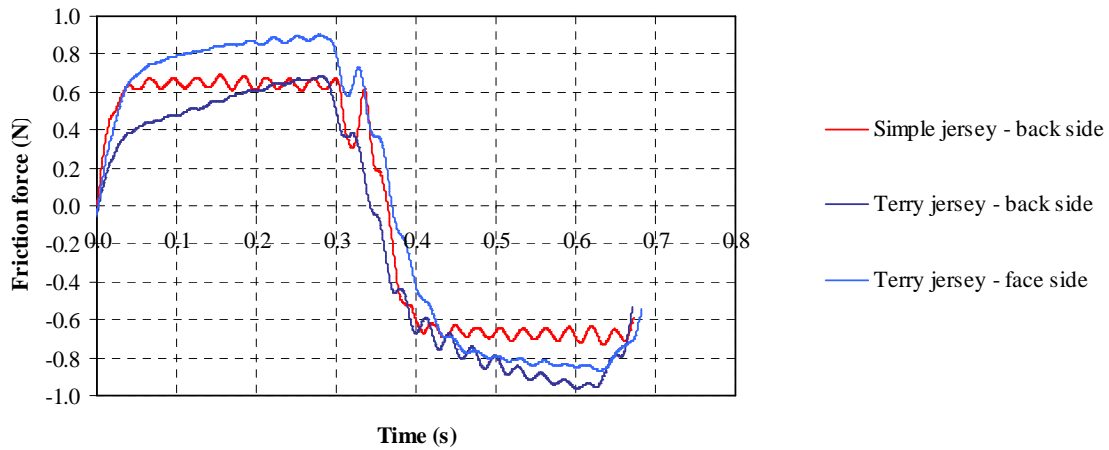


Figure 79: Friction force of Labonal terry jersey (face and back sides) and back side of Labonal simple jersey under 15 kPa in contact with the Lorica® pin. The experiment was carried out on the LPMT’s tribometer with a sliding distance of 5 mm and a sliding frequency of 1.5 Hz. The curves given here are mean curves from 5 measurements.

When running, the foot skin is first subjected to a shock and then to progressive compression and friction. It is not evident whether the shock or the friction energy has the greater influence on skin irritations. We can thus conclude that the simple jersey structure is better in terms of friction and quasi-static “damping effect” compared to the terry jersey structure whereas the terry jersey structure has a higher dynamic “damping effect” than the simple jersey structure. For hiking socks, we recommend wearing simple jersey socks and for running socks either simple jersey or terry jersey socks are suitable. Terry jersey socks should be worn with the terries in contact with the skin and oriented towards the toe for the friction on the skin to be reduced. Figure 43 indeed shows that for a normal pressure of 15 kPa, the friction force of the face of terry jersey (non terry side) is higher than the friction force of the back of terry jersey (terry side) and of the back side of simple jersey.

We compared the different sock structures in terms of friction induced on the foot during running. We have seen that Labonal terry jersey friction force has a particular shape that may be due to the rotation of terries during a friction cycle. We have also discussed the importance of the contribution of deformation and adhesion in friction for Labonal terry and simple jersey socks. From this experimental study, it can be concluded that the deformation



component of friction is important in the case of terry jersey. Based on this experimental result, we propose a discrete model of the friction of terry-covered textile surfaces described on the next chapter.

# Chapter IV: modelling of sock-to-skin friction

## Résumé

Les résultats expérimentaux ont montré que le frottement des surfaces recouvertes de bouclettes se déroule en 2 temps. Les bouclettes sont d'abord déformées i.e. orientées dans le sens du mouvement du palpeur, puis elles sont frottées. Nous avons modélisé ce comportement. Ce dernier chapitre présente tout d'abord les modèles de frottement et de compression disponibles dans la bibliographie puis détaille le modèle proposé.

Les modèles de « brosses » pourraient être adaptés à la simulation du frottement entre la peau et une chaussette bouclette car la structure d'une brosse et la déformation des poils de la brosse sont très similaires à la structure du jersey bouclette et au mouvement des boucles lorsqu'elles sont frottées. Comme dans les modèles de « brosses » étudiés, nous considérerons chaque bouclette de manière indépendante.

Les modèles de frottement d'un pneu sur la route sont également intéressants car la surface d'un pneumatique présente des sillons et pourrait être modélisée comme un polymère dont la surface est recouverte de poils. Nous nous sommes inspirés du modèle de LuGre qui permet la simulation de différents comportements en frottement, du purement élastique au viscoélastique. Nous n'avons considéré que la partie élastique des équations de ce modèle.

L'équation de Van Wyk nous permet de déterminer la limite entre la compression des bouclettes et la compression de la structure complète de la chaussette bouclette en réalisant un ajustement grâce à une courbe expérimentale.

Nous avons modélisé la force de frottement d'une surface tricotée recouverte de bouclettes sur la peau artificielle Lorica® Soft. Ce modèle à destination des industriels a pour objectif de comparer de manière simple différentes chaussettes en termes de frottement induit sur la peau afin de réduire le risque d'apparition d'irritations cutanées. Les modèles de frottement et de compression existants sont tous fondés sur le fléchissement des poils, fils ou fibres. Dans un premier temps, le mouvement des bouclettes a donc été simulé comme du fléchissement et de la compression mais cette première approche a donné une modélisation compliquée, très lente et peu satisfaisante. Nous avons donc simulé le comportement en frottement comme une rotation des bouclettes.

La partie expérimentale de ce travail a montré que la partie déformation du frottement était plus déterminante que la partie adhésive qui sera négligée dans notre simulation. Le frottement est divisé en deux phases, les bouclettes effectuent une rotation de leur angle initial à leur angle final sans qu'il y ait de glissement entre les boucles et le palpeur, puis elles restent en position finale et sont frottées avec un coefficient de frottement constant. Le comportement des boucles est supposé élastique même s'il est plus vraisemblablement viscoélastique. La partie non verticale des boucles n'est pas prise en compte. La force de frottement est modélisée comme une fonction de l'orientation des bouclettes i.e. comme une fonction du déplacement horizontal du palpeur. On considère deux groupes distincts de bouclettes ; celles qui sont sous le palpeur et celles à l'avant du palpeur au début du mouvement. La force de frottement totale résulte des forces de compression exercées par les boucles sur le palpeur et est égale à la somme des forces de frottement individuelles des bouclettes. L'instant auquel le palpeur touche la boucle, où la boucle arrive à sa position finale ou encore l'instant où elle est lâchée par le palpeur dépendent de la place de la bouclette dans la colonne de mailles. On calcule donc la force de frottement pour une colonne avant de multiplier cette dernière par le nombre de rangées présentes sous le palpeur. Les bouclettes sont considérées comme indépendantes les unes des autres.

Le moment d'un fil de bouclette peut être calculé à la fois à partir de la force de frottement et de la force de compression exercées sur ce fil (cf. équation [E1]).

$$M(\theta) = F_c L \sin \theta = F_f L \cos \theta \quad [E1]$$

M est le moment en N.mm,  $\theta$  l'angle formé par le fil de bouclette et la verticale au tricot en rad,  $F_c$  la force de compression en N,  $F_f$  la force de frottement en N, L la hauteur de la bouclette. Le déplacement vertical du fil de bouclette en mm est donné par l'équation [E2] :

$$d(\theta) = L(\cos \theta_i - \cos \theta) \quad [E2]$$

$\theta_i$  est l'angle initial du fil de bouclette en rad.

Des deux premières équations découle l'expression de la force de frottement [E3] :

$$F_f = \frac{F_c L \sin \theta}{L \cos \theta_i - d(\theta)} \quad [E3]$$

Le déplacement horizontal du fil de bouclette est donné par l'équation [E4] :

$$z(\theta) = L(\sin \theta - \sin \theta_i) \quad [E4]$$

Pour exprimer la force de frottement en fonction du déplacement horizontal du fil de bouclette, on suppose que :

$$F_f = \lambda(\theta)z(\theta) \quad [E5]$$

$\lambda(\theta)$  est déterminé à partir des équations [E3], [E4], et [E5] :

$$\lambda(\theta) = \frac{F_c \sin \theta}{(L \cos \theta - d(\theta))(\sin \theta - \sin \theta_i)} \quad [E6]$$

Nous avons considéré un coefficient  $\lambda_c$  constant pour calculer la force de frottement d'un fil de bouclette :

$$\lambda_c = \frac{F_{f \max}}{z_{\max}(\theta)} = \frac{F_{c \max} \sin \theta_{\max}}{(L \cos \theta_i - d_{\max}(\theta))(\sin \theta_{\max} - \sin \theta_i)} \quad [E7]$$

$\theta_{\max}$  est l'angle de rotation maximal,  $F_{c \max}$  et  $d_{\max}$  sont obtenus à partir des courbes de compression Kawabata en utilisant l'équation de Van Wyk. Pour le jersey bouclette Labonal,  $\lambda_c = 2,3 \times 10^{-3}$  N/mm/fil.

Les équations ci-dessus sont valables pour le sens aller du mouvement du palpeur.

La force de frottement modélisée est ajustée à une courbe expérimentale. L'ajustement est réalisé de manière indépendante en sens aller et retour. Le paramètre d'ajustement est l'angle de rotation maximal dans la direction considérée. Cet angle est calculé en appliquant la méthode des moindres carrés à une courbe expérimentale. Il correspond à l'inclinaison finale des bouclettes par rapport à la verticale au tricot. Les valeurs limites de cet angle sont estimées à partir de photographies afin de corroborer les résultats de la modélisation.

La modélisation est très proche des résultats expérimentaux en ce qui concerne le jersey bouclette Labonal. Afin d'obtenir un modèle simple facilement utilisable par des industriels, nous avons fait de nombreuses hypothèses, les différences observées entre les résultats de la simulation et les courbes expérimentales sont dues à ces hypothèses. Il se peut notamment que la force normale appliquée ne suffise pas à coucher complètement les bouclettes. Les bouclettes n'atteignent donc pas forcément leur angle maximal de rotation, surtout en sens retour lorsqu'elles s'opposent au mouvement du palpeur, ce qui explique l'asymétrie plus prononcée des résultats de la simulation.

L'introduction de la partie adhésive du frottement i.e. l'adhésion entre le palpeur et les bouclettes mais aussi les forces d'attraction exercées par une bouclette sur ses voisines devrait permettre d'améliorer le modèle. De plus, les bouclettes sont ici considérées comme indépendantes alors qu'en réalité, chaque boucle touche et déforme sa voisine lorsqu'elle

bouge. La prise en compte de la force de compression exercée par chaque boucle sur la suivante devrait également parfaire les résultats de la simulation.

# CONTENTS

<b>Chapter IV: modelling of sock-to-skin friction</b>	<b>161</b>
I. THEORETICAL BACKGROUND	167
1. Friction models	167
A. Brush models	167
B. Road/tire dynamic friction models	170
2. Compression models	172
II. DISCRETE MODEL OF SOCK-TO-SKIN FRICTION	176
1. Mechanical model's assumptions	177
2. Mathematical expression of the friction force	179
3. Results and discussion	183
Literature cited	186

The previous chapter detailed the experimental friction results. These results indicate that the friction of terry covered socks is a two stages process. First the terries are deformed i.e. they are oriented in the pin sliding direction and secondly they are rubbed by the pin. We modelled this behaviour and the simulation shows good correspondence with the experiment. In this last chapter, previous studies on friction and compression models will first be outlined then the model we propose will be fully detailed.

## **I. THEORETICAL BACKGROUND**

### **1. Friction models**

#### **A. Brush models**

Brush models may be adapted to simulate the friction between the skin and a terry jersey sock since the structure of a brush and the deformation of the hairs of a brush are respectively similar to the terry jersey structure and the movement of the terries when rubbed against a counterpart material.

Kotomin and Avdeev [1] proposed a macromodel approach for experimental studies of polymer brushes friction using ordinary tooth brushes with different stiffness. Experiments were performed on pairs of brushes with various mutual penetrations and speeds of displacement. Two types of toothbrushes were used for experiments: “medium” type brushes i.e. mild brushes and “hard” type brushes i.e. rigid brushes. The speed of the crosshead displacement varied in the range 1 – 500 mm/min. The penetration depth was 1, 3 and 7 mm. The displacement range was 10 mm. A simultaneous recording of the shear force and the normal displacement response with an accuracy of 0.2  $\mu\text{m}$  were realised. A force-displacement response during cyclic shift in two directions was studied. As could be expected, the rate of force growth was higher for rigid brushes than for mild brushes. This rate was therefore considered as characteristic of rigidity. Contrasting with the shear force, the normal repulsive reaction for mild brushes is stronger than that for rigid brushes. Considering the interaction of two single filaments of the opposite brushes, the authors identified two different rubbing mechanisms. At the beginning of the movement, the filaments ends transfer



the stress to the whole filaments which are bent (cf. figure 1). Then, the disconnection of the filaments of the two brushes may happen in two ways:

- The sliding of bent filaments ends along each other up to separate the brushes ends, called “slipping-pulling” mechanism
- The deviation across common axis of the filaments axis leading to an interpenetration of the opposite brushes without contact, called “rake-on-rake” mechanism

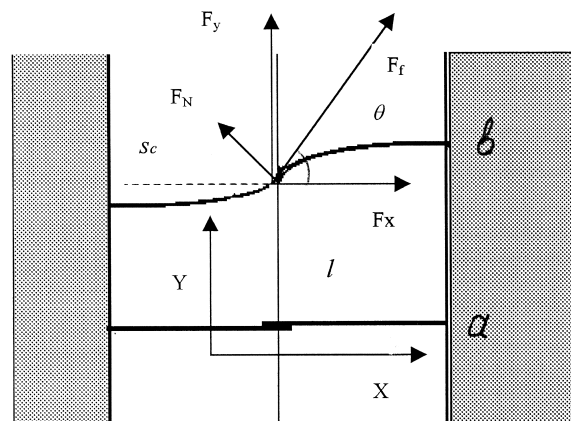


Figure 80: Geometric model for filaments interaction in a) initial and b) separation position [1].

The first mechanism was analysed to correspond to mild brushes with low penetration and the second for rigid brushes with deep mutual penetration. A rather unexpected phenomenon was observed: the normal displacement was negative at the beginning of the cycle which corresponds to an “attraction” of the rubbing brushes while moving. This attraction was considered as a consequence of the friction force reaction along the filament axis. The normal component of this reaction actually acted as an attraction force. This force was similar for both types of brushes as it depended mostly on the friction coefficient between filaments. The existence of a critical velocity for the drop of the friction force was proved and a possible link to critical displacement with interpenetration level was estimated.

Spiegelberg and Andersson [2] used surface velocities obtained from a rigid body model to simulate friction and wear in the contact between the rocker arm pad and valve bridge in the cam mechanism of a diesel engine. They simulated friction using two different friction models, a 3D brush model capable of handling transient conditions such as a varying normal load and varying surface velocities and a Coulombian friction model. The 3D brush model reproduced the friction in rolling and sliding contacts between rough surfaces. The surfaces were modelled by bristles that bend depending on the relative tangential displacement of the surfaces and the normal load at each point of contact. Each bristle was assumed to deform independently. In a real contact, however, the tangential deformation in a point would be influenced by the deformation in other points around it. Spiegelberg et al. [3] previously simulated the motion of a cylinder between two planes, first with a step change in velocity and then with an oscillating motion of the upper plane. They aimed to investigate the friction in the contacts and the movement of the roller when the planes are in motion. The friction in the rolling and sliding contacts was simulated with a brush model: one of the two surfaces in contact was modelled with bristles on it (cf. figure 2).

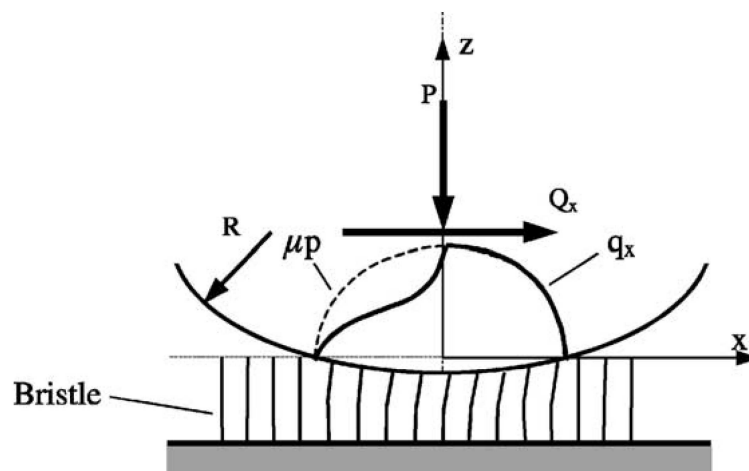


Figure 81: The brush model.  $P$ : normal load,  $Q_x$ : tangential load,  $R$ : equivalent contact radius,  $q_x$ : tangential traction,  $\mu P$ : limiting tangential traction [3].

The bristles were presumed to bend and give rise to traction when the opposite surface moves relative to them. The imaginary bristles represented here the elastic deformation of the

surfaces in contact. A characteristic of the brush model is that each bristle deformed independently of the others. The surfaces were assumed to be ideally smooth.

Brush models cited above all considered each bristle independently of the others. This is an interesting hypothesis in our case as the interaction between a terry and the other terries surrounding is complex to model.

Kotomin and Avdeev [1] investigated the interaction of two single filaments of two opposite brushes while we are interested in the interaction of one single hair and Lorica® smooth counterpart. Nevertheless, the analysis of the filaments deformation as bending may also be pertinent in the case of terry jersey rubbing against skin during running.

Spiegelberg and Andersson [2] studied the friction and wear of two mechanical pieces in contact. They considered that the hairs did not move vertically i.e. the distance between the two counterparts was constant which is not the case for the skin of the foot in contact with a sock. Spiegelberg et al. [3] first calculated the deformation of one single bristle then multiplied this expression by the number of bristles in the contact to obtain the total friction force. We followed a similar approach. However, they considered that sliding occurred in the movement of a cylinder between two planes while we simulated friction without sliding.

## **B. Road/tire dynamic friction models**

Road to tire friction is interesting in connection with textiles as tire surface with its tread designs may be modelled as a polymer with bristles on its surface.

Canudas de Wit et al. [4] suggested a dynamic model for friction, called the LuGre model, which includes most of the friction behaviours which can be observed experimentally. The model properties were investigated by analysis and simulation. Surfaces are very irregular at the microscopic level and two surfaces make contact at a number of asperities. This was modelled as two rigid bodies which make contact through elastic bristles (cf. figure 3). When a tangential force is applied, the bristles will deflect like springs leading to the friction force. If the force is sufficiently large, some of the bristles deflect so much that they will slip. The phenomenon is highly random due to the irregular forms of the surfaces. The LuGre model was based on the average behaviour of the bristles. The average deflection of the bristles was modelled by  $z$ :

$\frac{dz}{dt} = v - \frac{|v|}{g(v)}z$  where  $v$  is the relative velocity between the two surfaces. The

function  $g$  is positive and depends on many factors such as material properties, lubrication, and temperature. It needs not to be symmetrical. Direction dependent behaviour can therefore be simulated. For typical bearing friction,  $g(v)$  will decrease monotonically from  $g(0)$  when  $v$  increases which corresponds to the Stribeck effect (decrease of the friction force for low velocities). The friction force generated from the bending of the bristles was described as:

$F = \sigma_0 z + \sigma_1 \frac{dz}{dt}$  where  $\sigma_0$  is the stiffness and  $\sigma_1$  a damping coefficient.

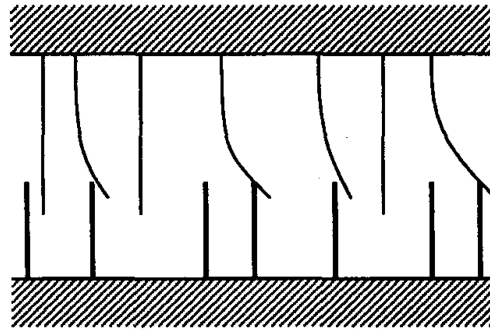


Figure 82: The friction interface between two surfaces is thought of as a contact between bristles [4]. For simplicity, the bristles on the lower part are shown as being rigid.

A term proportional to the relative velocity could be added to the friction force to account for viscous friction so that:

$$F = \sigma_0 z + \sigma_1 \frac{dz}{dt} + \sigma_2 v$$

Canudas de Wit and Tsiotras [5] later showed that the LuGre dynamic friction model accurately simulated velocity and road/surface dependence of the tire friction force. They therefore developed speed-dependent dynamic friction models based on simple punctual contacts which described the tire/road interaction. The input parameters of these models had a physical significance which allowed tuning the model parameters according to experimental data. The models were also speed-dependent, which agreed with experimental observations.

The LuGre model enables different friction behaviours to be simulated, from purely elastic to viscoelastic behaviour. We drew our inspiration from the LuGre model, only the elastic part of the equations above has been considered.

## 2. Compression models

Van Wyk [6] studied the compression behaviour of a fibre wool mat and found a mechanical expression allowing experimental curves to be adjusted. He exposed that the compression of a mass of fibres involves several processes but that the problem is considerably simplified when reduced to that of simple bending of the fibres. For a 3D fibre wad\*, it was assumed that the governing mechanism is that of fibres bending between contact points. He further assumed that the crimps and scales of the wool fibres prevent them from sliding at the contact points even though they may be tilted with respect to the loading axis. His key statement is that the vertical distance between contact points is proportional to the contact point spacing. In his developments, he ignored possible twisting and extension of the fibres. He further modelled the fibre elements as randomly oriented, the mass of fibres as uniformly packed and neglected frictional forces. The fibres were supposed to all have the same length and to be homogeneous, linearly elastic, with a round cross-section. It was assumed that all the fibres were laid perpendicular to compression forces direction. Compression and traction deformations at the contact points were ignored. He expressed compression solicitation as bending between fibres which gets higher with the decrease of the fibre mat volume during compression. Van Wyk's equation can be written as follows:

$$p = kY \frac{m^3}{\rho^3} \left( \frac{1}{V^3} - \frac{1}{V_0^3} \right)$$

$p$  is the pressure applied on the fibre wad,  $k$  is a constant,  $m$  is the fibre wad mass,  $Y$  is the Young's modulus of the fibres,  $\rho$  is the bulk density of the fibres,  $V$  is the volume filled with fibres under pressure, and  $V_0$  the volume filled with fibres under no pressure. Such a simplified equation cannot be used near the asymptote of compression i.e. for assemblies which have been compressed to a volume small enough for the incompressible volume of the fibres to become significant or for assemblies for which the volume at zero pressure is finite, so a more elaborate equation must be employed, such as:

---

\* fibre wad: *tampon fibreux* in French.

$$p = kY \left( \frac{m}{\rho} \right)^3 \left[ \frac{1}{(V - V')^3} - \frac{1}{(V_0 - V')^3} \right]$$

$V'$  is the maximum volume filled with a fibre wad under pressure i.e. the volume at the asymptote of the compression curve. From this equation, compression energy  $W$  can be calculated from 0 to  $p$ . Dupuis et al. [7] adapted the Van Wyk's equation to the study of textile fabrics. They considered De Jong et al. [8] assumption that the volume  $V_0$  is much bigger than the volumes  $V$  and  $V'$ , so that the parameter  $\frac{1}{(V_0 - V')^3}$  is very small compared to

the parameter  $\frac{1}{(V - V')^3}$ . If  $V_0$  is much higher than  $V$  and  $V'$ , then:

$$p \approx a \frac{1}{(V - V')^3} \text{ with } a = kY \left( \frac{m}{\rho} \right)^3$$

$$W = -\int_0^p p dv = -\int_{V_0}^V \frac{a}{(v - V')^3} dv = \frac{a}{2} \left[ \frac{1}{(V - V')^2} - \frac{1}{(V_0 - V')^2} \right]$$

Still supposing that  $V_0$  is much greater than  $V$ , it could be written:

$$W = \frac{a}{2} \frac{1}{(V - V')^2} = \frac{p}{2} (V - V')$$

This gave:

$$V' = V - \frac{2W}{p} \text{ and } a = \frac{8W^3}{p^2}$$

Calculating  $V'$  and  $a$  is therefore easy. For textile assemblies such as fabrics which do not verify the condition that  $V_0$  is very high compared with  $V$  and  $V'$ , the following equations were calculated:

$$p = a \left[ \frac{1}{(V - V')^3} - \frac{1}{(V_0 - V')^3} \right]$$

$$W = -\int_0^p p dv = \frac{p}{2} (V - V') + 1.5a \frac{V - V_0}{(V_0 - V')^3}$$

In order to get the minimum energy  $W$ , the parameters  $a$  and  $V'$  have to be minimum.  $W$  and  $V$  can be determined from experimental results. The couple  $a_{\min}$  and  $V'_{\min}$  whereby the Van Wyk's equation can be solved can thus be calculated. This equation enables us to

determine the limit between the compression of the terries of a terry jersey sock and the compression of the whole knitted structure fitting a compression curve.

Toll [9] developed theories of fibre packing for use in manufacturing composite materials. He defined the maximum unforced packing fraction as the volume fraction under which fibres are compressed without opposition. The maximum packing fraction of force free fibres was assessed from a statistical analysis of the distribution of fibre-fibre contact points. Any compression beyond this limit requires the application of external pressure. Two regimes have thus been defined in terms of fibre volume fraction: unforced packing, at sufficiently low volume fractions for fibres to be separated with no forces acting between them; and forced packing, at higher volume fractions where fibres formed a network and were bent between contact points so that overall elastic forces were needed to keep the network from expanding. Toll dealt with two aspects:

- The limit between the two regimes, i.e. the maximum unforced packing fraction
- The mechanics of forced packing

The forced packing was believed to be governed by the bending of fibre segments between contact points. A micromechanical theory was therefore developed, again based on the contact point statistics, and equations relating the force response per unit area of a fibre bed to the fibre volume fraction were derived for three basic types of assembly: a general 3D wad, a planar mat of dispersed fibres, and a bundle of almost parallel fibres. Other types of reinforcement structure, such as woven fabrics, and the effect of lubrication were also tackled.

Toll modelled the compressive response of fibres to network compression. His objective was to provide a set of simple, yet mechanistic, models to describe the observed phenomena and understand the underlying mechanisms. The fibre assembly was modelled as a volume in which fibres of uniform and circular cross section, straight or curved, are disposed at random positions, but without mutual intersection, and at orientations according to a statistically homogeneous orientation distribution. There was a slight contradiction between the randomness of position and the requirement of no intersection; the no intersection condition supposed a short range correlation in the spatial distribution of fibres.

If the fibres are non-parallel and approximately straight, the governing deformation mechanisms will be the same as for a fibre segment being bent between points of contact with other fibres. Each fibre segment will touch each other as the assembly is compressed and thus

form new contact points and new shorter fibre segments. This will happen at an increasing rate toward higher volume fractions since the rate of encounter will be proportional to the fibre volume fraction. Since a short segment is stiffer than a long one, and the number of segments increases at an increasing rate, the overall compressive force per unit area will be a nonlinear function of the fibre volume fraction. For the case of contact points formed by fibre-fibre crossover, the chosen deformation unit was one fibre segment supported by two other fibres and loaded by a third somewhere between the supports. The contact forces were considered as punctual acting forces, unless the contacting fibres were very close to parallel, in which case it was necessary to describe it as a line contact.

The contact zone therefore may no longer be confined to a negligibly small region around the contact point but have a size comparable to the free segment length and will grow along the fibres as they deflect. In the extreme case of closely packed, perfectly straight and parallel fibres, the network will be almost as stiff as the fibres themselves, which, in this context, are practically rigid. Consequently there must be some feature of the fibre arrangement that lowers the packing efficiency and provides flexibility. Toll identified two candidate mechanisms for this. One was that the fibres have a certain degree of misalignment after all, and that this misalignment causes the fibres to cross over each other and bend between the cross-over points in the same manner as in a non-aligned fibre network. The other proposition was that the fibres are not quite straight, but rather, “wavy”, with one wave corresponding to a beam segment loaded and supported at its extremities. Toll constructed a simple model of weaves and mats where the structure is divided into two distinct regions: a high volume fraction region a and a low volume fraction region b. He assumed that region a behaved like the bundle itself, and was much stiffer than b. He presumed that no sliding takes place across contact points and did not take the fibre length in account since fibre length is important only if the number of contact points per fibre is small, so that the compliance of the deformation units is influenced by the presence of free fibre ends. He considered that a fibre network with reasonably long fibres; fibre length / fibre diameter  $\sim 1000$  or more, would already form a large enough number of contact points per fibre under its self-load to behave as if the fibres were infinitely long.

Toll modelled a fibre assembly under compression. His results would be essential to take in account the action of each fibre on the surrounding fibres.

Dayiary et al. [10] investigated the mechanism of pile deformation under a compressive load in a cut-pile carpet and suggested a theoretical analysis of force and energy of deformation. The elastic-stored bending energy was derived, the frictional effect due to the



sliding pile yarn with its neighbour and the frictional bending couple were also considered. It was estimated that in a cut-pile carpet under vertical compressive load, the deformation of the piles occurs in three steps. The first process was the beginning of loading which could be different for new and used carpets because the hairs of a new carpet are quasi perfectly vertical while the ones of a used carpet present a residual bending. In the second process, the pile was deflected and a curvature occurred along its length. In this process, pile transferred from a curved form to two sectional forms including a curved portion in bottom and a straight portion on top. In the third and final position, there is a two-sectional form at the end of loading or at jamming mode. Dayiary et al. believed that such a deformation could not be created by bending phenomenon only and that friction between fibres into pile yarn may have also been involved. The following assumptions were made:

- A hair is an elastic vertical bar that is deflected under a compressive concentrated load
- A hair has a circular cross-section which is uniform along its length
- Gravity is neglected compared with applied force
- A hair has zero twist and consists of many fibres
- Back of carpet is rigid

The total energy in a hair under loading is composed of two terms namely the bending and the frictional energy. The total energy of pile deformation was shown to depend on geometrical properties of yarn such as pile length and radius, on mechanical properties of yarn including pile bending rigidity and coefficient of friction between pile yarns, and on applied compressive load.

## **II. DISCRETE MODEL OF SOCK-TO-SKIN FRICTION**

Previous models that have just been detailed were all based on the bending of elements that can be bristles, yarns or fibres. We modelled the friction force of knitted fabrics covered with terries rubbing on the mechanical model of skin used in our friction experiments i.e. Lorica® Soft. This model may be a useful tool to compare different socks and to assess the potential of sock constructions to reduce friction induced skin injuries. The movement of terries was first modelled as bending and compression as in previous studies but this model

was complicated, slow and did not give satisfying results. Therefore, the model we suggest is not based on the bending of terries but on the rotation of terries from an initial to a final position [11].

**1. Mechanical model’s assumptions**

Theoretical friction includes deformation and adhesion. Terry-covered knitted fabrics are very deformable materials. In the experimental chapter, it has been concluded that the friction behaviour of these fabrics is dominated by deformation mechanisms. The model will then consider the deformation of terries as the basic friction mechanism and adhesion will be neglected. Dynamic friction is believed to primarily result from two mechanisms namely terries rotation and friction. A similar two-phase mechanical sollicitation has previously been observed for velvet fabrics i.e. textile surfaces consisting of oriented hairiness of quasi-constant length [12]. Moreover, the rotation is assumed to be reversible, i.e., the loops are considered to have elastic or, more probably, viscoelastic behaviour. One loop is modelled as two cut yarns. The input parameters of the model are basic textile and geometrical characteristics of the sock. The modelling consists in formulating the friction force as a function of the terry orientation which is determined by the horizontal displacement of the contacting pin.

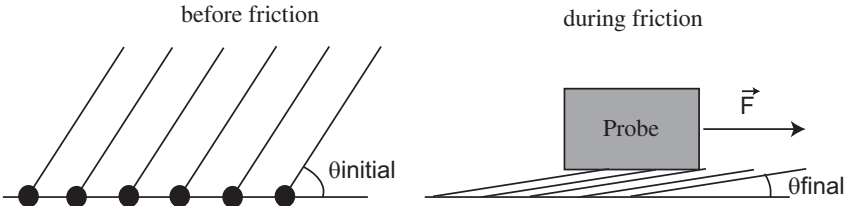


*Figure 83: two-phase friction of the terry yarns as simulated in the model.*

As it has been outlined, two different phases are distinguished in the terries movement. Hairs are supposed to first rotate from an initial to a final position or angle without sliding between them and the pin. Once in their final position, the hairs are assumed to keep this position and be rubbed by Lorica® with a constant friction coefficient equal to the friction force in final position divided by the normal load (cf. figure 4).

Two groups of terries are differentiated: terry yarns which are under the pin and terry yarns which are in front of the pin when the pin begins to move. The total friction force for a textile fabric is assumed to result from compression forces which are transmitted to the pin by the rotating terries and to be equal to the sum of the friction forces for all individual terries.

The instants when the pin touches the terry, when the loop reaches its final position and when it leaves the contact depend on the position of the terry in the wale. Therefore, the friction force of a stitch wale is first calculated before being multiplied by the number of rows present under the pin.

Each terry has been considered independent of the other terries. The final rotation angle of the terries before the change of the movement direction depends on the position of the terry. The last yarns taken by the pin have a smaller final angle than the other yarns. The friction force of a hair is thus not necessarily equal to zero at the beginning of the friction cycle. It is equal to zero for the yarns which are at the front of the pin while the terries under the pin have a residual deformation due to the precedent friction cycle. Once the yarn enters the contact, the friction force increases from its initial value to its maximal value in the forward direction i.e. the value corresponding either to the maximal angle of the yarn in this direction or to the maximal displacement of the pin. If the pin is not already at its maximal displacement, the friction force of the hair will keep its maximal value until the terry yarn leaves the contact or the pin reaches its maximal displacement. If the yarn leaves the contact, its friction force becomes equal to zero. Similar phenomena occur in the reverse direction.

The model input parameters for Labonal terry jersey are listed in Table 1.

PIN WIDTH	9 MM
Pin length	17 mm
Rubbing distance	5 mm
Period of the alternating movement	0.67 s
Number of terry yarns widthwise	1/mm
Number of terry yarns lengthwise	1.7/mm
Terries height	1.38 mm
Terries initial angle	7°

Table 19: Input parameters of the model for Labonal terry jersey sock.

## 2. Mathematical expression of the friction force

The equations which have been used to calculate the friction force as a function of the compression force and terry orientation are explained below. The notations used are listed in table 2 and some parameters are described in figure 5.

MODEL MATHEMATICAL NOTATION	DEFINITION
$d$	Terry yarn vertical displacement (mm)
$F_c$	Compression force (N)
$F_f$	Friction force (N)
$\theta$	Angle formed by the terry yarn and the vertical to the knitted fabric surface (rad)
$\theta_i$	Terry yarn initial angle (rad)
$L$	Terries height (mm)
$M$	Torque (N.mm)
$z$	Terry yarn horizontal displacement (mm)

Table 20: Model mathematical notations and definitions.

The torque of a single terry yarn can be computed from both friction and compression forces as expressed in equation [E1].

$$M(\theta) = F_c L \sin \theta = F_f L \cos \theta \quad [E1]$$

$$d(\theta) = L(\cos \theta_i - \cos \theta) \quad [E2]$$

The friction force [E3] can be expressed from equations [E1] and [E2] as:

$$F_f = \frac{F_c L \sin \theta}{L \cos \theta_i - d(\theta)} \quad [E3]$$

$$z(\theta) = L(\sin \theta - \sin \theta_i) \quad [E4]$$

We aim to plot the friction force in function of the terry yarn horizontal displacement. We thus write  $F_f$  as:

$$F_f = \lambda(\theta) z(\theta) \quad [E5]$$

Finally, [E3], [E4], and [E5] give the following expression of  $\lambda(\theta)$ :

$$\lambda(\theta) = \frac{F_c \sin \theta}{(L \cos \theta_i - d(\theta))(\sin \theta - \sin \theta_i)} \quad [E6]$$

$\lambda(\theta)$  is not constant as shown on figure 6. We nevertheless considered a constant coefficient  $\lambda_c$  to calculate the friction force of a single terry yarn.  $\lambda_c$  is the slope of the dotted line D and equals  $2.3 \times 10^{-3}$  N/mm/yarn for the Labonal terry jersey, it can be expressed as:

$$\lambda_c = \frac{F_{f \max}}{z_{\max}(\theta)} = \frac{F_{c \max} \sin \theta_{\max}}{(L \cos \theta_i - d_{\max}(\theta))(\sin \theta_{\max} - \sin \theta_i)} \quad [E7]$$

$\theta_{\max}$  is the maximal rotation angle.  $F_{c \max}$  and  $d_{\max}$  are determined from Kawabata compression curves using Van Wyk's equation [6].

Figure 5 schematizes the geometry of a terry yarn when the pin moves in the forward direction. The hair has a similar geometry when the pin goes in the reverse direction. The equations above are given for the forward direction of the pin. When the pin moves in the reverse direction, equations [E4], [E6] and [E7] are slightly modified:

$$z(\theta) = L(\sin \theta + \sin \theta_i) \quad [E8]$$

$$\lambda(\theta) = \frac{F_c \sin \theta}{(L \cos \theta_i - d(\theta))(\sin \theta + \sin \theta_i)} \quad [E9]$$

$$\lambda_c = \frac{F_{f \max}}{z_{\max}(\theta)} = \frac{F_{c \max} \sin \theta_{\max}}{(L \cos \theta_i - d_{\max}(\theta))(\sin \theta_{\max} + \sin \theta_i)} \quad [E10]$$

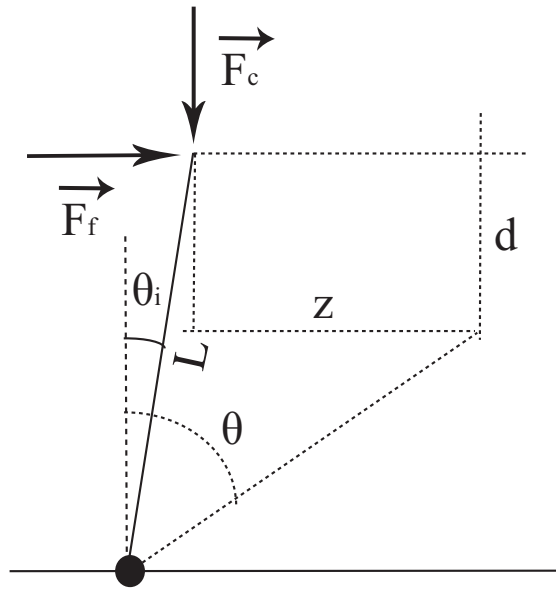


Figure 84: Geometrical characteristics and loading of a terry yarn.

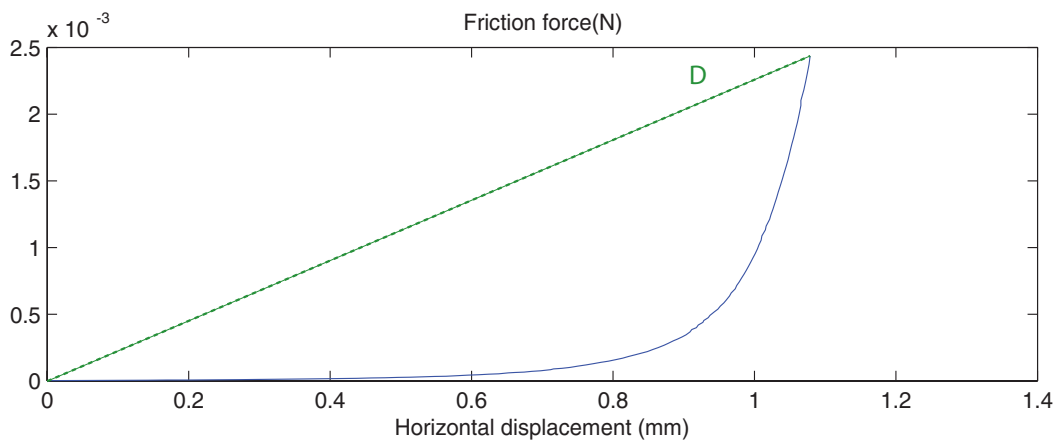
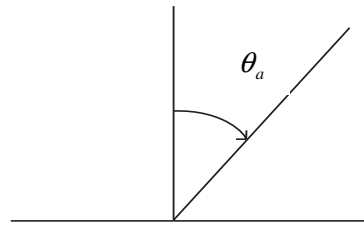
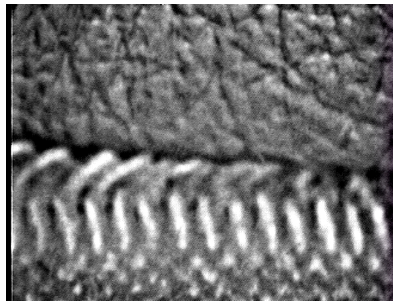


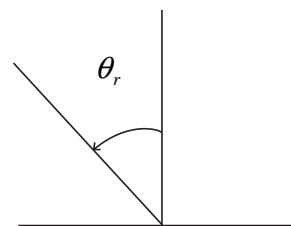
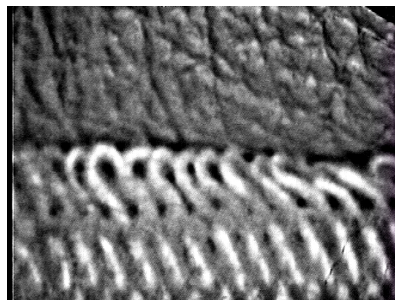
Figure 85: Calculated friction force of a single hair versus horizontal displacement.

SOCK	$\theta_a$ (°)	$\theta_r$ (°)
Labonal terry jersey	$41 \pm 6$	$-49 \pm 9$
Terry jersey 10 - 12	$40 \pm 12$	$-58 \pm 6$
Terry jersey 10 - 16	$56 \pm 9$	$-58 \pm 12$
Terry jersey 10 - 20	$53 \pm 12$	$-66 \pm 7$
Terry jersey 9 - 16	$36 \pm 16$	$-45 \pm 12$
Terry jersey 11 - 16	$54 \pm 6$	$-63 \pm 8$

Table 21: Mean maximal rotation angles in the forward ( $\theta_a$ ) and the reverse direction ( $\theta_r$ ) for terry jersey fabrics. These values were calculated from at least 9 measurements with ImageJ software.



(a)



(b)

Figure 86: Photographs (zoom  $\times 40$ ) used to estimate (a) terries maximal angle for the forward direction and (b) terries maximal angle for the reverse direction. These photographs were taken under 15 kPa during a static experiment with the Lorica® pin.

The modelled friction force is fitted to the experimental data. The fitting is realised in both forward and reverse directions independently. The fitted parameter is the maximal rotation angle in the studied direction. The maximal rotation angles in the forward and the reverse directions are calculated applying the least squares method to an experimental friction curve so that these angles do not exceed physical limits. These angles correspond to the final inclination between terries and the vertical axis, their limit values can be assessed from photographs as illustrated on figure 7. These estimations enable model results to be corroborated. The maximal angles in both the forward and the reverse direction, namely  $\theta_a$  and  $\theta_r$ , for the six terry jersey fabrics are given in table 3. Rotation angles for other terry jersey fabrics than Labonal are indicated as comparison in table 3. It can be seen that the standard deviations for these angles are very high; this is due to the heterogeneity of the fabrics. When rubbed, not all the terries show the same behaviour, some rotate when the pin moves, some just leave the contact. Simulations will therefore not be given for these fabrics.

### 3. Results and discussion

A good correspondence was found between modelled and measured friction forces for Labonal terry jersey as can be seen on figure 8.

Many hypotheses have been made to get a simple model. The differences between experimental data and simulated curves are attributed to the model's assumptions. A terry is considered as two yarns i.e. the non-vertical part of the loop is not taken into account. Textile fabrics are very deformable materials, especially terry jersey fabrics. The analysis of friction experiments indicates that for terry jersey fabrics, the major part of friction is due to sock deformation. The friction is thus restricted to terries rotation and rubbing i.e. adhesion is neglected whereas theoretical friction includes both deformation and adhesion. Moreover, terries are modelled as perfectly elastic while their real behaviour is rather viscoelastic. Finally, the applied normal force may not be sufficient for the terry yarns to reach their maximal rotation angles, especially in the reverse direction as they counter the movement since they are oriented in the opposite direction. This may explain the more pronounced asymmetry of simulated results compared to experimental data.



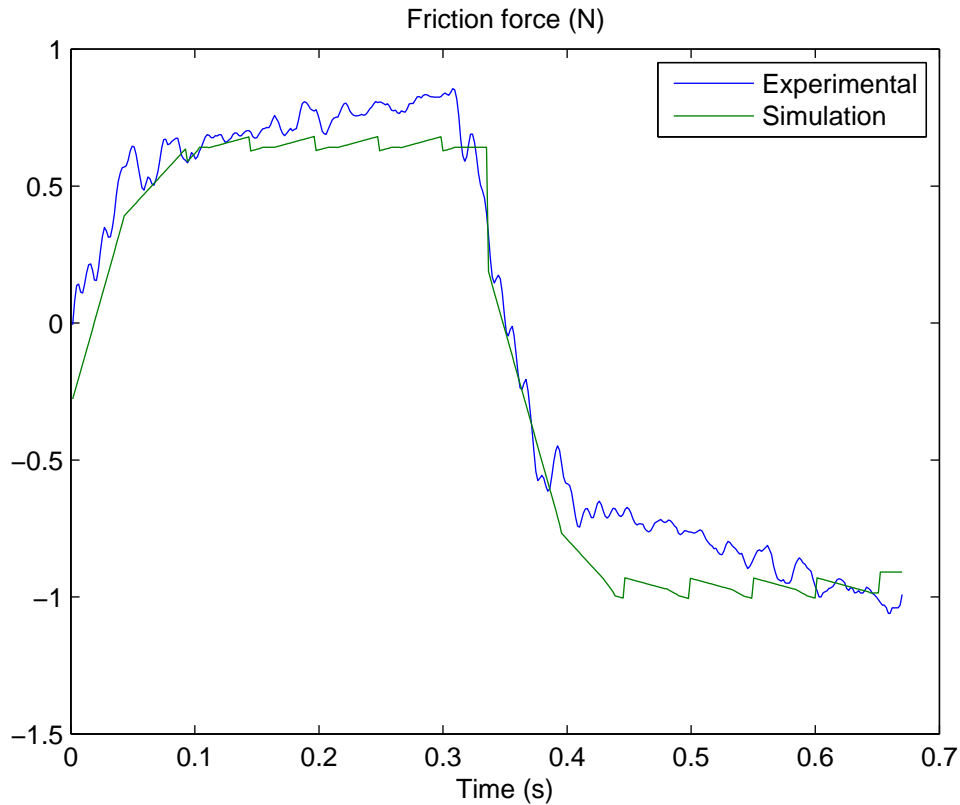


*Figure 87 : Comparison between experiment and model for an apparent pressure of 15 kPa.*

The displacement of the pin is modelled as a linear (triangular) displacement whereas the movement of the oscillating table of the LPMT's friction tester is sinusoidal. The model was modified in order to simulate the real pin displacement but the result is very similar and the computing interval was considerably increased. Some sliding was also introduced simulating the hairs which did not reach their maximal rotation angle at the end of the forward and the reverse movement to leave the contact once in their initial position. The correspondence to experimental data was better for the modelling without sliding than for the modelling including sliding. The maximal rotation angles of the terries were estimated using photographs taken during a static experiment while real rotation angles correspond to a dynamic situation. The angles that have been measured may therefore be overestimated as the angle will increase with the time of loading. The overestimation is thought to be more significant for the maximal rotation angle in the reverse direction since the resistance of terries to sliding is higher in this direction. The maximal rotation angle in the reverse direction was thus modelled as the angle for which the reaction of terries trims the pin weight. This

model gives similar results as the previous one for the steady states in the forward and the reverse sliding directions.

The model may be improved by the introduction of the adhesion part of friction; the adhesion between the pin and the yarns but also the attraction forces exerted by a yarn on the neighbouring yarns around it. Moreover, the terry yarns are simulated here as independent of each other while in reality, when the terry rotates, it will touch and deform the neighbouring terry and so on. The model can thus be improved by considering the compression force exerted by each hair on the next one.

The model may also be adapted to low and non hairy fabrics such as yarn bridges and simple or double jersey. The parameter  $L$  can be measured for the yarn bridges fabric and may be estimated as equal to the yarn diameter for non hairy fabrics. The initial angle is assumed to be around  $90^\circ$  for non-hairy fabrics. For yarn bridges, it seems difficult to neglect the non-vertical part of the loop as the most part of it is horizontal.

## Literature cited

1. Kotomin, S.V. and N.N. Avdeev, *Macromodel approach to experimental study of polymer brushes rubbing*. Wear, 1998. **222**(1): p. 21-28.
2. Spiegelberg, C. and S. Andersson, *Simulation of friction and wear in the contact between the valve bridge and rocker arm pad in a cam mechanism*. Wear, 2006. **261**(1): p. 58-67.
3. Spiegelberg, C., S. Björklund, and S. Andersson, *Simulation of transient friction of a cylinder between two planes*. Wear, 2003. **254**(11): p. 1170-1179.
4. Canudas-de-Wit, C., et al., *A New Model for Control of Systems with Friction*. IEEE Transactions on Automatic control, 1995. **40**(3): p. 419-425.
5. Canudas-de-Wit, C. and P. Tsiotras, *Dynamic Tire Friction Models for Vehicle Traction Control*, in *Conference on Decision and Control*. 1999: Phoenix (Arizona, USA).
6. Van-Wyk, C.M., *Note on the compressibility of wool*. Journal of Textile Institute, 1946: p. T285-T292.
7. Dupuis, D., G. Popov, and P. Viallier, *Compression of Greystate Fabrics as a Function of Yarn Structure*. Textile Research Journal, 1995. **65**(6): p. 309-316.
8. De-Jong, S., J.W. Snaith, and N.A. Michie, *A Mechanical Model for the Lateral Compression of Woven Fabrics*. Textile Research Journal, 1986(56): p. 759-767.
9. Toll, S., *Packing Mechanics of Fiber Reinforcements*. Polymer engineering and science, 1998. **38**(8): p. 1337-1350.
10. Dayiary, M., S.S. Najjar, and M. Shamsi, *A new theoretical approach to cut-pile carpet compression based on elastic-stored bending energy*. The Journal of The Textile Institute, 2009. **100**(8): p. 688-694.
11. Baussan, E., et al., *Experiments and modelling of skin-knitted fabric friction*. Wear, 2010. **268**(9-10): p. 1103-1110.
12. Praëne, J.M., *Modélisation phénoménologique du comportement tribologique des surfaces textiles*, in *Mécanique*. 2007, Université de Haute-Alsace: Mulhouse. p. 174.

# Conclusion

This study deals with the mechanical contact between the foot skin of the recreational runner and his socks. It aimed to determine which knitted structure should be recommended for runners. There have indeed been several studies on the influence of the sock fibre composition while the effect of the sock structure has not been investigated yet. The socks that people commonly choose and the areas where blisters may appear have been pointed out. The case of the plantar fascia zone is studied here. Cotton-made socks were investigated as cotton is the material the most used in basic running socks. Four knitted structures were chosen, namely simple jersey, double jersey, yarn bridges jersey and terry jersey. The socks were studied independently of the shoes. The pressure applied on the foot and the stride frequency have been determined using in-shoe measurements. In order to simulate the friction between the socks and a skin equivalent, the sliding frequency was then fixed to 1.5 Hz and the vertical forces ranged from 0.5 to 2.2 N. Friction experiments were carried out on two different tribometers; a linear alternating tribometer especially designed for this study and the EMPA Textile Friction Analyser. Neither the linear reciprocating dead weight tribometer nor the TFA exactly reproduces the friction of the foot with the sock in the shoe. In-shoe conditions are probably an intermediate between these two cases. The transverse properties of the different knitted structures were also examined through compression experiments and a first approach of shock absorption tests.

It is difficult to give universal conclusions about which sock is the best to wear during running as the pressure and friction the foot skin undergoes highly depend on the foot shape, the shoe shape, the mechanical properties of the shoe and the way to wear running shoes. The shoe is supposed to absorb a part of the shock energy generated at each stride when the foot contacts the ground. In order to reduce the pressure on the skin, the contact surface between the sock and the shoe should be as large as possible; the shape of the shoe should be adapted to the shape of the foot and the distance between the shoe and the skin should ideally be equal to the thickness of the sock when it is not compressed. A lower distance will lead to an increase of the contact pressure while a higher distance will increase the sliding distance of the foot within the shoe.

Double jersey and yarn bridges structures were investigated because they were supposed to be intermediates between the simple and the terry jersey structures. Their friction behaviour shows they are intermediates but much closer to simple jersey. Moreover, compression measurements revealed they are harder than the two other structures and

consequently less interesting for sports socks. To resume, terry and simple jersey structures were found to give better results than double jersey and yarn bridges structures in terms of friction and compression.

The conclusions drawn from this study will therefore only be about terry and simple jersey structures. The thickness of terry jersey socks is a good, easy and inexpensive way to reduce the pain people with bony prominences at specific areas of the foot or with pre-existing blisters suffer from. The friction, compression and shock absorption experiments we carried out showed that:

- For a given normal load, terry jersey socks generate less friction than simple jersey socks provided that the terries are compact, homogeneous and oriented in the direction of the friction force.
- Under progressive compression, for the same compression energy applied on the sock, the simple jersey structure transmits less energy to the skin than the terry jersey structure. Simple jersey socks consequently provide a better static or quasi-static “damping effect” than terry jersey socks.
- When a ball is dropped from a given height on simple and terry jersey structures, the height of the first rebound of the ball is lower for a terry jersey sock than for a simple jersey sock. The terry jersey structure thus gives a higher dynamic “damping effect” or shock absorption than the simple jersey structure.

We could thus conclude that:

- When walking, the foot undergoes friction and progressive compression, the confrontation of the friction and the compression results indicates that the best knitted structure for hiking socks is the simple jersey structure. This can be seen in the figure 1.
- When running, the foot skin is first subjected to a shock and then to progressive compression and friction. We do not know whether the shock, the friction force or the compression energy has the greater influence on skin irritations. The simple jersey structure is better in terms of friction and quasi-static “damping effect” compared to the terry jersey structure. Therefore, if the effect of the friction force and the compression energy is more important than

the influence of the maximal compression force on the formation of blisters, then we recommend wearing simple jersey socks when running.

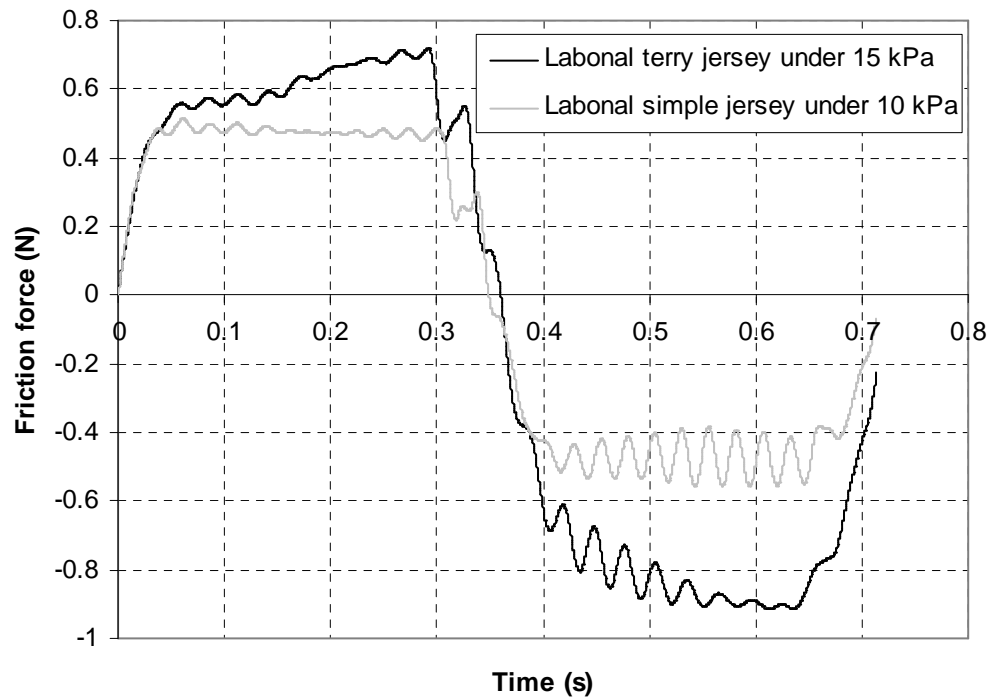


Figure 88: Friction force of Labonal terry jersey under 15 kPa and Labonal simple jersey under 10 kPa in contact with the Lorica® pin.

- On the other hand, the terry jersey structure seems to have a higher dynamic “damping effect” than the simple jersey structure. Consequently, if it is the shock absorption that is more important than the friction force and the compression energy regarding the formation of blisters, the knitted structure recommended for running socks would be the terry jersey structure. Moreover, this structure can be improved drastically with sufficiently compact and homogeneous terries in contact with the skin and oriented towards the toe so that the friction can be reduced when the foot slides towards the toe within the shoe i.e. when the foot contacts the ground and is loaded with significant normal and tangential forces. In that case terry jersey is better than simple jersey in terms of friction.

- If a recreational runner has only terry jersey socks, it is recommended to determine whether the terries are oriented towards the toes when worn in contact with the skin. If it is the case, the socks should be worn with the terries in contact with the skin. If the terries are oriented towards the heel when worn in contact with the skin, which is the case for most of the terry jersey socks which are commercialised, it is better to wear the socks with the terries in contact with the shoe because they will be oriented, in this case, in the direction of the friction force generated by the sliding of the foot in the shoe. It can indeed be seen in figure 2 that when the terries are well oriented, the back (terry side) of the terry jersey generates a lower friction force than the face (non terry side) of the terry jersey whereas when the terries are inclined in the wrong direction, it is the face of the terry jersey that gives less friction than the back.

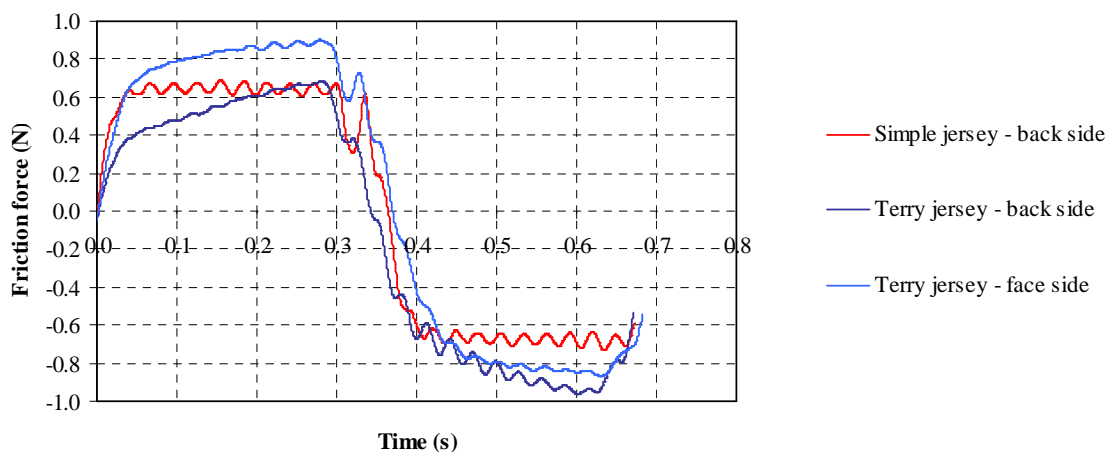


Figure 89: Friction force of the face (non terry side), the back (terry side) of Labonal terry jersey and the back of Labonal simple jersey under 15 kPa in contact with the Lorica® pin.

Moreover, we have seen that Labonal terry jersey friction force has a particular shape that may be due to the rotation of terries during a friction cycle. It has been found that the contribution of deformation is important in the case of the terry jersey structure. A discrete model for the friction of textile surfaces recovered with terries is thus proposed that considers the rotation and the rubbing of terries and neglects the adhesion. Hairs are supposed to first rotate from an initial to a final position without sliding between them and the pin. Once in



their final position, the hairs are assumed to keep this position and be rubbed with a constant friction coefficient. The modelled friction force is fitted to the experimental data. The fitting is realised in both forward and reverse directions independently. The fitted parameter is the maximal rotation angle in the studied direction. The maximal rotation angles in the forward and the reverse directions are calculated applying the least squares method to an experimental friction curve. After fitting, theoretical and experimental results are very similar.

The model may be improved by the introduction of the adhesion part of friction i.e. the adhesion between the pin and the yarns and the attraction forces exerted by a yarn on the neighbouring yarns around it. The terry yarns are simulated as independent of each other while in reality, when the terry rotates, it will touch and deform the neighbouring terry. The model may thus give better simulations by considering the compression force exerted by each hair on the next one. The model may also be adapted to low and non hairy fabrics such as yarn bridges and simple or double jersey. The height of the yarn can be measured for yarn bridges fabric and may be estimated as equal to the yarn diameter for non hairy fabrics. Initial angle may be assumed to be around  $90^\circ$  for non-hairy fabrics. In addition, the pin geometry may be modelled by dividing the space into small areas which can be active or not depending on the shape of the pin. The shapes of the foot and the shoe could thus be considered as these two geometries define the contact area.

The pressure the sock exerts on the foot skin is different from one area of the foot to another. The conclusions drawn by our study are given for vertical loads from 0.5 to 2.2N corresponding to the plantar fascia zone. Complementary friction and compression tests under higher normal loads can be carried out to investigate other areas of the foot.

Both TFA and LPMT's tribometer can be improved in order to better simulate the friction between the sock and the foot of a runner for example with the use of curved rubbing elements that could simulate the contact of textile fabrics against skin overlying bony prominences. The pin may also be designed in order to reproduce the shape of the tested foot area and a shoe insole may be placed under the sock. Moreover, during the friction experiments, no tension was applied to the sock whereas when it is worn the sock is subjected to multidirectional tensions. Both the friction devices used are alternating tribometers while in the shoe, the foot slides in a single direction. In addition, in the case of the LPMT's

tribometer, the normal load is kept constant whereas for the TFA, it is the distance between the pin and the sample that is fixed and we have seen that in-shoe conditions are probably intermediate. A unidirectional tribometer with constant normal load and constant distance between the pin and the sample may be developed in order to better simulate in-shoe friction.

Shock resistance tests may be carried out in order to determine which textile structure best absorbs the shock energy when the foot contacts the ground. The ability of the different socks to form folds which is related to their elasticity is also an important parameter to investigate in future works as folds will increase sharply the friction and compression forces the sock exerts on the foot. The ageing of the knitted structures is another important parameter which can be studied. The simple jersey structure is thought not to change much with time while for the terry jersey structure, the terries may be affected by repeated washings and we have seen that the quality of the terries is very important in terms of friction i.e. compact, vertical and homogeneous terries give reduced friction while heterogeneous and crushed terries do not present interesting friction properties.

Finally, the friction and compression tests we carried out were realised in a dry atmosphere. When running, the foot skin sweats and perspiration from other areas of the body is accumulated in the shoe. The conclusions drawn by this study are qualitatively true for a wet atmosphere but experiments on human subjects wearing well adapted socks (in terms of fibre composition and lacing conditions) could be carried out in order to give quantitative results.

Dix chaussettes ont été étudiées, toutes en coton : quatre d'entre elles pour évaluer l'influence de la structure tricotée sur le frottement (jerseys bouclette, simple, double et ponts de fil), trois sont identiques au titre du fil près, et les trois dernières à la pointure près. Nous nous sommes attachés au cas des phlyctènes apparaissant lors de la course à pied. Les zones du pied sujettes aux ampoules ont été déterminées grâce à un sondage. La pression s'exerçant sur ces zones et la fréquence des foulées ont été mesurées. Nous avons ainsi programmé une platine oscillante qui reproduit le frottement dans la chaussure. Les mesures obtenues sur ce dispositif ont été comparées à celles du Textile Friction Analyser de l'EMPA. En croisant ces résultats avec des mesures de compression et une première approche de test d'absorption des chocs, nous avons observé que le jersey simple est plus indiqué dans le cas de la marche car il exerce un frottement moins important que la bouclette et apporte un meilleur amortissement quasi-statique. Dans le cas de la course à pied, il reste à déterminer si le choc a un effet plus dommageable que le frottement et la compression exercée sur la peau. Si le choc est primordial, le jersey bouclette sera recommandé, sinon le jersey simple. Nous avons développé un modèle du frottement textile-peau en nous intéressant tout d'abord au cas des tricots bouclette. Le mouvement des bouclettes lors d'un cycle de frottement est assimilé à une rotation entre un angle maximal en sens bouclette et un angle maximal en sens inverse. Ce modèle donne des résultats très proches de l'expérience.

Mots clés : contact peau - textile, chaussette, phlyctène, frottement, pression, modèle

Ten cotton-made athletic socks were studied: four in order to evaluate the influence of the knitted structure on the sock - to - skin friction (terry, simple, double and yarn bridges jerseys), three differ from the yarn count and three from the size. We focused our research on the case of skin blisters generated during running. The areas of the foot where these skin affections may appear were determined using a survey. The pressure exerted on these areas and the stride frequency were measured whereby a linear alternative tribometer reproducing the friction in the shoe has been programmed. The results obtained on this device were compared with the results obtained on the EMPA's Textile Friction Analyser. Complementary compression and shock absorption tests were realised. It was observed that the best knitted structure for hiking socks is the simple jersey structure. For running socks, if the effect of the friction force and the compression energy is more important than the influence of the maximal compression force on the formation of blisters, then we recommend wearing simple jersey otherwise we advise to wear terry jersey socks. A discrete model for the friction of textile surfaces recovered with terries in contact with the skin is proposed. Terries are supposed to rotate from an initial to a final position both in the forward and the reverse direction. After fitting, theoretical and experimental results are very similar.

Key words: textile - to - skin contact, sock, skin blister, friction, pressure, model